

Aus dem Institut für Bodenkunde und Standortslehre

Universität Hohenheim

Fachgebiet: Biogeophysik – Prof. Dr. Thilo Streck

Microbial Regulation of Pesticide Degradation Coupled to Carbon Turnover in the Detritusphere

Dissertation

zur Erlangung des Grades eines Doktors der Agrarwissenschaften (Dr. sc. agr.)

vorgelegt der Fakultät Agrarwissenschaften von

Holger Pagel

aus Rostock

2015

Date of acceptance: 17.12.2014

Date of oral examination: 16.06.2015

Examination committee

Supervisor and Referee: Prof. Dr. Thilo Streck

Co-Referee: Prof. Dr. Claire Chenu

Additional Examiner: Prof. Dr. Ellen Kandeler

Head of the Committee: Prof. Dr. Dr. h.c. Rainer Mosenthin

Dean: Prof. Dr. Ralf T. Vögele

To my children,

Hannes Kostja - Greta Jule - Frieder Jurek,

for childlike curiosity and the power of asking "Why?".

Preface

My PhD project was part of the DFG priority program SPP 1315 “Biogeochemical interfaces in soil”. The joint scientific goal was “... to gain a [mechanistic] understanding of the interplay and interdependencies of the physical, chemical, and biological processes operating at biogeochemical interfaces in soil” (Totsche et al. 2010).

The SPP1315 gave me the great opportunity to easily meet (and partly collaborate) with many active scientists. Special thanks go to the coordinator Kai Uwe Totsche as well as to the scientific coordinators Thilo Rennert (first phase) and Joanna Ewa Hanzel (second phase) for setting up and organizing the priority programme.

Table of Contents

1	Summary	1
2	Zusammenfassung	4
3	General Introduction	7
3.1	Biogeochemical interfaces in soil	7
3.2	Biogeochemical hot spots and matter cycling in soil	8
3.3	Modeling microbial regulation of matter cycling in soil.....	12
3.4	The model pesticide 4-chloro-2-methylphenoxyacetic acid (MCPA).....	12
3.5	Scope of the thesis – Why study the detritusphere?	13
4	Regulation of bacterial and fungal MCPA degradation at the soil-litter interface ... 15	
4.1	Abstract	16
4.2	Introduction.....	17
4.3	Material and methods	18
4.4	Results	23
4.5	Discussion	27
4.6	Conclusions	30
4.7	Acknowledgement	30
4.8	References	30
5	Micro-scale modeling of pesticide degradation coupled to carbon turnover in the detritusphere - Model description and sensitivity analysis 34	
5.1	Abstract	35
5.2	Introduction.....	36
5.3	Model description.....	39
5.4	Global sensitivity analysis	49
5.5	Results and discussion	50
5.6	Conclusion and outlook.....	59
5.7	Acknowledgements.....	60
5.8	References	60
5.9	Online Resources	66
6	Regulation of pesticide degradation in the detritusphere: Integrating soil genomics and biogeochemical modeling	90
6.1	Abstract	91
6.2	Introduction.....	92
6.3	Material and Methods	95
6.4	Results and discussion	100
6.5	Conclusions	121
6.6	Acknowledgements.....	122
6.7	Literature cited.....	122
6.8	Appendices.....	133
7	General discussion	140

8	Final conclusions	143
9	References	144
	Curriculum vitae	153
	Acknowledgements.....	154

1 Summary

Many soil functions, such as nutrient cycling or pesticide degradation, are controlled by microorganisms. Dynamics of microbial populations and biogeochemical cycling in soil are largely determined by the availability of carbon (C). However, the underlying regulation mechanisms are still not well understood. The detritusphere is a microbial “hot spot” of C turnover. It is characterized by a pronounced concentration gradient of C from litter (high) into the adjacent soil (lower). Therefore, this microhabitat is very well suited to investigate the influence of C availability on microbial dynamics and biogeochemical processes. My thesis aimed at improving our understanding of biogeochemical interactions involved in pesticide degradation coupled to C turnover in the detritusphere. Thereby, the herbicide 4-chloro-2-methylphenoxyacetic acid (MCPA) served as a model xenobiotic.

In the first study, the influence of litter-C input on C and MCPA turnover as well as on the MCPA-degrading microbial community in soil was investigated spatially resolved in a three-week microcosm experiment. Based on these results, a new mathematical model was developed that simulates transport and degradation of MCPA depending on C turnover and microbial dynamics. High-leverage model parameters were identified by a global sensitivity analysis. A second microcosm experiment focused on the spatiotemporal dynamics of MCPA, C and microorganisms. It provided the data to parameterize the new model.

In the experiments MCPA, organic C (total and extractable) and microbial C as well as CO₂ production were analyzed to quantify matter cycling in soil. In the experiments ¹⁴C-labeled MCPA as well as litter and soil with different ¹³C signatures were applied. Thus, the fate of MCPA- and litter-C was traced by using isotopic analyses of CO₂, extractable and total organic C as well as microbial C. Information on composition and dynamics of the soil microbial community was obtained by quantifying three marker-genes: the 16S rRNA gene (bacteria), an internal transcribed spacer (ITS) fragment (fungi) and the functional gene *tfdA* (bacterial MCPA degrader)

The new model was formulated as a set of coupled ordinary and partial differential equations. It simulates the dynamics of MCPA, five C pools (litter, high-quality and low-quality dissolved organic C, insoluble soil organic matter, CO₂) and three microbial pools (bacteria, fungi, bacterial pesticide degraders). In addition, it considers physiological activity of microorganisms, transport and sorption of dissolved organic C and MCPA as well as the dynamics of C isotopes (¹⁴C, ¹³C). The model was calibrated using a Pareto optimization. In addition to the parameterization of the model, this method was used to analyze possible structural shortcomings of the model. For the first time, genetic information on abundances of total bacteria, fungi and specific pesticide degraders in soil were directly used as a proxy of the corresponding microbial pools in the model.

In the detritosphere, gradients of organic matter turnover from litter into the adjacent soil could be identified. Increased C availability, due to the transport of dissolved organic substances from litter into soil, resulted in the boost of microbial biomass and activity as well as in the acceleration of MCPA degradation. Fungi and bacterial MCPA-degraders profited most from litter-C input. Accelerated MCPA degradation was accompanied by increased incorporation of MCPA-C into soil organic matter. The experimental results show that the transport of dissolved organic substances from litter regulates C availability, microbial activity and finally MCPA degradation in the detritosphere. In general, litter-derived organic compounds provide energy and resources for microorganisms. The following possible regulation mechanisms were identified: i) Litter might directly supply the co-substrate α -ketoglutarate (or surrogates) required for enzymatic oxidation of MCPA by bacterial MCPA degraders. Alternatively, it might provide additional energy and resources for production and regeneration of the needed co-substrate. ii) Additional litter-C might alleviate substrate limitation of enzyme production by bacteria and bacterial consortia resulting in an increased activity of specific enzymes attacking MCPA. iii) Litter-derived organic substances might stimulate MCPA degradation via fungal co-metabolism by unspecific extracellular enzymes, either directly by inducing enzyme production, or by supplying primary substrates that provide the energy consumed by co-metabolic MCPA transformation.

The model abstracts these regulation mechanisms in such a way that C availability controls physiological activity, growth, death and maintenance of microbial pools. Accelerated pesticide degradation in the detritosphere was modeled by the two following mechanisms: i) Increasing C availability and turnover promotes activity and biomass of bacterial pesticide degraders. Thus, the pesticide is faster utilized as a growth substrate by this microbial pool. ii) By analogy, the model simulates accelerated co-metabolic pesticide transformation as a result of increased activity and biomass of the fungal pool due to increased C availability. Based on the global sensitivity analysis, 41% (n=33) of all considered parameters and input values were classified as “very important” and “important”. These mainly include biokinetic parameters and initial values. The Pareto-analysis showed that the model structure was adequate and the identified parameter values were reasonable to reproduce the observed dynamics of C and MCPA. The model satisfactorily matched observed abundances of 16S rRNA and *tfdA* genes. It underestimated, however, the steep increase of fungal ITS fragments, most probably because this gene-marker is only inadequately suited as a measure of fungal biomass. The model simulations indicate that soil fungi primarily benefit from low-quality C, whereas bacterial MCPA-degraders preferentially use high-quality C. According to the simulations, MCPA was predominantly transformed via co-metabolism to high-quality C. Subsequently, this C was primarily assimilated by bacterial MCPA-degraders. The highest turnover of litter-derived C occurred by substrate uptake for microbial growth. Input and microbial turnover of litter-C stimulated MCPA

degradation mainly in a soil layer at 0-3 mm distance to litter. As a consequence of this, a concentration gradient of MCPA formed, which triggered the diffusive upward transport of MCPA from deeper soil layers into the detritosphere.

The results of the three studies suggest that i) the detritosphere is a biogeochemical hot spot where microbial dynamics control matter cycling, ii) the integrated use of experiments and mathematical modelling gives detailed insight into matter cycling and dynamics of microorganisms in soil, and iii) microbial communities need to be explicitly considered to understand the regulation of soil functions.

2 Zusammenfassung

Viele Bodenfunktionen, wie zum Beispiel die Umsetzung von Nährstoffen oder der Abbau von Pestiziden, werden maßgeblich durch Mikroorganismen gesteuert. Die Verfügbarkeit von Kohlenstoff (C) bestimmt dabei signifikant die Dynamik der mikrobiellen Biomasse und biogeochemischer Umsetzungsprozesse im Boden. Ein „hot spot“ des mikrobiellen C-Umsatzes ist die Detritusphäre. Sie ist durch einen starken Gradienten der C-Konzentration von der Streu (hoch) in den angrenzenden Boden (niedriger) geprägt. Daher lässt sich der Einfluss der C-Verfügbarkeit auf mikrobielle Umsatzprozesse gerade in der Detritusphäre sehr gut untersuchen. Ziel meiner Dissertation war es, die am gekoppelten Pestizid-Abbau und C-Umsatz beteiligten biogeochemischen Wechselwirkungen in der Detritusphäre besser zu verstehen. Dabei diente das Herbizid 4-Chlor-2-methylphenoxyessigsäure (MCPA) als ein Modell-Xenobiotikum.

In der ersten Studie wurde in einem dreiwöchigen Mikrokosmenexperiment der Einfluss von Streu-C auf den Umsatz von C und MCPA sowie die MCPA-abbauende mikrobielle Gemeinschaft im Boden räumlich aufgelöst untersucht. Aufbauend auf diesen Ergebnissen wurde in der zweiten Arbeit ein neues mathematisches Modell entwickelt, das den Transport und den Abbau von MCPA in Abhängigkeit vom C-Umsatz und der mikrobiellen Dynamik simuliert. Anhand einer globalen Sensitivitätsanalyse wurden die Modellparameter identifiziert, die die Simulation am stärksten beeinflussen. Ein weiteres Mikrokosmenexperiment mit dem Focus auf der zeitlichen Dynamik von MCPA, C und Mikroorganismen diente zur Parametrisierung des neuen Modells (dritte Studie).

Zur Quantifizierung des Stoffumsatzes in den Experimenten wurden MCPA, organischer C (total und extrahierbar) und mikrobieller C im Boden sowie die CO₂-Produktion analysiert. Außerdem wurde ¹⁴C markiertes MCPA sowie Streu und Boden mit jeweils unterschiedlicher ¹³C-Signatur eingesetzt. Mithilfe isotopischer Analysen von CO₂, gelöstem und gesamtem organischen C sowie mikrobiellem C konnten so die Umsatzwege von MCPA- und Streu-C verfolgt werden. Informationen über die Zusammensetzung und Dynamik der mikrobiellen Gemeinschaft im Boden lieferte die Quantifizierung folgender Gen-Marker: das 16S rRNA Gen (Bakterien), ein internal transcribed spacer (ITS) Fragment (Pilze) und das Funktionsgen *tdfA* (bakterielle MCPA-Abbauer).

Das neue Modell wurde als System gekoppelter gewöhnlicher und partieller Differentialgleichungen formuliert. Es simuliert die Dynamik von MCPA, fünf C-Pools (Streu, gelöster organischer C hoher und niedriger Qualität, unlösliche organische Bodensubstanz, CO₂) und drei mikrobiellen Pools (Bakterien, Pilze, bakterielle Pestizidabbauer). Außerdem berücksichtigt es die physiologische Aktivität von Mikroorganismen, den Transport und die Sorption von gelöstem organischen C und MCPA sowie die Dynamik von C-Isotopen (¹⁴C; ¹³C). Das Modell wurde

mithilfe einer Pareto-Optimierung kalibriert. Dieses Verfahren erlaubte darüber hinaus eine Analyse möglicher struktureller Defizite des Modells. Für die Kalibrierung wurden erstmals direkt genetische Informationen über die Abundanz von gesamten Bakterien, Pilzen und spezifischen MCPA-Abbauern im Boden als Maß für die entsprechenden mikrobiellen Pools im Modell genutzt.

In der Detritusphäre zeigten sich Gradienten des Stoffumsatzes von der Streu in den angrenzenden Boden. Die erhöhte C-Verfügbarkeit in der Detritusphäre, infolge des Transports gelöster organischer Verbindungen aus der Streu in den Boden, führte zu einem Anstieg der mikrobiellen Biomasse und Aktivität sowie zu einem beschleunigten MCPA-Abbau. Pilze und bakterielle MCPA-Abbauer profitierten am stärksten von eingetragener Streu-C. Der beschleunigte MCPA-Abbau ging mit verstärktem Einbau von MCPA-C in die organische Bodensubstanz einher. Die experimentellen Ergebnisse zeigen, dass der Transport gelöster organischer Verbindungen aus der Streu die C-Verfügbarkeit und in der Folge sowohl die mikrobielle Aktivität als auch den MCPA-Umsatz im Boden reguliert. Generell stellen eingetragene Verbindungen aus der Streu Energie und Ressourcen für Mikroorganismen zur Verfügung. Als mögliche Regulationsmechanismen wurden identifiziert: i) Streu könnte direkt das Co-Substrat α -Ketoglutarat (oder Surrogate) liefern, das für die enzymatische Oxidation von MCPA durch bakterielle MCPA-Abbauer gebraucht wird. Alternativ könnten organische Verbindungen aus der Streu zusätzliche Energie und Ressourcen zur Produktion und Regeneration des benötigten Co-Substrats liefern. ii) Zusätzlicher Streu-C könnte die Substratlimitierung der Enzymproduktion von Bakterien und bakteriellen Konsortien vermindern und in der Folge zu höherer Aktivität von spezifischen MCPA-angreifenden Enzymen führen. iii) Organische Substanzen aus der Streu könnten den co-metabolischen MCPA-Abbau durch unspezifische extrazelluläre Enzyme von Bodenpilzen stimulieren, entweder direkt über die Induktion der Enzymproduktion oder indem aus Primärsubstraten Energie, die für die co-metabolische MCPA-Transformation verbraucht wird, gewonnen werden kann.

Das Modell abstrahiert diese Regulationsmechanismen, indem physiologische Aktivität, Wachstum, Absterben und Erhaltungsstoffwechsel der mikrobiellen Pools durch die C-Verfügbarkeit kontrolliert werden. Der beschleunigte MCPA-Abbau in der Detritusphäre wird durch folgende zwei Mechanismen abgebildet: i) Steigende C-Verfügbarkeit und erhöhter C-Umsatz fördern Aktivität und Biomasse bakterieller Pestizid-Abbauer. Infolgedessen wird durch diesen mikrobiellen Pool vermehrt Pestizid als Wachstumssubstrat umgesetzt. ii) Analog dazu simuliert das Modell den beschleunigten co-metabolischen MCPA-Umsatz als Folge erhöhter Aktivität und Biomasse des pilzlichen Pools aufgrund von höherer C-Verfügbarkeit. Auf Basis der globalen Sensitivitätsanalyse des Modells wurden 41% ($n = 33$) aller berücksichtigten Parameter bzw. Eingangsgrößen als „sehr wichtig“ und „wichtig“ klassifiziert. Dazu zählten vor al-

lem biokinetische Parameter und Anfangswerte. Die Pareto-Analyse ergab, dass die Modellstruktur geeignet war und sinnvolle Parameterwerte identifiziert werden konnten, um die gemessene Dynamik von C und MCPA abzubilden. Das Modell konnte die gemessenen Abundanz der 16S rRNA und *tfda* Gene zufriedenstellend wiedergeben. Es unterschätzte allerdings den extrem starken Anstieg der pilzlichen ITS-Fragmente, höchstwahrscheinlich weil dieser Gen-Marker nur unzureichend als Maß für die gesamte pilzliche Biomasse geeignet ist. Die Modellsimulationen zeigten, dass Bodenpilze vor allem von C niedriger Qualität profitierten, während bakterielle MCPA-Abbauer bevorzugt C hoher Qualität nutzten. In den Simulationen wurde MCPA überwiegend durch pilzlichen Co-Metabolismus zu C von hoher Qualität umgesetzt. Dieser C wurde anschließend primär von spezifischen bakteriellen MCPA-Abbauern assimiliert. Der größte Umsatz von eingetragenem Streu-C erfolgte durch Substrataufnahme für mikrobielles Wachstum. Eintrag und mikrobieller Umsatz von Streu-C förderte den Abbau von MCPA vor allem in einer Bodenschicht in 0-3 mm Abstand zur Streu. Infolgedessen bildete sich ein Gradient der MCPA-Konzentration aus, der den diffusiven MCPA Transport aus tieferen Bodenschichten in die Detritusphäre antrieb.

Die Ergebnisse der Studien zeigen: i) Die Detritusphäre ist ein biogeochemischer hot spot, in dem Stoffumsätze durch die mikrobielle Dynamik kontrolliert werden. ii) Die integrierte Anwendung von Experimenten und mathematischer Modellierung erlaubt einen erweiterten Einblick in die Dynamik von Stoffen und Mikroorganismen im Boden. iii) Mikrobielle Gemeinschaften müssen explizit berücksichtigt werden, um die Regulation von Bodenfunktionen zu verstehen.

3 General Introduction

3.1 Biogeochemical interfaces in soil

“Soil is the most complex biomaterial on the planet” (Young and Crawford 2004). It “is an extraordinarily complex medium, made up of a heterogeneous mixture of solid, liquid and gaseous material, as well as a diverse community of living organisms.” (Jury and Horton 2004; p. 1, first sentence). Consequently, a dynamic system of biogeochemical interfaces is formed at the points of contact between diverse inorganic, organic and living soil components (Totsche et al. 2010). Rennert et al. (2012) define a biogeochemical interface as a “3D domain with a thickness ranging from nanometers to micrometers” that “gradually or abruptly separate[s] bulk immobile phases from mobile liquid or gaseous phases”.

However, biogeochemical interfaces are not restricted to the nano- and microscale, and they can be viewed as being hierarchically organized across a much wider range of spatial scales (Vogel and Roth 2003; Totsche et al. 2010; Lin 2012). Thus, the spatially heterogeneous distribution of interfaces between solid, liquid and gas in combination with the spatially and temporally heterogeneous input of carbon, nutrients and other chemicals promotes the formation of microbially diverse niches in soil (Or et al. 2007; Totsche et al. 2010). Such microhabitats are biogeochemical interfaces themselves as they separate soil compartments with different biological and physicochemical properties. Ultimately at the highest hierarchical level, soil microhabitats are in turn integral parts of the pedosphere as the global interfacial domain between hydrosphere, atmosphere, biosphere and lithosphere (Blume et al. 2010).

Properties of interfaces between liquid, gas and solid (including microorganisms) fundamentally control biogeochemical processes occurring at a scale below micrometers (Chorover et al. 2007; Totsche et al. 2010). Such processes include the alteration of water-film thickness by capillary forces at the pore surface, sorption/ desorption of various solutes (e.g. cations, anions, natural organic carbon or pollutants), weathering of primary mineral surfaces and formation of secondary minerals as well as microbial uptake of diverse compounds from the solid, liquid and gaseous phases and their microbial transformation (Or et al. 2007). These nanoscale biogeochemical processes determine major soil functions, such as water storage, nutrient cycling or degradation of organic chemicals at the scale of microhabitats and in the pedosphere as a whole (Young and Crawford 2004; Chorover et al. 2007; Totsche et al. 2010).

How biogeochemical processes occurring at the nanoscale manifest at the higher hierarchical level of microhabitats and how they determine the functioning of microhabitats as biogeochemical interfaces is, however, regulated by microhabitat-specific characteristics, such as the availability of water and nutrients (Paul 2007, Chapter 11). Considering the pedosphere as the

biogeochemical interface at the highest hierarchical level, e.g., climatic conditions can regulate biogeochemical cycling at spatial scales of about 100 - 1000 km (Or et al. 2007).

Biogeochemical interfaces are often biogeochemical hot spots, because the continuous supply and junction of different, complementary reactants at such locations facilitates maintaining high rates of specific biogeochemical reactions (McClain et al. 2003; Hagedorn and Bellamy 2011). McClain et al. (2003) further state that hot spots of biogeochemical processing “may be defined at any spatial scale”. This is in perfect agreement with the hierarchical scale concept of biogeochemical interfaces stated above.

3.2 Biogeochemical hot spots and matter cycling in soil

“Microbial activity is vital to a wide range of soil functions. They [the microbes] play critical roles in most biogeochemical cycles on Earth, including those of carbon, nitrogen, phosphorus and sulphur.” (Or et al. 2007). Indeed, soil organic matter dynamics as well as cycling of inorganic nutrients and metals in soils are strongly driven by microbial action (Paul 2007 Ch. 12, 13,15; Gleixner 2013). Therefore, the understanding of biologically controlled soil processes is crucial to understand the response of the soil system to environmental impacts, such as those arising due to climate change or application of agrochemicals (e.g. fertilizers, pesticides) or contamination with pollutants (e.g. organic chemicals, heavy metals).

Despite its important role, microbial biomass represents only 2 - 5% of total terrestrial soil C (Paul 2007, p.286) and it accounts only for 1 - 6% of total organic matter in most soils (Blume et al. 2010, p.95). Only a small fraction of the potentially habitable space in soils is colonized by microorganisms. Based on microscopic investigations of a sand dune soil, Hissett and Gray (1976) estimated that 0.2% of the organic surfaces and 0.02% of the sand grain surfaces were occupied by bacteria. Young and Crawford (2004) estimated 10^{-6} % areal coverage of solid surfaces in soil by microorganisms and stated: “The important point here is not the absolute coverage, which can vary with clay content, moisture, and substrate availability, but the fact that it is considerably less than 1%, even with the most optimistic balance of inputs.”

The majority of soil bacteria resides in pores $> 0.8 \mu\text{m}$. They are most frequently found in pores with a maximum pore diameter ranging from 2.5 to 9 μm , where they are most protected against predators. In contrast, fungi, protozoa and algae mainly colonize pores larger than 5 μm (Paul 2007, p.297). Postma and van Veen (1990) found that microbial colonization in soil is not limited by the availability of protective and habitable pore space. In their study, less than 0.5% of this pore space were occupied by bacteria.

Instead of the available habitat space, the availability of resources largely determines how dense available solid surfaces in soil are populated. This view was nicely illustrated by microscopic images from thin sections by Nunan et al. (2003). The images show that soil surfaces were more densely colonized by bacteria, when glucose was added as additional carbon

source. The same authors suggested that bacteria are present at preferentially colonized patches. They accounted the observed heterogeneous bacterial distribution to an uneven distribution of soil organic matter at the micro-scale. Recent studies confirmed that bacterial cells aggregate at a scale of a few micrometers as a result of soil architecture and resource availability at the micro-scale (Raynaud and Nunan 2014). In general, “the structural organization of soil creates a mosaic of microenvironments” (Ranjard and Richaume 2001) with locally specific physicochemical characteristics (e.g., pH, redox potential, water availability, concentrations of nutrients, electron acceptors and signaling compounds), which determine diversity and abundance of microbial communities at the micro-scale (Foster 1988; Ranjard et al. 2000; Ettema and Wardle 2002; Grundmann 2004; Paul 2007, Chapter 11; Franklin and Mills 2009; Ruamps et al. 2011; Crawford et al. 2012; Prosser 2012; Vos et al. 2013).

Micro-environmental characteristics also regulate the physiological state of microorganisms. In their recent review, Blagodatskaya and Kuzyakov (2013) define four physiological states of microorganisms: i) *active*, ii) *potentially active*, iii) *dormant* and iv) *dead*. They stated that the portion of *active* microorganisms actually contributing to ongoing biogeochemical processes is as low as 0.1 – 2% and does not exceed 5% of the total microbial biomass in soil. The authors further speculate that this low *active* portion of the total microbial community in soil might reflect heterogeneously distributed “hot spots” of high substrate availability at the micro-scale, “where an important part of potentially active and partly dormant microorganisms switched to the active state.”

The activity state of microorganisms is directly linked to the production of extracellular enzymes (Kandeler et al. 1999a; Poll et al. 2006; Spohn and Kuzyakov 2013). However, the actual activity of extracellular enzymes in soil is, at least to some extent, decoupled from their active microbial producers (Nannipieri et al. 2002). For that, Burns et al. (2013) gave three reasons: First, “most extracellular enzymes diffuse away from their parent cell.” Second, “many extracellular enzymes become stabilized through association with clay minerals, humic acids and particulate organic matter and retain significant levels of activity for prolonged periods of time.” And third, extracellular enzyme activity may also originate from enzymes attached to or released from dead microorganisms.

As a result of soil’s heterogeneous nature, the biological functioning of soils is governed by high reaction rates occurring at distinct hot spots and hot moments (see McClain et al. 2003 for a definition), where life conditions of microbial communities and physicochemical constraints of extracellular enzymes are optimally met (Parkin 1993; Nannipieri et al. 2003; Nunan et al. 2003; Girish Shukla and A. Varma 2011, Chapter 12; Vos et al. 2013). Kandeler et al. (2001) stated: “... hot spots of activity may be <10% of the total soil volume, but may represent >90% of the total biological activity in most soils worldwide.” Consequently, we must study matter cycling in biochemical hot spots to improve our understanding of the dynamics of the

whole soil system (Kuzyakov et al. 2009). On the other hand, microbially-driven processes in “non hot spot” regions should not be neglected. In agreement with the “hot spot” point of view taken here, Young and Ritz (2005) draw the well-fitting picture of soils as “oases surrounded by deserts” and claim “that the desert regions have just as much to do with the functionality of the soil system as do the oases [the biochemical hot spots]”.

Biogeochemical hot spots in soils are found in numerous highly diverse soil microhabitats (Foster 1988; Beare et al. 1995). Physical fractionation of soil according to size and density of particles as well as aggregates was widely applied to study the association of microorganisms and microbially-driven soil processes (in particular SOM turnover) with defined micro-niches (Nishiyama et al. 1992; Kandeler et al. 1999b; Kandeler et al. 2000; Christensen 2001; Sessitsch et al. 2001; Poll et al. 2003; Marx et al. 2005; Dorodnikov et al. 2009; Lagomarsino et al. 2012; Bailey et al. 2013; Zhang et al. 2013; Rabbi et al. 2014). Small-size fractions (i.e. clay and silt) have been identified as microhabitats with high abundance and diversity of bacteria, whereas large-size fractions (aggregates > 2 mm) have been found to be fungal hot spots (Ranjard and Richaume 2001; Kögel-Knabner et al. 2008). Enzyme measurements further revealed that soil particles of clay- to silt-size and free particulate organic matter are biogeochemical hot spots of C, nitrogen, sulphur and phosphorus cycling (Kandeler et al. 1999b; Allison and Jastrow 2006; Lagomarsino et al. 2012).

On the basis of the conceptual soil aggregate hierarchy model by Tisdall and Oades (1982) and its later enhancements (Six et al. 2004), there is evidence that SOM is predominantly stabilized in micro-aggregates rather than in macro-aggregates (Jastrow et al. 2007). Accordingly, Dorodnikov et al. (2009) found that measured activities of enzymes involved in C, nitrogen, sulfur, phosphorus cycling and enzyme activity in bulk soil could be primarily attributed to macro-aggregates and that micro-aggregates (<250 μm) contributed only to a very minor part. Thus, macro-aggregates were identified as important micro-environments (i.e. hot spots) of matter cycling by these authors. Other studies focused on soil processes in the interior vs. the exterior of soil aggregates. For instance, Sexstone (1985) nicely demonstrated the importance of anaerobic zones within aggregates as hot spots of denitrification, whereas higher potential nitrification was found in aggregate exteriors (Hoffmann et al. 2007).

Biological studies employing physical particle size and aggregate fractionation greatly helped to improve the understanding how micro-environmental conditions regulate biological functioning. However, results from such studies should be interpreted with caution. Particle size fractionation destroys the natural micro-environment of particles and soil microorganisms (Kandeler and Dick 2007) and studies employing aggregate fractionation have been found to be strongly dependent on the used isolation procedure and prone to artefacts caused by sample preparation (Ashman et al. 2003; Bach and Hofmockel 2014). Consequently, the use of physically extracted particle size and aggregate fractions to understand functional consequences

of the intact soil structure *in situ* is somewhat limited (Young and Ritz 2005; von Lützow et al. 2007; Hallett et al. 2013).

Six and Paustian (2014) stated that by relying on isolation of aggregate structure to understand SOM dynamics, "...in some sense, we are looking at the walls of a house to understand what is happening in the living-room." Indeed, microbial activity immediately takes place in the pores ("the living-room") rather than within the solid matrix of soil ("the walls of a house"). The characteristics of the continuous soil pore network (e.g. connectivity and pore shape) determine microbial functioning and soil processes (Strong et al. 2004; Young and Ritz 2005; Or et al. 2007; Chenu and Cosentino 2011; Ananyeva et al. 2013). In particular, the pore network geometry regulates water distribution and resource availability at the micro-scale, which then determines at which location in the pore network microorganisms are most active (Or et al. 2007; Bouckaert et al. 2013; Ruamps et al. 2013). This relationship is nicely illustrated in several studies that identified preferential flow paths and macropores as hot spots of increased C and N turnover as well as accelerated degradation of pesticides (Pivetz and Steenhuis 1995; Vinther et al. 1999; Bundt et al. 2001a; Bundt et al. 2001b; Gaston and Locke 2002; Jarvis 2007; Badawi et al. 2013). The hot spots identified in these studies are characterized by better nutrient availability (as a result of root-, earthworm- and litter-derived biopore linings with SOM) and oxygen supply compared to the surrounding soil matrix.

The input of organic C and nutrients from external sources (e.g., litter, roots) generally triggers the formation of microbial hot spots as localized zones of increased matter cycling in soil. The rhizo-, drilo- and detritosphere are major biogeochemical interfaces (soil-roots, soil-earthworms, soil-litter) where C and nutrients enter soil (Beare et al. 1995). Several studies have shown that in these microhabitats C turnover can be accelerated and "priming effects", i.e. "...strong short-term changes in the turnover of soil organic matter caused by comparatively moderate treatments of the soil" (Kuzyakov et al. 2000), are typically occurring (Helal and Sauerbeck 1984; Bottner et al. 1999; Kandeler et al. 1999a; Don et al. 2008; Poll et al. 2008; Cheng 2009; Kuzyakov 2010; Bird et al. 2011; Schenck zu Schweinsberg-Mickan et al. 2012). Enhanced C turnover in the rhizo-, drilo- and detritosphere is often coupled to increased rates of other soil processes, such as the degradation of organic chemicals (Haby and Crowley 1996; Shaw and Burns 2003; Gerhardt et al. 2009; Liu et al. 2011; Chen and Yuan 2012; Blouin et al. 2013). However, the regulation mechanisms that are responsible for such priming phenomena (i.e., accelerated degradation of SOM and pesticides in response to supply with fresh C or nutrients) are not yet fully understood (Blagodatskaya and Kuzyakov 2008; Neill and Guenet 2010; Fontaine et al. 2011).

3.3 Modeling microbial regulation of matter cycling in soil

“Models provide a means of deconstructing the complexity of environmental systems...” (Wainwright and Mulligan 2013; chapter 2.1.4, p. 11). They serve as tools to test theory and can improve our understanding of observations in natural systems (Wainwright and Mulligan 2013, chapter 2.1.3).

The most widely applied simplification of decay processes in biochemical models employs first order kinetics assuming that degradation can be described as a strictly substrate-limited process. This formulation is used in most mathematical models in combination with equations describing transport and sorption of solutes to simulate the fate of C, N and pesticide pools in soils at different spatial and temporal scales (Köhne et al. 2009; Manzoni and Porporato 2009). It has been recognized that global scale models should explicitly account for the impact of microbial dynamics on degradation processes in order to realistically represent C dynamics in soil and to improve model predictions of the soil organic matter response to global change (Schmidt et al. 2011; Todd-Brown et al. 2012). Similarly, models must consider microbial dynamics to reproduce priming phenomena (Parnas 1976; Wutzler and Reichstein 2008).

Various mathematical models explicitly consider microbial regulation mechanisms of biochemical processes. They usually implement several functional groups of microorganisms and resource pools of differing quality (e.g.; Grant et al. 1993; Garnier et al. 2003; Kravchenko et al. 2004; Moorhead and Sinsabaugh 2006; Ingwersen et al. 2008; Gras et al. 2011; Aslam et al. 2014). In such models, dynamics of resources and microorganisms are typically coupled using Monod kinetics. Several models explicitly account for microbial traits, enzyme production and microbial physiology (Blagodatsky and Richter 1998; Schimel and Weintraub 2003; Allison 2012; Moorhead et al. 2012; Moore et al. 2014; Sistla et al. 2014; Wang et al. 2014; Wieder et al. 2014). Recently, the spatial heterogeneity of the pore space and the distribution of microorganisms in soil has been directly implemented (Masse et al. 2007; Gharasoo et al. 2012; Resat et al. 2012; Cazelles et al. 2013; Monga et al. 2014). Such models are complex, but they are powerful tools to enhance the mechanistic understanding of microbial dynamics and biogeochemical interactions involved in carbon and nutrient cycling as well as in the degradation of organic compounds in soil (Blagodatsky et al. 2010; Allison 2012; Möller and Hansen 2012; Banitz et al. 2013; Chalhoub et al. 2013; Perveen et al. 2014; Rosenbom et al. 2014).

3.4 The model pesticide 4-chloro-2-methylphenoxyacetic acid (MCPA)

MCPA is a systemic herbicide acting like naturally occurring phytohormones (auxins) causing abnormal growth responses and finally the death of target plants (Caux et al. 1995; British Crop Protection Council 2009). It is formulated into esters, salts and amine derivatives and often used in combination with other herbicides, such as Dicamba and Mecoprop-P (British Crop Protection Council 2009). The typical application rate is 0.2–2.3 kg of MCPA per hectare

(Caux et al. 1995; British Crop Protection Council 2009). The half-life of MCPA in soils is fairly short (7 – 41 days; European Commission 2005) and it is not strongly sorbed in soils ($k_{oc} = 10\text{-}157 \text{ L kg}^{-1}$; Jensen et al. 2004; European Commission 2005). Chlorophenoxy pesticides, such as MCPA, are widely applied as broad-spectrum, post-emergence herbicides against broad-leaved weeds in agricultural cultivation (cereals, vegetables) and grassland (British Crop Protection Council 2009). In Germany, phenoxy phytohormones represent about 6% of all sold herbicides (Status in 2013; BVL 2014).

Among the chlorophenoxy pesticides, mainly 2,4-dichlorophenoxyacetic acid and MCPA have been frequently used as model compounds to study the degradation of organic contaminants in soil (Torstensson et al. 1975; Loos et al. 1979; Soulas 1993; Crespin et al. 2001; Cederlund et al. 2007; Boivin et al. 2005). In soil, MCPA is predominantly degraded by microorganisms; exclusively under aerobic conditions (European Commission 2005). Bacterial pathways of MCPA degradation and enzymes as well as functional genes involved have been intensively studied (Helling et al. 1968; Don and Pemberton 1981; Pieper et al. 1988; Fukumori and Hausinger 1993; Smejkal et al. 2001; Laemmli et al. 2004; Ledger et al. 2006; Liu et al. 2013). The major bacterial pathway of biodegradation of MCPA and other chlorophenoxy herbicides is initiated by the cleavage of the ether-bonded acetate side chain, which is catalyzed by different oxygenases (Itoh et al. 2004; Müller et al. 2006; Baelum et al. 2010; Zaprasis et al. 2010; Nielsen et al. 2013; Liu et al. 2013). Fungal degradation pathways of chlorophenoxy herbicides and the fungal enzymes involved are less well understood. Evidence is growing, however, that many soil fungi are able to degrade chlorophenoxy herbicides (Torstensson et al. 1975; Vroumsia et al. 2005; Itoh et al. 2013).

3.5 Scope of the thesis – Why study the detritusphere?

“Plant litter materials provide the primary resources for organic matter formation in soil.” (Kögel-Knabner et al. 2008). Accordingly, the detritusphere is a highly relevant microhabitat in soils because it is the biogeochemical interface where soil gets into contact with fresh plant litter. It is a very important biochemical hot spot of microbial activity and matter cycling in soil (Beare et al. 1995; Kandeler et al. 1999a; Gaillard et al. 2003; Poll et al. 2008; Kuzyakov 2010). Consequently, the detritusphere is a well-suited to elucidate the regulation of crucial soil functions.

My thesis aims to clarify the biogeochemical interactions involved in MCPA degradation coupled to C turnover in the detritusphere. The herbicide MCPA serves as a model compound to elucidate how microbial dynamics in biogeochemical hot spots control the fate of organic chemicals, in particular pesticides.

The work is organized in three parts:

In the first study, the effect of litter addition on MCPA degradation as well as on the microbial community in soil was investigated in a laboratory experiment using a microcosm incubation system. Possible regulation mechanisms of accelerated MCPA degradation were identified.

Secondly, based on a detritusphere C turnover model (Ingwersen et al. 2008), a complex mathematical model was developed. It simulates coupled C turnover and pesticide degradation in the detritusphere by considering physicochemical processes (i.e. convective/ diffusive transport, sorption) as well as microbial dynamics. The model particularly includes two microbial regulation mechanisms of accelerated MCPA degradation in the detritusphere identified in the first study: i) stimulation of the activity of specific bacterial MCPA degraders, and ii) increased fungal production of unspecific enzymes that transform MCPA.

In the third study, a second microcosm experiment was performed. The experimental data were then utilized to parameterize the new model. In a novel approach, measured dynamics of microbial marker genes (*tfdA*, 16S rRNA, fungal ITS fragments) and carbon isotopes (^{13}C and ^{14}C) were used to calibrate simulated dynamics of microbial pools as well as of litter- and pesticide-derived organic carbon in soil. The parameterized model was then applied as an analytical tool to gain further insight into the microbial regulation of accelerated MCPA degradation in the detritusphere.

4 Regulation of bacterial and fungal MCPA degradation at the soil-litter interface

Soil Biology & Biochemistry 42 (2010), 1879 – 1887

DOI: 10.1016/j.soilbio.2010.07.013

Christian Poll^a, Holger Pagel^b, Marion Devers-Lamrani^c, Fabrice Martin-Laurent^c, Joachim Ingwersen^b, Thilo Streck^b, Ellen Kandeler^a

^a Institute of Soil Science and Land Evaluation, Soil Biology, University of Hohenheim, D-70593 Stuttgart, Germany

^b Institute of Soil Science and Land Evaluation, Biogeophysics, University of Hohenheim, D-70593 Stuttgart, Germany

^c Laboratory of Soil and Environmental Microbiology, INRA-University of Burgundy, F-21065 Dijon Cedex , France

© 2015, Elsevier B.V. This manuscript version is made available under the CC-BY-NC-ND 4.0 license <http://creativecommons.org/licenses/by-nc-nd/4.0/>

4.1 Abstract

Much is known about mechanisms and regulation of phenoxy acid herbicide degradation at the organism level, whereas the effects of environmental factors on the performance of the phenoxy acid degrading communities in soils are much less clear. In a microcosm experiment we investigated the small-scale effect of litter addition on the functioning of the MCPA degrading communities. ^{14}C labelled MCPA was applied and the functional genes *tfdA* and *tfdA α* were quantified to characterise bacterial MCPA degradation. We identify the transport of litter compounds as an important process that probably regulates the activity of the MCPA degrading community at the soil-litter interface. Two possible mechanisms can explain the increased *tfdA* abundance and MCPA degradation below the litter layer: 1) transport of α -ketoglutarate or its metabolic precursors reduces the costs for regenerating this co-substrate and thereby improves growth conditions for the MCPA degrading community; 2) external supply of energy and nutrients changes the internal resource allocation towards enzyme production and/or improves the activity of bacterial consortia involved in MCPA degradation. In addition, the presence of litter compounds might have induced fungal production of litter-decaying enzymes that are able to degrade MCPA as well.

4.2 Introduction

Soil microbial communities play a key role in degrading xenobiotic compounds. This function is part of the filter capabilities of soils and belongs to the ecosystem services listed by the Millennium Ecosystem Assessment (2005). MCPA (4-chloro-2-methylphenoxyacetic acid) and 2,4-D (2,4-dichlorophenoxyacetic acid) have been two of the most heavily used phenoxy acid herbicides against dicotyledonous plants for around 50 years. They were often studied as model compounds for the environmental fate of xenobiotics. Several environmental factors govern phenoxy acid degradation in soils. One such key factor is the soil organic matter content, which influences the ratio between sorbed and dissolved 2,4-D and thereby the degradation rate (Greer and Shelton, 1992). Recently, Vieublé-Gonod et al. (2003) suggested that uneven distribution of 2,4-D degradation in an arable soil at the millimeter scale might be explained by a heterogeneous distribution of the degrader community and of carbonaceous substrates required for co-metabolic 2,4-D degradation. Another study suggested that MCPA degradation is independent of the background density of the degrader community and more connected to growth of the microbial degraders (Fredslund et al., 2008). Therefore, microbial growth conditions might play an important role in MCPA degradation. This is in accordance with Cederlund et al. (2007), who suggested that MCPA mineralisation in railway embankments was N limited, and to Duah-Yentumi and Kuwatsuka (1980), who showed that adding plant residues increased MCPA degradation. The activity of the soil microbiota is favoured in hot-spots where more nutrients are available than in other more oligotrophic habitats of soils. Previous studies have shown enhanced degradation of several xenobiotics in the rhizosphere (Piutti et al., 2002; Shaw and Burns, 2004). Similar to the rhizosphere, the detritosphere is characterized by high availability of soluble litter compounds, which stimulates microbial activity, growth and C turnover (Poll et al., 2008). However, the effect of litter addition on pesticide degradation as well as on the involved functional microbial communities at the small-scale has not yet been investigated.

Several bacteria have been identified as 2,4-D or MCPA degraders (e.g. Bell, 1960; Bollag et al., 1967; Chaudhry and Huang, 1988; Pieper et al., 1988) and much is known about the mechanisms and regulation of the degradation processes at the organism level. The most intensively studied is the *tfd* pathway. The *tfd* genes are often located on plasmids (Don and Pemberton, 1985) and are seldom chromosomal. Bacteria might be capable of the complete degradation pathway or only harbour genes encoding a truncated degradation pathway (Ka et al., 1994; Top et al., 1996). The initial step of this pathway encoded by the *tfdA* gene (Streber et al., 1987) is the cleavage of the acetate side chain by an α -ketoglutarate-dependent dioxygenase (Fukumori and Hausinger, 1993). Beside bacteria that harbour genes of the *tfd* pathway, several other phenoxy acid degraders have been identified. Among these are slow-growing oligo-

trophic bacteria of the α subdivision of the class *Proteobacteria*, which were isolated from pristine soils. They harbour the *tfdA α* gene that encodes another α -ketoglutarate-dependent dioxygenase (Itoh et al., 2002; Kamagata et al., 1997). The degradation of phenoxy acid herbicides, however, is not restricted to bacteria. Fungi have been reported to degrade these compounds as well (Castillo et al., 2001; Reddy et al., 1997). Vroumsia et al. (2005) screened ninety fungal strains and found up to 52% of added 2,4-D degraded by single fungal strains after an incubation of 5 days. In contrast to bacteria, no distinct pathway of fungal phenoxy acid degradation is known. Non-specific enzymes like lignin peroxidase or manganese peroxidase/laccase are suggested to be involved in the degradation process (Castillo et al., 2001).

The direct effects of environmental factors on the performance of the phenoxy acid degrading community in soils, however, are poorly known. Small-scale studies provide the unique opportunity to directly relate environmental factors (e.g. substrate availability or soil texture) to the functioning of the microbial degrader community. We studied the effect of litter addition on MCPA degradation as well as on the MCPA degrading community at the small-scale. We hypothesise that i) MCPA degradation is enhanced due to increased substrate availability within the detritosphere and that ii) this is accompanied by an increase in the genetic potential for MCPA degradation. Since bacteria and fungi show different substrate utilization strategies within the detritosphere (Poll et al., 2006), we further expected that iii) these two microbial groups differentially respond to the addition of MCPA and litter. For this purpose, we studied the degradation of ^{14}C labelled MCPA in the detritosphere in a microcosm experiment over 20 days. The abundance of 16S rDNA and 18S rDNA sequences was quantified to detect the response of the bacterial and fungal components of the soil microbiota to MCPA and litter addition. Finally, we quantified *tfdA* and *tfdA α* sequences as indicators for the abundance of bacterial MCPA degraders. Our results elucidate the regulation of microbial MCPA degradation by the properties of the soil habitat.

4.3 Material and methods

4.3.1 Soil and plant residues

Soil was sampled from an agricultural field located at an experimental farm in Scheyern, north of Munich (Germany, 48° 30' N, 11° 21' E) in July 2007. Samples were taken from the loamy topsoil of a Luvisol (World Reference Base for Soil Resources) [pH (CaCl₂) 5.3, total C content 13.6 g kg⁻¹, total N content 1.32 g kg⁻¹]. After sampling, the soil was sieved (< 2 mm) and stored at -20°C to minimise disturbance by soil faunal activity during the experiments. For the incubation, maize (C/N ratio 48) residues were chosen. Maize leaf litter and stems were shredded into pieces of 2-10 mm length and stored air-dried until the start of the experiment. The soil was pre-incubated for 6 weeks at 20°C with an MCPA addition of 20 mg kg⁻¹ to increase the

initial number of MCPA degrading microorganisms (Baelum et al., 2008). Pre-experiments indicated that, after 6 weeks, MCPA is totally dissipated in this soil.

4.3.2 Experimental design

The experiment consisted of the following four treatments: (i) no MCPA and no litter addition, (ii) addition of litter, (iii) addition of MCPA, and (iv) addition of litter and MCPA. After thawing, the soil was homogenised and half of the soil was spiked with ^{14}C ring labelled MCPA (radioactive purity 91%, specific activity $60 \text{ MBq mmole}^{-1}$) at a concentration of 50 mg kg^{-1} . Labelled MCPA was mixed and dissolved in water with unlabelled MCPA to give a final activity of $26.4 \text{ kBq microcosm}^{-1}$. Soil moisture was adjusted to a volumetric water content of 35.2%, corresponding to a matric potential of -63 hPa . Finally, soil equivalent to 90 g dry soil was filled into cylinders (diameter= 5.6 cm ,

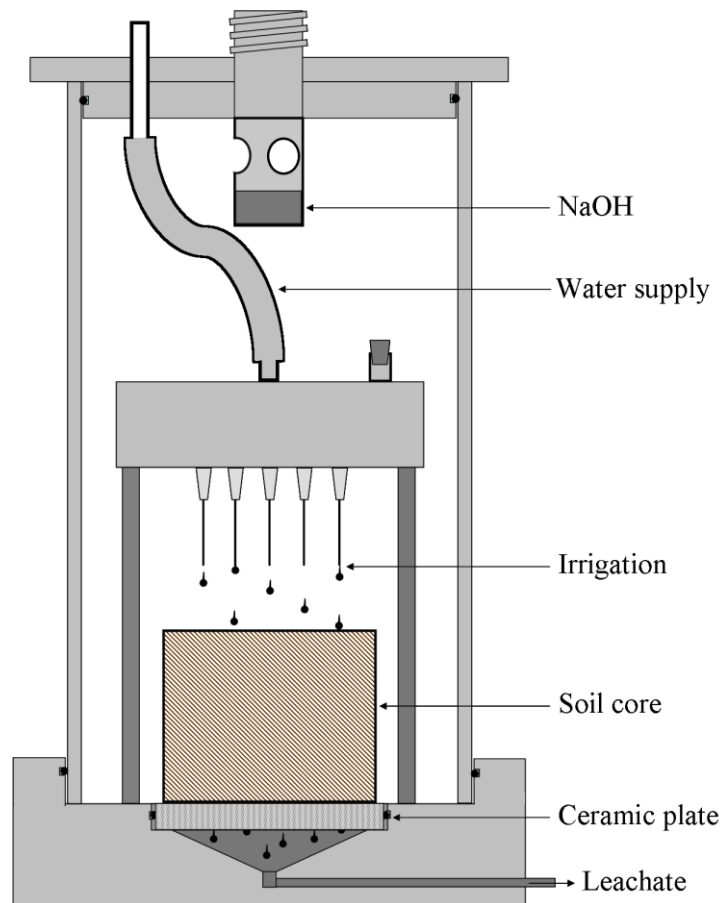


Fig. 1 Illustration of the microcosms used for the incubation experiment.

height= 4 cm) and covered with 0.5 g litter for the litter treatments. The litter was rewetted with 2 ml 0.01 M CaCl_2 before addition to the microcosms. The soil cores had a height of 3 cm and were compacted to a bulk density of 1.2 g cm^{-3} . For each treatment, 9 soil cores were prepared. Subsequently, each soil core was placed into an air-tight microcosm (Fig. 1) with a saturated ceramic plate beneath each cylinder. Ceramic plates were kept at a defined water suction of -63 hPa to maintain a defined lower boundary condition regarding water transport in the soil columns. The microcosms were incubated at $20 \text{ }^\circ\text{C}$. After 20 days, $^{14}\text{CO}_2$ production indicated a strong decrease in MCPA degradation activity and the experiment was ended. During the incubation, we irrigated the microcosms one time with 4 ml and four times with 3 ml 0.01 M CaCl_2 solution. We used CaCl_2 to avoid dispersion of clay. At the first irrigation event, we applied 4 ml CaCl_2 to account for differences in soil moisture originating from the preparation of soil cores. Leachates were sampled one day after each irrigation event.

4.3.3 Sample preparation

The litter was removed after the incubation and the soil cores were frozen and subsequently cut into thin slices using a cryostat microtome (HM 500 M, MICROM International GmbH). The respective slices of three soil cores were pooled together to obtain a sufficient amount of soil for analysis. This yielded three replicates of each treatment. The slices were taken from the following distances to the soil-litter interface: 0–1, 1–2, 2–3, 3–4, 4–5, 5–7 and 7–10 mm.

4.3.4 MCPA analysis of soil and leachates

We extracted 1.5 g fresh soil with 7.5 ml of methanol/water (1:1) for 1 h in a water bath (50°C) using 50 ml glass centrifuge tubes with Teflon-lined screw caps. After centrifugation, 2 ml of the supernatant were removed for analysis. Soil extracts and leachates were filtered (0.45 µm pore size) and the MCPA concentration was determined by HPLC (System Gold, Beckman Instruments) using a UV detector according to the method of Moret et al. (2006). The separation was carried out on a 200 mm×4.6 mm column packed with 5µm Kromasil 100 C18 material (MZ-Analysentechnik GmbH) at 20°C and a flow of 1 ml min⁻¹. MCPA was detected at a wavelength of 228 nm.

4.3.5 Respiration and ¹⁴C content of CO₂ and leachate

CO₂-C production was measured at regular intervals during the incubation. Evolved CO₂ was trapped in 2.5 ml of 1 M NaOH solution, which were added to small vessels fixed to the lids of the microcosms. An aliquot of 0.5 ml was taken, and trapped CO₂ was measured titrimetrically after precipitation of carbonate with 0.5 ml 1 M BaCl₂ solution using 0.1 M HCl.

For determining the ¹⁴C content of the CO₂-C, 1 ml NaOH was transferred into 5 mL scintillation vials (LDPE) and mixed with 4 ml scintillation fluid (Rotiszint eco-plus, Carl Roth GmbH+Co. KG). Similarly, 0.5 ml of each collected leachate were mixed with 4 ml scintillation fluid. The vials were shaken and then analysed for 10-20 min using a Wallac 1411 Liquid Scintillation System (Perkin Elmer Life Sciences). ¹⁴C activity was calculated and corrected for quenching using standard calibration.

We used the logistic model of Simkins and Alexander (1984) to estimate kinetic parameters of MCPA mineralisation:

$$-\frac{dC}{dt} = kC(X_0 + C_0 - C) \quad \text{Initial condition: } C(t = 0) = C_0$$

According to Fomsgaard (1997), the following analytical solution of the differential equation was obtained and fitted to ¹⁴C mineralisation data:

$$P = C_0 - C = C_0 - \frac{C_0 + X_0}{1 + \frac{X_0}{C_0} e^{k(C_0 + X_0)t}}$$

where C stands for the amount of MCPA in soil, k for the mineralisation rate constant, X_0 for the amount of MCPA required to produce the initial population density, C_0 for the total amount of MCPA converted to $^{14}\text{CO}_2$ by first order metabolism, P for the amount of MCPA mineralised at time t (% of initial ^{14}C), and t for the time in days.

4.3.6 ^{14}C content of soil organic matter

The ^{14}C activity in soil was determined by sample oxidation. Soil samples (0.13-0.35 g) were weighed into cellulose paper and combusted for 4 min (Biological Oxidizer OX 500 R.J. Harvey Instrument Corporation). Subsequently, $^{14}\text{CO}_2$ was trapped in Oxysolve C-400 (Zinsser Analytic GmbH) and quantified by liquid scintillation counting (Beckman Coulter LS6500 Multi-Purpose Scintillation Counter, Beckman Coulter Inc.). The trapping efficiency was >94%.

4.3.7 Microbial biomass and dissolved organic carbon (DOC)

Microbial biomass was determined using the chloroform-fumigation-extraction (CFE) method (Vance et al., 1987). One gram of soil was fumigated with ethanol-free chloroform for 24 h at room temperature in a desiccator. After the incubation, chloroform was removed. Fumigated and non-fumigated samples were dispersed in 10 ml 0.5 M K_2SO_4 and extracted on a horizontal shaker at 250 rev min^{-1} for 30 min. Then, samples were centrifuged at 4560 rev min^{-1} for 30 min. Two millimeters of the supernatant were diluted four times to avoid a high salt concentration for the subsequent analysis. Diluted extracts were analysed for DOC with a DIMATOC 100 (Dimatec GmbH). However, the microbial biomass was not detectable due to low contents and the high extraction ratio of 1:10, which was necessary because only small sample amounts were available and a minimum extraction volume for the subsequent analyses was needed. The ^{14}C activity of the microbial biomass was analysed as described above by mixing 15 ml scintillation fluid with 6 ml of the soil extracts. The ^{14}C activity of the non-fumigated samples were used as estimates for the ^{14}C DOC of the soils; the ^{14}C activity of the microbial biomass was calculated from the difference in the ^{14}C activity of the fumigated and non-fumigated samples using a k_{EC} factor of 0.45 (Joergensen, 1996).

4.3.8 DNA extraction

Total community DNA was extracted from 0.3 g soil using the FastDNA Spin Kit for soil (BIO101, MP Biomedicals) according to the manufacturer's instructions. The extracted DNA was quantified with a Nanodrop ND1000 Spectrophotometer (NanoDrop Technologies Inc.).

4.3.9 Quantitative PCR assay

We quantified copy numbers of *tfmA*, *tfmA α* , 16S rDNA and 18S rDNA with an ABI Prism 7900 (Applied Biosystems) using a SYBR green PCR master mix (QuantiTect SYBR green PCR Kit, QIAGEN). The primer sets and temperature programmes for quantifying *tfmA* and *tfmA α* genes were taken from Baelum et al. (2006) and Itoh et al. (2002), respectively (Table 1); 18S rDNA and 16S rDNA were analysed according to Manerkar et al. (2008) and López-Gutiérrez et al.

(2004), respectively. Each PCR contained 2 μ l of each primer (10 μ M), 10 μ l of SYBR green PCR master mix, 0.5 μ l of T4gp32 (Q-BIOgene), 3.5 μ l water and 2 μ l of diluted soil DNA corresponding to 20 ng of soil DNA. Selected *tfdA* and *tfdA α* PCR products were sequenced to confirm their specificity. 16S rDNA standard curves were obtained using 10-fold serial dilutions of a linearised plasmid containing cloned 16S rRNA genes from *Pseudomonas aeruginosa* PAO1 (Bru et al., 2008). 18S rDNA, *tfdA* and *tfdA α* standard curves were prepared by serial dilution of pGem-T clones of respective PCR products resulting from soil DNA amplification. Efficiencies of the qPCR reaction were 109%, 93%, 91% and 83% for 16S rDNA, 18S rDNA, *tfdA* and *tfdA α* , respectively. Inhibitory effects of co-extracted humic substances were tested by comparison of standard plasmid DNA quantification in the presence or absence of soil DNA (Philippot et al., 2009).

Table 1 Primers and conditions for quantitative PCR

Target sequence	Primer	qPCR conditions	Reference
16S rDNA	341F: CCT ACG GGA GGC AGC AG 515R: ATT CCG CGG CTG GCA	900s at 95°C, Cycle (35): 15s at 95°C, 30s at 60°C, 30s at 72°C, 30s at 80°C (detection)	Manerkar et al., 2008
18S rDNA	IST 3F: GCA TCG ATG AAG AAC GCA GC IST 4R: TCC TCC GCT TAT TGA TAT GC	900s at 95°C, Cycle (35): 15s at 95°C, 30s at 55°C, 30s at 72°C, 30s at 80°C (detection)	López-Gutiérrez et al., 2004
<i>tfdA</i>	F: GAG CAC TAC GCR CTG AAY TCC CG R: GTC GCG TGC TCG AGA AG	900s at 95°C, Cycle (40): 15s at 95°C, 30s at 64°C, 30s at 72°C (detection)	Baelum et al., 2006
<i>tfdAα</i>	F: ACS GAG TTC KSC GAC ATG CG R: GCG GTT GTC CCA CAT CAC	900s at 95°C, Cycle (40): 15s at 95°C, 30s at 64°C, 30s at 72°C (detection)	Itoh et al., 2002

R, G/A; Y, T/C; S, G/C; K, G/T;

4.3.10 Statistics

The results were calculated based on oven-dried soil. Soil water content was determined by weighing 0.3 g of fresh soil into vessels and drying at 60°C for 72 h.

Cumulative CO₂ production and the abundance of 16S rDNA, 18S rDNA, *tfdA* and *tfdA α* sequences were tested for significant differences by two-way ANOVA with the fixed factors litter and MCPA. The data for the abundance of 18S rDNA were log-transformed before analysis because of heterogeneity of variances. For the comparison of the gene copy numbers, only the first layer (0-1 mm from the litter) was chosen because we expected the effects to be greatest within this layer. The results of the ¹⁴CO₂ production rate were compared by one-way ANOVA with repeated measure. We used student's t-test to compare the parameters derived

from the modified Gompertz model and the ^{14}C content of the microbial biomass within the first layer. The ^{14}C content of the soil organic matter showed heterogeneous variances even after transformation and, additionally, some missing values. We therefore performed no statistical test for these data.

4.4 Results

4.4.1 Soil respiration and MCPA degradation

Litter addition significantly increased the cumulative $\text{CO}_2\text{-C}$ production ($F_{1,32} = 2548$, $P < 0.001$) by about 42 mg per microcosm (Fig. 2A). MCPA significantly increased this production ($F_{1,32} = 79.4$, $P < 0.001$) by 7.4 mg per microcosm. The differences in the cumulative $\text{CO}_2\text{-C}$ production due to MCPA addition mainly reflected increased respiration rates during the first five days (Fig. 2A), whereas after this initial phase nearly no differences in response to MCPA addition occurred.

Mineralisation of ^{14}C labelled MCPA showed a lag phase of about seven days (Fig. 2B). Thereafter, the presence of litter significantly increased the $^{14}\text{CO}_2$ production ($F_{1,16} = 27.2$, $P < 0.001$). Sixteen days after MCPA addition, the $^{14}\text{CO}_2$ production strongly decreased in soil cores covered with maize litter, whereas this decrease was delayed by about two days in microcosms without litter (data not shown). At the end of the incubation, about 38% and 46% of the initially added ^{14}C

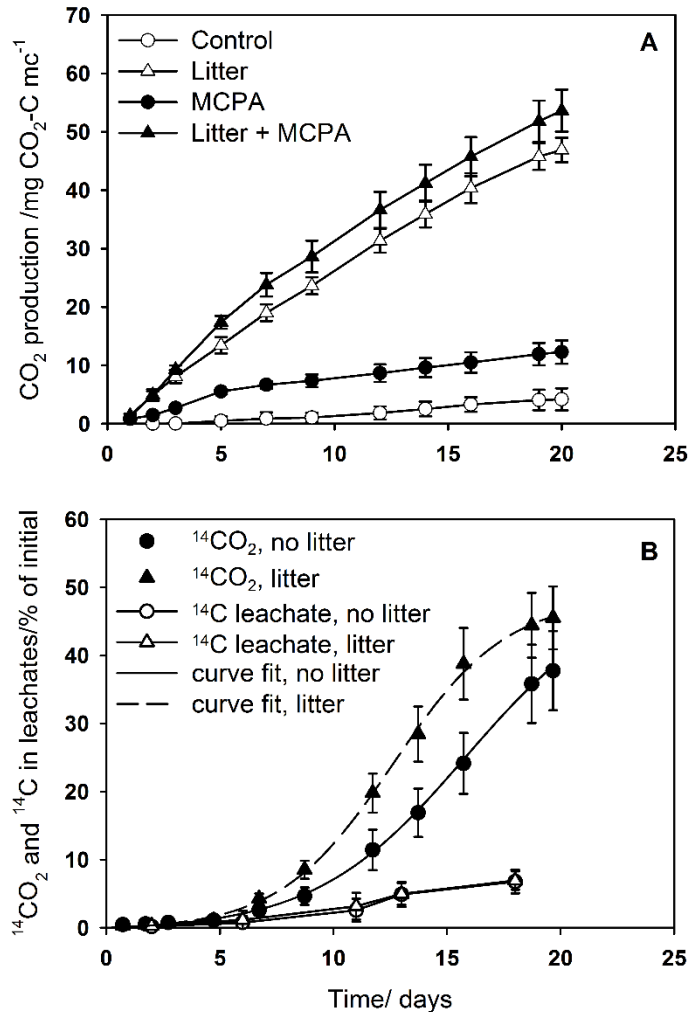


Fig. 2 Cumulative $\text{CO}_2\text{-C}$ production (A), MCPA mineralisation and leaching of ^{14}C (B). Curves are fitted to a logistic model with the following parameters (\pm standard error): *no litter* $C_0=50.6$ (± 5.5), $X_0=0.43$ (± 0.20), $k=0.0059$ (± 0.0014); *litter* $C_0=48.5$ (± 1.3), $X_0=0.31$ (± 0.10), $k=0.0082$ (± 0.0008). Values are means of nine microcosms (mc), error bars show standard deviation.

were mineralised in microcosms without and with litter, respectively. The logistic model fitted the $^{14}\text{CO}_2$ production with model efficiencies of 0.95 and 0.97 for the control and the litter treatment, respectively. The mineralisation rate constant k increased from 0.0059 to 0.0082 % day $^{-1}$ with litter addition (t-test, $P < 0.05$), C_0 indicated a maximum percentage of mineralisation of

about 49% with no differences between treatments. These results were supported by the extractable MCPA and the ^{14}C activity of the DOC (Fig. 3A, C). We extracted 4-6% of the initially added MCPA from microcosms without litter addition, whereas less than 1% was extractable after litter addition. The ^{14}C activity of the DOC showed a similar pattern: more of the initially added ^{14}C remained within the DOC in microcosms without (8-10.5%) than in microcosms with (3-5%) litter addition.

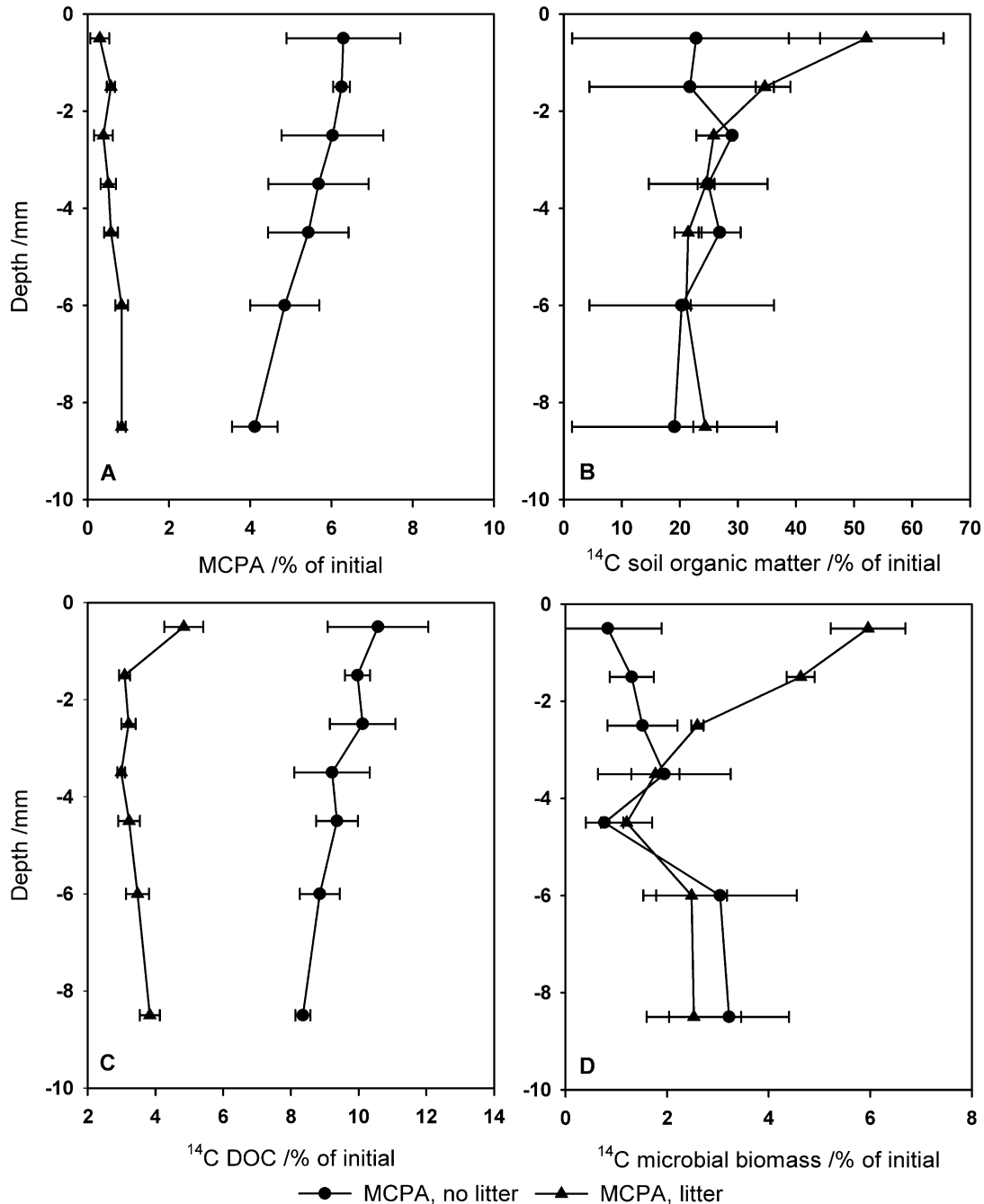


Fig. 3 Depth profiles of the extractable MCPA (A), and of the ^{14}C activity of the soil organic matter (B), the DOC (C) and the microbial biomass (D). Values are means of three replicates, error bars show standard deviation.

Nearly seven percent of the added ^{14}C were leached from the soil columns (Fig. 2B). However, no differences between microcosms with and without litter were detected. In the top layer (0-1

mm) of microcosms with litter, about 52% of the added ^{14}C remained in the soil organic matter (Fig. 3B). This value decreased with increasing distance to the litter and reached the control level of 20-25% at 3 mm depth. However, the difference between microcosms due to litter addition was statistically not significant. In total, we recovered 70-75% of the added ^{14}C as CO_2 , soil organic carbon and leachate. The ^{14}C activity of the microbial biomass reflected the ^{14}C activity pattern of the soil organic matter: the top layer of microcosms covered with maize litter showed significantly higher activities (t-test, $P < 0.01$) than in microcosms without litter (Fig. 3D). These differences decreased with increasing depth and became negligible below 3 mm.

4.4.2 16S rDNA/18S rDNA

The abundance of the soil microflora was estimated by qPCR assay targeting the 16S rDNA sequence of the bacterial ribosomal operon. We detected 16S rDNA sequences within the range of 7.9×10^{10} to 1.7×10^{11} copy numbers g^{-1} (Fig. 4A). Litter addition significantly increased the abundance of 16S rDNA sequences ($F_{1,8} = 607.6$, $P < 0.001$) by 83% within the first layer. The increase in copy numbers due to litter addition was detectable up to a distance of 3-4 mm to the litter. MCPA addition significantly increased the abundance of 16S rDNA sequences ($F_{1,8} = 33.3$, $P < 0.001$) as well, although to a much smaller extent (+14%) than litter.

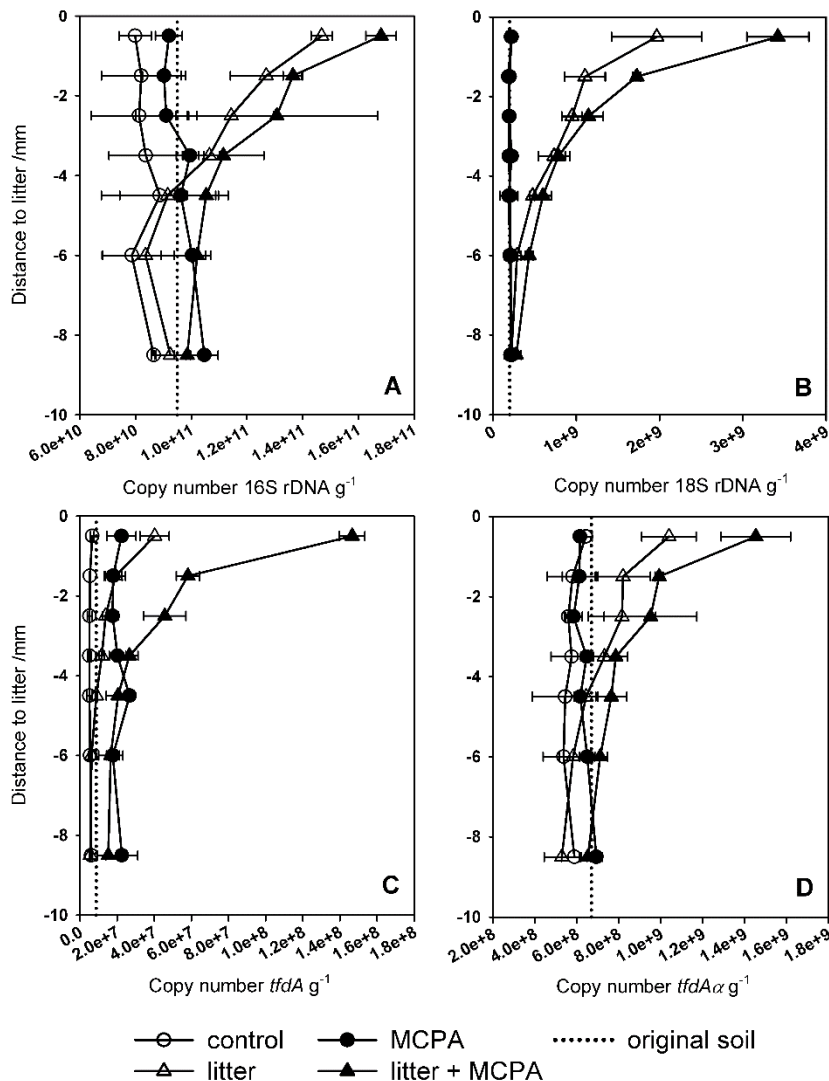
The abundance of the fungal community was estimated by qPCR targeting the 18S rDNA sequence of the fungal ribosomal operon. Copy numbers of 18S rDNA sequences were within a range of 1.9×10^8 to 3.4×10^9 g^{-1} (Fig. 4B). Litter addition significantly increased the abundance of 18S rDNA sequences ($F_{1,8} = 673.7$, $P < 0.001$) 12-fold within the first layer. This effect was detectable up to 5 mm away from the litter. Overall, MCPA addition significantly increased copy numbers of 18S rDNA sequences ($F_{1,8} = 8.9$, $P < 0.05$) by 66% within the first layer. In contrast to 16S rDNA, however, MCPA addition increased 18S rDNA sequence copy numbers only in the presence of litter ($F_{1,8} = 9.9$, $P < 0.05$).

4.4.3 *tfdA/tfdA α*

The abundance of the MCPA degrading community was estimated by qPCR targeting either *tfdA* or *tfdA α* sequences. We detected *tfdA* sequences within the range of 5.1×10^6 to 1.5×10^8 copy numbers g^{-1} (Fig. 4C). Litter addition significantly increased the abundance of *tfdA* sequences ($F_{1,8} = 434.2$, $P < 0.001$) 6-fold within the first layer. The gradient in the copy number of *tfdA* sequences within 3-4 mm of the litter was similar to that found for 16S rDNA. MCPA addition increased the abundance of *tfdA* sequences in microcosms with and without litter over the complete range of 10 mm. However, the significant 3-fold increase ($F_{1,8} = 260.5$, $P < 0.001$) within the first layer was much stronger than for 16S rDNA. Furthermore, litter and MCPA addition showed a significant interaction ($F_{1,8} = 143.0$, $P < 0.001$), with the increase in copy numbers being much stronger in soils exposed to both litter and MCPA (22-fold) than in soils

exposed to MCPA (3-fold) or litter (6-fold) alone. The gradients and effects were similar when considering the relative abundance of *tfdA* sequences in the soil microflora (data not shown).

Copy numbers of *tfdA α* sequences ranged from 5.3×10^8 to 1.5×10^9 g⁻¹ (Fig. 4D). Litter addition significantly increased their abundance ($F_{1,8} = 101.3$, $P < 0.001$) 2-fold within the first layer. Again, we detected a gradient within 3-4 mm of the litter. The effect of MCPA addition on the abundance of *tfdA α* sequences was more similar to the pattern found for 18S rDNA than for *tfdA*. MCPA addition significantly increased copy numbers ($F_{1,8} = 9.9$, $P < 0.05$) by 23%. As for 18S rDNA, however, this effect was restricted to microcosms with MCPA and litter addition due to a significant interaction of both factors ($F_{1,8} = 13.0$, $P < 0.01$). In contrast to *tfdA*, litter and MCPA addition did not affect the relative abundance of *tfdA α* sequences in the soil microflora (data not shown), and almost all data were within the range of the original soil.



4.5 Discussion

4.5.1 MCPA degradation

In the present experiment, 38% to 46% of the added ^{14}C evolved into $^{14}\text{CO}_2$ over a period of 20 days. This value is within the range found in the literature for phenoxy acid herbicides (Boivin et al., 2005; Fredslund et al., 2008; Nicolaisen et al., 2008). As we hypothesised, MCPA degradation was enhanced after litter addition. This agrees with the result of Duah-Yentumi and Kuwatsuka (1982), who found an increased degradation rate of MCPA after adding plant residues. Furthermore, those authors found no effect of plant residues on the lag phase, which supports our results. In contrast, Nicolaisen et al. (2008) did not detect any lag phase after pre-incubation of the soil with 20 mg kg^{-1} MCPA. Vieublé Gonod et al. (2003) explained the lag phase prior to MCPA degradation as the time required to promote the growth of low-density, degrading microbial populations. We detected relatively high copy numbers of the *tfdA* sequence. Therefore, differences in soil properties, which affect MCPA availability, are probably more important for the contradictory effects of repeated MCPA addition on the lag phase. Overall, we found an increased cumulative respiration by $7.4 \text{ mg CO}_2\text{-C}$ due to MCPA addition, which is distinctly more than the initially applied 2.4 mg MCPA-C . One possible explanation for this priming effect is an increased mineralisation of soil organic matter due to the added energy source (Fontaine et al., 2003), in our case MCPA. However, the observed difference in respiration occurred mainly during the lag phase of MCPA mineralisation. We suggest cryptic growth (Jenkinson and Parry, 1989) or a stress reaction due to toxic effects of MCPA on soil microorganisms as reasons for the observed effect. Vieublé Gonod et al. (2006) detected a change in the genetic structure of the bacterial community during the first 4 days after 2,4-D application. The authors explained this effect by growth of 2,4-D degraders or by toxic effects on parts of the microbial community. The latter is supported by results of Saleh et al. (unpublished), who found a decrease in bacterial PLFAs after MCPA addition, and of S. Schulz (personal communication), who detected a negative effect of MCPA on the abundance of *alkB* genes.

We found about 1 to 6% of the added ^{14}C bound in the microbial biomass, which is within the range of the 5% observed by Vieublé Gonod et al. (2006) 15 days after 2,4-D application. Significantly more ^{14}C was bound in the microbial biomass and the soil organic matter when soil cores were covered by litter, whereas less MCPA was extracted and less ^{14}C was found as dissolved organic carbon. Therefore, we suggest that litter addition induced greater MCPA degradation and assimilation of ^{14}C by the MCPA degrading community. At the same time, a higher assimilation rate would result in more MCPA-C bound in the soil organic matter as cell tissue. A possible explanation for this observation is a greater availability of α -ketoglutarate due to either direct transport or improved delivery of α -ketoglutarate through the Krebs cycle by increased metabolic activity of MCPA degraders. Müller and Babel (2000) reported that a

considerable portion of the energy resulting from MCPA metabolism is used to regenerate α -ketoglutarate, which is used as a co-substrate during the initial degradation step. Adding this co-substrate increased 2,4-D degradation (Müller, 2007). Therefore, transport of litter-derived α -ketoglutarate or its metabolic precursors into the soil might have on the one hand decreased the portion of MCPA carbon used to regenerate α -ketoglutarate and on the other hand increased the portion used for microbial growth. This hypothesis of transport-regulated MCPA degradation at the soil-litter interface is further supported by the gradients we observed within the first 3 mm for the ^{14}C content of the soil organic matter and the microbial biomass. In a previous study, such gradients were detected in the detritosphere as the result of transport of litter-derived substrates (Poll et al., 2006). Another possibility is a change in internal resource allocation within the bacterial cells. Beside the availability of α -ketoglutarate, the transport of litter compounds potentially regulated MCPA degradation by improving the energy- and nutrient-intensive enzyme production (Schimel and Weintraub, 2003). In this case, the MCPA degrading community might have allocated more resources into the production of *tfd* enzymes after litter addition. This agrees with Cederlund et al. (2007), who found MCPA degradation along a railway embankment to be N-limited.

4.5.2 Quantification of functional genes

We detected $5 \times 10^6 \text{ g}^{-1}$ copy numbers of the *tfdA* sequence in the control soil, which is within the range reported in the literature (Baelum et al., 2008; Nicolaisen et al., 2008; Vieublé Gonod et al., 2006). The *tfdA α* abundances are two orders of magnitude greater in the control soil than for *tfdA* and represented about 0.6% of the copy numbers of 16S rDNA. Itoh et al. (2004) suggested the existence of a natural substrate for the enzyme encoded by *tfdA α* . The high abundance of *tfdA α* indicates that this natural substrate might be relatively common in the soil used here. Litter addition induced a gradient in the abundance of the *tfdA α* bacterial community, whereas MCPA affected *tfdA α* only in the presence of litter, which indicates that adding litter compounds induces the *tfdA α* pathway. However, at least some of the *tfdA α* enrichment is due to an overall increase in bacterial abundance. We therefore suggest, that bacteria harbouring *tfdA α* contributed little to MCPA degradation in the detritosphere.

Note that the *tfdA* sequence abundance showed a much stronger response to the addition of MCPA or litter both in absolute numbers and in relation to 16S rDNA. This agrees with previous studies (Baelum et al., 2008; Vieublé Gonod et al., 2006) that found a similar increase in *tfdA* copy numbers after 2,4-D and MCPA addition. For example, Baelum et al. (2008) detected an increase from 2×10^6 copy numbers g^{-1} to 8×10^6 copy numbers g^{-1} . However, litter addition combined with MCPA boosted the value to $1.5 \times 10^8 \text{ g}^{-1}$, which is two-fold higher than any literature value. The positive response of the *tfd* bacterial community to increased substrate availability along a gradient at the soil-litter interface corroborates our second hypothesis of an improved

genetic potential of MCPA degraders within the detritusphere. This further indicates that the detritusphere represents a hotspot for MCPA degradation and that the above-mentioned regulation mechanisms are relevant within this microhabitat. Furthermore, the increased MCPA degradation and assimilation of MCPA derived C seems to be due to a pronounced activity of the *tfd* bacterial community. Shaw and Burns (2004) observed an increased 2,4-D mineralisation in the rhizosphere of *Trifolium pratense* but no enrichment in the degrading populations (based on the most probable number method). Plasmids carrying the *tfdA* gene are present at a single or low copy number per cell (Leveau et al., 1999). Therefore, the increase in copy numbers of the *tfdA* sequence in our experiment was probably due to growth of the *tfd* bacterial community. Hogan et al. (1997) also detected *tfdA* genes in bacterial populations unable to degrade 2,4-D. Therefore, litter addition might also have favoured non-degrading bacterial populations carrying the *tfdA* gene. However, litter addition enhanced MCPA degradation, and a positive interaction between MCPA and litter on the abundance of *tfdA* genes occurred: both results indicate that litter addition favoured MCPA degrading populations. Beside the above-mentioned transport of α -ketoglutarate and its metabolic precursors, other regulation mechanisms potentially explain the positive effect of litter addition on MCPA degradation. Microbial populations might act as a consortium during MCPA degradation (Ka et al., 1994; Top et al., 1996), which reduces the benefit from each single population. This is especially true for populations that harbour only the *tfdA* gene encoding the initial degradation step (Müller and Babel, 2001). Adding external C sources like α -ketoglutarate or fructose induced degradation activity by such strains. In our experiment, transport of litter compounds might have alleviated substrate limitation. Accordingly, bacterial populations only capable of the initial degradation step boosted MCPA degradation and *tfdA* abundance. Finally, litter substrates probably induced co-metabolic MCPA degradation. We suggest that, in our experiment, co-metabolic MCPA degradation might be partly connected to fungal communities. Fungal degradation of 2,4-D and MCPA has been shown by several studies (e.g. Reddy et al., 1997; Vroumsia et al., 1999). For example, Castillo et al. (2001) revealed that MCPA degradation on unsterile straw was connected to the activity of fungal lignin-degrading enzymes like lignin peroxidase and manganese peroxidase/laccase. We observed an effect of MCPA on the abundance of 18S rDNA only in the presence of litter. We therefore suggest that litter addition stimulates the development of fungal populations and non-specific enzymes able to transform MCPA. This hypothesis is supported by findings of Vroumsia et al. (1999), who observed that fungal degradation of 2,4-D in medium was improved in the presence of glucose and nitrogen. Finally, the specific conditions in the detritusphere might have promoted the development of fungal populations able to transform MCPA. *Mortierella isabellina* was one of the two most efficient fungi out of ninety strains tested for their ability to degrade 2,4-D (Vroumsia et al., 2005). In a previous study using a similar experimental set-up, we identified *Mortierellaceae* as pioneer colonisers

in the detritosphere (Poll et al., 2010). Therefore, we suggest that adding litter provided conditions for the growth of specific fungal populations that can degrade MCPA.

4.6 Conclusions

In conclusion, our study exemplified how substrate availability regulates the functioning of microbial communities. Furthermore, soil represents a highly structured environment, and the regulation of microbial activity therefore often depends on small-scale processes, which form micro-habitats with specific conditions. At the soil-litter interface, transport of litter compounds increased the abundance and activity of the *tfd* bacterial community probably by: a) supplying α -ketoglutarate due to either direct transport or increased delivery through the Krebs cycle or b) supplying energy and nutrients, which improve bacterial enzyme production or the activity of bacterial consortia involved in MCPA degradation. Induction of non-specific fungal enzymes that transform MCPA is another possible regulation mechanism of MCPA degradation at the soil-litter interface. Finally, the observed effects of litter addition are a good example of priming effects in soil, and the suggested regulation mechanisms might be of more general relevance.

4.7 Acknowledgement

We thank Sabine Rudolph, David Bru, Erhard Strohm and Christoph Schweizer for their excellent technical assistance. Funding was provided by the Deutsche Forschungsgemeinschaft (DFG) priority program SPP 1315: "Biogeochemical Interfaces in Soil".

4.8 References

- Baelum, J., Henriksen, T., Hansen, H.C.B., Jacobsen, C.S., 2006. Degradation of 4-Chloro-2-Methylphenoxyacetic Acid in top- and subsoil is quantitatively linked to the class III *tfdA* gene. *Applied and Environmental Microbiology* 72, 1476-1486.
- Baelum, J., Nicolaisen, M.H., Holben, W.E., Strobel, B.W., Sørensen, J., Jacobsen, C.S., 2008. Direct analysis of *tfdA* gene expression by indigenous bacteria in phenoxy acid amended agricultural soil. *The ISME Journal* 2, 677-687.
- Bell, G.R., 1960. Studies on a soil *Achromobacter* which degrades 2,4-dichlorophenoxyacetic acid. *Canadian Journal of Microbiology* 6, 325-337.
- Boivin, A., Amellal, S., Schiavon, M., van Genuchten, M. T., 2005. 2,4-Dichlorophenoxyacetic acid (2,4-D) sorption and degradation in three agricultural soils. *Environmental Pollution* 138, 92-99.
- Bru, D., Martin-Laurent, F., Philippot, L., 2008. Quantification of the detrimental effect of a single primer-template mismatch by real-time PCR using the 16S rRNA gene as an example. *Applied and Environmental Microbiology* 74, 1660-1663.
- Castillo, M.D.P., Andersson, A., Ander, P., Stenström, J., Torstensson, L., 2001. Establishment of the white rot fungus *Phanerochaete chrysosporium* on unsterile straw in solid substrate fermentation systems intended for degradation of pesticides. *World Journal of Microbiology and Biotechnology* 17, 627-633.
- Cederlund, H., Börjesson, E., Önnby, K., Stenström, J., 2007. Metabolic and cometabolic degradation of herbicides in the fine material of railway ballast. *Soil Biology and Biochemistry* 39, 473-484.

- Chaudhry, G.R., Huang, G.H., 1988. Isolation and characterization of a new plasmid from a *Flavobacterium* sp. which carries the genes for degradation of 2,4-dichlorophenoxyacetate. *Journal of Bacteriology* 170, 3897-3902.
- Don, R.H., Pemberton, J.M., 1985. Genetic and physical map of the 2,4-dichlorophenoxyacetic acid-degradative plasmid pJP4. *Journal of Bacteriology* 161, 466-468.
- Duah-Yentumi, S., Kuwatsuka, S., 1980. Effect of organic matter and chemical fertilizers on the degradation of benthicarb and MCPA herbicides in the soil. *Soil Science and Plant Nutrition* 26, 541-549.
- Duah-Yentumi, S., Kuwatsuka, S., 1982. Microbial degradation of benthicarb, MCPA and 2,4-D herbicides in perfused soils amended with organic matter and chemical fertilizers. *Soil Science and Plant Nutrition* 28, 19-26.
- Fomsgaard, I.S., 1997. Modelling the mineralization kinetics for low concentrations of pesticides in surface and subsurface soil. *Ecological Modelling* 102, 175-208.
- Fontaine, S., Mariotti, A., Abbadie, L., 2003. The priming effect of organic matter: a question of microbial competition? *Soil Biology and Biochemistry* 35, 837-843.
- Fredslund, L., Vinther, F.P., Brinch, U.C., Elsgaard, L., Rosenberg, P., Jacobsen, C.S., 2008. Spatial variation in 2-Methyl-4-chlorophenoxyacetic acid mineralization and sorption in a sandy soil at field level. *Journal of Environmental Quality* 37, 1918-1928.
- Fukumori, F., Hausinger, R.P., 1993. *Alcaligenes eutrophus* JMP134 "2,4-dichlorophenoxyacetate monooxygenase" is an α -ketoglutarate-dependent dioxygenase. *Journal of Bacteriology* 175, 2083-2086.
- Greer, L.E., Shelton, D.R., 1992. Effect of inoculant strain and organic matter content on kinetics of 2,4-dichlorophenoxyacetic acid degradation in soil. *Applied and Environmental Microbiology* 58, 1459-1465.
- Hogan, D.A., Buckley, D.H., Nakatsu, C.H., Schmidt, T.M., Hausinger, R.P., 1997. Distribution of the *tfdA* gene in soil bacteria that do not degrade 2,4-dichlorophenoxyacetic acid (2,4-D). *Microbial Ecology* 34, 90-96.
- Itoh, K., Kanda, R., Sumita, Y., Kim, H., Kamagata, Y., Suyama, K., Yamamoto, H., Hausinger, R.P., Tiedje, J.M., 2002. *tfdA*-like genes in 2,4-dichlorophenoxyacetic acid-degrading bacteria belonging to the *Bradyrhizobium-Agromonas-Nitrobacter-Afipia* cluster in α -Proteobacteria. *Applied and Environmental Microbiology* 68, 3449-3454.
- Itoh, K., Tashiro, Y., Uobe, K., Kamagata, Y., Suyama, K., Yamamoto, H., 2004. Root nodule *Bradyrhizobium* spp. harbor *tfdAa* and *cadA*, homologous with genes encoding 2,4-dichlorophenoxyacetic acid degrading proteins. *Applied and Environmental Microbiology* 70, 2110-2118.
- Jenkinson, D.S., Parry, L.C., 1989. The nitrogen cycle in the broadbalk wheat experiment: A model for the turnover of nitrogen through the soil microbial biomass. *Soil Biology and Biochemistry* 21, 535-541.
- Joergensen, R.G., 1996. The fumigation-extraction method to estimate soil microbial biomass: Calibration of the *k*EC value. *Soil Biology and Biochemistry* 28, 25-31.
- Ka, J.O., Holben, W.E., Tiedje, J.M., 1994. Genetic and phenotypic diversity of 2,4-dichlorophenoxyacetic acid (2,4-D)-degrading bacteria isolated from 2,4-D-treated field soils. *Applied and Environmental Microbiology* 60, 1106-1115.
- Kamagata, Y., Fulthorpe, R., Tamura, K., Takami, H., Forney, L.J., Tiedje, J.M., 1997. Pristine environments harbor a new group of oligotrophic 2,4-dichlorophenoxyacetic acid-degrading bacteria. *Applied and Environmental Microbiology* 63, 226-2272.
- Leveau, J.H.J., König, F., Fuchsli, H., Werlen, C., van der Meer, J.R., 1999. Dynamics of multigene expression during catabolic adaptation of *Ralstonia eutropha* JMP134 (pJP4) to the herbicide 2,4-dichlorophenoxyacetate. *Molecular Microbiology* 33, 396-406.
- Lopez-Gutierrez, J.C., Henry, S., Hallet, S., Martin-Laurent, F., Catroux, G., Philippot, L., 2004. Quantification of a novel group of nitrate-reducing bacteria in the environment by real-time PCR. *Journal of Microbiological Methods* 57, 399-407.

- Manerkar, M.A., Seena, S., Bärlocher, F., 2008. Q-RT-PCR for assessing archaea, bacteria, and fungi during leaf decomposition in a stream. *Microbial Ecology* 56, 467-473.
- Millennium Ecosystem Assessment, 2005. *Ecosystems and Human Well-Being: Synthesis*. Island Press, Washington DC.
- Moret, S., Hidalgo, M., Sanchez, J. M., 2006. Development of an ion-pairing liquid chromatography method for the determination of phenoxyacetic herbicides and their main metabolites: Application to the analysis of soil samples. *Chromatographia* 63, 109-115.
- Müller, R.H., 2007. Activity and reaction mechanism of the initial enzymatic step specifying the microbial degradation of 2,4-Dichlorophenoxyacetate. *Engineering in Life Science* 7, 311-321.
- Müller, R.H., Babel, W., 2000. A theoretical study on the metabolic requirements resulting from a-ketoglutarate-dependent cleavage of phenoxyalkanoates. *Applied and Environmental Microbiology* 66, 339-344.
- Müller, R.H., Babel, W., 2001. Pseudo-recalcitrance of chlorophenoxyalkanoate herbicides- correlation to the availability of a-ketoglutarate. *Acta Biotechnologica* 21, 227-242.
- Nicolaisen, M.H., Baelum, J., Jacobsen, C.S., Sørensen, J., 2008. Transcription dynamics of the functional *tfdA* gene during MCPA herbicide degradation by *Cupriavidus necator* AEO106 (pRO101) in agricultural soil. *Environmental Microbiology* 10, 571-579.
- Philippot, L., Cuhel, J., Saby, N.P.A., Cheneby, D., Chronakova, A., Bru, D., Arrouays, D., Martin-Laurent, F., Simek, M., 2009. Mapping field-scale spatial patterns of size and activity of the denitrifier community. *Environmental Microbiology* 11, 1518-1526.
- Pieper, D.H., Reineke, W., Engesser, K.-H., Knackmuss, H.-J., 1988. Metabolism of 2,4-dichlorophenoxyacetic acid, 4-chloro-2-methylphenoxyacetic acid and 2-methylphenoxyacetic acid by *Alcaligenes eutrophus* JMP 134. *Archives of Microbiology* 150, 95-102.
- Piutti, S., Hallet, S., Rousseaux, S., Philippot, L., Soulas, G., Martin-Laurent, F., 2002. Accelerated mineralisation of atrazine in maize rhizosphere soil. *Biology and Fertility of Soils* 36, 434-441.
- Poll, C., Ingwersen, J., Stemmer, M., Gerzabek, M.H., Kandeler, E., 2006. Mechanisms of solute transport affect small-scale abundance and function of soil microorganisms in the detritusphere. *European Journal of Soil Science* 57, 583-595.
- Poll, C., Marhan, S., Ingwersen, J., Kandeler, E., 2008. Dynamics of litter carbon turnover and microbial abundance in a rye detritusphere. *Soil Biology and Biochemistry* 40, 1306-1321.
- Poll, C., Brune, T., Begerow, D., Kandeler, E., 2010. Small-scale diversity and succession of fungi in the detritusphere of rye residues. *Microbial Ecology* 59, 130-140.
- Reddy, G.V.B., Joshi, D.K., Gold, M.H., 1997. Degradation of chlorophenoxyacetic acids by the lignin-degrading fungus *Dichomitus squalens*. *Microbiology* 143, 2353-2360.
- Schimel, J.P., Weintraub, M.N., 2003. The implications of exoenzyme activity on microbial carbon and nitrogen limitation in soil: a theoretical model. *Soil Biology and Biochemistry* 35, 549-563.
- Shaw, L.J., Burns, R.G., 2004. Enhanced mineralization of [U-14C]2,4-Dichlorophenoxyacetic acid in soil from the rhizosphere of *Trifolium pratense*. *Applied and Environmental Microbiology* 70, 4766-4774.
- Simkins, S., Alexander, M., 1984. Models for mineralization kinetics with the variables of substrate concentration and population density. *Applied and Environmental Microbiology* 47, 1299-1306.
- Streber, W.R., Timmis, K.N., Zenk, M.H., 1987. Analysis, cloning, and high-level expression of 2,4-dichlorophenoxyacetate monooxygenase gene *tfdA* of *Alcaligenes eutrophus* JMP134. *Journal of Bacteriology* 169, 2950-2955.
- Top, E.M., Maltseva, O.V., Forney, L.J., 1996. Capture of a catabolic plasmid that encodes only 2,4-dichlorophenoxyacetic acid:a-ketoglutaric acid dioxygenase (TfdA) by genetic complementation. *Applied and Environmental Microbiology* 62, 2470-2476.

- Vance, E.D., Brookes, P.C., Jenkinson, D.S., 1987. An extraction method for measuring soil microbial biomass C. *Soil Biology and Biochemistry* 19, 703-707.
- Vieublé Gonod, L., Chenu, C., Soulas, G., 2003. Spatial variability of 2,4-dichlorophenoxyacetic acid (2,4-D) mineralisation potential at a millimetre scale in soil. *Soil Biology and Biochemistry* 35, 373-382.
- Vieublé Gonod, L., Martin-Laurent, F., Chenu, C., 2006. 2,4-D impact on bacterial communities, and the activity and genetic potential of 2,4-D degrading communities in soil. *FEMS Microbiology Ecology* 58, 529-537.
- Vroumsia, T., Steiman, R., Seigle-Murandi, F., Benoit-Guyod, J.-L., 1999. Effects of culture parameters on the degradation of 2,4-dichlorophenoxyacetic acid (2,4-D) and 2,4-dichlorophenol (2,4-DCP) by selected fungi. *Chemosphere* 39, 1397-1405.
- Vroumsia, T., Steiman, R., Seigle-Murandi, F., Benoit-Guyod, J.-L., 2005. Fungal bioconversion of 2,4-dichlorophenoxyacetic acid (2,4-D) and 2,4-dichlorophenol (2,4-DCP). *Chemosphere* 60, 1471-1480.

5 Micro-scale modeling of pesticide degradation coupled to carbon turnover in the detritosphere - Model description and sensitivity analysis

Biogeochemistry 117 (2014), 185–204

DOI: 10.1007/s10533-013-9851-3

Holger Pagel¹, Joachim Ingwersen¹, Christian Poll², Ellen Kandeler², Thilo Streck¹

¹ Institute of Soil Science and Land Evaluation, Biogeophysics, University of Hohenheim, D-70593 Stuttgart, Germany

² Institute of Soil Science and Land Evaluation, Soil Biology, University of Hohenheim, D-70593 Stuttgart, Germany

The final publication is available at "link.springer.com".

5.1 Abstract

Microbiologically active biogeochemical interfaces are excellent systems to study soil functions such as pesticide degradation at the micro-scale. In particular, in the detritusphere pesticide degradation is accelerated by input of fresh organic carbon from litter into the adjacent soil. This observed priming effect suggests: *i*) pesticide degradation is strongly coupled to carbon turnover, *ii*) it is controlled by size and activity of the microbial community and *iii*) sorption and transport of dissolved carbonaceous compounds and pesticides might regulate substrate availability and in turn decomposition processes. We present a new mechanistic 1D model (*PEsticide degradation Coupled to CARbon turnover in the Detritusphere, PECCAD*) which implements these hypotheses. The new model explicitly considers growth and activity of bacteria, fungi and specific pesticide degraders in response to substrate availability. Enhanced pesticide degradation due to availability of a second source of carbon (dissolved organic carbon) is implemented in the model structure via two mechanisms. First, additional substrate is utilized simultaneously with the pesticide by bacterial pesticide degraders resulting in an increase in their size and activity. Second, stimulation of fungal growth and activity by additional substrates leads directly to higher pesticide degradation via co-metabolism. Thus, PECCAD implicitly accounts for litter-stimulated production and activity of unspecific fungal enzymes responsible for co-metabolic pesticide degradation. With a global sensitivity analysis we identified high-leverage model parameters and input. In combination with appropriate experimental data, PECCAD can serve as a tool to elucidate regulation mechanisms of accelerated pesticide degradation in the detritusphere.

5.2 Introduction

The detritusphere is a microbiologically highly active biogeochemical interface in soil. It includes the litter and the adjacent soil influenced by litter (Ingwersen et al. 2008; Poll et al. 2006). The dimension of this microhabitat is typically in the range of only a few millimeters (Gaillard et al. 2003; Kandeler et al. 1999). However, the rates at which biogeochemical processes occur at such microsites determine the functioning of the soil ecosystem at the large scale (Beare et al. 1995; Totsche et al. 2010; Young et al. 2009).

The degradation of pesticides is one important biogeochemical process in soils. It can be substantially accelerated by readily available organic substrates. The stimulation of pesticide degradation by root exudates is well documented (Gerhardt et al. 2009; Shaw and Burns 2003), but little information is available about the effect of litter carbon (C) on pesticide degradation. For example, Ghani and Wardle (2001) killed *Carduus nutans* L. plants (musk thistle) by the application of the ^{14}C -labelled herbicide metsulfuron-methyl and studied the influence of the remaining plant litter on metsulfuron-methyl degradation. They found a significant effect of plant litter on herbicide degradation and mineralization accompanied by increased incorporation of herbicide- ^{14}C into the microbial biomass compared to the control without plants. Similarly, we also found a significant stimulating effect of maize litter on the mineralization and utilization of the herbicide MCPA (4-chloro-2-methylphenoxyacetic acid) as well as on specific MCPA degraders in the detritusphere (Poll et al. 2010).

Considering pesticides as a part of the soil organic matter (SOM) pool, such a short-term stimulation effect due to fresh C or nutrient input can be seen as a 'priming effect' (Kuzyakov et al. 2000). The detritusphere is one of the microbial 'hot spots' in soils for priming phenomena (Kuzyakov 2010).

Microorganisms are the drivers of observed priming effects in soil (Blagodatskaya and Kuzyakov 2008; Shaw and Burns 2003). While the number of soil C models has increased exponentially in the last decades, this active role of microorganisms in SOM dynamics has not been taken into account by most models. A comprehensive overview about available SOM models can be found in a recent review by Manzoni and Porporato (2009). The majority of SOM models use a first-order approach to describe the SOM decomposition as an exclusively substrate-controlled process. They typically partition SOM into several compartments including one biomass pool (e.g., Braakhekke et al. 2011; Jenkinson and Rayner 1977; Parton 1993; Van Veen and Paul 1981). However, the decomposition of single SOM compartments is then calculated using biomass-independent pool-specific decomposition rates, thereby neglecting soil microorganisms as the real drivers. Nevertheless, such models have been successfully used to simulate long term C dynamics in soil (Smith et al. 1997).

Despite the dominance of first-order approaches, some detailed SOM models have been developed which explicitly consider that SOM decomposition processes are regulated by the pool size and activity of soil microorganisms (Allison 2012; Blagodatsky et al. 2011; Ingwersen et al. 2008; Moorhead and Sinsabaugh 2006; Parnas 1976; Paustian and Schnürer 1987; Schimel and Weintraub 2003). Other than first-order linear models, such models are principally able to simulate priming phenomena (Wutzler and Reichstein 2008) and they are mostly employed to capture C dynamics at a small spatial ($\sim \mu\text{m}$ to mm) and temporal (\sim hours to days) scale. The detailed models typically assume Monod-type kinetics for microbial growth and account for microbial maintenance and death. Blagodatsky and Richter (1998) were the first to explicitly consider the “activity state” of microbial biomass as a function of substrate concentration in a combined C and nitrogen (N) model. This unique feature was based on the work of Panikov (1995). Various models differentiate between distinct functional microbial groups, typically based on physiological characteristics of individual populations. In some of these approaches the decomposition of specific SOM fractions is then explicitly attributed to defined functional groups of microorganisms. For instance, the CANTIS model (Garnier et al. 2001) splits total microbial biomass into zymogenous and autochthonous pools. Fontaine et al. (2003) define *r*- and *K*-strategist microorganisms according to the paradigm of an *r*- to *K*-selection continuum, which has been recently suggested as a basic classification scheme in soil microbial ecology (Fierer et al. 2007). Similarly, in both models the zymogenous organisms (i.e. *r*-strategists) feed only on fresh and soluble organic matter, whereas the autochthonous (i.e. *K*-strategists) predominately utilize less energy-rich SOM compounds. In the model of Ingwersen et al. (2008), decomposition of “initial-stage” (is) dissolved organic carbon (DOC) is exclusively attributed to is-decomposers, whereas “late-stage” (ls) DOC is only utilized by ls-decomposers. Indeed, is- and ls-decomposers were thought to predominantly reflect bacterial and fungal physiology, respectively. The theoretical guild-based decomposition model (GDM) of Moorhead and Sinsabaugh (2006) defines three guilds of microorganisms (opportunists, decomposers and miners); each simultaneously utilizing three C pools (soluble compounds, holocellulose and lignin). The synthetic chemostat model (SCM; Panikov 1999) is based on similar theoretical foundations using the concept of *r*-, *K*- or *L*-selected microbial life strategies.

Litter and SOM are heterogeneous mixtures of substances ranging from readily degradable components such as sugars, proteins or amino acids to more recalcitrant components such as cellulose or lignin (Blume et al. 2010; Kögel-Knabner 2002; Paul 2007). This has led to the concept of a “dynamic continuum of decomposability”. This concept uses a distribution function describing organic matter quality to model litter and SOM decomposition (Bosatta and Ågren 1991; Carpenter 1981; Feng 2009). However, it results in complex model structures. Its usability is further limited by the lack of detailed knowledge about SOM chemistry for model validation (Bosatta and Ågren 2003; Gignoux et al. 2001; Moorhead and Sinsabaugh 2006). The

majority of models simplify the SOM quality continuum by partitioning SOM into discrete pools with differing decomposition rates, which are considered empirical functions of bulk soil variables such as moisture, temperature or clay content (Manzoni and Porporato 2009). For the widely-used RothC model (Jenkinson and Rayner 1977) it was shown that the sizes of the C pools can be calibrated via measurement (Skjemstad et al. 2004; Zimmermann et al. 2007) or inverse parameter optimization (Scharnagl et al. 2010).

However, decomposition rates and stability of SOM compounds are not exclusively regulated by their molecular structure (as recently reviewed by Dungait et al. 2012). Rather, microbial activity at the micro-scale is strongly influenced by the conditions (e.g., pH; moisture; availability of co-substrates or nutrients) in the immediate soil micro-environment (Ekschmitt et al. 2008; Schmidt et al. 2011). Physicochemical characteristics of soil also control sorption and transport processes, which in turn can regulate the microbial degradation of DOC and pesticides (Ghafoor et al. 2011; Jensen et al. 2004; Marschner and Kalbitz 2003; Poll et al. 2006; Poll et al. 2010; Scow and Johnson 1996; Zander et al. 1999). Several SOM and litter turnover models explicitly include microbial dynamics, but treat the soil as a bulk phase, thereby neglecting these physical processes (e.g., Allison 2012; Blagodatsky and Richter 1998; Moorhead and Sinsabaugh 2006, but see Garnier et al. 2001; Ingwersen et al. 2008).

On the other hand, a couple of models simulating DOC dynamics (e.g., Fan et al. 2010; Gjettermann et al. 2008; Michalzik et al. 2003; Neff and Asner 2001; Yurova et al. 2008) and many pesticide fate models (e.g., Köhne et al. 2006; Leistra et al. 2001; Roulier and Jarvis 2003; Šimůnek et al. 2008; Streck and Richter 1999) mechanistically consider sorption and transport processes in great detail, but they typically oversimplify decomposition as a process exclusively determined by substrate concentration using first order approaches. Although Monod-type kinetics were successfully applied to account for growth-linked pesticide degradation (Cheyns et al. 2010; De Wilde et al. 2009; Shelton and Doherty 1997) potentially synergistic or antagonistic effects due to simultaneous utilization of other available substrates, such as DOC, are rarely considered (but see Richter et al. 1996; p.76). Modeling approaches for co-metabolic degradation of organic chemicals have been proposed, but data for estimating kinetic parameters are scarce (Alvarez-Cohen and Speitel Jr 2001).

Complex models can represent biophysical processes in great detail, but the estimation of the resulting high number of unknown parameters is a challenge. Biokinetic parameters typically depend strongly on the conditions under which they are determined and in most cases they cannot be estimated independently (Brusseu et al. 2006; Estrella et al. 1993; Langner et al. 1998). Fortunately, in recent years sophisticated codes for inverse parameter optimization have become available (e.g., Doherty 2005; Vrugt and Robinson 2007). These techniques have been successfully applied to simultaneously estimate sorption, degradation and transport

parameters of pesticide models (Cheyons et al. 2010; Dubus et al. 2004; Mertens et al. 2009). In addition, modern molecular biological tools, such as quantitative real time PCR (Higuchi et al. 1993) allow direct measurement of specific degrader populations in soil and thus reduce an important source of uncertainty in coupled biophysical models. These developments offer a promising way to obtain meaningful parameter estimates of complex biophysical models.

In this paper we present a new biophysical model intended to serve as a tool to elucidate regulation mechanisms of litter-C stimulated pesticide degradation in the detritusphere. We modified and extended the micro-scale C model of Ingwersen et al. (2008) to cover coupled transport, sorption and biodegradation processes of SOM and pesticide C with special emphasis on the dynamics of microbial degrader populations. In a series of microcosm experiments we study the transport and degradation of the model pesticide MCPA in the detritusphere. Isotopic measurements as well as the abundance of taxonomic and functional genes (as a proxy for specific microbial populations in soil) supplement measured concentrations of SOM constituents and MCPA. These data will provide the basis for identification of biokinetic parameters and input variables of the PECCAD model by inverse parameter optimization in future studies. Here, we give a detailed overview of the new PECCAD model and present the results of a global sensitivity analysis conducted to identify the high-leverage model parameters and input values.

5.3 Model description

5.3.1 General structure

The PECCAD model is based on a detritusphere model described in detail by Ingwersen et al. (2008). This model was successfully applied to simulate the two-phase dynamics of litter decomposition and microbial succession observed in a microcosm study (Poll et al. 2008). In the model, litter is split into two C pools, one decomposing rapidly (*is*), the other slowly (*ls*). The release of C from litter to the corresponding DOC_{is} and DOC_{ls} pools is controlled by a Weibull function. While the DOC_{is} pool serves as a growth substrate for specific *is*-decomposers, the DOC_{ls} pool and an insoluble SOM pool serve as growth substrates for *ls*-decomposers. As in the NICA model (Blagodatsky and Richter 1998), microbial growth is coupled with the consumption of substrate via Monod kinetics, which is controlled by a physiological state variable regulating the fractions of active and dormant microorganisms. The model of Ingwersen et al. (2008) simulates C-linked N dynamics and accounts for diffusive transport of DOC and inorganic N. Moreover, it can handle different C isotopes (^{12}C , ^{13}C).

The generic structure of the PECCAD model is given in Fig. 1. Following Ingwersen et al. (2008) we defined two litter C fractions: a readily available high quality (*hiq*) pool and a less easily decomposable low quality (*loq*) pool. We changed the nomenclature from “initial stage” and “late stage” C pools to “high quality” and “low quality”, because the successive stages of

litter/ DOC decomposition can be thought as being primarily caused by C quality. Each litter pool is decomposed and partly mineralized to CO_2 . The remaining part is transferred to soil by convective and diffusive-dispersive transport. These two processes form the upper boundary conditions for DOC dynamics in soil. The *hiq* DOC pool (C_{hiq}) is primarily fed by the decomposition of *hiq* litter, but dissolved pesticide carbon (C_P) also contributes to the supply of C_{hiq} via co-metabolic pesticide degradation. In contrast, the *loq* DOC pool (C_{loq}) is replenished by decomposition of *loq* litter and insoluble SOM (C_I).

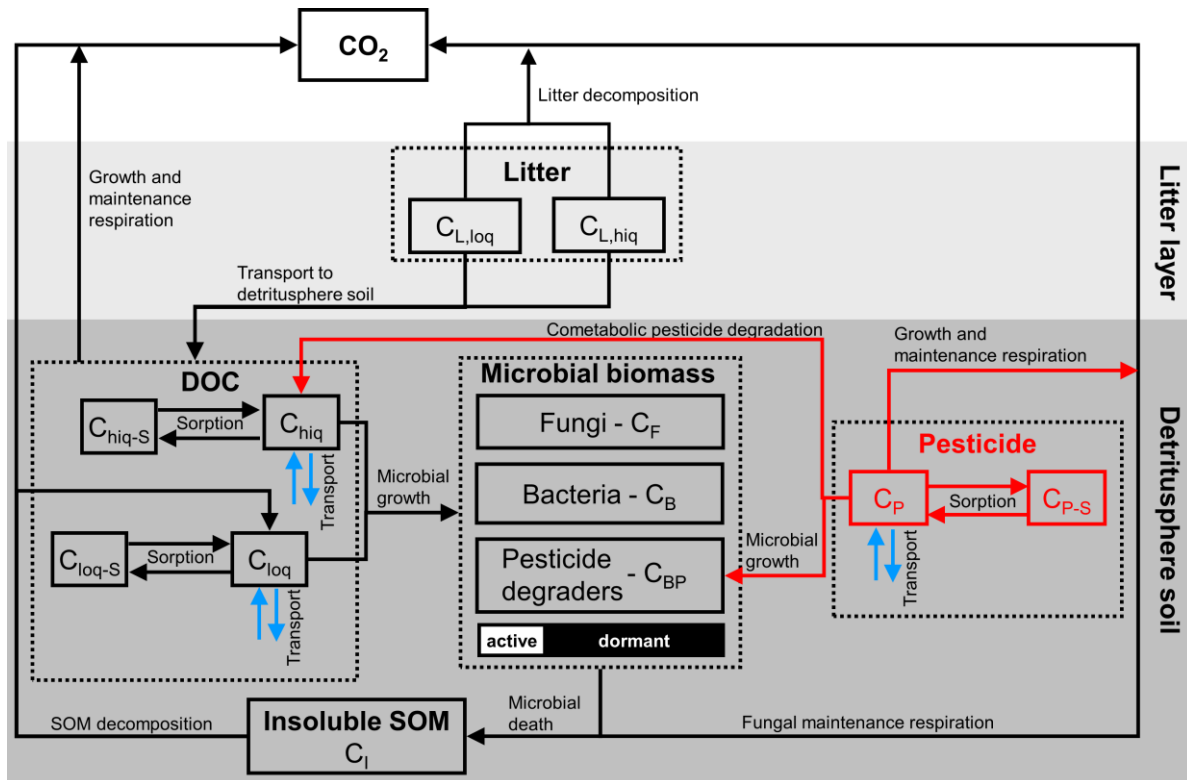


Fig. 1 Schematic diagram of the new PECCAD model. Boxes indicate carbon pools and arrows symbolize carbon fluxes. The abbreviations *hiq* and *loq* stand for high and low quality.

The model is formulated as a set of coupled partial and ordinary differential equations, which are given in Table 1. All functions as well as parameters and other inputs are listed in Table 2 and Online Resource 1, respectively. Technical details on specific key features of the model are given in Online Resource 2. In these equations z (mm) stands for soil depth or distance to litter and t (d) for time. The locations of the upper and lower boundaries are given by $z = 0$ and $z = L$, respectively.

Compared to the detritosphere model of Ingwersen et al. (2008), the PECCAD model has been extended by the following features:

- (1) We implemented an empirical decomposition model (Rovira and Rovira 2010) to simulate the input of *hiq* and *loq* DOC originating from litter at the soil surface (see Online Resource 3). The change in decomposed litter quality depends on the time dependent

rate function of litter decomposition. The empirical Weibull function mentioned above was therefore not needed.

- (2) We explicitly account for sorption of DOC by including pools for the solution and sorbed phases of *hiq* and *loq* DOC (C_{hiq} / C_{loq} and C_{hiq-S} / C_{loq-S}), which are related by a linear sorption isotherm. Further, we added two pools for pesticide solution and sorbed phases (C_P and C_{P-S}) in soil. The phase concentrations are expressed in terms of C and related by the nonlinear Freundlich sorption isotherm.
- (3) PECCAD assumes three microbial pools: bacteria, fungi and specific pesticide degraders. A multi-substrate Monod kinetics approach was introduced to couple microbial growth with the consumption of *hiq* and *loq* DOC as well as pesticide C.
- (4) N turnover has not yet been considered in the current model version to restrict the model complexity. The dynamics of inorganic N were shown to be unimportant for modeled C turnover in the study of Ingwersen et al. (2008).
- (5) Convective and diffusive transport of DOC and pesticide are accounted for.
- (6) We explicitly account for total C, ^{13}C and ^{14}C pools and fluxes to trace the C flow from litter and pesticide into other C pools.
- (7) Ingwersen et al. (2008) used the method of lines with a finite difference scheme and employed Berkeley Madonna (Macey et al. 2000) as solver. We used the software FlexPDE (PDE solutions Inc. 2011) for discretization with finite elements to solve the resulting system of equations.

5.3.2 Microbial physiology

In the PECCAD approach the microbial community consists of three specific populations, which differ in their physiological traits. Thus, only specific bacterial pesticide degraders (C_{BP}) can utilize the pesticide as growth substrate (Table 2; Eq. 31). On the other hand, only unspecific extracellular enzymes produced by fungi (C_F) can co-metabolically degrade the pesticide (Table 2; Eq. 33; See Online Resource 2 for the rationale). In contrast to the two bacterial populations (C_B and C_{BP}), which possess exogenous maintenance, we use an endogenous maintenance function for fungi (For details refer to Online Resource 2). Following Ingwersen et al. (2008), this is based on the fact that fungi are able to autolyse their old hyphae (Jennings and Lysek 1999) and use the reallocated nutrients for maintenance-related functions, whereas most bacteria utilize exogenous substrates to gain energy for maintenance (Russell and Cook 1995).

Beside these specific traits of single populations, all microbial groups share some common traits. However, the individual level of ability for a specific trait is assigned by population-specific parameters. For example, the level of utilization of *hiq* and *loq* DOC by bacteria, fungi and specific pesticide degraders is strongly determined by their individual growth rates (Table 1; Eq. 11, 15). The growth rates in turn are controlled by the actual values of individual maximum growth rates and substrate affinity coefficients (Table 2, Eq. 28, 29, 31) as fundamental properties of each microbial population. In analogy, the microbial pools can respond differently to substrate availability in terms of activity. The active part of individual microbial pools is determined by their physiological state index (Table 1, Eq. 8, 9, 10). Here, activity inhibition coefficients are assigned as fundamental properties of individual populations that regulate how single functional groups of microorganisms become active or dormant in response to substrate availability (For details refer to Online Resource 2). Other individual traits of the microbial pools implemented in PECCAD regulate ecological processes such as the decomposition of insoluble SOM (C_I) by extracellular enzymes (Table 1; Eq. 19)

Table 1 Governing differential equations of the PECCAD model

Stock	Differential equation
Litter layer	
Litter carbon (mg C)	$\frac{dC_{L,tot}}{dt} = -k_L \cdot C_{L,tot} \quad (1)$
hiq litter derived dissolved organic carbon (mg C)	$\frac{dC_{L,hiq}}{dt} = Y_{L,hiq}^* \cdot f_L \cdot k_L \cdot C_{L,tot} \quad (2)$
loq litter derived dissolved organic carbon (mg C)	$\frac{dC_{L,loq}}{dt} = Y_{L,loq}^* \cdot (1 - f_L) \cdot k_L \cdot C_{L,tot} \quad (3)$
Litter derived CO ₂ (mg C)	$\frac{dCO_{2-L}}{dt} = (1 - Y_{L,hiq}^* \cdot f_L - Y_{L,loq}^* \cdot (1 - f_L)) \cdot k_L \cdot C_{L,tot} \quad (4)$
Detritosphere soil	
Bacteria (mg C g ⁻¹ soil)	$\frac{\partial C_B}{\partial t} = C_B \cdot r_B \cdot (\mu_{B,hiq} + \mu_{B,loq} - a_B) \quad (5)$
Fungi (mg C g ⁻¹ soil)	$\frac{\partial C_F}{\partial t} = C_F \cdot r_F \cdot (\mu_{F,hiq} + \mu_{F,loq} - a_F - a_{max-F}^* \cdot (1 - Y_{r-F}^*) - m_{F,P}) \quad (6)$
Bacterial pesticide degraders (mg C g ⁻¹ soil)	$\frac{\partial C_{BP}}{\partial t} = C_{BP} \cdot r_{BP} \cdot (\mu_{BP,P} + \mu_{BP,hiq} + \mu_{BP,loq} - a_{BP}) \quad (7)$
Physiological state index of bacteria	$\frac{\partial r_B}{\partial t} = (\mu_{B,hiq} + \mu_{B,loq}) \cdot (\phi_B - r_B) \quad (8)$
Physiological state index of fungi	$\frac{\partial r_F}{\partial t} = (\mu_{F,hiq} + \mu_{F,loq}) \cdot (\phi_F - r_F) \quad (9)$
Physiological state index of bacterial pesticide degraders	$\frac{\partial r_{BP}}{\partial t} = (\mu_{BP,P} + \mu_{BP,hiq} + \mu_{BP,loq}) \cdot (\phi_{BP} - r_{BP}) \quad (10)$
hiq dissolved organic carbon (mg C g ⁻¹ soil)	$\begin{aligned} \frac{\partial (C_{hiq})}{\partial t} = & C_B \cdot r_B \cdot \left(-\frac{1}{Y_{S-B,hiq}^*} \cdot \mu_{B,hiq} - m_{B,hiq} \right) \\ & + C_{BP} \cdot r_{BP} \cdot \left(-\frac{1}{Y_{S-BP,hiq}^*} \cdot \mu_{BP,hiq} - m_{BP,hiq} \right) \\ & + C_F \cdot r_F \cdot \left(-\frac{1}{Y_{S-F,hiq}^*} \cdot \mu_{F,hiq} + q_{F,P} \cdot Y_{R-F,P}^* \right) \\ & + D_{e-hiq} \cdot \frac{\partial^2 C_{hiq}}{\partial z^2} - v \cdot \frac{\partial C_{hiq}}{\partial z} - \frac{\partial C_{S,hiq}}{\partial t} \end{aligned} \quad (11)$
Sorbed phase	
	$C_{hiq-S} = \frac{\rho_B^*}{\theta^*} \cdot K_{d-hiq}^* \cdot C_{hiq} \quad (12)$

Boundary conditions

$$v \cdot C_{\text{hiq}}(0, t) - D_{e\text{-hiq}} \left. \frac{\partial C_{\text{hiq}}}{\partial z} \right|_{z=0} = \frac{1000}{A^* \cdot \rho_B} \cdot Y_{L,\text{hiq}}^* \cdot f_L \cdot k_L \cdot C_{L,\text{tot}} \quad (13)$$

$$D_{e\text{-hiq}} \left. \frac{\partial C_{\text{hiq}}}{\partial z} \right|_{z=L} = 0 \quad (14)$$

loq dissolved organic carbon
(mg C g⁻¹ soil)

$$\begin{aligned} \frac{\partial (C_{\text{loq}})}{\partial t} = & C_B \cdot r_B \left(-\frac{1}{Y_{S-B,\text{loq}}^*} \cdot \mu_{B,\text{loq}} - m_{B,\text{loq}} + q_B \cdot Y_{r-B}^* \right) \\ & + C_{BP} \cdot r_{BP} \left(-\frac{1}{Y_{S-BP,\text{loq}}^*} \cdot \mu_{BP,\text{loq}} - m_{BP,\text{loq}} + q_B \cdot Y_{r-B}^* \right) \\ & + C_F \cdot r_F \left(-\frac{1}{Y_{S-F,\text{loq}}^*} \cdot \mu_{F,\text{loq}} + q_F \cdot Y_{r-F}^* \right) \\ & + D_{e\text{-loq}} \frac{\partial^2 C_{\text{loq}}}{\partial z^2} - v \cdot \frac{\partial C_{\text{loq}}}{\partial z} - \frac{\partial C_{S,\text{loq}}}{\partial t} \end{aligned} \quad (15)$$

Sorbed phase

$$C_{\text{loq-S}} = \frac{\rho_B^*}{\theta^*} \cdot K_{d\text{-loq}}^* \cdot C_{\text{loq}} \quad (16)$$

Boundary conditions

$$v \cdot C_{\text{loq}}(0, t) - D_{e\text{-loq}} \left. \frac{\partial C_{\text{loq}}}{\partial z} \right|_{z=0} = \frac{1000}{A^* \cdot \rho_B} \cdot Y_{L,\text{loq}}^* \cdot (1 - f_L) \cdot k_L \cdot C_{L,\text{tot}} \quad (17)$$

$$D_{e\text{-loq}} \left. \frac{\partial C_{\text{loq}}}{\partial z} \right|_{z=L} = 0 \quad (18)$$

Insoluble soil organic matter
(mg C g⁻¹ soil)

$$\frac{\partial C_I}{\partial t} = C_B \cdot r_B \cdot (a_B - q_B) + C_{BP} \cdot r_{BP} \cdot (a_{BP} - q_B) + C_F \cdot r_F \cdot (a_F - q_F) \quad (19)$$

Pesticide
(mg C g⁻¹ soil)

$$\begin{aligned} \frac{\partial (C_P + C_{P-S})}{\partial t} = & C_{BP} \cdot r_{BP} \left(-\frac{1}{Y_{S-BP,P}^*} \cdot \mu_{BP,P} - m_{BP,P} \right) \\ & - C_F \cdot r_F \cdot q_{F,P} + D_{e-P} \frac{\partial^2 C_P}{\partial z^2} - v \cdot \frac{\partial C_P}{\partial z} \end{aligned} \quad (20)$$

Sorbed phase

$$C_{P-S} = K_{F-P}^* \cdot \left(C_P \cdot \frac{1000 \cdot \rho_B^* \cdot M_P^*}{9 \cdot \theta^* \cdot M_C^*} \right)^{n_{F-P}} \quad (21)$$

Boundary conditions

$$v \cdot C_P(0, t) - D_{e-P} \left. \frac{\partial C_P}{\partial z} \right|_{z=0} = 0 \quad (22)$$

$$D_{e-P} \left. \frac{\partial C_P}{\partial z} \right|_{z=L} = 0 \quad (23)$$

CO₂
(mg C g⁻¹ soil)

$$\frac{\partial \text{CO}_2}{\partial t} = C_B \cdot r_B \cdot \left(\begin{array}{l} \mu_{B,\text{hiq}} \cdot \frac{1 - Y_{S-B,\text{hiq}}^*}{Y_{S-B,\text{hiq}}^*} + \mu_{B,\text{loq}} \cdot \frac{1 - Y_{S-B,\text{loq}}^*}{Y_{S-B,\text{loq}}^*} \\ + m_{B,\text{hiq}} + m_{B,\text{loq}} + q_B \cdot (1 - Y_{r-B}^*) \end{array} \right)$$

$$+ C_{BP} \cdot r_{BP} \cdot \left(\begin{array}{l} \mu_{BP,P} \cdot \frac{1 - Y_{S-BP,P}^*}{Y_{S-BP,P}^*} + \mu_{BP,\text{hiq}} \cdot \frac{1 - Y_{S-BP,\text{hiq}}^*}{Y_{S-BP,\text{hiq}}^*} + \mu_{BP,\text{loq}} \cdot \frac{1 - Y_{S-BP,\text{loq}}^*}{Y_{S-BP,\text{loq}}^*} \\ + m_{BP,P} + m_{BP,\text{hiq}} + m_{BP,\text{loq}} + q_B \cdot (1 - Y_{r-B}^*) \end{array} \right) \quad (24)$$

$$+ C_F \cdot r_F \cdot \left(\begin{array}{l} \mu_{F,\text{hiq}} \cdot \frac{1 - Y_{S-F,\text{hiq}}^*}{Y_{S-F,\text{hiq}}^*} + \mu_{F,\text{loq}} \cdot \frac{1 - Y_{S-F,\text{loq}}^*}{Y_{S-F,\text{loq}}^*} \\ + a_{\text{max-F}}^* \cdot (1 - Y_{r-F}^*) + m_{F,P} + q_{F,P} \cdot (1 - Y_{R-F,P}^*) \end{array} \right)$$

Biokinetic functions and composite parameter expressions are defined in Table 2.

* indicates defined parameters, input values and material constants that are given in Online Resource 1.

Table 2 Biokinetic functions and composite parameter expressions used in the PECCAD model

Definition	Expression	Unit	
Litter layer			
Rate of total litter decomposition ^a	$k_L = c_L^* + \left(\frac{t}{t^2 + b_L^*} \right)^3$	d ⁻¹	(25)
Fraction of hiq litter on total decomposed litter	$f_L = \frac{k_L - c_L^*}{k_{L,max}}$	Unitless	(26)
Maximum rate of total litter decomposition	with $k_{L,max} = c_L^* + \left(\frac{1}{2 \cdot \sqrt{b_L^*}} \right)^3$	d ⁻¹	(27)
Detritosphere soil			
	with $i = \{hiq, loq\}$:		
Substrate dependent specific growth rate of bacteria ^b	$\mu_{B,i} = \frac{\mu_{max-B}^* \cdot C_i \cdot k_{B,i}^*}{\mu_{max-B}^* + \sum C_i \cdot k_{B,i}^*}$	d ⁻¹	(28)
Substrate dependent specific growth rate of fungi ^b	$\mu_{F,i} = \frac{\mu_{max-F}^* \cdot C_i \cdot k_{F,i}^*}{\mu_{max-F}^* + \sum C_i \cdot k_{F,i}^*}$	d ⁻¹	(29)
Substrate dependent specific rate of maintenance respiration of bacteria ^b	$m_{B,i} = \frac{m_{max-B}^* \cdot C_i \cdot k_{m-B,i}^*}{m_{max-B}^* + \sum C_i \cdot k_{m-B,i}^*}$	d ⁻¹	(30)
	with $i = \{P, hiq, loq\}$:		
Substrate dependent specific growth rate of bacterial pesticide degraders ^b	$\mu_{BP,i} = \frac{\mu_{max-BP}^* \cdot C_i \cdot k_{BP,i}^*}{\mu_{max-BP}^* + \sum C_i \cdot k_{BP,i}^*}$	d ⁻¹	(31)
Substrate dependent specific rate of maintenance respiration of bacterial pesticide degraders ^b	$m_{BP,i} = \frac{m_{max-BP}^* \cdot C_i \cdot k_{m-BP,i}^*}{m_{max-BP}^* + \sum C_i \cdot k_{m-BP,i}^*}$	d ⁻¹	(32)
Co-metabolic pesticide consumption rate of fungi ^c	$q_{F,P} = \left(T_{y-F}^* (\mu_{F,hiq} + \mu_{F,loq}) + k_{F,P}^* \right) \frac{C_P}{K_{S-F,P}^* + C_P}$	d ⁻¹	(33)
Endogenous maintenance rate of fungi due to co-metabolic pesticide degradation ^c	$m_{F,P} = \frac{q_{F,P}}{T_{F,P}^*}$	d ⁻¹	(34)
Specific death rate of bacteria ^d	$a_B = \frac{a_{max-B}^*}{1 + K_{a-B,hiq}^* \cdot C_{hiq} + K_{a-B,loq}^* \cdot C_{loq}}$	d ⁻¹	(35)

Specific death rate of fungi ^d	$a_F = \frac{a_{\max-F}^*}{1 + K_{a-F,hiq}^* \cdot C_{hiq} + K_{a-F,loq}^* \cdot C_{loq}}$	d^{-1}	(36)
Specific death rate of bacterial pesticide degraders ^d	$a_{BP} = \frac{a_{\max-BP}^*}{1 + K_{a-BP,P}^* \cdot C_P + K_{a-BP,hiq}^* \cdot C_{hiq} + K_{a-BP,loq}^* \cdot C_{loq}}$	d^{-1}	(37)
Specific rate of insoluble SOM decomposition by bacteria and bacterial pesticide degraders ^d	$q_B = \frac{q_{\max-B}^* \cdot C_I}{K_{I-B}^* + C_I}$	d^{-1}	(38)
Specific rate of insoluble SOM decomposition by fungi ^d	$q_F = \frac{q_{\max-F}^* \cdot C_I}{K_{I-F}^* + C_I}$	d^{-1}	(39)
Limiting factor of activity increase of bacteria ^d	$\Phi_B = \frac{C_{hiq} / k_{r-B,hiq}^* + C_{loq} / k_{r-B,loq}^*}{1 + C_{hiq} / k_{r-B,hiq}^* + C_{loq} / k_{r-B,loq}^*}$	Unitless	(40)
Limiting factor of activity increase of fungi ^d	$\Phi_F = \frac{C_{hiq} / k_{r-F,hiq}^* + C_{loq} / k_{r-F,loq}^*}{1 + C_{hiq} / k_{r-F,hiq}^* + C_{loq} / k_{r-F,loq}^*}$	Unitless	(41)
Limiting factor of activity increase of bacterial pesticide degraders ^d	$\Phi_{BP} = \frac{C_{hiq} / k_{r-BP,hiq}^* + C_{loq} / k_{r-BP,loq}^* + C_P / k_{r-BP,P}^*}{1 + C_{hiq} / k_{r-BP,hiq}^* + C_{loq} / k_{r-BP,loq}^* + C_P / k_{r-BP,P}^*}$	Unitless	(42)
Pore water velocity	$v = \frac{J_w^*}{\theta^*}$	mm d ⁻¹	(43)
Effective diffusion-dispersion coefficient of hiq DOC	$D_{e-hiq} = \lambda^* \cdot v + \xi \cdot D_{hiq}^*$	mm ² d ⁻¹	(44)
Effective diffusion-dispersion coefficient of loq DOC	$D_{e-loq} = \lambda^* \cdot v + \xi \cdot D_{loq}^*$	mm ² d ⁻¹	(45)
Effective diffusion-dispersion coefficient of pesticide	$D_{e-P} = \lambda^* \cdot v + \xi \cdot D_P^*$	mm ² d ⁻¹	(46)
Soil liquid tortuosity factor ^e	$\xi = \frac{\theta^{*7}}{\phi^2}$	Unitless	(47)
Porosity of soil	$\phi = 1 - \frac{\rho_B^*}{\rho_S^*}$	Unitless	(48)
Conversion factor to calculate the abundance of 16S rRNA genes from bacterial biomass	$f_{16S\ rRNA} = \frac{16S\ rRNA(t=0)^*}{f_B(t=0)^* \cdot C_{mic}(t=0)^*}$	copy number · (mg C) ⁻¹	(49)

Conversion factor to calculate the abundance of 18S rRNA genes from fungal biomass

$$f_{18S\ rRNA} = \frac{18S\ rRNA(t=0)^*}{(1-f_B(t=0)^*) \cdot C_{mic}(t=0)^*} \quad \text{copy number} \cdot (\text{mg C})^{-1} \quad (50)$$

Conversion factor to calculate the abundance of tfdA genes from biomass of bacterial pesticide degraders

$$f_{tfdA} = \frac{tfdA(t=0)^*}{f_{BP-B}(t=0)^* \cdot f_B(t=0)^* \cdot C_{mic}(t=0)^*} \quad \text{copy number} \cdot (\text{mg C})^{-1} \quad (51)$$

* indicates defined parameters, input values and material constants that are given in Online Resource 1.

^a modified from case 4 in (Rovira and Rovira 2010).

^b according to (Lendenmann and Egli 1998)

^c derived from (Criddle 1993)

^d based on (Blagodatsky and Richter 1998)

^e after (Millington and Quirk 1961)

5.4 Global sensitivity analysis

For simplicity, we use only the term “parameter”, even though we included both parameters and other model input, e.g. boundary conditions, in the sensitivity analysis. The PECCAD model is complex. Consequently, it contains a high number of parameters ($n=81$; see Online Resource 1). They can be derived *i*) from direct measurements, *ii*) by the use of data from independent experiments or *iii*) by calibrating the model against the target data set (inverse simulation). See Addiscott et al. (1995) for a discussion of how the way of parameter evaluation affects model validation. A global sensitivity analysis helps to identify the most important factors of model dynamics and efficiently reduces the number of parameters that require fitting (Saltelli 2008). Such, overparameterization can be avoided, which often occurs with complex non-linear environmental models as a consequence of equifinality (Beven and Freer 2001).

The global sensitivity analysis was performed in line with a series of microcosm experiments conducted to explore the temporally and spatially resolved dynamics of SOM and the model pesticide MCPA in soil.

The experiments are similar to those described by Poll et al. (2010). Briefly, small soil columns of 30 mm length and 56 mm diameter are filled with a homogeneous soil spiked with MCPA. We used a fertilized topsoil (loamy Luvisol; WRB 2006) from an agricultural field at the research station Scheyern (Germany; 48°30'N, 11°21'E; <http://www.helmholtz-muenchen.de/en/scheyern2/home/index.html>). Maize litter is placed on top of the soil cores and the cores are irrigated regularly. The soil cores are placed on suction plates to control the lower boundary condition and incubated in an airtight microcosm system.

In line with actually measured quantities in the related microcosm experiments, we chose 411 model outputs to be considered in the sensitivity analysis. The set of model outputs included several aggregated C pools and gene abundances in soil integrated over seven layers (0-1, 1-2, 2-3, 3-4, 4-6, 6-10 and 10-20 mm below a litter layer) at five sampling dates (4.89, 7.84, 10.03, 13.93 and 22.81 days of incubation) as well as ^{14}C and total CO_2 -fluxes released from the whole soil column at 13 sampling dates (0.83, 1.79, 3.76, 4.86, 5.77, 7.74, 8.75, 9.97, 13.76, 15.73, 18.77, 20.76, 22.74 days of incubation). CO_2 fluxes were averaged over each of the 13 sampling intervals. Simulated abundances of 16S rRNA and 18S rRNA genes as well as of the functional gene *tfmA* were derived from the modeled biomass of bacteria, fungi and bacterial pesticide degraders, respectively, using conversion factors (Eqs. 49-51; Table 2). Total DOC was calculated as:

$$DOC = C_{hiq} + C_{loq} + C_P \quad (52)$$

Total pesticide concentration was given by:

$$P = C_P + C_{S-P} \quad (53)$$

Total microbial biomass was derived by:

$$C_{mic} = C_F + C_B + C_{BP} \quad (54)$$

Several C pools were then aggregated as total organic carbon:

$$TOC = DOC + C_{S,hiq} + C_{S,loq} + P + C_{mic} \quad (55)$$

Accordingly, ^{13}C abundances and ^{14}C activities of these aggregated model outputs were calculated as $A_{^{14}\text{C}} CO_2$, $A_{^{14}\text{C}} C_{mic}$, $\delta^{13}\text{C} TOC$ and $A_{^{14}\text{C}} TOC$.

5.4.1 Methodology

We adopted the LH-OAT (“Latin Hypercube – One At a Time”) method of van Griensven et al. (2006), who used this method to analyze parameter sensitivities of a hydrological model (Soil and Water Assessment Tool, SWAT; Arnold et al. 1998). In brief, we sampled the parameter space by a Latin Hypercube method (McKay et al. 1979) at 100 different locations. At each sampling point individual parameter values were slightly varied (“one at a time”). We used the resulting parameter-sets (81 parameters, $n=8200$) as input for PECCAD and calculated the model outputs needed to determine relative parameter sensitivities. Global parameter sensitivities were calculated as the 90th percentile of partial relative sensitivities. Further methodical details are given in Online Resource 4.

5.5 Results and discussion

5.5.1 Model concept

To our knowledge, PECCAD is the first model that mechanistically simulates microbial dynamics and explicitly couples pesticide degradation with C dynamics in soil. The model is able to reproduce accelerated pesticide degradation due to fresh litter-C input. The acceleration is due to two mechanisms: *i*) direct stimulation of activity and growth of specific pesticide degraders and *ii*) increase in fungal activity and growth causing enhanced fungal co-metabolic degradation of the pesticide.

Soil microorganisms are genetically highly diverse (Whitman et al. 1998; Hawksworth 2001), leading to a multitude of potential microbial characteristics. Partitioning of the microbial community into a limited number of functional groups is an unavoidable simplification, necessary to obtain applicable C turnover models. Physiological traits of microorganisms substantially determine rates of ecological processes in response to environmental conditions. Thus, a next step towards a more mechanistic treatment of microbial-driven ecological functions in SOM

turnover models may be achieved by a more comprehensive incorporation of functional microbial traits on the community level linked with the explicit consideration of enzyme kinetics (Wallenstein and Hall 2012). A recent implementation of this concept can be found in the litter decomposition model DEMENT (Allison 2012). DEMENT explicitly considers the characteristics of microbial communities as well as those of various extracellular enzymes ($n=20-50$) and accounts for interactions between multiple microbial taxa ($n=100-200$). While these developments are promising, there is still a lack of available data to properly validate such complex models (Allison 2012). Wallenstein et al. (2012) explicitly addressed this issue as one outcome of the recent “*Second International Enzymes in the Environment Research Coordination Network Workshop: Incorporating Enzymes and Microbial Physiology*” by stating that “... Model development should occur in tandem with experimental design and data acquisition...”. With PECCAD we follow this suggestion. Thus, we consider only three microbial pools with a limited number of functional microbial traits. However, in contrast to other mechanistic models (e.g., Allison 2012, Moorhead and Sinsabaugh 2006), microbial pools in PECCAD have been chosen such that they can be measured directly by their taxonomic and functional genes. We think that this is a promising feature for a successful parameterization.

Similarly to the GDM model (Moorhead and Sinsabaugh 2006), each microbial pool simultaneously utilizes two pools containing DOC of differing quality. Compared to the detritusphere model of Ingwersen et al. (2008) this new feature makes the model more realistic and flexible, but it increases the number of parameters.

The mechanistic integration of microorganisms in C models has the potential to improve predictions of ecological functioning in response to climate change (McGuire and Treseder 2010; Todd-Brown et al. 2012). Likewise, modeling of priming effects induced by easily available C sources requires an explicit incorporation of microbial processes (Wutzler and Reichstein

2008). Accordingly, this also holds true for the main purpose of PECCAD: modeling the stimulating effect of litter-C (i.e. 'priming effect') on pesticide degradation in the detritosphere.

Mathematically, stimulated activity and growth due to additional substrate availability are primarily implemented by means of the multi-substrate growth of specific pesticide degraders and fungi (Table 2; Eqs. 31-32) in combination with the functions Φ_{BP} and Φ_F (Table 2; Eqs. 41, 42) regulating the activity of pesticide degraders and fungi. As illustrated in Fig. 2, the additional availability of *hiq* or *loq* DOC has a synergistic effect on both the activity state and the overall growth rate of specific pesticide degraders and fungi. Due to the nonlinearity of both functions, the increase in microbial activity and growth rate by the synergistic effect of additional substrates is relatively higher at low substrate availability and becomes constant if the concentration of at least one readily usable C source (such as C_{hiq}) is high. This feature supports the wide-spread observation that microbes adapt their strategy from simultaneous substrate utilization at low substrate levels to preferential utilization of the most growth-supporting substrate at high (i.e. not growth-limiting) substrate levels (Egli 2010; Harder and Dijkhuizen 1982).

In addition to stimulated pesticide degradation, the PECCAD model is able to simulate accelerated SOM decomposition triggered by the input of fresh DOC, since the decomposition of the insoluble SOM pool is controlled by the biomass of microbial pools (Table 1; Eq. 19). Higher growth and activity of microorganisms due to additional DOC input directly leads to increased insoluble SOM decomposition ('priming effect'). This feedback reflects the increased production of extracellular enzymes as a consequence of additional DOC input. The action of non-specific ox-

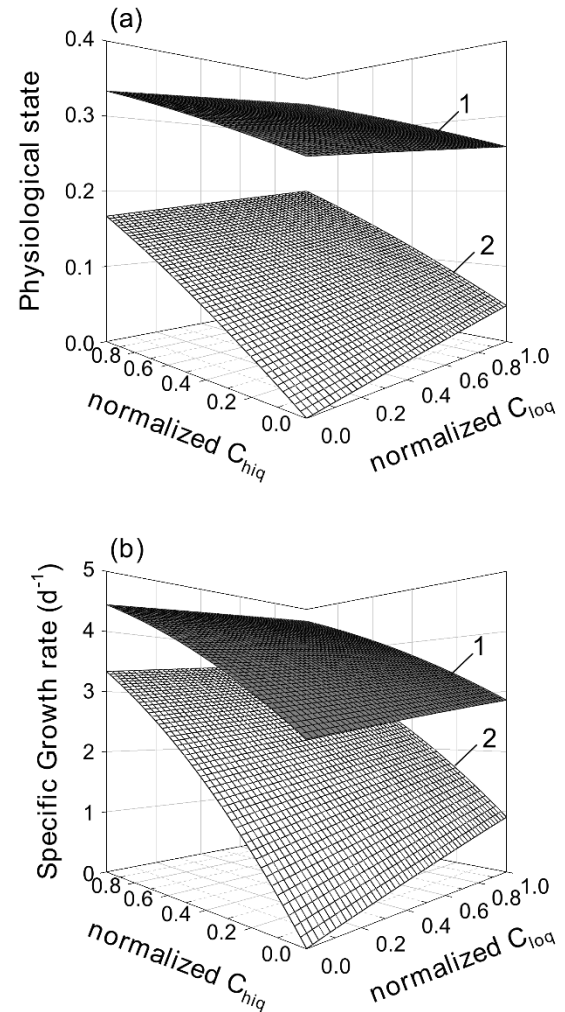


Fig. 2 Effect of substrate availability on **a** physiological state at steady state and **b** growth rate of microorganisms for pesticide levels of $C_P = 0.015 \text{ mg C g}^{-1}$ (1) and $C_P = 0 \text{ mg C g}^{-1}$ (2). Both functions were calculated according to corresponding formulations of specific pesticide degraders (Table 2, Eqs. 31, 42). Concentrations of *hiq* and *loq* DOC (C_{hiq} , C_{loq}) were assumed to be in the range of 0 to 0.1 mg C g^{-1} . Individual values of both variables were normalized to the maximum resulting in a range of [0...1]. Parameter values were chosen for illustrative purposes as follows:
 $k_{r-BP,P} = 0.05 \text{ mg C g}^{-1}$, $k_{r-BP,hiq} = 0.5 \text{ mg C g}^{-1}$
 $k_{r-BP,loq} = 2 \text{ mg C g}^{-1}$, $\mu_{max-BP} = 10 \text{ d}^{-1}$
 $k_{BP,P} = 200 \text{ g (mg C d)}^{-1}$, $k_{BP,hiq} = 50 \text{ g (mg C d)}^{-1}$
 $k_{BP,loq} = 50 \text{ g (mg C d)}^{-1}$

idative enzymes on both the insoluble SOM pool and the dissolved pesticide pool is only implicitly considered in the current version of the PECCAD model. Insoluble SOM decomposition and fungal co-metabolic pesticide decomposition are defined as flows that are directly controlled by the size and activity of biomass pools. This implementation implicitly reflects a biomass-coupled dynamic of enzyme production. An increase in microbial activity/ size results in higher production of non-specific enzymes and finally leads to increased decomposition of SOM and pesticide. A more direct coupling of SOM decomposition with the non-specific degradation of pesticide could be obtained by explicitly considering an additional independent pool of extracellular enzymes in a future version of the PECCAD model.

It is worthwhile to compare the basic concept of PECCAD to other studies modeling priming effects in soil. For instance, Blagodatsky et al. (2010) modeled enhanced SOM decomposition induced by addition of ^{14}C glucose in a short-term laboratory incubation experiment. They found that approaches considering microbial activity were best suited to match experimental $^{14}\text{CO}_2$ production data. However, for simplicity they considered only one microbial pool. Yet, the basic mechanism of accelerated decomposition of one C pool due to higher microbial activity and growth induced by a second pool of fresh C in soil is the same as that implemented in PECCAD. Other models also include formulations to capture enhanced growth of one or several specific microbial pools in response to additional fresh C or other nutrients (e.g., Fontaine and Barot 2005; Moorhead and Sinsabaugh 2006; Neill and Gignoux 2006; Parnas 1976), but other than PECCAD, they usually do not account for interactions between differing simultaneously utilized C substrates. In addition to the complex representation of microbial-driven processes, PECCAD considers sorption as well as convective and diffusive transport of both DOC and the pesticide as regulation mechanisms of substrate availability in soil.

Several studies have demonstrated that including $^{13}\text{C}/^{14}\text{C}$ pools or fluxes combined with appropriate isotopic measurement data can be very useful in parameterizing SOM models (e.g., Blagodatsky et al. 2010; Ingwersen et al. 2008; Niklaus and Falloon 2006; Pansu et al. 2009). Likewise, measurements of $^{14}\text{CO}_2$ mineralized from ^{14}C -labeled pesticides are often used to calibrate relatively simple pesticide decomposition models (e.g., Gaultier et al. 2008; Poll et al. 2010; Simkins and Alexander 1984). Isotopic labeling of pesticides generally allows for tracing the flow of pesticide C into soil pools, such as microbial biomass (Gonod et al. 2006; Lerch et al. 2009; Poll et al. 2010) and biogenic residues (Nowak et al. 2011). Accordingly, PECCAD explicitly simulates ^{13}C and ^{14}C isotopes, providing a basis for the use of isotopic data from the accompanying microcosm studies to facilitate parameter identification by inverse simulation.

5.5.2 Model dynamics

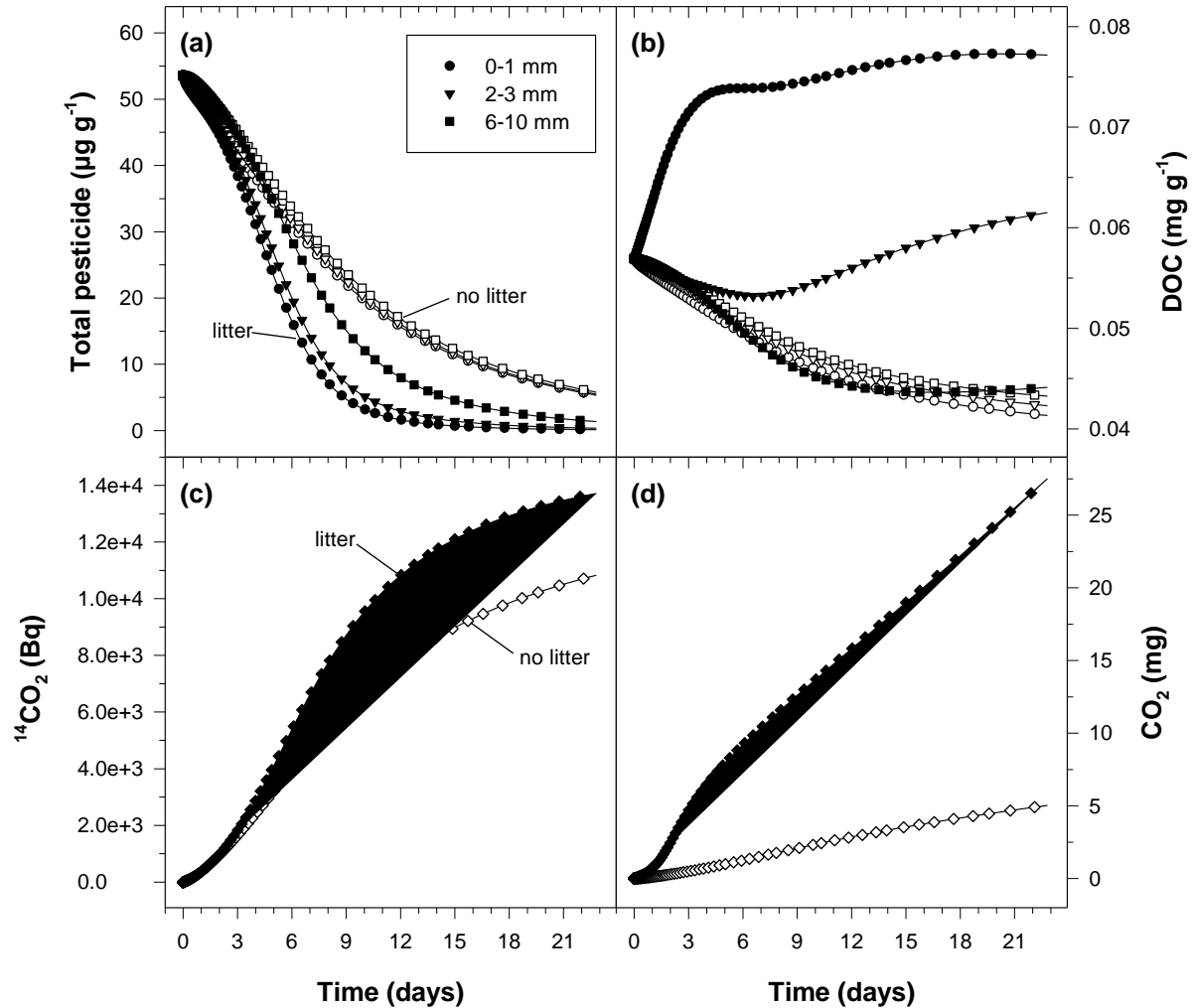


Fig. 3 Simulated substrate pools integrated over selected soil layers of 0-1 mm, 2-3 mm and 6-10 mm distance to litter (**a, b**); cumulative pesticide-derived $^{14}\text{CO}_2$ (**c**) and cumulative total CO_2 (**d**). PECCAD was run with default parameter and input values as given in Online Resource 1. Open symbols represent a simulation with-out litter addition and filled symbols for a simulation with litter addition ($C_{L,\text{tot}}(t=0) = 0$ vs. $C_{L,\text{tot}}(t=0) = 206 \text{ mg C}$).

We used the default parameter values given in Online Resource 1 to investigate the dynamics of soil and biomass pools in PECCAD with special emphasis on the effect of litter on pesticide (MCPA) degradation. We ran two PECCAD simulations with *i*) addition of litter, i.e. existence of soil-litter interface or *ii*) no addition of litter. PECCAD predicted accelerated pesticide degradation close to the soil-litter interface (Fig. 3a) and overall increased mineralization of ^{14}C -labelled pesticide in response to litter addition (Fig. 3b). Further, litter addition led to increased DOC concentration at the soil-litter interface (Fig. 3c) and higher CO_2 production (Fig. 3d). The simulated CO_2 and $^{14}\text{CO}_2$ dynamics are comparable to experimental observations in a previous microcosm study (Poll et al. 2010). Increased DOC concentrations at the soil-litter interface

induced enhanced activity and abundance of microbial populations (Fig. 4), with the most pronounced response nearest to the litter (0-1 mm distance).

Fungi benefit more from litter-derived DOC than bacteria. Higher proliferation of fungi is due to their lower maximal specific death rate coefficient ($a_{\max-F} = 0.35 d^{-1}$ vs. $a_{\max-B} = a_{\max-BP} = 1.30 d^{-1}$; Online Resource 1). The detritosphere model of Ingwersen et al. (2008) predicted higher growth of late-stage decomposers (dominated by fungi) at the soil-litter interface. Thus, despite its structural differences from Ingwersen et al. (2008), the PECCAD model with its flexible structure is able to simulate similar biomass dynamics.

The set of parameter values and in particular initial conditions used are related to microcosm studies conducted in our lab. They give only one possible realization of the PECCAD model but are suitable to generally demonstrate PECCAD's ability to simulate litter-stimulated pesticide degradation. In a next step, the model will be thoroughly tested and calibrated against data from a series of ongoing microcosm experiments.

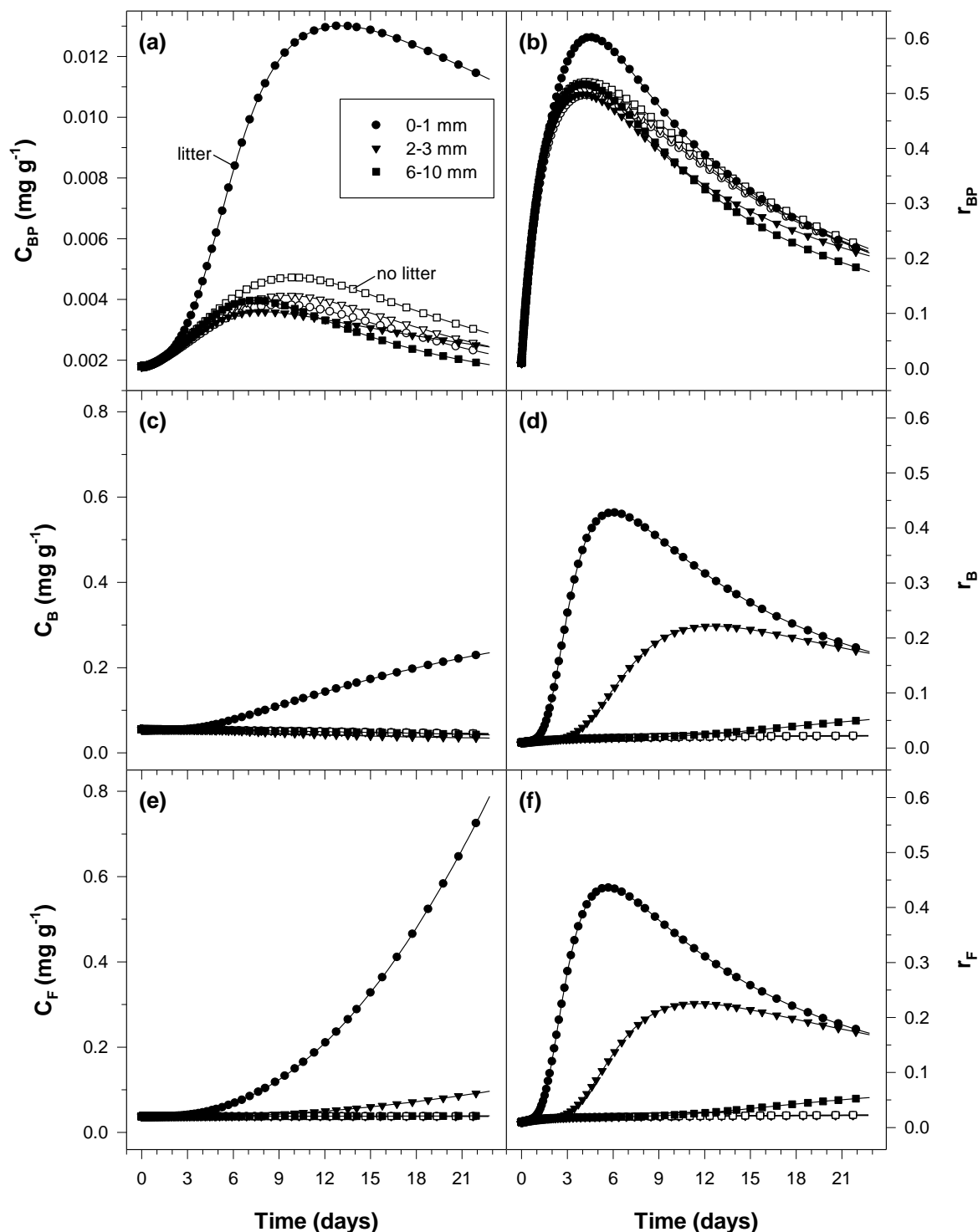


Fig. 4 Simulated dynamics of microbial biomass (a, c, e) and activity (b, d, f) integrated over selected soil layers of 0-1 mm, 2-3 mm and 6-10 mm distance to litter: a, b are specific bacterial pesticide degraders; c, d are bacteria; e, f are fungi. PECCAD was run with default parameter and input values as given in Online Resource 1. Open symbols stand for a simulation without litter addition and filled symbols for a simulation with litter addition ($C_{L,tot}(t=0) = 0$ vs. $C_{L,tot}(t=0) = 206 \text{ mg C}$).

5.5.3 Global sensitivity analysis

Estimated sensitivity indices of all considered parameters for all criteria are given in Online Resource 5. We defined the global sensitivity index (*GSI*); that is, the maximum taken over all sensitivity indices of a single criterion. Based on this *GSI* we classified parameters and input values as *i*) *very important* ($1.0 \geq GSI \geq 0.75$; $n=22$), *ii*) *important* ($0.75 > GSI \geq 0.50$; $n=11$), *iii*) *less important* ($0.50 > GSI \geq 0.25$; $n=28$) and *iv*) *not important* ($0.25 > GSI \geq 0.00$; $n=20$). The sensitivity of model output to *very important* and *important* parameters is illustrated in Fig. 5.

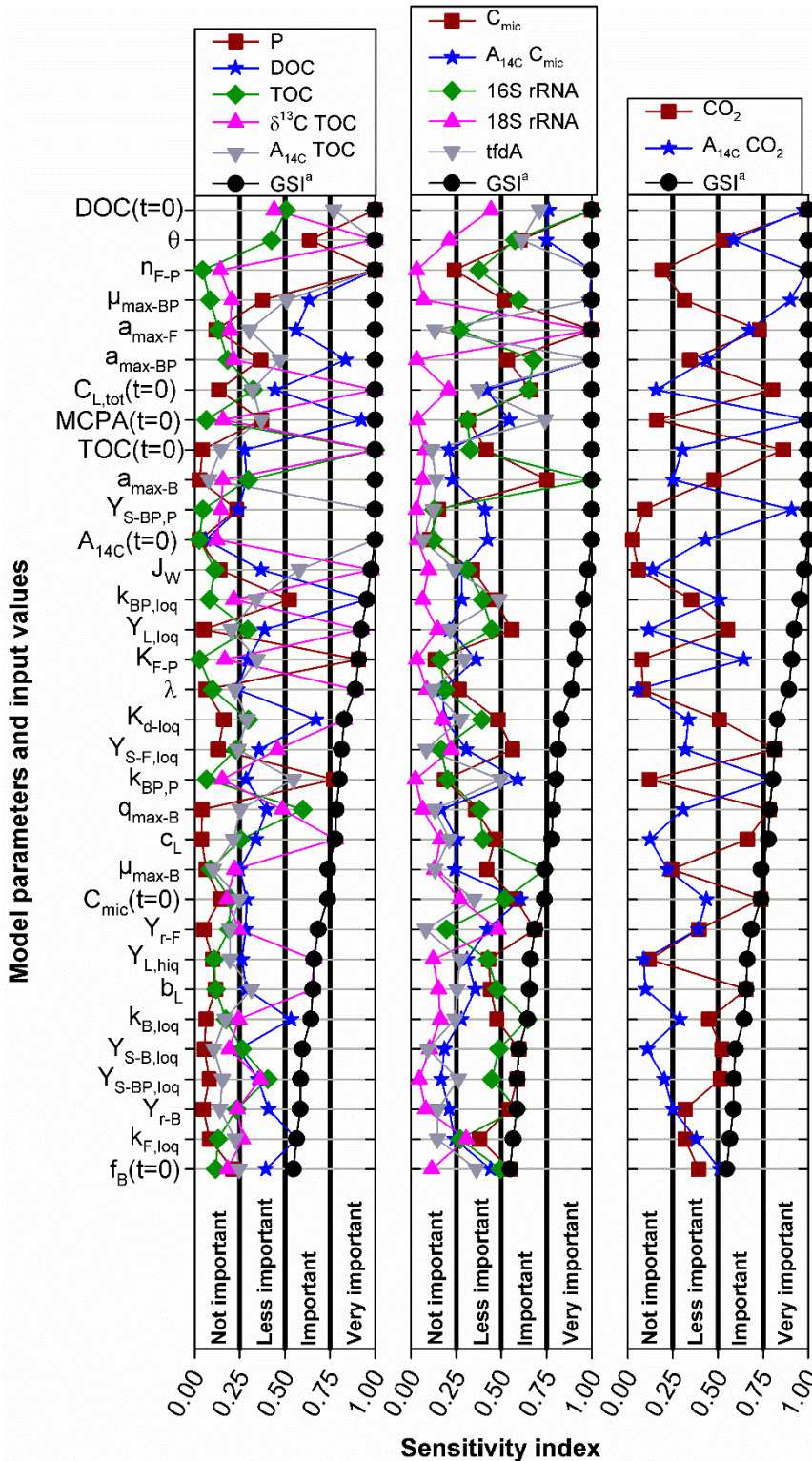


Fig. 5 Sensitivity of model output to *very important* and *important* parameters
(^a Global sensitivity index as defined in Online Resource 4)

Model parameters can be grouped into two categories. They can be either (A) directly measured or estimated from independent experiments, or they must be (B) fitted by inverse simulation. Category A parameter ranges were set according to uncertainty estimates (i.e. primarily 95% confidence limits) of mean values (Online Resource 1), whereas those of category B were defined on the basis of literature data. Thus, the calculated sensitivities of category A parameters will be used to discuss the impact of their uncertainty on the dynamics of PECCAD model pools.

About 41% ($n=33$) of all considered parameters are regarded as *important* or *very important*. Out of these 33 parameters 11 belong to category A and 22 are associated with category B.

Among the *important* or *very important* category B parameters are biokinetic parameters such as maximum growth and death rates (μ_{max} and a_{max}) of bacteria, fungi and bacterial pesticide degraders. Likewise, substrate affinity coefficients for growth on *loq* DOC ($k_{BP,loq}$, $k_{B,loq}$ and $k_{F,loq}$) have a high impact on model dynamics. Further, model output is highly sensitive to parameters controlling the decomposition of the insoluble SOM pool C_I ($q_{max,B}$, Y_{r-F} , Y_{r-B} and Y_{r-B}), substrate uptake efficiencies ($Y_{S-BP,P}$, $Y_{S-F,loq}$, $Y_{S-B,loq}$ and $Y_{S-BP,loq}$), parameters controlling sorption (K_{d-loq}) and transport with the soil solution ($Y_{L,loq}$, λ and $Y_{L,hiq}$) as well as to the initial composition of the microbial community ($f_B(t=0)$). Our sensitivity results are essentially in line with those of Ingwersen et al. (2008). They found highest sensitivities for maximum growth, death and SOM decomposition rates as well as for the fractions of initial and late stage litter (equivalent to *hiq* and *loq* litter in PECCAD) transferred to soil. Parameters controlling the activity of microbial pools ($r(t=0)$ and k_r) show the lowest sensitivity in their study, which is consistent with the results presented here. In addition to microbial activity parameters, we also identified coefficients linked with bacterial maintenance kinetics (C_B , C_{BP}) as *not important*. These parameters were fixed to default values in the study of Ingwersen et al. (2008). The low importance of parameters related to exogenous maintenance results from the relatively low contribution of the corresponding C fluxes to total C turnover compared to microbial growth and death processes. In contrast, model output shows a higher sensitivity to parameters related to fungal endogenous maintenance (a_{max-F} , Y_{r-F}) because this process has a larger contribution on overall C turnover. Recall that, although the detritusphere model of Ingwersen et al. (2008) served as a basis for the development of PECCAD, there are distinct differences between the models, in particular in the structure of microbial populations.

Among the category A parameters, uncertainties of initial DOC concentration ($DOC(t=0)$) and volumetric water content (θ) have the greatest influence of all considered input on several

outputs simultaneously. *Very important* and *important* category A parameters are several measured initial quantities ($C_{L,tot}(t=0)$, $MCPA(t=0)$, $TOC(t=0)$, $A_{14C}(t=0)$, $C_{mic}(t=0)$) as well as independently estimated sorption parameters ($n_{F,P}$, K_{F-P}) and parameters used with the empirical litter decomposition model (b_L , c_L). Both litter decomposition parameters are included in the function f_L (Table 2, Eq. 26), which calculates the fraction of *hiq* litter on total litter decomposition and controls the associated fluxes of *hiq* and *loq* DOC from litter into soil. Ingwersen et al. (2008) also found high sensitivities for the parameters of a Weibull function that regulates the fraction of initial-stage litter (equivalent to *hiq* litter in PECCAD) on total litter decomposition.

The global sensitivity analysis gave reasonable and coherent results in terms of causes and effects. Thus, highest biokinetic parameter sensitivities of specific microbial pools are typically linked to corresponding microbial proxies (16S rRNA, 18S rRNA, *tfmA*) and associated substrate pools. Likewise, parameter sensitivities properly reflect simulated decomposition and transport processes of the model. For instance, several parameters linked with fungi or specific bacterial pesticide degraders show a high sensitivity for pesticide and ^{14}C pools in soil in conjunction with the production rate of $^{14}CO_2$, thereby reflecting the direct utilization of pesticide by both microbial populations. In contrast, ^{14}C model output is typically less sensitive to parameters associated with bacteria. This makes sense because bacteria do not directly utilize ^{14}C -labeled pesticide. Another example of consistent sensitivity results is related to the high-leverage transport parameters λ , $Y_{L,hiq}$ and $Y_{L,loq}$. These parameters have a strong impact on the modeled $\delta^{13}C - TOC$ dynamics, which reflects their direct effect on litter-C transport.

5.6 Conclusion and outlook

Due to its sophisticated representation of microbial populations and microbial-driven processes the PECCAD model can be utilized as a tool for studying regulation mechanisms of accelerated pesticide degradation (i.e. priming effects) in the detritusphere. The model will be particularly useful to evaluate ^{13}C and ^{14}C data from microcosm experiments. As a consequence of the sensitivity analysis we recommend to setting all parameters classified as *not important* (and perhaps also the *less important* ones) to default values.

The new model will be calibrated and validated using the data from a series of microcosm experiments. The simulation of experimentally amenable gene abundances and isotopic C pools is a promising feature to successfully parameterize PECCAD using sophisticated inverse techniques.

5.7 Acknowledgements

We thank Kathleen Regan for English corrections and gratefully acknowledge the funding (KA 1590/5-2 and STR 481/3-2) by Deutsche Forschungsgemeinschaft (DFG) in the frame of the priority program SPP 1315: "Biogeochemical Interfaces in Soil". We gratefully appreciate the valuable recommendations of three unknown reviewers.

5.8 References

- Addiscott T, Smith J, Bradbury N (1995) Critical evaluation of models and their parameters. *J Environ Qual* 24 (5):803-807
- Allison SD (2012) A trait-based approach for modelling microbial litter decomposition. *Ecol Lett* 15 (9):1058-1070. doi:10.1111/j.1461-0248.2012.01807.x
- Alvarez-Cohen L, Speitel Jr GE (2001) Kinetics of aerobic cometabolism of chlorinated solvents. *Biodegrad* 12 (2):105-126
- Arnold JG, Srinivasan R, Muttiah RS, Williams JR (1998) Large area hydrologic modeling and assessment part I: Model development. *J Am Water Resour Assoc* 34 (1):73-89
- Beare MH, Coleman DC, Crossley Jr DA, Hendrix PF, Odum EP (1995) A hierarchical approach to evaluating the significance of soil biodiversity to biogeochemical cycling. *Plant Soil* 170 (1):5-22
- Beven K, Freer J (2001) Equifinality, data assimilation, and uncertainty estimation in mechanistic modelling of complex environmental systems using the GLUE methodology. *J Hydrol* 249 (1-4):11-29. doi:10.1016/s0022-1694(01)00421-8
- Blagodatskaya E, Kuzyakov Y (2008) Mechanisms of real and apparent priming effects and their dependence on soil microbial biomass and community structure: Critical review. *Biol Fert Soils* 45 (2):115-131. doi:10.1007/s00374-008-0334-y
- Blagodatsky S, Blagodatskaya E, Yuyukina T, Kuzyakov Y (2010) Model of apparent and real priming effects: Linking microbial activity with soil organic matter decomposition. *Soil Biol Biochem* 42 (8):1275-1283. doi:10.1016/j.soilbio.2010.04.005
- Blagodatsky S, Grote R, Kiese R, Werner C, Butterbach-Bahl K (2011) Modelling of microbial carbon and nitrogen turnover in soil with special emphasis on N-trace gases emission. *Plant Soil* 346 (1):297-330. doi:10.1007/s11104-011-0821-z
- Blagodatsky SA, Richter O (1998) Microbial growth in soil and nitrogen turnover: A theoretical model considering the activity state of microorganisms. *Soil Biol Biochem* 30 (13):1743-1755
- Blume H-P, Brümmer GW, Horn R, Kandeler E, Kögel-Knabner I, Kretzschmar R, Stahr K, Wilke B-M (2010) Scheffer/Schachtschabel: Lehrbuch der Bodenkunde. 16 ed. Spektrum Akademischer Verlag, Heidelberg
- Bosatta E, Ågren GI (2003) Exact solutions to the continuous-quality equation for soil organic matter turnover. *J Theor Biol* 224 (1):97-105. doi:10.1016/s0022-5193(03)00147-4
- Bosatta E, Ågren GI (1991) Dynamics of carbon and nitrogen in the organic matter of the soil: a generic theory. *Am Nat* 138 (1):227-245
- Braakhekke MC, Beer C, Hoosbeek MR, Reichstein M, Kruijt B, Schrumph M, Kabat P (2011) Somprof: A vertically explicit soil organic matter model. *Ecol Model* 222 (10):1712-1730. doi:10.1016/j.ecolmodel.2011.02.015
- Brusseu ML, Sandrin SK, Li L, Yolcubal I, Jordan FL, Maier RM (2006) Biodegradation during contaminant transport in porous media: 8. The influence of microbial system variability on transport behavior and parameter determination. *W Resour Res* 42 (4):W04406. doi:10.1029/2005wr004112
- Carpenter SR (1981) Decay of heterogenous detritus: A general model. *J Theor Biol* 89 (4):539-547

- Cheyens K, Mertens J, Diels J, Smolders E, Springael D (2010) Monod kinetics rather than a first-order degradation model explains atrazine fate in soil mini-columns: Implications for pesticide fate modelling. *Environ Pollut* 158 (5):1405-1411. doi:10.1016/j.envpol.2009.12.041
- Criddle CS (1993) The kinetics of cometabolism. *Biotechnol Bioeng* 41 (11):1048-1056
- De Wilde T, Mertens J, Šimunek J, Sniegowksi K, Ryckeboer J, Jaeken P, Springael D, Spanoghe P (2009) Characterizing pesticide sorption and degradation in microscale biopurification systems using column displacement experiments. *Environ Pollut* 157 (2):463-473. doi:10.1016/j.envpol.2008.09.008
- Doherty J (2005) PEST: Model Independent Parameter Estimation. 5th ed. Watermark Numerical Computing, Brisbane, Australia
- Dubus IG, Beulke S, Brown CD, Gottesbüren B, Dieses A (2004) Inverse modelling for estimating sorption and degradation parameters for pesticides. *Pest Manag Sci* 60 (9):859-874. doi:10.1002/ps.893
- Dungait JAJ, Hopkins DW, Gregory AS, Whitmore AP (2012) Soil organic matter turnover is governed by accessibility not recalcitrance. *Glob Chang Biol* 18 (6):1781-1796. doi:10.1111/j.1365-2486.2012.02665.x
- Egli T (2010) How to live at very low substrate concentration. *W Res* 44 (17):4826-4837. doi:10.1016/j.watres.2010.07.023
- Ekschmitt K, Kandeler E, Poll C, Brune A, Buscot F, Friedrich M, Gleixner G, Hartmann A, Kästner M, Marhan S, Miltner A, Scheu S, Wolters V (2008) Soil-carbon preservation through habitat constraints and biological limitations on decomposer activity. *J Plant Nutr Soil Sci* 171 (1):27-35. doi:10.1002/jpln.200700051
- Estrella MR, Brusseau ML, Maier RS, Pepper IL, Wierenga PJ, Miller RM (1993) Biodegradation, sorption, and transport of 2,4-dichlorophenoxyacetic acid in saturated and unsaturated soils. *Appl Environ Microbiol* 59 (12):4266-4273
- Fan Z, Neff JC, Wickland KP (2010) Modeling the production, decomposition, and transport of dissolved organic carbon in boreal soils. *Soil Sci* 175 (5):223-232. doi:10.1097/SS.0b013e3181e0559a
- Feng Y (2009) K-model-A continuous model of soil organic carbon dynamics: Theory. *Soil Sci* 174 (9):482-493. doi:10.1097/SS.0b013e3181bb0f80
- Fierer N, Bradford MA, Jackson RB (2007) Toward an ecological classification of soil bacteria. *Ecol* 88 (6):1354-1364. doi:10.1890/05-1839
- Fontaine S, Barot S (2005) Size and functional diversity of microbe populations control plant persistence and long-term soil carbon accumulation. *Ecol Lett* 8 (10):1075-1087. doi:10.1111/j.1461-0248.2005.00813.x
- Fontaine S, Mariotti A, Abbadie L (2003) The priming effect of organic matter: A question of microbial competition? *Soil Biol Biochem* 35 (6):837-843. doi:10.1016/s0038-0717(03)00123-8
- Gaillard V, Chenu C, Recous S (2003) Carbon mineralisation in soil adjacent to plant residues of contrasting biochemical quality. *Soil Biol Biochem* 35 (1):93-99
- Garnier P, Néel C, Mary B, Lafolie F (2001) Evaluation of a nitrogen transport and transformation model in a bare soil. *Eur J Soil Sci* 52 (2):253-268
- Gaultier J, Farenhorst A, Cathcart J, Goddard T (2008) Degradation of [carboxyl-14C] 2,4-D and [ring-U-14C] 2,4-D in 114 agricultural soils as affected by soil organic carbon content. *Soil Biol Biochem* 40 (1):217-227. doi:10.1016/j.soilbio.2007.08.003
- Gerhardt KE, Huang XD, Glick BR, Greenberg BM (2009) Phytoremediation and rhizoremediation of organic soil contaminants: Potential and challenges. *Plant Sci* 176 (1):20-30. doi:10.1016/j.plantsci.2008.09.014
- Ghafoor A, Jarvis NJ, Thierfelder T, Stenström J (2011) Measurements and modeling of pesticide persistence in soil at the catchment scale. *Sci Total Environ* 409 (10):1900-1908. doi:10.1016/j.scitotenv.2011.01.049
- Ghani A, Wardle DA (2001) Fate of 14C from glucose and the herbicide metsulfuron-methyl in a plant-soil microcosm system. *Soil Biol Biochem* 33 (6):777-785. doi:10.1016/s0038-0717(00)00225-x
- Gignoux J, House J, Hall D, Masse D, Nacro HB, Abbadie L (2001) Design and test of a generic cohort model of soil organic matter decomposition: The SOMKO model. *Glob Ecol and Biogeogr* 10 (6):639-660

- Gjettermann B, Styczen M, Hansen HCB, Vinther FP, Hansen S (2008) Challenges in modelling dissolved organic matter dynamics in agricultural soil using DAISY. *Soil Biol Biochem* 40 (6):1506-1518. doi:10.1016/j.soilbio.2008.01.005
- Gonod LV, Martin-Laurent F, Chenu C (2006) 2,4-D impact on bacterial communities, and the activity and genetic potential of 2,4-D degrading communities in soil. *FEMS Microbiol Ecol* 58 (3):529-537. doi:10.1111/j.1574-6941.2006.00159.x
- Harder W, Dijkhuizen L (1982) Strategies of mixed substrate utilization in microorganisms. *Philos Trans R Soc Lond Ser B: Biol Sci* 297 (1088):459-480
- Hawksworth DL (2001) The magnitude of fungal diversity: The 1.5 million species estimate revisited. *Mycol Res* 105 (12):1422-1432
- Henriksen TM, Breland TA (1999) Nitrogen availability effects on carbon mineralization, fungal and bacterial growth, and enzyme activities during decomposition of wheat straw in soil. *Soil Biol Biochem* 31 (8):1121-1134. doi:10.1016/s0038-0717(99)00030-9
- Higuchi R, Fockler C, Dollinger G, Watson R (1993) Kinetic PCR analysis: Real-time monitoring of DNA amplification reactions. *Nat Biotechnol* 11 (9):1026-1030
- Ingwersen J, Poll C, Streck T, Kandeler E (2008) Micro-scale modelling of carbon turnover driven by microbial succession at a biogeochemical interface. *Soil Biol Biochem* 40 (4):872-886
- Jenkinson DS, Rayner JH (1977) The turnover of soil organic matter in some of the Rothamsted classical experiments. *Soil Sci* 123 (5):298-305
- Jennings DH, Lysek G (1999) *Fungal biology: understanding the fungal lifestyle*. 2nd edn. Bios Scientific Publishers, Oxford
- Jensen PH, Hansen HCB, Rasmussen J, Jacobsen OS (2004) Sorption-controlled degradation kinetics of MCPA in soil. *Environ Sci Technol* 38 (24):6662-6668
- Kandeler E, Luxhøi J, Tschirko D, Magid J (1999) Xylanase, invertase and protease at the soil-litter interface of a loamy sand. *Soil Biol Biochem* 31 (8):1171-1179
- Kögel-Knabner I (2002) The macromolecular organic composition of Plant and microbial residues as inputs to soil organic matter. *Soil Biol Biochem* 34 (2):139-162
- Köhne JM, Köhne S, Šimunek J (2006) Multi-process herbicide transport in structured soil columns: Experiments and model analysis. *J Contaminant Hydrology* 85 (1-2):1-32. doi:10.1016/j.jconhyd.2006.01.001
- Kuzyakov Y (2010) Priming effects: Interactions between living and dead organic matter. *Soil Biol Biochem* 42 (9):1363-1371. doi:10.1016/j.soilbio.2010.04.003
- Kuzyakov Y, Friedel JK, Stahr K (2000) Review of mechanisms and quantification of priming effects. *Soil Biol Biochem* 32 (11-12):1485-1498. doi:10.1016/s0038-0717(00)00084-5
- Langner HW, Inskeep WP, Gaber HM, Jones WL, Das BS, Wraith JM (1998) Pore water velocity and residence time effects on the degradation 2,4-D during transport. *Environ Sci Technol* 32 (9):1308-1315. doi:10.1021/es970834q
- Leistra M, van der Linden AMA, Boesten JJTI, Tiktak A, van den Berg F (2001) PEARL model for pesticide behaviour and emissions in soil-plant systems: Description of the processes in FOCUS PEARL version 1.1.1. Alterra Rep. 013. Alterra, Wageningen
- Lendenmann U, Egli T (1998) Kinetic models for the growth of *Escherichia coli* with mixtures of sugars under carbon-limited conditions. *Biotechnol and Bioeng* 59 (1):99-107
- Lerch TZ, Dignac MF, Nunan N, Bardoux G, Barriuso E, Mariotti A (2009) Dynamics of soil microbial populations involved in 2,4-D biodegradation revealed by FAME-based Stable Isotope Probing. *Soil Biol Biochem* 41 (1):77-85
- Macey R, Oster G, Zahnley T (2000) *Berkeley Madonna User's Guide 8.0*. University of California, Department of Molecular and Cellular Biology, Berkeley

- McKay MD, Beckman RJ, Conover WJ (1979) Comparison of three methods for selecting values of input variables in the analysis of output from a computer code. *Technometrics* 21 (2):239-245
- Manzoni S, Porporato A (2009) Soil carbon and nitrogen mineralization: Theory and models across scales. *Soil Biol Biochem* 41 (7):1355-1379
- Marschner B, Kalbitz K (2003) Controls of bioavailability and biodegradability of dissolved organic matter in soils. *Geoderma* 113 (3-4):211-235. doi:10.1016/s0016-7061(02)00362-2
- McGuire KL, Treseder KK (2010) Microbial communities and their relevance for ecosystem models: Decomposition as a case study. *Soil Biol Biochem* 42 (4):529-535. doi:10.1016/j.soilbio.2009.11.016
- Mertens J, Kahl G, Gottesbüren B, Vanderborgh J (2009) Inverse modeling of pesticide leaching in lysimeters: Local versus global and sequential single-objective versus multiobjective approaches. *Vadose Zone J* 8 (3):793-804. doi:10.2136/vzj2008.0029
- Michalzik B, Tipping E, Mulder J, Gallardo Lancho JF, Matzner E, Bryant CL, Clarke N, Lofts S, Vicente Esteban MA (2003) Modelling the production and transport of dissolved organic carbon in forest soils. *Biogeochem* 66 (3):241-264. doi:10.1023/b:biog.0000005329.68861.27
- Millington RJ, Quirk JP (1961) Permeability of porous solids. *Trans Faraday Soc* 57:1200-1207. doi:10.1039/tf9615701200
- Moorhead DL, Sinsabaugh RL (2006) A theoretical model of litter decay and microbial interaction. *Ecol Monogr* 76 (2):151-174
- Neff JC, Asner GP (2001) Dissolved organic carbon in terrestrial ecosystems: Synthesis and a model. *Ecosyst* 4 (1):29-48. doi:10.1007/s100210000058
- Neill C, Gignoux J (2006) Soil organic matter decomposition driven by microbial growth: A simple model for a complex network of interactions. *Soil Biol Biochem* 38 (4):803-811
- Niklaus PA, Falloon P (2006) Estimating soil carbon sequestration under elevated CO₂ by combining carbon isotope labelling with soil carbon cycle modelling. *Glob Change Biol* 12 (10):1909-1921. doi:10.1111/j.1365-2486.2006.01215.x
- Nowak KM, Miltner A, Gehre M, Schäffer A, Kästner M (2011) Formation and fate of bound residues from microbial biomass during 2, 4-D degradation in soil. *Environ Sci Technol* 45 (3):999-1006. doi:10.1021/es103097f
- Panikov NS (1995) *Microbial growth kinetics*. 1 ed. Chapman & Hall, Weinheim
- Panikov NS (1999) Understanding and prediction of soil microbial community dynamics under global change. *Appl Soil Ecol* 11 (2-3):161-176. doi:10.1016/s0929-1393(98)00143-7
- Pansu M, Martineau Y, Saugier B (2009) A modelling method to quantify in situ the input of carbon from roots and the resulting C turnover in soil. *Plant Soil* 317 (1-2):103-120. doi:10.1007/s11104-008-9791-1
- Parnas H (1976) A theoretical explanation of the priming effect based on microbial growth with two limiting substrates. *Soil Biol Biochem* 8 (2):139-144
- Parton WJ (1993) Observations and modeling of biomass and soil organic matter dynamics for the grassland biome worldwide. *Glob Biogeochem Cycle* 7 (4):785-809
- Paul EA (2007) *Soil microbiology, ecology, and biochemistry*. 3. ed. Academic Press, Amsterdam
- Paustian K, Schnürer J (1987) Fungal growth response to carbon and nitrogen limitation: A theoretical model. *Soil Biol Biochem* 19 (5):613-620
- PDE Solutions Inc. (2011) *FlexPDE 6.20 - finite element model builder for Partial Differential Equations*. WA, USA
- Poll C, Ingwersen J, Stemmer M, Gerzabek MH, Kandeler E (2006) Mechanisms of solute transport affect small-scale abundance and function of soil microorganisms in the detritosphere. *Eur J Soil Sci* 57 (4):583-595
- Poll C, Marhan S, Ingwersen J, Kandeler E (2008) Dynamics of litter carbon turnover and microbial abundance in a rye detritosphere. *Soil Biol Biochem* 40 (6):1306-1321

- Poll C, Pagel H, Devers-Lamrani M, Martin-Laurent F, Ingwersen J, Streck T, Kandeler E (2010) Regulation of bacterial and fungal MCPA degradation at the soil-litter interface. *Soil Biol Biochem* 42 (10):1879-1887. doi:10.1016/j.soilbio.2010.07.013
- Richter O, Diekkrüger B, Nörtersheuser P (1996) Environmental fate modelling of pesticides: from the laboratory to the field scale. VCH, Weinheim
- Roulier S, Jarvis N (2003) Modeling macropore flow effects on pesticide leaching: Inverse parameter estimation using microlysimeters. *J Environ Qual* 32 (6):2341-2353
- Rovira P, Rovira R (2010) Fitting litter decomposition datasets to mathematical curves: Towards a generalised exponential approach. *Geoderma* 155 (3-4):329-343. doi:10.1016/j.geoderma.2009.11.033
- Russell JB, Cook GM (1995) Energetics of bacterial growth: Balance of anabolic and catabolic reactions. *Microbiol Rev* 59 (1):48-62
- Saltelli A (2008) Global sensitivity analysis. the primer. Wiley, Chichester
- Scharnagl B, Vrugt JA, Vereecken H, Herbst M (2010) Information content of incubation experiments for inverse estimation of pools in the Rothamsted carbon model: A Bayesian perspective. *Biogeosci* 7 (2):763-776
- Schimel JP, Weintraub MN (2003) The implications of exoenzyme activity on microbial carbon and nitrogen limitation in soil: A theoretical model. *Soil Biol Biochem* 35 (4):549-563. doi:10.1016/s0038-0717(03)00015-4
- Schmidt MWI, Torn MS, Abiven S, Dittmar T, Guggenberger G, Janssens IA, Kleber M, Kögel-Knabner I, Lehmann J, Manning DAC, Nannipieri P, Rasse DP, Weiner S, Trumbore SE (2011) Persistence of soil organic matter as an ecosystem property. *Nat* 478 (7367):49-56. doi:10.1038/nature10386
- Scow KM, Johnson CR (1996) Effect of Sorption on Biodegradation of Soil Pollutants. *Adv Agron* 58 (C):1-56. doi:10.1016/s0065-2113(08)60252-7
- Shaw LJ, Burns RG (2003) Biodegradation of Organic Pollutants in the Rhizosphere. *Adv Appl Microbiol* 53:60-1. doi:10.1016/s0065-2164(03)53001-5
- Shelton DR, Doherty MA (1997) A model describing pesticide bioavailability and biodegradation in soil. *Soil Sci Soc Am J* 61 (4):1078-1084
- Simkins S, Alexander M (1984) Models for mineralization kinetics with the variables of substrate concentration and population density. *Appl Environ Microbiol* 47 (6):1299-1306
- Šimůnek J, Šejna M, Saito H, Sakai M, van Genuchten MT (2008) The HYDRUS-1D Software Package for Simulating the Movement of Water, Heat, and Multiple Solutes in Variably Saturated Media, Version 4.08. HYDRUS Software Series 3. Department of Environmental Sciences, University of California Riverside, Riverside
- Skjemstad JO, Spouncer LR, Cowie B, Swift RS (2004) Calibration of the Rothamsted organic carbon turnover model (RothC ver. 26.3), using measurable soil organic carbon pools. *Aust J Soil Res* 42 (1):79-88. doi:10.1071/sr03013
- Smith P, Smith JU, Powlson DS, McGill WB, Arah JRM, Chertov OG, Coleman K, Franko U, Frolking S, Jenkinson DS, Jensen LS, Kelly RH, Klein-Gunnewiek H, Komarov AS, Li C, Molina JAE, Mueller T, Parton WJ, Thornley JHM, Whitmore AP (1997) A comparison of the performance of nine soil organic matter models using datasets from seven long-term experiments. *Geoderma* 81 (1-2):153-225. doi:10.1016/s0016-7061(97)00087-6
- Streck T, Richter J (1999) Field-scale study of chlortoluron movement in a sandy soil over winter: II. Modeling. *J Environ Qual* 28 (6):1824-1831
- Todd-Brown KEO, Hopkins FM, Kivlin SN, Talbot JM, Allison SD (2012) A framework for representing microbial decomposition in coupled climate models. *Biogeochem* 109 (1-3):19-33. doi:10.1007/s10533-011-9635-6
- Totsche KU, Rennert T, Gerzabek MH, Kögel-Knabner I, Smalla K, Spiteller M, Vogel HJ (2010) Biogeochemical interfaces in soil: The interdisciplinary challenge for soil science. *J Plant Nutr Soil Sci* 173 (1):88-99. doi:10.1002/jpln.200900105

- van Griensven A, Meixner T, Grunwald S, Bishop T, Diluzio M, Srinivasan R (2006) A global sensitivity analysis tool for the parameters of multi-variable catchment models. *J Hydrol* 324 (1-4):10-23
- Van Veen JA, Paul EA (1981) Organic carbon dynamics in grassland soils. 1. Background information and computer simulation. *Can J Soil Sci* 61 (2):185-201. doi:10.4141/cjss81-024
- Vrugt JA, Robinson BA (2007) Improved evolutionary optimization from genetically adaptive multimethod search. *Proc Natl Acad Sci U S A* 104 (3):708-711. doi:10.1073/pnas.0610471104
- Wallenstein M, Stromberger M, Bell C (2012) Bridging the gap between modelers and experimentalists. *Eos Trans AGU* 93 (32). doi:10.1029/2012eo320005
- Wallenstein MD, Hall EK (2012) A trait-based framework for predicting when and where microbial adaptation to climate change will affect ecosystem functioning. *Biogeochem* 109 (1-3):35-47. doi:10.1007/s10533-011-9641-8
- Whitman WB, Coleman DC, Wiebe WJ (1998) Prokaryotes: The unseen majority. *Proc Natl Acad Sci U S A* 95 (12):6578-6583. doi:10.1073/pnas.95.12.6578
- WRB (2006) World reference base for soil resources 2006. *World Soil Res Rep*. FAO, Rome
- Wutzler T, Reichstein M (2008) Colimitation of decomposition by substrate and decomposers - A comparison of model formulations. *Biogeosci* 5 (3):749-759
- Young IM, Crawford JW, Nunan N, Otten W, Spiers A (2009) Chapter 4 Microbial Distribution in Soils. *Physics and Scaling*. *Adv Agron* 100 (C):81-121. doi:10.1016/s0065-2113(08)00604-4
- Yurova A, Sirin A, Buffam I, Bishop K, Laudon H (2008) Modeling the dissolved organic carbon output from a boreal mire using the convection-dispersion equation: Importance of representing sorption. *W Resour Res* 44 (7):W07411. doi:10.1029/2007wr006523
- Zander C, Streck T, Kumke T, Altfelder S, Richter J (1999) Field-scale study of chlortoluron movement in a sandy soil over winter: I. Experiments. *J Environ Qual* 28 (6):1817-1823
- Zimmermann M, Leifeld J, Schmidt MWI, Smith P, Fuhrer J (2007) Measured soil organic matter fractions can be related to pools in the RothC model. *Eur J Soil Sci* 58 (3):658-667. doi:10.1111/j.1365-2389.2006.00855.x

5.9 Online Resources

Online Resource 1:

Parameters, input variables and material constants used in the PECCAD model

Corresponding paper:

Micro-scale modeling of pesticide degradation coupled to carbon turnover in the detritosphere - Model description and sensitivity analysis

Holger Pagel¹, Joachim Ingwersen¹, Christian Poll², Ellen Kandeler², Thilo Streck¹

¹ *Institute of Soil Science and Land Evaluation, Biogeophysics, University of Hohenheim, D-70593 Stuttgart, Germany*

² *Institute of Soil Science and Land Evaluation, Soil Biology, University of Hohenheim, D-70593 Stuttgart, Germany*

Corresponding author:

Holger Pagel

Institute of Soil Science and Land Evaluation, Biogeophysics
University of Hohenheim
Emil-Wolff-Str. 27
D-70593 Stuttgart, Germany

Tel.: (+49)711 459 23383

Fax: (+49)711 459 23117

holgerp@uni-hohenheim.de

Table 1 Parameters, input variables and material constants used in the PECCAD model

Symbol	Definition	Default Value	Lower bound	Upper bound	Unit	Source
<i>Litter layer</i>						
b_L	Empirical parameter of litter decomposition rate At time $\sqrt{b_L}$ the decomposition rate reaches its maximum value $k_{L,max}$	4.79 ^a	1.85 ^a	7.73 ^a	d ²	Fitted ^b
c_L	Rate coefficient of litter decomposition function, analogous to a first order decomposition coefficient	1.17×10^{-2} a	9.15×10^{-3} a	1.43×10^{-2} a	d ⁻¹	Fitted ^b
$Y_{L,hiq}$	Fraction of the decomposed <i>hiq</i> litter transferred to soil	0.3	0.01	1	Unitless	(Ingwersen et al. 2008)
$Y_{L,loq}$	Fraction of the decomposed <i>loq</i> litter transferred to soil	0.829	0.01	1	Unitless	(Ingwersen et al. 2008)
$C_{L,tot}(t=0)$	Initial litter carbon	206 ^a	201 ^a	211 ^a	mg C	Measured
<i>Detritosphere soil</i>						
μ_{max-B}	Maximal specific growth rate of bacteria	25.5	0.1	50	d ⁻¹	(Ingwersen et al. 2008)
μ_{max-F}	Maximal specific growth rate of fungi	2.60	0.1	50	d ⁻¹	(Ingwersen et al. 2008)
μ_{max-BP}	Maximal specific growth rate of bacterial pesticide degraders	25.5	0.1	50	d ⁻¹	(Ingwersen et al. 2008)
$k_{B,hiq}$	<i>hiq</i> DOC growth substrate affinity coefficient of bacteria	96.5	1	5×10^2	$g(mgC \cdot d)^{-1}$	(Ingwersen et al. 2008)
$k_{B,loq}$	<i>loq</i> DOC growth substrate affinity coefficient of bacteria	9.81	1	5×10^2	$g(mgC \cdot d)^{-1}$	(Ingwersen et al. 2008)
$k_{F,hiq}$	<i>hiq</i> DOC growth substrate affinity coefficient of fungi	96.5	1	5×10^2	$g(mgC \cdot d)^{-1}$	(Ingwersen et al. 2008)
$k_{F,loq}$	<i>loq</i> DOC growth substrate affinity coefficient of fungi	9.81	1	5×10^2	$g(mgC \cdot d)^{-1}$	(Ingwersen et al. 2008)
$k_{BP,P}$	<i>Pesticide</i> growth substrate affinity coefficient of bacterial pesticide degraders	96.5	1	5×10^2	$g(mgC \cdot d)^{-1}$	(Ingwersen et al. 2008)
$k_{BP,hiq}$	<i>hiq</i> DOC growth substrate affinity coefficient of bacterial pesticide degraders	96.5	1	5×10^2	$g(mgC \cdot d)^{-1}$	(Ingwersen et al. 2008)

$k_{BP,loq}$	<i>loq</i> DOC growth substrate affinity coefficient of bacterial pesticide degraders	2.5	1	5×10^2	$g \cdot (mgC \cdot d)^{-1}$	
m_{max-B}	Maximal specific maintenance rate of bacteria	0.250	0.01	2	d^{-1}	(Gignoux et al. 2001)
m_{max-BP}	Maximal specific maintenance rate of bacterial pesticide degraders	0.250	0.01	2	d^{-1}	(Gignoux et al. 2001)
$k_{m-B,hiq}$	<i>hiq</i> DOC maintenance substrate affinity coefficient of bacteria	250	1	1.5×10^3	$g \cdot (mgC \cdot d)^{-1}$	(Ingwersen et al. 2008)
$k_{m-B,loq}$	<i>loq</i> DOC maintenance substrate affinity coefficient of bacteria	250	1	1.5×10^3	$g \cdot (mgC \cdot d)^{-1}$	(Ingwersen et al. 2008)
$k_{m-BP,P}$	<i>Pesticide</i> maintenance substrate affinity coefficient of bacterial pesticide degraders	250	1	1.5×10^3	$g \cdot (mgC \cdot d)^{-1}$	(Ingwersen et al. 2008)
$k_{m-BP,hiq}$	<i>hiq</i> DOC maintenance substrate affinity coefficient of bacterial pesticide degraders	250	1	1.5×10^3	$g \cdot (mgC \cdot d)^{-1}$	(Ingwersen et al. 2008)
$k_{m-BP,loq}$	<i>loq</i> DOC maintenance substrate affinity coefficient of bacterial pesticide degraders	250	1	1.5×10^3	$g \cdot (mgC \cdot d)^{-1}$	(Ingwersen et al. 2008)
$k_{F,P}$	Maximum specific rate of pesticide utilization in the absence of growth substrates	4	1×10^{-5}	5	d^{-1}	
T_{y-F}	Growth substrate transformation capacity	1	1×10^{-4}	1	$mgC \cdot (mgC)^{-1}$	
$K_{S-F,P}$	Substrate affinity coefficient of fungal co-metabolic <i>pesticide</i> transformation kinetic	0.1	0.01	5	$mgC \cdot g^{-1}$	
$T_{F,P}$	Co-metabolic pesticide transformation capacity of fungi	1×10^3	1	1×10^4	$mgC \cdot (mgC)^{-1}$	
a_{max-B}	Maximal specific death rate of bacteria	1.30	0.1	3	d^{-1}	(Blagodatsky et al. 1998)
a_{max-F}	Maximal specific death rate of fungi	0.35	0.1	3	d^{-1}	
a_{max-BP}	Maximal specific death rate of bacterial pesticide degraders	1.30	0.1	3	d^{-1}	(Blagodatsky et al. 1998)

$K_{a-B,hiq}$	Inhibition coefficient of bacterial death rate in response to <i>hiq</i> DOC	12.4	1	100	$g(mgC)^{-1}$	(Blagodatsky et al. 1998)
$K_{a-B,loq}$	Inhibition coefficient of bacterial death rate in response to <i>loq</i> DOC	12.4	1	100	$g(mgC)^{-1}$	(Blagodatsky et al. 1998)
$K_{a-F,hiq}$	Inhibition coefficient of fungal death rate in response to <i>hiq</i> DOC	12.4	1	100	$g(mgC)^{-1}$	(Blagodatsky et al. 1998)
$K_{a-F,loq}$	Inhibition coefficient of fungal death rate in response to <i>loq</i> DOC	12.4	1	100	$g(mgC)^{-1}$	(Blagodatsky et al. 1998)
$K_{a-BP,P}$	Inhibition coefficient of death rate of bacterial pesticide degraders in response to <i>pesticide</i>	12.4	1	100	$g(mgC)^{-1}$	(Blagodatsky et al. 1998)
$K_{a-BP,hiq}$	Inhibition coefficient of death rate of bacterial pesticide degraders in response to <i>hiq</i> DOC	12.4	1	100	$g(mgC)^{-1}$	(Blagodatsky et al. 1998)
$K_{a-BP,loq}$	Inhibition coefficient of death rate of bacterial pesticide degraders in response to <i>loq</i> DOC	12.4	1	100	$g(mgC)^{-1}$	(Blagodatsky et al. 1998)
q_{max-B}	Maximal specific decomposition rate of insoluble organic matter (C_1) of bacteria and bacterial pesticide degraders	1.62	0.1	10	d^{-1}	(Ingwersen et al. 2008)
q_{max-F}	Maximal specific decomposition rate of insoluble organic matter (C_1) of fungi	1.62	0.1	10	d^{-1}	(Ingwersen et al. 2008)
K_{I-B}	Substrate affinity coefficient of insoluble organic matter (C_1) decomposition kinetics of bacteria and bacterial pesticide degraders	13.8	1	100	$g(mgC)^{-1}$	(Blagodatsky et al. 1998)
K_{I-F}	Substrate affinity coefficient of insoluble organic matter (C_1) decomposition kinetics of fungi	13.8	1	100	$g(mgC)^{-1}$	(Blagodatsky et al. 1998)
$k_{r-B,hiq}$	Inhibition coefficient of bacterial activity in response to <i>hiq</i> DOC	5.06×10^{-2}	1×10^{-3}	10	$mgC \cdot g^{-1}$	(Ingwersen et al. 2008)
$k_{r-B,loq}$	Inhibition coefficient of bacterial activity in response to <i>loq</i> DOC	2.33	1×10^{-3}	10	$mgC \cdot g^{-1}$	(Ingwersen et al. 2008)

$k_{r-F,hiq}$	Inhibition coefficient of fungal activity in response to <i>hiq</i> DOC	5.06×10^{-3}	1×10^{-3}	10	$\text{mgC} \cdot \text{g}^{-1}$	(Ingwersen et al. 2008)
$k_{r-F,loq}$	Inhibition coefficient of fungal activity in response to <i>loq</i> DOC	2.33	1×10^{-3}	10	$\text{mgC} \cdot \text{g}^{-1}$	(Ingwersen et al. 2008)
$k_{r-BP,P}$	Inhibition coefficient of activity of bacterial pesticide degraders in response to <i>pesticide</i>	5.06×10^{-3}	1×10^{-3}	10	$\text{mgC} \cdot \text{g}^{-1}$	(Ingwersen et al. 2008)
$k_{r-BP,hiq}$	Inhibition coefficient of activity of bacterial pesticide degraders in response to <i>hiq</i> DOC	1×10^{-3}	1×10^{-3}	10	$\text{mgC} \cdot \text{g}^{-1}$	
$k_{r-BP,loq}$	Inhibition coefficient of activity of bacterial pesticide degraders in response to <i>loq</i> DOC	2.33	1×10^{-3}	10	$\text{mgC} \cdot \text{g}^{-1}$	(Ingwersen et al. 2008)
Y_{r-B}	Efficiency of insoluble organic matter (C_1) decomposition by bacteria and bacterial pesticide degraders	0.570	0.1	1	Unitless	(Blagodatsky et al. 1998)
Y_{r-F}	Efficiency of insoluble organic matter (C_1) decomposition and biomass reutilisation by fungi	0.570	0.1	1	Unitless	(Blagodatsky et al. 1998)
$Y_{R-F,P}$	Efficiency of co-metabolic pesticide transformation by fungi	0.316	0.1	1	Unitless	
$Y_{S-B,hiq}$	Substrate uptake efficiency of <i>hiq</i> DOC by bacteria	0.850	0.5	1	Unitless	(Blagodatsky et al. 1998)
$Y_{S-B,loq}$	Substrate uptake efficiency of <i>loq</i> DOC by bacteria	0.850	0.5	1	Unitless	(Blagodatsky et al. 1998)
$Y_{S-F,hiq}$	Substrate uptake efficiency of <i>hiq</i> DOC by fungi	0.850	0.5	1	Unitless	(Blagodatsky et al. 1998)
$Y_{S-F,loq}$	Substrate uptake efficiency of <i>loq</i> DOC by fungi	0.850	0.5	1	Unitless	(Blagodatsky et al. 1998)
$Y_{S-BP,P}$	Substrate uptake efficiency of <i>pesticide</i> by bacterial pesticide degraders	0.850	0.5	1	Unitless	(Blagodatsky et al. 1998)
$Y_{S-BP,hiq}$	Substrate uptake efficiency of <i>hiq</i> DOC by bacterial pesticide degraders	0.850	0.5	1	Unitless	(Blagodatsky et al. 1998)
$Y_{S-BP,loq}$	Substrate uptake efficiency of <i>loq</i> DOC by bacterial pesticide degraders	0.850	0.5	1	Unitless	(Blagodatsky et al. 1998)
D_{hiq}	Diffusion coefficient of <i>hiq</i> DOC in water	16.4	1	100	$\text{mm}^2 \cdot \text{d}^{-1}$	(Hendry et al. 2003)

D_{loq}	Diffusion coefficient of <i>loq</i> DOC in water	16.4	1	100	$\text{mm}^2 \cdot \text{d}^{-1}$	(Hendry et al. 2003)
D_p	Diffusion coefficient of <i>pesticide</i> in water	54.7	1	100	$\text{mm}^2 \cdot \text{d}^{-1}$	Calculated for MCPA after (Worch 1993)
K_{d-hiq}	Linear sorption coefficient of <i>hiq</i> DOC	26.0	1	100	$\text{mm}^3 \cdot \text{mg}^{-1}$	Fitted ^c
K_{d-loq}	Linear sorption coefficient of <i>loq</i> DOC	26.0	1	100	Unitless	Fitted ^c
K_{F-P}	“Freundlich”-coefficient of <i>pesticide</i> sorption isotherm	0.538 ^a	0.326 ^a	0.750 ^a	$(\text{mm}^3 \cdot \text{mg}^{-1})^{n_F}$	Fitted ^d
n_{F-P}	“Freundlich”-exponent of <i>pesticide</i> sorption isotherm	0.859 ^a	0.788 ^a	0.932 ^a	Unitless	Fitted ^d
λ	Dispersivity	10	1	50	mm	(Jury and Horton 2004)
J_w	Average soil water flux	0.190 ^e	0.171 ^e	0.209 ^e	$\text{mm} \cdot \text{d}^{-1}$	Calculated
θ	Average volumetric soil water content	0.360 ^e	0.324 ^e	0.396 ^e	$\text{mm}^3 \cdot \text{mm}^{-3}$	Calculated
ρ_B	Bulk density of soil	1.20	-	-	$\text{mm}^3 \cdot \text{mm}^{-3}$	Adjusted
ρ_S	Soil particle density	2.65	-	-	$\text{mg} \cdot \text{mm}^{-3}$	(Jury and Horton 2004)
M_p	Molar weight of pesticide	201	-	-	$\text{g} \cdot \text{mol}^{-1}$	Calculated for MCPA from (Wieser and Coplen 2011)
M_C	Molar weight of carbon	12.0	-	-	$\text{g} \cdot \text{mol}^{-1}$	(Wieser and Coplen 2011)
$r_B(t=0)$	Initial physiological state index of bacterial	0.1	0.01	1	Unitless	(Blagodatsky et al. 1998)
$r_F(t=0)$	Initial physiological state index of fungi	0.165	0.01	1	Unitless	(Ingwersen et al. 2008)
$r_{BP}(t=0)$	Initial physiological state index of bacterial pesticide degraders	0.1	0.01	1	Unitless	(Blagodatsky et al. 1998)
$f_B(t=0)$	Initial fraction of bacteria on total biomass	0.1	0.05	0.95	Unitless	(Ingwersen et al. 2008)
$f_{BP-B}(t=0)$	Initial fraction of bacterial pesticide degraders on total bacterial biomass	3.16×10^{-4}	1×10^{-6}	1×10^{-1}	Unitless	
$f_{DOC,hiq}(t=0)$	Initial fraction of <i>hiq</i> DOC on total DOC	1×10^{-5}	1×10^{-5}	1	Unitless	Lower bound
$TOC(t=0)$	Initial total organic carbon in soil	15.0 ^a	14.3 ^a	15.7 ^a	$\text{mgC} \cdot \text{g}^{-1}$	Measured
$DOC(t=0)$	Initial total dissolved organic carbon in soil	4.21×10^{-2} ^a	4.00×10^{-2} ^a	4.42×10^{-2} ^a	$\text{mgC} \cdot \text{g}^{-1}$	Measured

$C_{mic}(t=0)$	Initial microbial biomass in soil	$9.46 \times 10^{-2}{}^a$	$8.86 \times 10^{-2}{}^a$	$0.101{}^a$	$\text{mgC} \cdot \text{g}^{-1}$	Measured
MCPA($t=0$)	Initial MCPA concentration in soil	$53.6{}^a$	$49.7{}^a$	$57.4{}^a$	$\text{mgMCPA} \cdot \text{kg}^{-1}$	Measured
$A_{14C}(t=0)$	Initial total ^{14}C activity in soil due to MCPA amendment	$341{}^a$	$318{}^a$	$365{}^a$	$\text{Bq} \cdot \text{g}^{-1}$	Measured
16S rRNA($t=0$)	Initial abundance of 16S rRNA genes in soil	$2.48 \times 10^{12}{}^a$	$2.18 \times 10^{12}{}^a$	$2.77 \times 10^{12}{}^a$	$\text{copy number} \cdot \text{g}^{-1}$	Measured
18S rRNA($t=0$)	Initial abundance of 18S rRNA genes in soil	$8.51 \times 10^9{}^a$	$7.80 \times 10^9{}^a$	$9.22 \times 10^9{}^a$	$\text{copy number} \cdot \text{g}^{-1}$	Measured
$tfdA(t=0)$	Initial abundance of <i>tfdA</i> genes in soil	$1.49 \times 10^6{}^a$	$1.36 \times 10^6{}^a$	$1.63 \times 10^6{}^a$	$\text{copy number} \cdot \text{g}^{-1}$	Measured

^a Mean and 95% confidence limits of estimated and measured values.

^b Estimated by fitting Equation 1 (main paper ; Table 1) to litter mass loss data obtained from the microcosm experiment that provided the data base for model calibration.

^c Average soil water flux and volumetric soil water content were estimated from a transient water flow simulation. An uncertainty of the estimated values of $\pm 10\%$ was assumed.

^d Estimated by fitting an initial mass isotherm (Nodvin et al. 1986) to sorption data of water extracted litter DOC on a Luvisol soil. The same soil was used in the microcosm experiment that provided the data base for model calibration.

^e Estimated by fitting a Freundlich-isotherm to 24h batch sorption data of MCPA on a Luvisol soil. The same soil was used in the microcosm experiment that provided the data base for model calibration.

References

- Blagodatsky SA, Yevdokimov IV, Larionova AA, Richter J (1998) Microbial growth in soil and nitrogen turnover: Model calibration with laboratory data. *Soil Biol Biochem* 30 (13):1757-1764
- Gignoux J, House J, Hall D, Masse D, Nacro HB, Abbadie L (2001) Design and test of a generic cohort model of soil organic matter decomposition: The SOMKO model. *Glob Ecol and Biogeogr* 10 (6):639-660
- Hendry MJ, Ranville JR, Boldt-Leppin BEJ, Wassenaar LI (2003) Geochemical and transport properties of dissolved organic carbon in a clay-rich aquitard. *W Resour Res* 39 (7):SBH91
- Ingwersen J, Poll C, Streck T, Kandeler E (2008) Micro-scale modelling of carbon turnover driven by microbial succession at a biogeochemical interface. *Soil Biol Biochem* 40 (4):872-886
- Jury WA, Horton R (2004) *Soil physics*. 6. ed. John Wiley & Sons, New York
- Nodvin SC, Driscoll CT, Likens GE (1986) Simple partitioning of anions and dissolved organic carbon in a forest soil. *Soil Sci* 142 (1):27-35
- Wieser ME, Coplen TBC (2011) Atomic weights of the elements 2009 (IUPAC Technical Report). *Pure Appl Chem* 83 (2):359-396
- Worch E (1993) Eine neue Gleichung zur Berechnung von Diffusionskoeffizienten gelöster Stoffe. *Vom Wasser* 81:289-297

Online Resource 2:

Technical details on the implementation of PECCAD key features

Corresponding paper:

Micro-scale modeling of pesticide degradation coupled to carbon turnover in the detritosphere - Model description and sensitivity analysis

Holger Pagel¹, Joachim Ingwersen¹, Christian Poll², Ellen Kandeler², Thilo Streck¹

¹ *Institute of Soil Science and Land Evaluation, Biogeophysics, University of Hohenheim, D-70593 Stuttgart, Germany*

² *Institute of Soil Science and Land Evaluation, Soil Biology, University of Hohenheim, D-70593 Stuttgart, Germany*

Corresponding author:

Holger Pagel

Institute of Soil Science and Land Evaluation, Biogeophysics

University of Hohenheim

Emil-Wolff-Str. 27

D-70593 Stuttgart, Germany

Tel.: (+49)711 459 23383

Fax: (+49)711 459 23117

holgerp@uni-hohenheim.de

Microbial dynamics

In our model, the microbial pools change through growth, maintenance and death. Each microbial pool has a specific activity state. It is reasonable to assume that multiple carbonaceous compounds are utilized simultaneously as homologous substrates by microorganisms in natural C-limited environments. Indeed, there is some experimental evidence for mixtures of naturally occurring organic compounds and organic pollutants (e.g., Egli 2010; Knightes and Peters 2006; Wick et al. 2003). In line with this concept all three microbial pools are able to grow on both *hiq* and *loq* DOC. The specific pesticide degraders are in addition capable of using dissolved pesticide C as a third growth substrate.

To model this simultaneous utilization of growth substrates we applied a Monod type kinetic for mixed substrate growth developed by Lendenmann and Egli (1998). These authors successfully modeled the simultaneous utilization of mixtures of different sugars by *Escherichia coli* in a C-limited chemostat culture. We slightly modified their approach by defining substrate specific affinity coefficients k_i for each microbial pool (main paper; Table 2; Eqs. 28, 29, 31), such that:

$$k_i = \frac{\mu_{max,i}}{K_i} \quad (1)$$

where $\mu_{max,i}$ and K_i are parameters of the single Monod kinetic that describe utilization of substrate i . The fraction of DOC and pesticide C that is utilized due to exogenous maintenance respiration of bacteria and bacterial pesticide degraders is modeled by analogy to microbial growth using a mixed substrate Monod kinetics (main paper; Table 2; Eqs. 30, 32). In contrast the endogenous maintenance of fungi is represented by the term $a_{max-F} \cdot (1 - Y_{r,F})$ (main paper; Table 1; Eq. 6) and a second function (main paper; $m_{F,P}$; Table 2; Eq. 34). The latter reflects an additional maintenance burden imposed on fungal cells due to co-metabolic pesticide degradation.

Wang and Post (2012) recently suggested an interesting compromise approach for microbial maintenance, which is able to reflect a change from exogenous maintenance at high substrate availability to endogenous maintenance at low substrate availability. The rationale behind this approach was based on studies of bacterial maintenance by Dawes and Ribbons (1964). The shift to endogenous maintenance results in relatively higher microbial death at low substrate availability. Our modeling approach is similarly able to simulate such an increased microbial

decay at low substrate concentration, because microbial death is directly considered by multi-substrate dependent death rates (main paper; Table 2; Eqs. 35-37) as proposed by Blagodatsky and Richter (1998). In contrast, Wang and Post (2012) assumed in their simplified model of SOM decomposition that microbial death rates are independent of substrates.

In their review (Lennon and Jones 2011) showed that dormancy of microorganisms plays a very important role to deal with variable environmental conditions in ecosystems, in particular in soil. We account for possible dormancy of soil microorganisms by employing a physiological state index r first introduced by Panikov (1995) with each microbial pool (main paper; Table 1; Eqs. 8-10). This index r ranges from $[0 \dots 1]$ and reflects the proportion of actively growing (r) vs. dormant ($1-r$) microorganisms. The change in the physiological state of each microbial pool is regulated by a multi-substrate dependent response function (main paper; Table 2; Eqs. 40-42). The utilization of a physiological state variable results in a lagged response of the microbial biomass to a change in substrate availability, because all microbial life processes (i.e. growth, death or maintenance) are directly controlled by r (main paper; Table 1; Eqs. 5-7). As excellently illustrated by Blagodatsky and Richter (1998), the consideration of microbial activity allows a more realistic simulation of the long term behavior of microbial populations in soil compared to standard approaches that do not account for it. With our formulation at very low substrate concentrations a large part of a certain microbial pool persists at a dormant state or in turn only a minor part of microorganisms is still active. Since only the active part of a microbial pool is depleted by maintenance and death processes in PECCAD's model structure, microbes do not die off relatively fast due to substrate deficiencies. Instead the microbial biomass decreases slowly with time and is able to recover as substrates are available again. An increase in substrate availability first triggers microbial activity and is then followed by higher growth.

Co-metabolic pesticide degradation by fungi

Because we use the herbicide MCPA as a model pesticide in accompanying microcosm studies, we model pesticide decomposition by fungi with strong reference to chlorophenoxyacetic acids. Several studies have indicated that unspecific fungal lignin-degrading enzymes, such as manganese and lignin peroxidase, are involved in co-metabolic transformation of chlorophenoxyacetic acids (Castillo et al. 2001; Reddy et al. 1997; Vroumsia et al. 2005). This pathway also applies to pesticides from other substance classes (Bumpus et al. 1985). There is also some evidence of growth-linked degradation of halogenated aromatic compounds by fungi (e.g., Shailubhai et al. 1983). In a previous microcosm experiment we observed an increased

abundance of the fungal taxonomic marker 18S rRNA gene (Manerkar et al. 2008) in detritusphere soil amended with MCPA (Poll et al. 2010). The effect of MCPA was not visible in soil not influenced by litter, which suggests that the conditions in the detritusphere promoted the development of a specific fungal community capable of degrading MCPA either by growth-linked metabolism or co-metabolism. However, we found a much more pronounced stimulating effect of MCPA on the abundance of specific bacterial MCPA degraders using quantitative PCR targeting the functional gene *tfdA*. This gene encodes for a bacterial dioxygenase, which catalyzes the cleavage of the acetate side chain of the MCPA molecule as the first step of its biodegradation (Fukumori and Hausinger 1993).

Against this background, we simplified the pesticide degradation in the PECCAD model, such that it is performed by specific bacterial pesticide degraders with growth-linked metabolism. In contrast, pesticide transformation by fungi is modeled as a strictly co-metabolic process. We adopted a kinetic approach from Criddle (1993), which couples fungal utilization of pesticide-C to the fungal growth rates on *hiq* and *loq* DOC (main paper; Table 2; Eq. 33). This expression implies that the pesticide is co-metabolically transformed by fungal cells at a maximum rate defined by the parameter $k_{F,P}$, even in the absence of growth substrates. If *hiq* or *loq* DOC is present and fungi grow, the maximum rate of co-metabolic pesticide utilization is further increased. The increase is regulated by the transformation capacity T_{y-F} . This parameter reflects the mass of pesticide C transformed per unit mass of *hiq* or *loq* DOC and effectively links co-metabolic pesticide transformation with fungal growth.

Water regime and transport of DOC and pesticide

We assumed homogeneous soil and a stationary water regime. An extension of the model to account for a transient water regime would be straightforward, but is out of the scope of the present study. Transport of DOC and pesticide is simulated by the one-dimensional convection-dispersion equation (Jury and Horton 2004, Chapter 7) with apparent diffusion-dispersion coefficients (main paper; Table 2; Eqs. 44-66).

Dynamics of ^{13}C and ^{14}C pools

The dynamics of ^{13}C and ^{14}C pools are calculated from total C dynamics (Ingwersen et al. 2008). We defined ^{13}C and ^{14}C mass fractions of each C pool in the model. To calculate a ^{13}C or ^{14}C flux, the respective total C flux is multiplied with the current ^{13}C or ^{14}C mass fraction

of the source pool. Diffusion and convection of isotopic DOC pools are computed independently based on the $^{13}\text{C}/^{14}\text{C}$ concentrations of DOC. Isotopic pools of the pesticide (C_P and $C_{P,S}$) are directly calculated from total C pools assuming constant ^{13}C and ^{14}C mass fractions.

Boundary conditions and numerical integration

At the upper boundary of the detritosphere (soil surface) the influx densities of *hiq* and *loq* DOC were set according to the second terms in Eq. 13 and 17 (main paper; Table 1); that is, the influx of *hiq* and *loq* DOC from litter is defined by a given proportion of the total litter decomposition flux $k_L \cdot C_{L,tot}$. The actual time-dependent values of *hiq* and *loq* DOC influx densities are controlled by the parameters $Y_{L,hiq}$ and $Y_{L,loq}$ as well as by the function f_L (main paper; Table 2; Eq. 26), which partitions the total decomposition flux into *hiq* and *loq* C fluxes. At the upper boundary we assumed infiltration of pesticide-free water (main paper; Table 1; Eq. 22). At the lower boundary we applied a Neumann-type boundary condition (main paper; Table 1, Eqs. 14, 18, 23).

The system of non-linear partial and ordinary differential equations (main paper; Table 1) was numerically solved with the finite element solver FlexPDE (PDE solutions Inc. 2011) using a fully implicit Galerkin scheme in conjunction with the Newton-Raphson algorithm and a second-order two-step backward difference formula for solution in time.

References

- Blagodatsky SA, Richter O (1998) Microbial growth in soil and nitrogen turnover: A theoretical model considering the activity state of microorganisms. *Soil Biol Biochem* 30 (13):1743-1755
- Bumpus JA, Tien M, Wright D, Aust SD (1985) Oxidation of persistent environmental pollutants by a white rot fungus. *Sci* 228 (4706):1434-1436
- Castillo MdP, Andersson A, Ander P, Stenström J, Torstensson L (2001) Establishment of the white rot fungus *Phanerochaete chrysosporium* on unsterile straw in solid substrate fermentation systems intended for degradation of pesticides. *World J Microbiol Biotechnol* 17 (6):627-633
- Criddle CS (1993) The kinetics of cometabolism. *Biotechnol Bioeng* 41 (11):1048-1056
- Dawes EA, Ribbons DW (1964) Some aspects of the endogenous metabolism of bacteria. *Bacteriol Rev* 28:126-149
- Egli T (2010) How to live at very low substrate concentration. *W Res* 44 (17):4826-4837. doi:10.1016/j.watres.2010.07.023
- Fukumori F, Hausinger RP (1993) *Alcaligenes eutrophus* JMP134 “2,4-dichlorophenoxyacetate monooxygenase” is an α -ketoglutarate-dependent dioxygenase. *J Bacteriol* 175 (7):2083-2086

- Ingwersen J, Poll C, Streck T, Kandeler E (2008) Micro-scale modelling of carbon turnover driven by microbial succession at a biogeochemical interface. *Soil Biol Biochem* 40 (4):872-886
- Jury WA, Horton R (2004) *Soil physics*. 6. ed. John Wiley & Sons, New York
- Knights CD, Peters CA (2006) Multisubstrate biodegradation kinetics for binary and complex mixtures of polycyclic aromatic hydrocarbons. *Environ Toxicol Chem* 25 (7):1746-1756. doi:10.1897/05-483r.1
- Lendenmann U, Egli T (1998) Kinetic models for the growth of *Escherichia coli* with mixtures of sugars under carbon-limited conditions. *Biotechnol and Bioeng* 59 (1):99-107
- Lennon JT, Jones SE (2011) Microbial seed banks: The ecological and evolutionary implications of dormancy. *Nat Rev Microbiol* 9 (2):119-130. doi:10.1038/nrmicro2504
- Manerkar MA, Seena S, Bärlocher F (2008) Q-RT-PCR for assessing archaea, bacteria, and fungi during leaf decomposition in a stream. *Microb Ecol* 56 (3):467-473. doi:10.1007/s00248-008-9365-z
- Panikov NS (1995) *Microbial growth kinetics*. 1 ed. Chapman & Hall, Weinheim
- PDE Solutions Inc. (2011) FlexPDE 6.20 - finite element model builder for Partial Differential Equations. WA, USA
- Poll C, Pagel H, Devers-Lamrani M, Martin-Laurent F, Ingwersen J, Streck T, Kandeler E (2010) Regulation of bacterial and fungal MCPA degradation at the soil-litter interface. *Soil Biol Biochem* 42 (10):1879-1887. doi:10.1016/j.soilbio.2010.07.013
- Reddy GVB, Joshi DK, Gold MH (1997) Degradation of chlorophenoxyacetic acids by the lignin-degrading fungus *Dichomitus squalens*. *Microbiol* 143 (7):2353-2360
- Shailubhai K, Sahasrabudhe SR, Vora KA, Modi VV (1983) Degradation of chlorinated derivatives of phenoxyacetic acid and benzoic acid by *Aspergillus niger*. *FEMS Microbiol Lett* 18 (3):279-282. doi:10.1016/0378-1097(83)90341-5
- Vroumsia T, Steiman R, Seigle-Murandi F, Benoit-Guyod JL (2005) Fungal bioconversion of 2,4-dichlorophenoxyacetic acid (2,4-D) and 2,4-dichlorophenol (2,4-DCP). *Chemosphere* 60 (10):1471-1480
- Wang G, Post WM (2012) A theoretical reassessment of microbial maintenance and implications for microbial ecology modeling. *FEMS Microbiol Ecol*. doi:10.1111/j.1574-6941.2012.01389.x
- Wick LY, Pasche N, Bernasconi SM, Pelz O, Harms H (2003) Characterization of Multiple-Substrate Utilization by Anthracene-Degrading *Mycobacterium frederiksbergense* LB501T. *Appl Environ Microbiol* 69 (10):6133-6142. doi:10.1128/aem.69.10.6133-6142.2003

Online Resource 3:

Description of the litter decomposition submodel and the parameter estimation procedure

Corresponding paper:

Micro-scale modeling of pesticide degradation coupled to carbon turnover in the detritosphere - Model description and sensitivity analysis

Holger Pagel¹, Joachim Ingwersen¹, Christian Poll², Ellen Kandeler², Thilo Streck¹

¹ *Institute of Soil Science and Land Evaluation, Biogeophysics, University of Hohenheim, D-70593 Stuttgart, Germany*

² *Institute of Soil Science and Land Evaluation, Soil Biology, University of Hohenheim, D-70593 Stuttgart, Germany*

Corresponding author:

Holger Pagel

Institute of Soil Science and Land Evaluation, Biogeophysics

University of Hohenheim

Emil-Wolff-Str. 27

D-70593 Stuttgart, Germany

Tel.: (+49)711 459 23383

Fax: (+49)711 459 23117

holgerp@uni-hohenheim.de

Litter decomposition model

We applied a power function to model the litter decomposition rate (main paper; Table 2; Eq. 25; Rovira and Rovira 2010). This function shows a strong initial increase followed by a slow decrease with time. We postulate a short initial lag phase before litter C is successively decomposed. The original expression

$$f(t) = c + \left(\frac{at}{t^2 + b} \right)^3 \quad (1)$$

was modified by setting $a=1$. By this simplification the specific shape characteristics of the original expression is basically maintained (at least for $b < 10 \text{ d}^2$) and only two instead of three parameters have to be estimated by inverse simulation.

Compared to the complex structure implemented for soil pools with explicit consideration of defined microbial populations we are currently using a relatively simple empirical model to simulate litter decomposition. A more mechanistic approach could not be justified because, at the current state, data on microbial litter communities is not available from the related microcosm experiments. However, this information would be needed as a prerequisite to successfully estimate the additionally introduced parameters.

A biomass-driven litter decomposition model validated on the basis of suitable experiments would be a very promising feature to substantially improve the representation of DOC input at the soil-litter interface towards more generality, but it is out of the scope of this study.

Parameter estimation

The parameters b_L and c_L of the time-dependent decomposition rate k_L were estimated by fitting Eq. 1 (main paper; Table 1) to litter mass loss data of the accompanying microcosm experiment (Fig. 1). The ordinary differential equation that describes total litter mass loss (main paper; Table 1; Eq. 1) was numerically solved with FlexPDE (PDE solution Inc. 2011).

FlexPDE was coupled to PEST (Doherty 2005) to optimize the two parameters by applying a least squares criterion to the residual amount of litter C using the Levenberg-Marquardt algorithm. Estimated means as well as 95% confidence limits of b_L and c_L are given in Online Resource 1. The litter decomposition model performed well as indicated by a model efficiency (EF ; Loague and Green 1991) of $EF=0.956$.

The value $\sqrt{b_L} = 2.19 d$ gives the time when the decomposition rate reaches the maximum of $k_{L,max} = 2.44 \times 10^{-2} d^{-1}$ (main paper; Table 2; Eq. 27). The partitioning of total litter decomposition between *hiq* and *loq* C is directly coupled to the litter decomposition rate by Eq. 26 (main paper; Table 2). This function implies an initial pulse of *hiq* C, which is transferred to CO₂ and to the *hiq* DOC pool in soil.

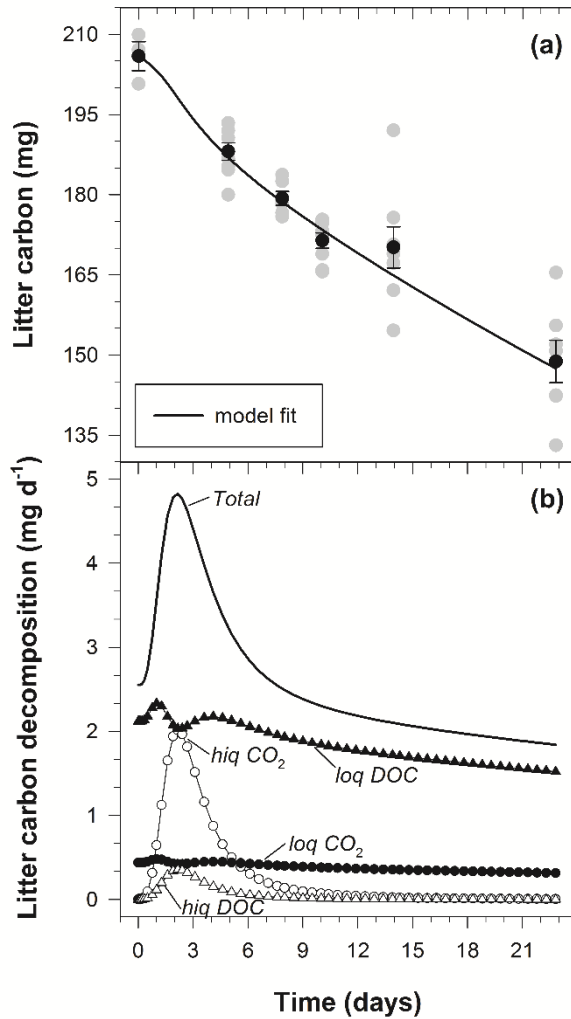


Fig. 1 Reconstructed litter decomposition: **a** measured litter mass loss data and fit (solid line) of litter decomposition model (main paper; Table 1; Eq. 1); grey symbols indicate individual measured values, black symbols show means and standard deviations of the means; **b** total litter C decomposition rate (solid line) and partitioning between *hiq* and *loq* C. Portion transferred to CO₂ as well as to DOC pools in soil are indicated by patterned lines, using the default values of $Y_{L,hiq}=0.15$ and $Y_{L,loq}=0.829$ (Online Resource 1)

References

- Doherty J (2005) PEST: Model Independent Parameter Estimation. 5th ed. Watermark Numerical Computing, Brisbane, Australia
- Loague K, Green RE (1991) Statistical and graphical methods for evaluating solute transport models: Overview and application. *J Contam Hydrol* 7 (1-2):51-73. doi:10.1016/0169-7722(91)90038-3
- PDE Solutions Inc. (2011) FlexPDE 6.20 - finite element model builder for Partial Differential Equations. WA, USA
- Rovira P, Rovira R (2010) Fitting litter decomposition datasets to mathematical curves: Towards a generalised exponential approach. *Geoderma* 155 (3-4):329-343. doi:10.1016/j.geoderma.2009.11.033

Online Resource 4:

Description of the LH-OAT approach for global sensitivity analysis

Corresponding paper:

Micro-scale modeling of pesticide degradation coupled to carbon turnover in the detritosphere - Model description and sensitivity analysis

Holger Pagel¹, Joachim Ingwersen¹, Christian Poll², Ellen Kandeler², Thilo Streck¹

¹ *Institute of Soil Science and Land Evaluation, Biogeophysics, University of Hohenheim, D-70593 Stuttgart, Germany*

² *Institute of Soil Science and Land Evaluation, Soil Biology, University of Hohenheim, D-70593 Stuttgart, Germany*

Corresponding author:

Holger Pagel

Institute of Soil Science and Land Evaluation, Biogeophysics

University of Hohenheim

Emil-Wolff-Str. 27

D-70593 Stuttgart, Germany

Tel.: (+49)711 459 23383

Fax: (+49)711 459 23117

holgerp@uni-hohenheim.de

LH-OAT approach for global sensitivity analysis

The parameter distributions were subdivided into $N_i=100$ strata of equal probability. We assumed a log-uniform distribution of parameters. Lower (LB) and upper (UB) parameter bounds (as stated in Online Resource 1; Table 1) were first transformed by taking the logarithm to base 10. The resulting log-transformed parameter range was then subdivided into $N_i=100$ intervals of width:

$$\frac{1}{N_i} \cdot (\log UB - \log LB) \quad (1)$$

We randomly chose 100 parameter values, such that for each parameter each interval was only sampled once. At each sampling point we calculated the relative parameter sensitivity as follows (van Griensven et al. 2006):

$$s_{i,j,k} = \frac{\partial M_k(p_{i,j})}{\partial p_{i,j}} \cdot \frac{p_{i,j}}{M_k(p_{i,j})} = \left| \frac{M_k(p_{i,j} \cdot (1+f)) - M_k(p_{i,j})}{p_{i,j} \cdot (1+f) - p_{i,j}} \cdot \frac{p_{i,j}}{M_k(p_{i,j})} \right| \quad (2)$$

where $s_{i,j,k}$ is the partial relative sensitivity of parameter p_i at LH sampling point j for each model output M_k and f was set to 0.001.

The global parameter sensitivity was calculated as a normalized measure over all LH intervals:

$$\hat{S}_{i,k} = \frac{\tilde{s}_{i,k}}{\text{MAX}(\tilde{s}_{1,k} \dots \tilde{s}_{Np,k})} \quad (3)$$

where $\hat{S}_{i,k}$ denotes the normalized global parameter sensitivity of parameter p_i for model output M_k , $\tilde{s}_{i,k}$ is the 90th percentile of partial relative sensitivities over all LH intervals of parameter p_i for model output M_k . Np stands for the total number of parameters.

The LH-OAT approach resulted in $N_i \cdot (Np + 1) = 8200$ parameter-sets and model runs. The number of parameters considered was $Np = 81$.

Reference

van Griensven A, Meixner T, Grunwald S, Bishop T, Diluzio M, Srinivasan R (2006) A global sensitivity analysis tool for the parameters of multi-variable catchment models. J Hydrol 324 (1-4):10-23

Online Resource 5:

Sensitivity indices of PECCAD parameters and input values for key model outputs

Corresponding paper:

Micro-scale modeling of pesticide degradation coupled to carbon turnover in the detritosphere - Model description and sensitivity analysis

Holger Pagel¹, Joachim Ingwersen¹, Christian Poll², Ellen Kandeler², Thilo Streck¹

¹ *Institute of Soil Science and Land Evaluation, Biogeophysics, University of Hohenheim, D-70593 Stuttgart, Germany*

² *Institute of Soil Science and Land Evaluation, Soil Biology, University of Hohenheim, D-70593 Stuttgart, Germany*

Corresponding author:

Holger Pagel

Institute of Soil Science and Land Evaluation, Biogeophysics
University of Hohenheim
Emil-Wolff-Str. 27
D-70593 Stuttgart, Germany

Tel.: (+49)711 459 23383

Fax: (+49)711 459 23117

holgerp@uni-hohenheim.de

Table 1 Sensitivity indices of PECCAD parameters and input values for key model outputs

Model input ^b	Model output ^a												GSI ^c
	DOC	P	TOC	$\delta^{13}\text{C}$	$A_{14\text{C}}$	C_{mic}	$A_{14\text{C}}$	16S	18S	tfdA	CO_2	CO_2	
DOC(t = 0)	1.000	1.000	0.508	0.442	0.772	1.000	0.764	1.000	0.443	0.712	1.000	0.977	1.000
θ	1.000	0.639	0.426	1.000	1.000	0.603	0.749	0.576	0.213	0.612	0.533	0.586	1.000
$n_{\text{F-P}}$	1.000	1.000	0.045	0.143	1.000	0.239	1.000	0.376	0.031	1.000	0.192	1.000	1.000
$\mu_{\text{max-BP}}$	0.636	0.378	0.086	0.207	0.511	0.517	0.988	0.596	0.069	1.000	0.315	0.901	1.000
$a_{\text{max-F}}$	0.563	0.118	0.134	0.197	0.304	1.000	1.000	0.270	1.000	0.132	0.729	0.672	1.000
$a_{\text{max-BP}}$	0.838	0.366	0.184	0.216	0.474	0.533	1.000	0.677	0.031	1.000	0.344	0.439	1.000
$C_{\text{L,tot}}(t = 0)$	0.447	0.135	0.325	1.000	0.322	0.664	0.419	0.653	0.208	0.374	0.801	0.157	1.000
MCPA(t = 0)	0.925	0.370	0.066	0.157	0.370	0.317	0.544	0.313	0.035	0.742	0.160	1.000	1.000
TOC(t = 0)	0.278	0.045	1.000	1.000	0.146	0.415	0.210	0.328	0.079	0.114	0.861	0.303	1.000
$a_{\text{max-B}}$	0.289	0.028	0.297	0.157	0.079	0.753	0.228	1.000	0.064	0.139	0.478	0.251	1.000
$Y_{\text{S-BP,P}}$	0.243	0.233	0.046	0.147	1.000	0.152	0.409	0.128	0.030	0.123	0.093	0.908	1.000
$A_{14\text{C}}(t = 0)$	0.061	0.029	0.027	0.123	1.000	0.102	0.424	0.124	0.036	0.067	0.027	0.432	1.000
J_{w}	0.368	0.140	0.114	0.979	0.580	0.340	0.281	0.310	0.097	0.241	0.059	0.138	0.979
$k_{\text{BP,loq}}$	0.955	0.526	0.084	0.218	0.341	0.459	0.281	0.396	0.064	0.486	0.353	0.510	0.955
$Y_{\text{L,loq}}$	0.389	0.052	0.296	0.923	0.204	0.559	0.212	0.447	0.147	0.217	0.554	0.115	0.923
$K_{\text{F-P}}$	0.296	0.909	0.028	0.168	0.346	0.135	0.360	0.160	0.031	0.296	0.077	0.643	0.909
λ	0.237	0.062	0.100	0.892	0.224	0.267	0.171	0.187	0.087	0.119	0.085	0.054	0.892
$K_{\text{d-loq}}$	0.673	0.163	0.298	0.830	0.291	0.481	0.187	0.392	0.173	0.274	0.508	0.337	0.830
$Y_{\text{S-F,loq}}$	0.358	0.131	0.229	0.460	0.240	0.563	0.306	0.166	0.223	0.084	0.815	0.319	0.815
$k_{\text{BP,P}}$	0.285	0.773	0.067	0.154	0.548	0.185	0.591	0.201	0.024	0.495	0.119	0.803	0.803
$q_{\text{max-B}}$	0.400	0.042	0.600	0.487	0.254	0.358	0.166	0.380	0.064	0.132	0.785	0.306	0.785
c_{L}	0.340	0.039	0.256	0.780	0.217	0.466	0.254	0.398	0.163	0.212	0.662	0.123	0.780
$\mu_{\text{max-B}}$	0.252	0.066	0.088	0.223	0.103	0.420	0.242	0.739	0.130	0.133	0.243	0.220	0.739
$C_{\text{mic}}(t = 0)$	0.289	0.144	0.199	0.179	0.249	0.579	0.606	0.519	0.270	0.349	0.738	0.436	0.738
$Y_{\text{r-F}}$	0.284	0.052	0.193	0.243	0.196	0.685	0.423	0.196	0.483	0.081	0.395	0.391	0.685
$Y_{\text{L,hiq}}$	0.263	0.101	0.108	0.662	0.197	0.429	0.309	0.424	0.122	0.272	0.119	0.089	0.662
b_{L}	0.288	0.116	0.118	0.652	0.316	0.442	0.355	0.476	0.152	0.255	0.656	0.098	0.656
$k_{\text{B,loq}}$	0.535	0.065	0.173	0.244	0.170	0.474	0.279	0.645	0.162	0.243	0.451	0.289	0.645
$Y_{\text{S-B,loq}}$	0.245	0.054	0.263	0.193	0.107	0.597	0.184	0.487	0.103	0.092	0.523	0.109	0.597
$Y_{\text{S-BP,loq}}$	0.351	0.082	0.406	0.364	0.155	0.588	0.167	0.447	0.045	0.262	0.513	0.203	0.588
$Y_{\text{r-B}}$	0.410	0.049	0.233	0.237	0.141	0.545	0.211	0.586	0.081	0.149	0.319	0.251	0.586
$k_{\text{F,loq}}$	0.566	0.084	0.132	0.266	0.226	0.380	0.241	0.272	0.305	0.146	0.318	0.380	0.566
$f_{\text{B}}(t = 0)$	0.395	0.213	0.117	0.183	0.247	0.548	0.441	0.494	0.114	0.361	0.393	0.510	0.548

Very important (0.750 – 1.000)

Important (0.500 – 0.750)

Model input ^b	Model output ^a												GSI ^c	
	DOC	P	TOC	$\delta^{13}\text{C}$ TOC	$A_{14\text{C}}$ TOC	C_{mic}	$A_{14\text{C}}$ C_{mic}	16S rRNA	18S rRNA	tfdA	CO_2	$A_{14\text{C}}$ CO_2		
16S rDNA ($t = 0$)	0.000	0.000	0.000	0.000	0.000	0.000	0.000	0.491	0.000	0.000	0.000	0.000	Less important (0.250 - 0.500)	0.491
$k_{r-B,\text{loq}}$	0.242	0.057	0.186	0.174	0.075	0.391	0.193	0.470	0.060	0.089	0.308	0.124		0.470
$k_{r-BP,\text{loq}}$	0.375	0.107	0.107	0.144	0.242	0.231	0.435	0.208	0.049	0.282	0.232	0.325		0.435
$\mu_{\text{max}-F}$	0.329	0.061	0.082	0.181	0.101	0.359	0.332	0.210	0.408	0.113	0.291	0.426		0.426
$K_{S-F,P}$	0.226	0.138	0.025	0.086	0.261	0.093	0.382	0.061	0.022	0.046	0.035	0.421		0.421
$k_{F,P}$	0.116	0.102	0.034	0.143	0.139	0.080	0.335	0.098	0.021	0.032	0.033	0.420		0.420
T_{y-F}	0.214	0.070	0.041	0.163	0.125	0.097	0.313	0.060	0.024	0.040	0.032	0.418		0.418
$Y_{R-F,P}$	0.046	0.024	0.027	0.077	0.177	0.055	0.417	0.058	0.036	0.025	0.030	0.375		0.417
$f_{BP-B}(t = 0)$	0.200	0.157	0.052	0.155	0.153	0.172	0.401	0.206	0.038	0.332	0.072	0.410		0.410
$r_F(t = 0)$	0.133	0.045	0.039	0.100	0.085	0.182	0.124	0.088	0.307	0.072	0.391	0.354		0.391
$f_{\text{DOC},\text{hiq}}(t = 0)$	0.363	0.157	0.079	0.143	0.108	0.276	0.321	0.280	0.142	0.226	0.323	0.242		0.363
$q_{\text{max}-F}$	0.187	0.035	0.192	0.240	0.150	0.299	0.168	0.126	0.097	0.076	0.360	0.172		0.360
$K_{a-B,\text{loq}}$	0.117	0.038	0.067	0.118	0.080	0.240	0.104	0.357	0.022	0.055	0.143	0.060		0.357
$Y_{S-F,\text{hiq}}$	0.253	0.094	0.041	0.155	0.173	0.164	0.356	0.112	0.089	0.116	0.057	0.157		0.356
$K_{d-\text{hiq}}$	0.350	0.173	0.089	0.328	0.139	0.283	0.337	0.269	0.077	0.178	0.172	0.191		0.350
tfdA ($t = 0$)	0.000	0.000	0.000	0.000	0.000	0.000	0.000	0.000	0.000	0.345	0.000	0.000		0.345
$k_{r-F,\text{loq}}$	0.342	0.061	0.123	0.228	0.129	0.298	0.328	0.144	0.255	0.097	0.226	0.237		0.342
$K_{a-BP,\text{loq}}$	0.180	0.064	0.079	0.193	0.078	0.223	0.228	0.208	0.022	0.342	0.105	0.189		0.342
$r_B(t = 0)$	0.136	0.027	0.072	0.181	0.050	0.225	0.081	0.334	0.036	0.068	0.256	0.065		0.334
K_{l-B}	0.162	0.035	0.299	0.281	0.088	0.249	0.092	0.184	0.034	0.095	0.331	0.172		0.331
$k_{F,\text{hiq}}$	0.117	0.029	0.037	0.113	0.057	0.124	0.311	0.118	0.142	0.091	0.049	0.094		0.311
$Y_{S-B,\text{hiq}}$	0.170	0.033	0.072	0.305	0.070	0.187	0.270	0.215	0.039	0.067	0.106	0.116		0.305
$k_{r-BP,\text{hiq}}$	0.188	0.062	0.050	0.142	0.088	0.152	0.295	0.165	0.050	0.180	0.048	0.101		0.295
$k_{r-BP,P}$	0.127	0.217	0.039	0.101	0.109	0.107	0.184	0.088	0.034	0.193	0.046	0.293		0.293
$k_{BP,\text{hiq}}$	0.258	0.108	0.050	0.196	0.229	0.218	0.289	0.219	0.041	0.265	0.095	0.115		0.289
$k_{r-B,\text{hiq}}$	0.169	0.050	0.066	0.182	0.070	0.286	0.119	0.269	0.077	0.121	0.087	0.042		0.286
18S rDNA ($t = 0$)	0.000	0.000	0.000	0.000	0.000	0.000	0.000	0.000	0.267	0.000	0.000	0.000		0.267
$k_{B,\text{hiq}}$	0.174	0.068	0.059	0.150	0.079	0.237	0.254	0.225	0.072	0.106	0.133	0.076		0.254

Model input ^b	Model output ^a													GSI ^c
	DOC	P	TOC	$\delta^{13}\text{C}$	$A_{14\text{C}}$	C_{mic}	$A_{14\text{C}}$	16S	18S	tfdA	CO_2	CO_2	$A_{14\text{C}}$	
$K_{a-F,\text{loq}}$	0.116	0.042	0.074	0.180	0.074	0.249	0.125	0.075	0.177	0.052	0.114	0.103		0.249
$k_{m-BP,P}$	0.087	0.045	0.019	0.092	0.248	0.065	0.113	0.073	0.028	0.030	0.031	0.122		0.248
$Y_{S-BP,\text{hiq}}$	0.237	0.157	0.040	0.167	0.067	0.160	0.076	0.170	0.029	0.132	0.103	0.065		0.237
K_{I-F}	0.185	0.038	0.222	0.204	0.098	0.197	0.091	0.121	0.073	0.081	0.235	0.101		0.235
$m_{\text{max}-BP}$	0.106	0.043	0.035	0.117	0.233	0.087	0.136	0.086	0.019	0.065	0.059	0.194		0.233
D_{loq}	0.183	0.042	0.044	0.230	0.076	0.185	0.076	0.084	0.043	0.071	0.033	0.043		0.230
$K_{a-F,\text{hiq}}$	0.131	0.028	0.057	0.221	0.080	0.110	0.079	0.126	0.081	0.122	0.035	0.053		0.221
$r_{BP}(t=0)$	0.099	0.049	0.037	0.136	0.072	0.104	0.210	0.124	0.027	0.213	0.038	0.211		0.213
D_p	0.165	0.059	0.028	0.086	0.203	0.083	0.120	0.075	0.024	0.082	0.038	0.072		0.203
$k_{r-F,\text{hiq}}$	0.119	0.064	0.051	0.106	0.051	0.184	0.150	0.097	0.129	0.077	0.065	0.084		0.184
$m_{\text{max}-B}$	0.165	0.030	0.089	0.139	0.078	0.180	0.112	0.136	0.074	0.092	0.073	0.069		0.180
D_{hiq}	0.110	0.033	0.028	0.163	0.069	0.122	0.128	0.104	0.032	0.053	0.032	0.043		0.163
$k_{m-BP,\text{hiq}}$	0.143	0.060	0.042	0.156	0.067	0.146	0.063	0.069	0.045	0.058	0.042	0.062		0.156
$K_{a-BP,P}$	0.078	0.073	0.033	0.077	0.094	0.095	0.126	0.091	0.029	0.150	0.037	0.101		0.150
$k_{m-BP,\text{loq}}$	0.112	0.042	0.054	0.130	0.129	0.104	0.105	0.139	0.049	0.069	0.041	0.079		0.139
$k_{m-B,\text{loq}}$	0.047	0.032	0.045	0.127	0.040	0.111	0.043	0.087	0.031	0.035	0.040	0.056		0.127
$K_{a-B,\text{hiq}}$	0.074	0.054	0.020	0.092	0.043	0.106	0.054	0.126	0.018	0.077	0.028	0.052		0.126
$K_{a-BP,\text{hiq}}$	0.090	0.047	0.041	0.120	0.081	0.098	0.099	0.069	0.056	0.109	0.056	0.070		0.120
$T_{F,P}$	0.056	0.022	0.012	0.068	0.044	0.072	0.048	0.068	0.029	0.045	0.035	0.035		0.072
$k_{m-B,\text{hiq}}$	0.067	0.027	0.016	0.065	0.050	0.057	0.064	0.047	0.019	0.026	0.028	0.067		0.067

Not important (0.000 – 0.250)

^asee Section 3 of the main paper for definition of key model output criteria^bsee Online Resource 1 for definition of parameters and input values^cGlobal sensitivity index, that is the maximum sensitivity index over all single model output criteria

6 Regulation of pesticide degradation in the detritosphere: Integrating soil genomics and biogeochemical modeling

Submitted to Ecological Monographs

Holger Pagel¹, Christian Poll², Joachim Ingwersen¹, Ellen Kandeler², Thilo Streck¹

¹ Institute of Soil Science and Land Evaluation, Biogeophysics, University of Hohenheim, D-70593 Stuttgart, Germany

² Institute of Soil Science and Land Evaluation, Soil Biology, University of Hohenheim, D-70593 Stuttgart, Germany

6.1 Abstract

The mechanistic integration of microbial behavior is still one of the greatest challenges facing biogeochemical models of organic matter cycling in soil. We recently introduced dynamic feedbacks between specific microbial groups and their micro-environment to model pesticide degradation coupled to carbon (C) turnover in the detritusphere (*PECCAD*). In the detritusphere, pesticide degradation by bacteria and fungi is stimulated by the transport of organic substances from the litter into the adjacent soil. In this study, we applied the *PECCAD* model to the data of a microcosm experiment to enhance our understanding of regulation mechanisms involved in coupled C turnover and degradation of the model compound MCPA (4-chloro-2-methylphenoxyacetic acid). With our novel modeling approach we link genetic information on abundances of total bacteria, fungi and specific pesticide degraders in soil to the biogeochemical dynamics of C and MCPA.

We utilized a Pareto optimization for multi-criteria calibration of the *PECCAD* model to determine the trade-off in estimating parameters from the data of three experimental treatments. The analysis revealed that the *PECCAD* model structure was adequate and the identified parameter values were reasonable. The model was able to reproduce the observed dynamics of C and MCPA. The simulations matched the measured increase of dissolved organic C (DOC) and microbial C as well as the accelerated MCPA degradation in soil up to a 6 mm distance to litter (detritusphere). Whereas the observed increase of bacteria and pesticide degrader populations was simulated satisfactorily, the model could not reproduce the steep increase of fungi indicated by the fungal marker gene. Our simulations suggest that fungal activity and growth was specifically stimulated by low-quality DOC, whereas bacterial MCPA degraders mostly benefited from high-quality DOC. According to the simulations, MCPA predominantly degraded via fungal co-metabolism. Our study demonstrates: i) Genetic information has a high potential to parameterize and evaluate complex mechanistic models, but model approaches must be improved based on extended information on gene dynamics at the cellular level, and ii) mathematical modeling is a powerful tool to gain comprehensive insight into microbial regulation of matter cycling in soil.

6.2 Introduction

The dynamics of biogeochemical processes in soil microhabitats strongly control matter cycling and ecosystem functioning (Beare et al. 1995, Young et al. 2009, Totsche et al. 2010). Small-scale habitats, such as the rhizosphere, drilosphere or detritusphere are characterized by high availability of readily utilizable carbon (C) resulting in high microbial abundance and activity compared to bulk soil (Lavelle 1988, Kandeler et al. 1999, Brown et al. 2000, Tiunov et al. 2001, Gaillard et al. 2003, Dazzo and Ganter 2009, Marschner et al. 2012). They are hot spots of C turnover (Helal and Sauerbeck 1984, Bottner et al. 1999, Kandeler et al. 1999, Don et al. 2008, Poll et al. 2008, Cheng 2009, Kuzyakov 2010, Bird et al. 2011, Schenck zu Schweinsberg-Mickan et al. 2012) and degradation of organic chemicals (particularly pesticides) in soils (Haby and Crowley 1996, Shaw and Burns 2005, Gerhardt et al. 2009, Poll et al. 2010, Liu et al. 2011, Chen and Yuan 2012, Blouin et al. 2013).

In the detritusphere, litter-derived C stimulates the degradation of herbicides (Duah-Yentumi and Kuwatsuka 1980, Ghani and Wardle 2001, Poll et al. 2010, Ditterich et al. 2013). The herbicide 4-chloro-2-methylphenoxyacetic acid (MCPA) is well suited to study the microbially-driven interactions between C turnover and pesticide degradation in the detritusphere. MCPA and other chlorophenoxy herbicides are widely applied against broad leaf weeds and have frequently been used as model compounds to study the degradation of organic contaminants in soil (Torstensson et al. 1975, Loos et al. 1979, Soulas 1993, Crespín et al. 2001, Boivin et al. 2005, Cederlund et al. 2007). The half-life of MCPA in soils is reasonably fairly short (7 – 41 days; European Commission 2005) and has been studied in detailed laboratory experiments.

Bacterial pathways of MCPA degradation and functional genes involved have been intensively studied (e.g., Helling et al. 1968, Don and Pemberton 1981, Pieper et al. 1988, Fukumori and Hausinger 1993, Smejkal et al. 2001, Laemmli et al. 2004, Ledger et al. 2006, Liu et al. 2013). The major bacterial pathway of biodegradation of MCPA and other chlorophenoxy herbicides is initiated by the cleavage of the ether-bonded acetate side chain. This reaction is catalyzed by different oxygenases encoded by *tfdA*/ *tfdA-like*, *cadA* and *r/sdpA* genes (Itoh et al. 2004, Müller et al. 2006, Baelum et al. 2010, Zaprasis et al. 2010, Liu et al. 2013, Nielsen et al. 2013). It has been shown that MCPA degradation in soil is quantitatively linked to the abundance of *tfdA* genes (Baelum et al. 2006, Nicolaisen et al. 2008, Poll et al. 2010, Ditterich et al. 2013, Liu et al. 2013).

Fungal degradation pathways of chlorophenoxy herbicides and the fungal enzymes involved are less well understood. Thus, Vroumsia et al. (2005) concluded: “*Although 2,4-D is a herbicide used world-wide in crop control and its bacterial degradation has been extensively stud-*

ied, there is a noticeable lack of knowledge on its degradation by fungi ...". To date this statement still holds true, and it does so for MCPA. Evidence is growing, however, that many soil fungi are able to degrade chlorophenoxy herbicides (Torstensson et al. 1975, Vroumsia et al. 2005, Itoh et al. 2013). In analogy to bacterial pathways the cleavage of the ether-bond appears as one of the major reactions, which initiate chlorophenoxyacetic acid degradation by fungi (Shailubhai et al. 1983, Reddy et al. 1997, Vroumsia et al. 2005, Itoh et al. 2013). Although Faulkner and Woodcock (1965) reported in an early study that the fungus *Aspergillus niger* transformed MCPA and 2,4-D by direct hydroxylation of the phenyl ring, later 2,4-Dichlorophenol was found as major metabolite of 2,4-D degradation by *A. niger* suggesting initial ether-bond cleavage (Shailubhai et al. 1983). The activity of lignolytic enzymes, such as lignin and manganese peroxidases or laccases, has been associated with chlorophenoxyacetic acid degradation (Castillo et al. 2001). However, there is some evidence that the initial cleavage of the ether-bond is catalyzed by non-lignolytic enzymes and that the lignolytic enzymes are rather involved in the degradation of the chlorinated aromatic moiety (Reddy et al. 1997). Indeed, the degradation of chlorophenols by fungal lignin and manganese peroxidases as well as laccases is well documented (Gianfreda and Bollag 1994, Field and Sierra-Alvarez 2008, Rubilar et al. 2008). Reports on side-chain cleavage of 2,4,6-Trichloroanisole (Campoy et al. 2009) and phenoxybutyrate herbicides (Sträuber et al. 2003) by cytochrome P450 monooxygenases indicate that this intracellular enzyme might be involved in the initial cleavage of the ether-bond of chlorophenoxyacetic acids by fungi.

An *Aspergillus niger* strain was able to use 2,4-D as sole source of C and energy (Shailubhai et al. 1983). In contrast, the majority of isolated fungal strains from an agricultural soil were not able to degrade chlorophenoxyacetic acids as sole source of C and energy (Han Sung and New 1994). The latter fact in combination with the putative involvement of lignolytic enzymes suggests that fungal MCPA degradation proceeds at least in part co-metabolically. There are two fundamental explanations of co-metabolic substrate utilization. First, the presence of primary substrates can be necessary to induce the respective enzymes, which catalyze the transformation of a secondary substrate. And second, the utilization of primary substrates can provide the energy to produce the reduction equivalents (e.g., NAD(P)H) needed for the enzymatically catalyzed reaction to attack the secondary substrate (Dalton and Stirling 1982, Brandt et al. 2003).

Litter-derived compounds could serve as inducers of enzyme production or as additional C and energy source at the soil-litter interface. In a previous study we found that fungal growth was stimulated by MCPA only if litter-derived C was also available (Poll et al. 2010). Thus, the observed accelerated degradation of MCPA at the soil-litter interface could be explained at least in part by litter-induced co-metabolic transformation of MCPA and formation of com-

pounds that can then be used as growth substrates by fungi. On the other hand, specific bacterial MCPA degraders were stimulated and apparently contributed to enhanced MCPA degradation at the soil-litter interface as well. Based on these considerations, we hypothesized that litter-derived C stimulates the growth and activity of i) specific bacterial degraders capable of using MCPA as sole source of C and energy and ii) fungal populations capable of producing unspecific enzymes that catalyze the co-metabolic degradation of MCPA (Poll et al. 2010). Both regulation mechanisms of MCPA degradation at the soil-litter interface were recently implemented in the PECCAD model (Pesticide degradation Coupled to CARbon turnover in the Detritosphere; Pagel et al. 2014).

The representation of soil biochemical processes in mathematical models can be substantially improved by explicitly considering microbial dynamics and several models (including the PECCAD model) already incorporate microbial physiology or enzyme dynamics (Gras et al. 2011, Allison 2012, Aslam et al. 2014, Perveen et al. 2014, Sistla et al. 2014, Wieder et al. 2014). However, such models typically have complex structures resulting in a high number of parameters that are largely unknown. Their parameterization can highly benefit from genomic and proteomic data (von Bergen et al. 2013, Myrold et al. 2014), which provide detailed information on the abundance and function of soil microorganisms. A promising approach to simplify the representation of complex soil microbial communities in models is to explicitly consider microbial traits identified by molecular biological analyses (Green et al. 2008, Wallenstein and Hall 2012, Trivedi et al. 2013, Krause et al. 2014). First approaches already integrate functional genes with biochemical models (Reed et al. 2014) and, indeed, measurements of *tfdA* class I and III genes in streambed sediments have been recently utilized to calibrate the initial biomass of MCPA degraders in a simple biokinetic model used to simulate the dynamics of MCPA degraders and MCPA mineralization in a microcosm experiment (Batoglu-Pazarbasi et al. 2013). Nonetheless, genomic data are not yet widely used to calibrate complex biochemical models, but it is promising to tackle this challenge.

Further progress in the mechanistic modeling of microbial traits and coupled enzyme dynamics may be fostered by the availability of advanced parameter estimation techniques (Trigueros et al. 2010, Gao et al. 2011, Kügler 2012, Laloy et al. 2013, Sambridge 2013, Vrugt and Sadegh 2013, Zhang et al. 2013). In particular, it has been demonstrated, albeit primarily in hydrological applications, that multiobjective optimization can be effectively utilized to parameterize and analyze complex models (Efstratiadis and Koutsoyiannis 2010, Moore et al. 2011, Price et al. 2012, Wöhling et al. 2013). Multiobjective optimization results in a Pareto set of parameter values, which reflect the global trade-off between multiple objectives by mapping from the parameter space to the objective space. Pareto optimal solutions have the property that moving from one solution to another results in the improvement of one objective while causing deterioration in at least one of the others (Vrugt et al. 2003). In contrast to using single objective

functions, multiobjective frameworks provide a better understanding of structural limitations of a model by quantifying the trade-off between model fits employing multiple characteristic criteria (Wöhling et al. 2013).

Our objectives in the present study were: i) to assess the capability of the PECCAD model to reproduce the experimental data from a complex microcosm experiment on MCPA degradation, ii) to evaluate the structural limitations of the PECCAD model, and iii) to gain new insights into the biophysicochemical interactions involved in MCPA degradation in the detritusphere by applying the calibrated PECCAD model.

6.3 Material and Methods

6.3.1 Microcosm experiment

We conducted a microcosm experiment focusing on the spatiotemporal dynamics of MCPA, C and microorganisms. Details on the setup and the technical procedures are given elsewhere (Poll et al. 2010, Ditterich et al. 2013).

Experimental design

We used topsoil from a loamy Luvisol (WRB 2006) from an agricultural field at the research station Scheyern (Germany; 48°30'N, 11°21'E; <http://www.helmholtz-muenchen.de/en/scheyern2/home/index.html>). The soil was sampled, sieved (< 2 mm) and stored in the dark at -20°C in July 2008. Before use the soil was thawed and its initial gravimetric water content (θ_g) of 27% was reduced to 22% by air drying at 20°C during an acclimatization period of 10 days in the dark. Then the soil was mixed with unlabeled MCPA (Sigma-Aldrich, PESTANAL®) dissolved in distilled water to give a final concentration of 20 µg/g and incubated at 20°C in the dark for 29 days. This pre-incubation was carried out to increase the abundance of MCPA degrading bacteria. The pre-incubated soil ($\theta_g = 22\%$) was then immediately used in the microcosm experiment. It contained some residual MCPA (0.18 ± 0.03 µg/g), which was considered negligible in relation to the subsequent MCPA amendment. To induce the formation of a detritusphere we employed a one-to-one mixture of shredded (2-10 mm) maize leaves and stems. See Appendix A: Table A1 for basic soil and litter properties.

We set up three experimental treatments: A) addition of litter (L), B) addition of MCPA (M), and C) combined addition of MCPA and litter (ML). All treatments were performed with four replicates. We prepared a mixture of unlabeled and ¹⁴C-labeled MCPA (ring-U-¹⁴C, >95% radiochemical and chemical purity, Izotop, Hungary) dissolved in distilled water and adjusted to pH 5.3 with NaOH. The pre-incubated soil was then homogeneously spiked with this stock solu-

tion. On average we obtained a final MCPA concentration of 53.6 $\mu\text{g/g}$ and a specific ^{14}C activity of 341 Bq/g (see Online Resource 1; Pagel et al. 2014). In the litter treatment we only added distilled water to the soil.

The soil was filled to a height of 30 mm into stainless steel cylinders (diameter = 56 mm, height = 40 mm) and compacted to a bulk density of 1.2 g/cm^3 . The soil had a volumetric water content of 35%, corresponding to a matric potential of -63 hPa. In L and ML treatments we placed 0.5 g of maize residues (rewetted with 2 ml 0.01 M CaCl_2) as a thin layer on top of the soil cores. Soil cores were placed in airtight microcosms on ceramic plates, which were kept at a defined suction of -63 hPa (Poll et al. 2010). We incubated the microcosms at 20°C in the dark. The soil was irrigated with 0.01 M CaCl_2 solution at a rate of 0.2 ml/min on four events (1.97, 8.92, 14.76 and 21.95 days). In total we applied 13 ml solution, 4 ml at the first irrigation event and 3 ml at each of the remaining three events. Based on a transient simulation of water movement using the Richards equation we calculated an average water flow rate of 0.191 mm/d, which was then used to model the steady state water flow with PECCAD.

Analysis of litter and soil pools

We destructively sampled four microcosms of each treatment after 4.9, 7.8, 10.0, 13.9 and 22.8 days. After removing the litter layer the soil cores were immediately frozen at -20°C. Subsequently, they were sliced using a cryostat microtome (HM 500 M, MICROM International GmbH, Walldorf, Germany) in 0-1, 1-2, 2-3, 3-4, 4-6, 6-10 and 10-20 mm layers. To obtain sufficient material for analyses, we combined and homogeneously mixed the soil from the associated layers of two soil cores. This procedure yielded two replicate samples per treatment, layer and sampling date derived from four replicate soil cores.

Residual MCPA in soil was extracted by agitation of 1.5 g soil with a 7.5 mL methanol/ H_2O (1:1 by volume) solution in 15 ml centrifuge tubes (polyethylene) on a horizontal shaker at 200 rpm for 10 min. The tubes were then heated in a water bath for 60 min at 50°C. After repeated agitation on a horizontal shaker (200 rpm for 10 min) and centrifugation (4500g, 10 min) an aliquot of 1.5 ml supernatant was filtered (0.45 μm syringe filters, regenerated cellulose) directly into HPLC vials for further analysis. MCPA in the extracts was determined by HPLC with a UV-detector (System Gold, Beckman Instruments) at a wavelength of 228 nm using acetonitrile/water (ratio 32:68) with 20 mmol/l H_3PO_4 as mobile phase at a flow rate of 0.5 ml/min on a 150 mm \times 3 mm column packed with 3 μm MZ Aqua Perfect C18 material column (MZ-Analysentechnik GmbH, Germany). Identification and quantification was done by external calibration using freshly prepared MCPA standards dissolved in methanol/ H_2O (1:1 by volume). The detection limit of MCPA in soil was 0.05 $\mu\text{g/g}$, and the recovery of total MCPA from freshly spiked soil samples was 96%.

Oven-dried (105°C for 24h) ground soil samples were used to determine total ^{14}C activity by liquid scintillation counting of trapped $^{14}\text{CO}_2$ after complete combustion as well as ^{13}C abundance by an elemental analyser coupled with an isotope ratio mass spectrometer (EA-IRMS). See Poll et al. (2010; ^{14}C) and Poll et al. (2008; ^{13}C) for technical and instrumental details. Total organic C (TOC) contents of soil were directly obtained from the ^{13}C EA-IRMS measurements. Quantification of TOC and TO^{13}C in soil was verified using weighted samples of a certified low organic content soil standard (C: $15.2 \pm 0.2 \mu\text{g/g}$, $\delta^{13}\text{C}_{\text{V-PDB}}$: $-27.46 \pm 0.11\text{‰}$; Certificate No. 114524, IVA Analysentechnik e.K., Germany).

Microbial biomass was determined by the chloroform-fumigation-extraction method (Vance et al. 1987). Briefly, we applied 4 mL 0.025 M K_2SO_4 solution to 1 g of fumigated (24h, ethanol-free CH_3Cl) and non-fumigated soil. An aliquot of the soil extracts was then analyzed for dissolved organic carbon (DOC) using a DIMATOC 100 (Dimatec GmbH). The ^{14}C activity of soil extracts was determined by liquid scintillation counting (Wallac 1411, Perkin Elmer) after mixing 0.5 ml soil extract with 4.5 ml scintillation fluid (Rotiszint eco-plus, Carl Roth GmbH&Co. KG, Germany). Total C content and ^{14}C activity of the microbial biomass (C_{mic} , mg/g; $^{14}\text{C}_{\text{mic}}$, Bq/g) were calculated as follows:

$$C_{\text{mic}} = \frac{\text{DOC}_{\text{fum}} - \text{DOC}_{\text{control}}}{k_{\text{EC}}}$$

$$^{14}\text{C}_{\text{mic}} = \frac{\text{DO}^{14}\text{C}_{\text{fum}} - \text{DO}^{14}\text{C}_{\text{control}}}{k_{\text{EC}}}$$

Here DOC_{fum} ($\text{DO}^{14}\text{C}_{\text{fum}}$) and $\text{DOC}_{\text{control}}$ ($\text{DO}^{14}\text{C}_{\text{control}}$) stand for organic C (^{14}C) extracted with 0.025 M K_2SO_4 solution from fumigated and non-fumigated soil samples, respectively. We used $k_{\text{EC}} = 0.45$ to account for incomplete extraction of microbial biomass C after fumigation (Joergensen 1996).

The quantification of 16S rRNA genes, fungal ITS fragments and *tdfA* genes was performed by quantitative PCR after DNA extraction from fresh soil samples and was described in detail by Poll et al. (2010) and Ditterich et al. (2013).

Production rate of total CO_2 and $^{14}\text{CO}_2$

We determined the CO_2 -C production from the whole soil column at regular intervals during the experiment using a 1 M NaOH solution to trap evolved CO_2 in the headspace of the microcosms. Sampling of NaOH and analysis of total CO and $^{14}\text{CO}_2$ were done as described in Poll et al. (2010). Time-averaged CO_2 production rates ($r_{\text{CO}_2,i}$, mg C/d; $^{14}r_{\text{CO}_2,i}$, Bq/d) were estimated at 13 sampling dates ($T_{\text{CO}_2,i} = [0.83, 1.79, 3.76, 4.86, 5.77, 7.74, 8.75, 9.97, 13.76, 15.73, 18.77, 20.76, 22.74]$ days):

$$r_{CO_2,i} = \frac{C_{CO_2,i}}{\Delta t_i}$$

$$^{14}r_{CO_2,i} = \frac{^{14}C_{CO_2,i}}{\Delta t_i}$$

Here $C_{CO_2,i}$ ($^{14}C_{CO_2,i}$) denotes the amount of CO_2 ($^{14}CO_2$) produced during the sampling period Δt_i measured at sampling date $T_{CO_2,i}$.

6.3.2 PECCAD model

Setup

The PECCAD model is described in detail in Pagel et al. (2014). Briefly, PECCAD simulates the coupled dynamics of several C pools (high and low quality [*hiq* and *loq*] DOC, insoluble soil organic matter [SOM]), two pesticide pools (dissolved and sorbed phase) as well as size and activity of three microbial populations (bacteria, fungi and specific bacterial pesticide degraders). It simulates abundances of 16S rRNA genes and fungal ITS fragments as well as of the functional gene *tfdA* calculated from the modeled biomass of bacteria, fungi and bacterial MCPA degraders, respectively. It considers the vertical transport (diffusion and convection) of DOC and pesticide and accounts for ^{13}C and ^{14}C pools. The model is formulated as a set of non-linear partial and ordinary differential equations, which were numerically solved using the finite element solver FlexPDE (PDE_Solutions 2011). Influx of litter-derived *hiq* and *loq* DOC at the upper soil boundary was simulated by an empirical litter decomposition model. Its parameters were estimated from litter mass loss in microcosms by inverse simulation. Further details on the litter submodel can be found in Pagel et al. (2014). PECCAD is capable of mechanistically simulating enhanced pesticide degradation in soil due to the input of fresh organic C, which stimulates *i*) growth and activity of specific (bacterial) pesticide degraders and *ii*) fungal co-metabolism by unspecific fungal enzymes.

Calibration

To parameterize the PECCAD model, we performed a calibration against the measured data of the microcosm experiment. In total, we simultaneously estimated 67 parameters including *i*) *biokinetic parameters* such as maximal growth and decomposition rates, substrate affinities coefficients, inhibition coefficients controlling the activity of microbial pools and substrate uptake efficiencies, *ii*) *physicochemical parameters* such as the dispersivity or sorption and diffusion coefficients of *hiq* and *loq* DOC and *iii*) *initial values* such as the initial physiological state index of microbial pools and coefficients defining the initial fraction of bacteria, fungi and specific MCPA degraders on the total microbial biomass in soil. Lower and upper boundary constraints of parameters are given in Appendix B: Table B1.

We conducted a multi-criteria Pareto analysis using the AMALGAM (a multi-algorithm, genetically adaptive multiobjective; Vrugt and Robinson 2007) method to obtain parameter sets that reflect Pareto-efficient solutions of the data from the three experimental treatments (L, M, ML). Consequently, we used three aggregated objective functions to quantify the fit of PECCAD simulations with the respective observations for each experimental treatment

$$F_i = \frac{1}{N_i^P} \sum_{j=1}^{N_i^P} \frac{MSE_{i,j}}{MSE_{i,j}^{MIN}},$$

$$MSE_{i,j} = \frac{1}{N_{i,j}^S} \sum_{k=1}^{N_{i,j}^S} \left(\frac{P_{i,j,k} - O_{i,j,k}}{\text{MAX}(O_{i,j,1} \dots O_{i,j,N_{i,j}^S})} \right)^2$$

where F_i is the objective function of treatment i (L, M or ML) to be minimized, N_i^P denotes the treatment-specific total number of considered pools and $MSE_{i,j}$ stands for the mean squared error as treatment- (i) and pool- (j) specific criterion of goodness of fit. The individual $MSE_{i,j}$ were normalized with corresponding minimum mean squared error values $MSE_{i,j}^{MIN}$, which were estimated from an initial “burn-in” AMALGAM run of about 10000 model evaluations. We applied this normalization to balance the weights of individual $MSE_{i,j}$ and that of the three objective functions F_i . The $MSE_{i,j}$ were calculated from the difference of model predictions $P_{i,j,k}$ and measured observations $O_{i,j,k}$. The constant $N_{i,j}^S$ is the total number of samples of pool j and treatment i . These 1 ... k samples include the measured and corresponding modelled values on a given sampling date and in the case of soil pools also at different soil layers. Individual $P_{i,j,k}$ and $O_{i,j,k}$ were normalized to lie in an interval of $\{0 \dots 1\}$ by dividing its value by the maximum observed value of the respective pool.

There are three Pareto extremes, where F_L , F_M or F_{ML} reach their minima. Each of these Pareto extremes corresponds to a parameter set, which produces the model realization that best fits the data of a single experimental treatment. Additionally, we defined a Pareto point, referred in the following as the compromise solution, where the Euclidean distance to the origin $(\langle 0, 0, 0 \rangle)$ in the three-dimensional objective space is at its minimum:

$$F_{Comp} = \sqrt{F_L^2 + F_M^2 + F_{ML}^2}$$

The corresponding parameter set leads to a model realization that, by definition, simultaneously best matches the data of all three experimental treatments.

6.4 Results and discussion

6.4.1 Model parameterization

Trade-offs between treatments: Litter, MCPA and MCPA & litter

Out of 156,800 parameter sets sampled by the AMALGAM algorithm, we identified in total 108 Pareto solutions. These Pareto points lie on a three-dimensional Pareto surface that defines the trade-off between the F_L , F_M and F_{ML} objectives, respectively. Fig. 1 shows the three Pareto fronts, each with regard to two of the three objectives. Pareto points away from the projected fronts indicate model parameterizations that perform well on the third objective not shown in the bi-criterion plots, but not on the two objectives shown.

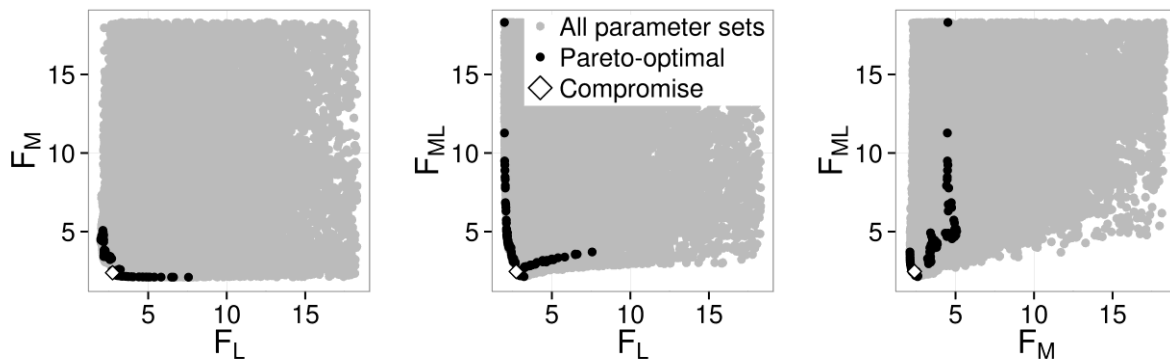


Fig. 1 Projection of the objective functions for all simulations onto the $F_M - F_L$, $F_{ML} - F_L$ and $F_{ML} - F_M$ planes. The axes represent the values of three objective functions (F ; normalized squared errors) that were minimized during calibration of the PECCAD model with AMALGAM to the experimental data of the three treatments: Litter (L), MCPA (M) and MCPA & litter (ML).

In general, the shapes of the Pareto fronts are only slightly non-rectangular indicating that it was possible to significantly improve the predictions of one treatment without losing too much performance with regard to the other two treatments. Accordingly, the Pareto extreme that best matches the data of the ML treatment (lowest F_{ML}) results in individual objective values ($F_L = 3.22$, $F_M = 2.58$, $F_{ML} = 2.14$) that are close to the values of the compromise solution ($F_L = 2.73$, $F_M = 2.38$, $F_{ML} = 2.46$). The objective values ($\Delta F_L = 0.75$ vs. $\Delta F_M = 0.28$ and $\Delta F_{ML} = 0.32$) of the compromise solution, in turn, are only slightly larger than the single best values with the highest deviation found for the L treatment. All these findings imply that the trade-off for matching the data of the three treatments is relatively low. However, the curvature (i.e. the deviation from a rectangular shape) of the Pareto fronts is most pronounced for the F_L and F_M objectives, which points to some structural deficits of the PECCAD model in simulating the coupled C and MCPA dynamics in soil. The largest trade-off was found between the objectives $F_L - F_{ML}$ and $F_L - F_M$. Here, the best fit to the experimental data of the L treatment ($F_L = 1.98$) is accompanied by substantially higher values for the other two objectives ($F_{ML} = 18.3$ and $F_M = 4.52$). Also the minimum Pareto extreme related to the M treatment ($F_M = 2.10$) is contrasted by F_L and F_{ML} values of 7.48 and 3.70, respectively.

Numerical models need to simplify the complexity of interacting processes in real-world systems (Wainwright and Mulligan 2013). Hence, every model has structural deficits and trade-offs between different objectives have to be expected. From a more detailed view on the performance of PECCAD (Table 2) it becomes evident that the observed trade-off in fitting the data of different experimental treatments is largely driven by conflicts in simultaneously matching the observed microbial dynamics of all three treatments. This indicates that there is space for improvement with regard to the structural representation of microbial dynamics in PECCAD. One should, however, be aware that the trade-offs between objectives arise not only from structural deficits of the PECCAD model, but that they will partly also be due to other sources such as errors in measuring input and output values (Wöhling et al. 2013). Measurement errors are much higher for microbial data (e.g. microbial biomass, gene abundances) than for other measurements (e.g. MCPA concentration, $\delta^{13}\text{C}$ abundance).

The F_L - F_{ML} Pareto front close the F_L Pareto optimum appears patchy and could have been explored further by AMALGAM. However, the bi-criterion Pareto fronts did not substantially improve during the last 30,000 model evaluations, and the Pareto analysis was stopped since the Pareto fronts were stable. Wöhling and Vrugt (2011) argued similarly regarding a patchy Pareto front observed in their AMALGAM optimization using a hydrological model.

The final Pareto analysis with AMALGAM needed about four months of computation time running PECCAD in parallel on a six-core workstation. Due to computational limitations, we restricted the Pareto analysis to the use of three objective functions. Direct utilization of different data types as individual objective values would have given a more detailed insight into model structural inadequacies. However, the computer power needed would then dramatically increase because of the much higher number of model evaluations required to sample the resulting high-dimensional (>10) Pareto surface. This limitation could be compensated for by running the AMALGAM code coupled with the model on a computer cluster, but this was out of the scope of the present study. The experimental data of the three treatments represent different degrees of biogeochemical complexity; with the ML treatment as the most complex system. Thus, we think that the applied information reduction to three treatment-specific objectives was reasonable and efficient to assess the structure of the PECCAD model.

Optimized parameters

In total, 67 parameters were simultaneously optimized with AMALGAM (Table 1). The majority of parameters directly controls biokinetic functions and microbial dynamics in soil. The remaining parameters essentially control transport and sorption of litter-, MCPA- and soil-C, respectively. Most parameters take on similar values in treatment-specific and the overall (compromise) optimization, in line with the low trade-offs between the objectives found with the Pareto

analysis. However, model parameterizations optimal for L and M treatments do not reflect interactions between litter-C and pesticide dynamics. Accordingly, the optimization with regard to only one objective is not sufficient alone to constrain the values of the full set of PECCAD's parameters. This is obvious for parameters directly related to pesticide degradation (e.g. $k_{BP,P}$, $Y_{S-BP,P}$ or $k_{F,P}$) in case of the L treatment or for that directly related to litter-C input ($Y_{L,hiq}$ and $Y_{L,loq}$) in case of the M treatment. Also, e.g., parameters related to *hiq* DOC dynamics are excited most with the data of L and ML treatments, because the *hiq* DOC pool in soil is mostly supplied directly from *hiq* litter-C. The model parameterization optimal for ML reflects interactions between C and pesticide dynamics, but does not necessarily capture the dynamics of microbial pools and substrate pools in absence of either MCPA-C or litter-C. Thus, only the compromise solution integrates all of the information about different states of the system observed in the three treatments. In contrast, parameters optimized for only a subset of the data take partly unrealistic values. Therefore, unless stated otherwise, we refer only to the parameter set of the overall optimization in the following discussion.

Based on our simulations, we can state that the fraction of decomposed litter-C transferred to soil is approximately four times larger for *hiq* than for *loq* litter ($Y_{L,hiq}$ vs. $Y_{L,loq}$; Table 1). In contrast, Ingwersen et al. (2008) found a much lower fraction of decomposed initial-stage litter transferred to soil (corresponding to $Y_{L,hiq}$) compared to that of late-stage litter (corresponding to $Y_{L,loq}$). In the present study, 45% of the decomposed *hiq* litter-C and 12% of the decomposed *loq* litter-C were transferred to soil, whereas according to the detritosphere model of Ingwersen et al. (2008) only 15% of decomposed initial-stage litter-C, but 83% of decomposed late-stage litter-C were transferred to soil. Despite the fact that rye litter was applied by Ingwersen et al. (2008), whereas maize litter was used in our experiment, these differences result mainly from a different reconstruction of litter decomposition. PECCAD simulates a successive decomposition of both litter fractions. The maximum proportion of *hiq* litter-C decomposition on the total rate reaches a maximum value of 0.5 after 2 days, and litter decomposition is almost completely fed by *loq* C after 15 days (Pagel et al. 2014; see appendix x for details). In contrast, Ingwersen et al. (2008) used a Weibull function to model a continuous sigmoidal shift in decomposition from initial-stage litter-C dominated to almost complete dominance of late-stage litter-C after 37 days. By that, they applied a strictly sequential litter decomposition scheme. In consequence of the different schemes, Ingwersen et al. (2008) simulate relatively higher amounts of decomposed initial-stage litter-C compared to the amounts of *hiq* litter-C simulated in PECCAD. Thus, the optimized fractions of initial-stage vs. *hiq* and late-stage vs. *loq* litter-C transferred to soil partly compensate for the uncertainty in the reconstruction of litter decomposition dynamics. Nonetheless, the fast initial turnover of *hiq* litter-C simulated by PECCAD agrees well with a study by Kalbitz et al. (2003). By applying a double-exponential first-order decomposition model to CO₂ mineralization data, they performed an incubation

Table 1 Parameter values of best fits of the PECCAD model to the data of three experimental treatments obtained by Pareto analysis: litter (L), MCPA (M) and MCPA & litter (ML). The compromise solution (Comp) indicates the parameters of the overall best fit. See Appendix B: Table B1 for parameter bounds and units.

Parameter	L	M	ML	Comp	Parameter	F _L	F _M	F _{ML}	Comp
$Y_{L,hiq}$	0.453	-	0.467	0.463	q_{max-F}	8.67	0.44	0.44	0.72
$Y_{L,loq}$	0.116	-	0.119	0.120	K_{L-B}	1.74	1.17	1.07	1.04
μ_{max-B}	0.174	37.7	1.01	0.704	K_{I-F}	1.21	1.28	1.20	1.18
μ_{max-F}	0.728	0.198	0.153	0.171	$k_{r-B,hiq}$	6.13	8.06	5.83	6.93
μ_{max-BP}	12.4	4.37	8.35	4.69	$k_{r-B,loq}$	9.18	9.51	8.80	7.66
$k_{B,hiq}$	4.05	1.56	2.40	3.95	$k_{r-F,hiq}$	0.144	0.0013	0.0010	0.0010
$k_{B,loq}$	1.27	44.8	29.7	1.77	$k_{r-F,loq}$	1.28	10.0	7.82	5.84
$k_{F,hiq}$	1.00	1.31	1.25	1.31	$k_{r-BP,P}$	-	0.0789	0.0042	0.0634
$k_{F,loq}$	432	478	479	467	$k_{r-BP,hiq}$	3.40	10.0	3.12	2.53
$k_{BP,P}$	-	1.13	1.21	1.07	$k_{r-BP,loq}$	10.0	9.12	8.25	9.69
$k_{BP,hiq}$	32.0	9.34	6.61	34.7	Y_{r-B}	0.855	0.929	0.901	0.851
$k_{BP,loq}$	2.64	1.25	1.27	1.32	Y_{r-F}	0.986	0.997	0.996	0.998
m_{max-B}	0.0469	0.0214	0.0231	0.0166	$Y_{R-F,P}$	-	0.299	0.307	0.285
m_{max-BP}	0.0523	0.0265	0.0243	0.0269	$Y_{S-B,hiq}$	0.700	0.520	0.539	0.809
$k_{m-B,hiq}$	102	1370	418	1468	$Y_{S-B,loq}$	0.867	0.996	0.998	1.000
$k_{m-B,loq}$	1175	5.89	522	726	$Y_{S-F,hiq}$	0.608	0.593	0.671	0.612
$k_{m-BP,P}$	-	280	295	264	$Y_{S-F,loq}$	0.871	0.775	0.891	0.891
$k_{m-BP,hiq}$	5.81	8.93	2.80	1.81	$Y_{S-BP,P}$	-	0.999	0.750	0.712
$k_{m-BP,loq}$	13.1	1288	1500	1261	$Y_{S-BP,hiq}$	0.555	0.527	0.500	0.500
$k_{F,P}$	-	9.69	9.76	9.77	$Y_{S-BP,loq}$	0.990	0.853	0.742	0.841
T_{y-F}	-	0.0414	0.0343	0.444	D_{hiq}	17.1	11.5	4.02	15.9
$K_{S-F,P}$	-	0.14	0.11	0.10	D_{loq}	2.59	3.85	3.86	4.98
$T_{F,P}$	-	18.4	32.3	27.4	K_{d-hiq}	1.58	1.28	2.94	2.46
a_{max-B}	0.183	0.318	0.413	0.272	K_{d-loq}	9.05	11.5	10.5	9.23
a_{max-F}	0.156	0.257	0.263	0.274	λ	2.30	7.25	3.61	2.61
a_{max-BP}	0.196	0.136	0.135	0.139	$r_B(t=0)$	0.0212	0.0100	0.0101	0.0100
$K_{a-B,hiq}$	1.33	4.99	1.60	1.79	$r_F(t=0)$	0.0107	0.0101	0.0102	0.0106
$K_{a-B,loq}$	1.05	5.47	5.12	5.20	$r_{BP}(t=0)$	0.965	0.999	0.897	0.907
$K_{a-F,hiq}$	92.8	99.0	100	90.5	$f_B(t=0)$	0.950	0.306	0.365	0.407
$K_{a-F,loq}$	1.54	1.09	1.08	1.22	$f_{BP-B}(t=0)$	0.488	0.434	0.500	0.346
$K_{a-BP,P}$	-	4.04	2.52	1.95	$f_{DOC,hiq}(t=0)$	2.1×10^{-3}	1.1×10^{-4}	8.5×10^{-4}	3.0×10^{-4}
$K_{a-BP,hiq}$	23.7	3.90	5.05	5.02	f_{DOC}	0.630	0.848	0.778	0.762
$K_{a-BP,loq}$	1.57	2.84	2.75	2.86	f_P	-	0.891	0.888	0.890
q_{max-B}	2.02	8.99	6.51	6.76					

experiment with DOC extracted from fresh maize litter and estimated a half-life of 4.4 days for the labile DOC pool. Moreover, our finding of $Y_{L,hiq} > Y_{L,loq}$ is consistent with the mechanistic conception that the *hiq* litter fraction mainly contains readily soluble compounds released as initial flush, whereas *loq* litter largely consists of insoluble particulate material successively degraded by extracellular enzymes (Berg and McClaugherty 2008, Moorhead et al. 2013, Rinkes et al. 2014).

We found about three times higher diffusion coefficients and four times lower sorption coefficients of *hiq* DOC compared to *loq* DOC (Table 1). This indicates faster transport and lower retardation of *hiq* DOC vs. *loq* DOC. Diffusion and sorption coefficients implicitly reflect physicochemical characteristics associated with the two organic C fractions utilized in the model. Thus, based on the empirical correlation of Polson (1950), molecular diffusion coefficients in water for substances with a molar mass greater than 1 kg/mol can be calculated as

$$D = \frac{2.74 \times 10^{-5}}{M^{\frac{1}{3}}},$$

where D is the molecular diffusion coefficient in water (cm²/s) and M denotes the molar mass (g/mol). Recalculated from this equation, the fitted diffusion coefficients (compromise solution, Table 1) of *hiq* DOC correspond to molar masses of 2.60 – 204 kg/mol, those of *loq* DOC correspond to molar masses of 107 – 764 kg/mol. These values are in the range typically observed with DOC sampled from soil and litter (Kiikkilä et al. 2013, Malik and Gleixner 2013). Similar to the PECCAD model, a site-specific version (silt loam forest soil) of the DyDOC (dynamic DOC) model distinguishes between two different DOC fractions: PDOM1 is associated to hydrophilic compounds, PDOM2 to more hydrophobic DOC compounds (Tipping et al. 2012). The linear sorption coefficients $K_{d,hiq}$ and $K_{d,loq}$ optimized with the PECCAD model (Table 1) were lower than the corresponding values optimized with DyDOC ($K_{d-PDOM1} = 5 - 5.8$ mm³/d, $K_{d-PDOM1} = 140 - 160$ mm³/d). Note, differences between their and our estimates may of course arise due to differing sorbent properties and DOC compositions of the studied soils. The implementation of *hiq* and *loq* C pools in PECCAD is based on the fact that physicochemical characteristics of DOC compounds determine their degradability, availability and, hence, their quality as substrate for microbes (Kalbitz et al. 2003; Kiikkilä et al. 2013). In accordance with that, it follows from the above that the estimates of sorption and diffusion coefficients reasonably indicate association of small hydrophilic compounds with the *hiq* DOC pool, whereas the *loq* DOC pool is rather associated with large less hydrophilic compounds.

Comparing optimized values of PECCAD's biokinetic parameters with values obtained with other models is limited by the fact that the exact model parameterization is closely linked to the structure of biological processes implemented. In addition, the optimized values of bioki-

netic parameter values typically depend on experimental conditions (e.g. pF, pH or temperature) that influence microbial functioning but are currently not explicitly considered in the PECCAD model (Estrella et al. 1993, Langner et al. 1998, Brusseau et al. 2006). Nonetheless, comparisons with other studies can help to reveal if the optimized biokinetic parameters of the PECCAD model are reasonable or not.

Optimized values of maximum growth rates of bacteria and fungi (μ_{max} , Table 1) are 1-2 orders of magnitude lower than the corresponding values (2.59 d^{-1} and 25.5 d^{-1}) estimated in the study of Ingwersen et al. (2008). Neglecting differences in experimental conditions and model structure, this difference may originate from the fact that Ingwersen et al. (2008) used fixed and equal substrate affinity coefficients for the two DOC pools. Both parameters are, however, highly correlated and several different combinations of both values can result in similar growth kinetics (Kovarova-Kovar and Egli 1998). In contrast to Ingwersen et al. (2008), PECCAD assumes multi-substrate Monod kinetics employing substrate- and decomposer-specific affinity constants. These parameters have been identified to strongly affect model dynamics (Pagel et al. 2014). In this study, other than in Ingwersen et al. (2008), they were fitted together with the maximum growth rates. Further, maximum growth rates in the range from 1 to 29 d^{-1} have been typically utilized in studies investigating the dynamics of either single species (mostly *E. coli*) growing on glucose and other easily degradable substrates (Simkins and Alexander 1984, Kovarova-Kovar and Egli 1998, Lendenmann and Egli 1998), soil microorganisms after glucose amendment (Smith 1979, Blagodatsky et al. 2000), or of microbial pools in soil associated with the degradation of labile C pools (Paustian and Schnürer 1987, Toal et al. 2000). That is, maximum growth rates $> 1 \text{ d}^{-1}$ correspond to fast growing microorganisms utilizing easily degradable substrates (Wutzler and Reichstein 2013). In contrast, Zelenev et al. (2005) apply a much lower maximum growth rate of 0.24 d^{-1} for oligotrophic soil microbes, Moorhead and Sinsabaugh (2006) give a “C uptake rate coefficient” (corresponding to the maximal growth rate parameter of PECCAD) for microorganisms involved in litter decay from $0.04 \text{ d}^{-1} - 0.10 \text{ d}^{-1}$, and recently Sistla et al. (2014) reported a value of 0.15 d^{-1} . Our estimated maximum growth rates of bacteria and fungi are relatively close to the latter values. Modeled bacterial and fungal pools are dominated by species growing relatively slowly.

The maximum growth rate of specific bacterial pesticide degraders is in the range of $3.12-5.76 \text{ d}^{-1}$ estimated by others for 2,4-D and MCPA degraders in pure culture and soil (Shelton and Doherty 1997, Föchslin et al. 2003, Rosenbom et al. 2014). Cederlund (2007) determined specific growth rates of up to 10 d^{-1} for MCPA degrading microorganisms in the soil of a railway embankment.

The optimized maximum growth rate of bacterial pesticide degraders (Table 1; overall optimum) is ~ 6-times higher than those of bacteria in general and even ~27-times higher than those of

fungi. Higher growth rates of bacteria compared to fungi are in line with lower experimentally estimated turnover times of bacteria (0.5 – 215 days) vs. fungi (20 – 580 days) in soil (Rousk and Bååth 2011) and higher net growth rates of bacteria ($9 - 60 \text{ d}^{-1}$) than fungi ($0.3 - 8.4 \text{ d}^{-1}$) determined in solution culture under optimum conditions (McGill et al. 1981). The highest substrate affinity to *hiq* DOC (k_{hiq}) is attributed to bacterial pesticide degraders followed by bacteria and fungi, whereas fungi show dramatically higher (>250 times) substrate affinities to *loq* DOC than bacteria and pesticide degraders.

The growth parameters characterize the population of bacterial pesticide degraders and to a less extent also that of other bacteria as relatively fast growing microorganisms specialized on easily degradable substrates (*hiq* DOC). In contrast fungi are simulated as rather slow growing microorganisms specialized on less easily degradable substrates (*loq* DOC).

Optimized values of substrate uptake efficiencies (Y_S) differ primarily with the kind of substrate. Thus, Y_S is lower for *hiq* DOC and MCPA (0.50 – 0.809) than for *loq* DOC (0.841 – 1.00). How substrate quality (i.e. chemical composition and molecular size) controls Y_S is not yet fully understood. In general, Y_S varies with substrate quality because of differences in metabolic assimilation pathways (Gommers et al. 1988, Van Hees et al. 2005). On the one hand, substrate uptake efficiencies may be low if many enzymatic steps are needed until the C contained in a compound can be assimilated (Manzoni et al. 2012, Sinsabaugh et al. 2013). Higher optimized Y_S values for *loq* DOC (i.e. large molecules) vs. *hiq* DOC/MCPA (i.e. small molecules which are readily available) stand in contrast to this argumentation, but may be explained in accordance with a counteracting mechanism that controls Y_S due to the degree of reduction of substrates. The degree of reduction is defined as “the number of available electrons per unit carbon atom of a substance which can be transferred to oxygen” (Minkevich and Eroshin 1973, Battley 2009). It is a measure of the chemical energy content of organic substances (for details see Gommers et al. 1988, Manzoni et al. 2012). Considering a single compound as energy and growth substrate, Y_S approaches the theoretical limit of unity at a degree of reduction of a substrate larger than five (Gommers et al. 1988). Indeed, many readily available substrates (corresponding to *hiq* DOC) used by microorganisms (e.g. miscellaneous organic acids, amino acids and carbohydrates) as well as MCPA have a degree of reduction smaller than five (Manzoni et al. 2012). They can be classified as energy-limited, i.e. their energy content per C is not sufficient to completely transform all substrate-C into biomass-C. This results in Y_S values smaller than unity down to extremely low values such as, e.g., < 0.2 in the case of oxalate (Gommers et al. 1988). Following this line of argumentation higher Y_S values for *loq* DOC vs. *hiq* DOC/MCPA would reflect that the modeled *loq* DOC is dominated by compounds not energy-limited, whereas *hiq* DOC rather consists of energy-limited substances. In addition, Y_S of a substrate utilized as carbon and energy source can also increase if a second substrate is dominantly utilized as energy source during mixed substrate utilization (Gommers et al. 1988).

Thus, preferential use of *hiq* DOC compounds and MCPA as energy source vs. *loq* DOC compounds might also explain higher Y_S of *loq* DOC than *hiq* DOC and MCPA. More detailed characterization of measured DOC, e.g. by electrospray ionization combined with ultra-high-resolution mass spectrometry (Reemtsma 2009, Roth et al. 2014), would probably allow to constrain identified substrate-specific Y_S . Considering the same substrate, differences of Y_S attributed to microbial pools were much less pronounced. This latter finding is in line with recent studies, where no differences in carbon use efficiency (which is conceptually similar to Y_S) between bacteria and fungi were found (Thiet et al. 2006, Dijkstra et al. 2011). In contrast, earlier experimental observations and model implementations (e.g. in the CENTURY model; Parton et al. 1987) suggested higher carbon use efficiency of fungi than of bacteria (see review by Manzoni et al. 2012).

Other than most models, PECCAD applies a microbial death rate function that depends on the substrate concentration. It is controlled by two parameters: a_{max} and K_a . Model outputs are highly sensitive to maximum specific death rates (a_{max}), but the inhibition coefficients of microbial death rates (K_a) show low sensitivity indices (Pagel et al. 2014). Therefore, we will only compare the estimated a_{max} values to those from other studies. The maximal specific death rates of all three microbial populations are four to ten times lower than the value (1.3 d^{-1}) estimated by Blagodatsky et al. (1998) and applied by Ingwersen et al. (2008). However, they were close to values (0.12 and 0.24 d^{-1}) used in other models (Smith 1979, Gras et al. 2011, Lashermes et al. 2013). Zelenev et al. (2005) utilized maximum specific death rates of 0.12 d^{-1} and 5.76 d^{-1} for copiotrophic and oligotrophic soil bacteria, respectively. Compared with estimates of Blagodatsky et al. (1998), we probably found lower a_{max} , because these authors studied a glucose-amended soil, in which the proportion of active copiotrophic microorganisms was higher than in our soil. Similarly, Monga et al. (2014) estimated mortality rates of five different bacterial species incubated with fructose in sand microcosms in the range of $0.22 - 1.4 \text{ d}^{-1}$. We found very similar a_{max} values for bacteria and fungi. This result is supported by a recent experimental study, in which mortalities of bacteria and fungi (25% and 27%) within the first three hours following the rewetting of a seasonally dried soil were similar (Blazewicz et al. 2014).

The estimated maximum specific maintenance rates of bacteria and MCPA degraders (m_{max}) are about 1-2 magnitudes lower than their corresponding maximum growth and death rate coefficients. In line with Ingwersen et al. (2008), this suggests that exogenous maintenance respiration plays a minor role compared to growth and death fluxes. However, they used an about tenfold higher value (0.25 d^{-1}) in their model based on literature data from Gignoux et al. (2001). These authors pointed to the scarcity and the large uncertainty of m_{max} estimates. Published estimates of specific maintenance rates corresponding to m_{max} can be found to be in the

range of 0.0017 – 0.744 d⁻¹ (Anderson and Domsch 1985a, 1985b, Mueller et al. 1997, Blagodatsky et al. 2010, Gras et al. 2011, Wang et al. 2014). This wide variety of estimates arises partly because various maintenance concepts are still debated. As a consequence, very different approaches are utilized in models (Van Bodegom 2007, Blagodatsky et al. 2010, Wang and Post 2012).

The inhibition coefficients (k_r) are parameters of three functions, which control the physiological state r of the three microbial pools, i.e. their transition from the dormant to the active state and vice versa (Pagel et al. 2014). Our k_r estimates (Table 1) extend the range of 0.051 to 2.3 mg C/g reported by Blagodatsky et al. (1998) and Ingwersen et al. (2008). Yet, it must be noted that absolute k_r values cannot be directly compared. The number and structural integration of microbial pools differs between the three models. Considering each microbial population individually, our fitted k_r values were lowest for *hiq* DOC/MCPA and highest for *loq* DOC. This means that microorganisms respond more sensitively to changes in the supply with *hiq* DOC and MCPA than to alterations of *loq* DOC. This finding is basically in line with Ingwersen et al. (2008). However, they had set up their model in such a way that initial-stage DOC (corresponding to *hiq* DOC) was exclusively consumed by initial-stage decomposers, whereas late-stage DOC (corresponding to *loq* DOC) was exclusively consumed by late-stage decomposers. Much lower values of $k_{r-F,hiq}$ and $k_{r-BP,P}$ compared to the other k_r estimates indicate that the onset of activity of fungi and specific bacterial MCPA degraders is triggered already at relatively low concentrations of *hiq* DOC and MCPA, respectively. In particular, fungi respond faster to additional supply of *hiq* DOC by switching to the active state than bacteria. Specific bacterial MCPA degraders respond more strongly to MCPA-C than to *hiq* and *loq* DOC. The high sensitivity of the physiological state of specific MCPA degraders to changes in MCPA supply is reasonable. In contrast, the high sensitivity of fungal physiological activity to *hiq* DOC is somewhat unexpected in view of the fact that we estimated a high fungal substrate affinity to *loq* DOC and a relatively low maximum growth rate of fungi (see above). On the other hand, these values might be interpreted as implicitly reflecting fungal activity stimulation by intermediate degradation products of extracellular enzymes (associated with *hiq* DOC) that act as inducers of enzyme production (Allison et al. 2011).

Based on the identified biokinetic parameter, the simulated microbial pools of the PECCAD model can be ecologically categorized as follows. The two bacterial pools mainly reflect the characteristics of r-strategists/copiotrophs, whereas the fungal pool predominantly consists of K-strategist/oligotrophs (Fierer, Bradford, and Jackson 2007). We must be aware of the fact, however, that bacterial and fungal populations in soil are complex and consist of numerous species, which cover a broad continuum of ecological characteristics. How to best simplify the high complexity of soil microbial community composition in mathematical models remains a big challenge.

Studies on co-metabolic transformation of pesticides in soil by fungi are scarce (Ellegaard-Jensen et al. 2013). Recently, Aslam et al. (2014) modeled the enhanced degradation of the herbicide glyphosate in a maize detritusphere. They attributed its biodegradation exclusively to co-metabolic transformation. To our knowledge, there is no study in which the co-metabolic transformation of MCPA is simulated. Our estimated value of the maximum specific rate of MCPA utilization via co-metabolism by fungi in the absence of growth substrates ($k_{F,P}$) reaches almost 10 d^{-1} (Table 1). This high $k_{F,P}$ in relation to a μ_{max-F} value $< 1 \text{ d}^{-1}$ in combination with a $T_{y,F}$ estimate < 0.5 indicates that the co-metabolic pesticide consumption rate function of fungi (Eq. 33; Pagel et al. 2014) is dominantly controlled by the $k_{F,P}$ and $K_{S-F,P}$ parameters. Overall, the parameterization of the co-metabolic pesticide consumption rate function suggests an essential contribution of co-metabolic MCPA transformation by fungi on the total MCPA dissipation. The $Y_{R-F,P}$ estimate reveals that about 70% of the total co-metabolically transformed MCPA-C is directly mineralized to CO_2 . Such a high proportion of CO_2 production associated with co-metabolic MCPA transformation would be in line with the mechanism that intermediate metabolites are to a large extent directly utilized for the resupply of energy or reduction equivalents, which have been consumed in the initial enzymatic attack of the MCPA molecule (Brandt et al. 2003). Consequently, only a small percentage of co-metabolized MCPA-C is then released as *hiq* DOC. The $T_{F,P}$ value (Table 1) indicates an approx. 30-fold lower maintenance burden to the fungal biomass compared to the total flux of co-metabolic MCPA transformation by fungi (compare Eqs. 6, 20,34; Pagel et al. 2014). In contrast, other studies report transformation capacity values corresponding to $T_{F,P}$ values $\ll 1$ for more toxic compounds (e.g. Trichlorethylene) than MCPA (Alvarez-Cohen and Speitel Jr 2001, Chen et al. 2008, Sedighi and Vahabzadeh 2014). Thus, for such substrates the maintenance burden to microorganisms in terms of C is severalfold higher than the substrate-C actually transformed via co-metabolism. Because such a strong adverse impact of MCPA or its degradation products is not documented, we set the lower bound of $T_{F,P}$ to unity (see Appendix B: Table B1).

Compared to that of fungi the maximal specific insoluble SOM decomposition rate of bacteria is much higher ($q_{max-B} = 6.76 \text{ d}^{-1}$, $q_{max-F} = 0.72 \text{ d}^{-1}$; Table 1). Note, however, the high uncertainty of the q_{max-F} estimate as reflected in the large difference between the fitted values associated with the L treatment and the compromise solution. This is mainly caused by the low sensitivity of model outputs to q_{max-F} (Pagel et al. 2014). In addition, the estimation of parameters of SOM kinetics is weakened by the large uncertainty of TOC measurements (see below). The q_{max} estimates of Ingwersen et al. (2008) and Blagodatsky et al. (1998) (1.6 and 2.3 d^{-1}) lie between our two values, but these two models applied only one mutual q_{max} parameter for the total microbial community. Our q_{max} estimates are 3-4 orders of magnitudes higher than the decomposition rate constants of insoluble SOM pools applied by widely used C turnover models such as RothC, CENTURY or DAISY (Parton 1993, Gjettermann et al. 2008, Rampazzo Todorovic

et al. 2010). Other than in these models, however, in the PECCAD model the apparent insoluble SOM decomposition rate is limited by the biomass and physiological state of microbial pools. This explains higher absolute values of q_{max} (Wutzler and Reichstein 2013). The substrate affinity coefficients of insoluble organic matter (K_i) approach their lower bound, whereby K_i estimates of fungi and bacteria are very close (Table 1; Appendix B: Table B1). In contrast to the K_i values estimated by Blagodatsky et al. (1998) and used by Ingwersen et al. (2008), our K_i estimates are approximately one order of magnitude lower than the average insoluble SOM concentration. This indicates that the SOM decomposition rate is not limited by SOM substrate availability. Rather, PECCAD's model structure and parameterization implicitly reflect that production and activity of extracellular enzymes are strongly regulated by microbial dynamics, which is highly consistent with recent experimental results (Kramer et al. 2013, Spohn and Kuzyakov 2014, Talbot et al. 2014) and mathematical models that explicitly account for enzyme dynamics (Allison et al. 2010, He et al. 2014, Moore et al. 2014).

A small number of parameters that characterize the initial conditions in soil had to be calibrated, because these values were not accessible to direct measurement. The low $f_{DOC,hiq}(t=0)$ values means that the total DOC in soil initially contains only a minor fraction of *hiq* DOC (< 0.3%). Hence, litter-C input was the major source of *hiq* DOC. This is in accordance with simulations by others (Ingwersen et al. 2008, Wutzler and Reichstein 2013, Aslam et al. 2014). The estimated initial fraction of bacteria on the total microbial biomass $f_B(t=0)$ of 0.41 corresponds well to a fungi-to-bacteria ratio of 37 - 76% as reported by Joergensen and Wichern (2008) for the microbial biomass of arable soils. The values of $f_B(t=0)$ and $f_{BP-B}(t=0)$ (initial fraction of bacterial MCPA degraders on the total bacterial biomass) were used to compute conversion factors from copy numbers of 16S rRNA genes, fungal ITS fragments and *tfdA* genes to C contents of the microbial model pools and vice versa. Based on the compromise values of $f_B(t=0)$ and $f_{BP-B}(t=0)$ and the gene abundances measured in soil before the start of the experiment, we calculated the following ratios (copy numbers per mg C):

16S rRNA genes/bacterial C = 6.44×10^{11} ,

fungal ITS fragments/fungal C = 1.52×10^9 , and

tfdA genes/bacterial degrader C = 1.12×10^8

Assuming that the mass of bacterial C ranges from 10 to 100 fg/cell (McMahon and Parnell 2014) the ratio of 16S rRNA genes to bacterial C results in a range of 6.4 - 64 copies of 16S rRNA genes/cell. Despite this wide uncertainty range, our assessment is close to the measured 16S rRNA gene copy numbers/cell in bacteria ranging from 1 - 15 (Kembel et al. 2012). Klappenbach et al. (2000) proposed that the number of rRNA operons in a bacterial genome represents one microbial trait allowing bacteria with a higher number of rRNA operons (≥ 5) to respond faster to resource availability. Our lowest estimate of 6.4 copies/cell might be biased

towards a higher value, because the extraction of extracellular DNA originating from dead bacteria results in an overestimation of the 16S rRNA gene abundance in relation to the living microbial biomass captured by the chloroform fumigation-extraction method (Pietramellara et al. 2009). Further uncertainty arises because extraction efficiencies of DNA and fumigated biomass-C both vary with soil characteristics (Joergensen 1996, Anderson and Martens 2013). The fraction of fungal ITS fragments/fungal C indicates a much lower number of gene copies per biomass-C in fungi than in bacteria. Baldrian et al. (2013) report a comparable ratio of fungal ITS fragments/dry biomass of 0.794×10^9 copies/mg C for fruit bodies of several fungi collected at a forest site. The authors explicitly point to the high level of variation in ITS copy number estimates even within one species. Performing the same calculation as for 16S rRNA genes (see above), the ratio *tfdA* genes/bacterial degrader C results in much less than one *tfdA* gene copy/cell (0.001 – 0.012). Consequently, the initial proportion of bacterial MCPA degraders has been probably overestimated considering the relatively high estimate that about 14% of the total microbial biomass initially consists of bacterial pesticide degraders (Table 1). On the other hand, specific bacterial MCPA degraders were substantially enriched by the pre-incubation of soil carried out after amendment of 20 $\mu\text{g/g}$ MCPA (see Material & Methods). Similarly, Klappenbach et al. (2000) reported a high relative enrichment of 2,4-D-degrading bacteria, which represented up to 10% of the total culturable bacteria from soil microcosms after one-time pulses of 2,4-D addition. Moreover, whereas MCPA-degrading bacteria carry *tfdA* genes, also bacteria harboring *cadA* and *r/sdpA* genes have been identified to degrade MCPA (Liu et al. 2013). Thus, the modeled pool of bacterial MCPA degraders may be considered to only partly consist of microorganisms carrying *tfdA* genes, albeit we implicitly assume that the abundance of *tfdA* genes can be used as a genetic proxy reflecting the total MCPA-degrading bacterial community. The fitted initial physiological states of bacteria and fungi $r_B(t=0)$ and $r_F(t=0)$ approached its lower bound of 0.01 (Table 1; Appendix B: Table B1). In comparison, Blagodatsky et al. (1998) and Ingwersen et al. (2008) report values of 0.1 – 0.165, whereas Wutzler et al. (2012) estimated the mean $r(t=0)$ of 32 arable soil samples by kinetic respiration analysis to be 0.004. Further, a low proportion of active microbes is in agreement with estimates that typically less than 20% of the total microbial community in soils is in an active state (Lennon and Jones 2011, Wang et al. 2014). In their recent review on the activity state of microorganisms in soil (Blagodatskaya and Kuzyakov 2013) even state that the portion of active microorganisms actually contributing to ongoing biogeochemical processes is as low as 0.1 – 2% and does not exceed 5% of the total microbial biomass in soil. In contrast, the initial physiological activity of the bacterial MCPA degrader pool $r_{BP}(t=0)$ was very high. Although an initially higher proportion of active bacterial MCPA degraders compared to the total bacteria and fungi can be reasonably attributed to the pre-incubation of the soil with MCPA, the $r_{BP}(t=0)$ parameter is probably overestimated. This is substantiated considering that the

steady state value of r_{BP} at $t=0$ is 0.19, which can be calculated from the initial MCPA and DOC concentrations and the k_{r-BP} estimates according to the compromise solution. With steady state, the values of r_B and r_F at $t=0$ are much lower (5.5×10^{-3} and 1.9×10^{-2}).

The applied batch extraction of DOC (see material and methods) overestimates the *in situ* DOC in the soil solution as simulated with PECCAD, because the DOC captured in the extracts additionally contains some sorbed phase C as a result of the lower soil/solution ratio used in extraction than *in situ*. To account for this potential overestimation and to assure compatibility of PECCAD model outputs and measurements, we fitted the parameter f_{DOC} . Its value of 0.76 (Table 1) suggests that DOC measured in K_2SO_4 extracts overestimates the *in situ* DOC concentration in the soil solution by a factor of 1.3 ($1/0.76$). This is in good agreement with the data on differentially extracted DOC from a silty loam soil Zsolnay (Zsolnay 2003).

The estimate of f_P (Table 1) confirms a slightly reduced extraction efficiency of MCPA with K_2SO_4 solution in comparison to the MeOH/H₂O extraction. The lower efficiency had to be considered to avoid unrealistic high model outputs of ¹⁴C activity in K_2SO_4 extractable DOC.

The parameter values given in Table 1 yield relevant model realizations that optimally match the observed dynamics of C, MCPA and microorganisms. We are, however, aware of parameter uncertainty arising from errors of input and calibration data as well as from structural errors of the model (Vrugt and Sadegh 2013). The available data might also not have been sufficient to simultaneously identify the large number of parameters associated with the high complexity of the PECCAD model (Young 2013). Thus, the identified Pareto parameter sets might represent only a subset of suitable model realizations (equifinality, Beven 2006). It is impossible to infer the uncertainty associated with the optimized parameter set from the Pareto analysis alone. In future studies, for instance approximate Bayesian computation (Vrugt and Sadegh 2013) could be used for an enhanced investigation of the Pareto solution space in the front region.

6.4.2 *Microbial regulation of MCPA degradation coupled to C turnover in the detritusphere*

Measured dynamics of C, MCPA and microorganisms

The presence of litter resulted in up to five times higher respiration rates in comparison to the control (M treatment) (Fig. 2) as well as in increases in extractable DOC (Fig. 3), microbial biomass C and abundances of genetic proxies (Fig. 4) in the soil close to the soil-litter interface. The soil data in combination with the $\delta^{13}C$ abundance of TOC (Fig. 3) suggest a detritusphere dimension of up to 6 mm (see Appendix C). The concentration/abundance gradients were most pronounced in the 0 - 3 mm soil layer adjacent to litter in good agreement with other studies (Gaillard et al. 2003, Poll et al. 2006, 2008, Marschner et al. 2012).

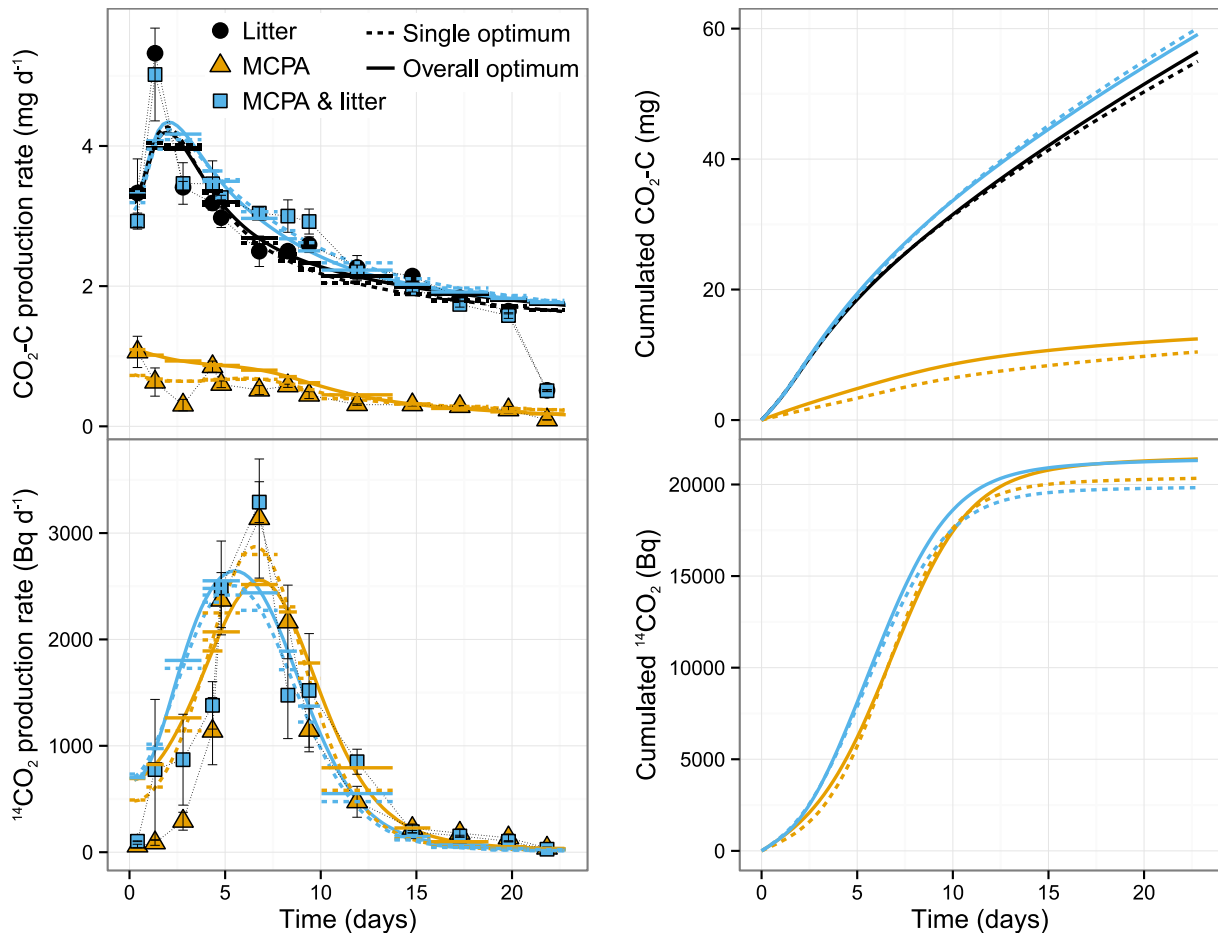


Fig. 2 Measured and simulated respiration and MCPA mineralization of the entire soil cores. Symbols show means and error bars indicate standard errors of four replicates. Horizontal line segments represent the model fits to the observed average CO₂ production rates. Continuous lines show simulated CO₂/¹⁴CO₂ production rates and cumulated CO₂/¹⁴CO₂ using either the treatment specific optimal parameters (dashed line) or the compromise parameter set (solid).

In the detritosphere, we found accelerated MCPA degradation in combination with increased incorporation of ¹⁴C into the microbial biomass and into TOC (Fig. 5). This confirms our previous results (Poll et al. 2010). Nowak et al. (2011) showed that the C in non-extractable residues of 2,4-D can be almost completely assigned to microbial residues. Hence, we suppose that at the end of the experiment, the largest part of the non-extractable ¹⁴C TOC (Fig. 5) can be primarily ascribed to residues of microorganisms that had assimilated MCPA-C before, either directly from the parent compound or indirectly as part of the C cycling in soil. Our results thus point to accelerated and increased formation of MCPA-derived biogenic residues in the detritosphere. The measured dynamics of extractable ¹⁴C-DOC essentially paralleled that of MCPA (Fig. 5). Thus, any metabolites and co-metabolic transformation products of MCPA that might had been formed were not accumulated, but rapidly converted.

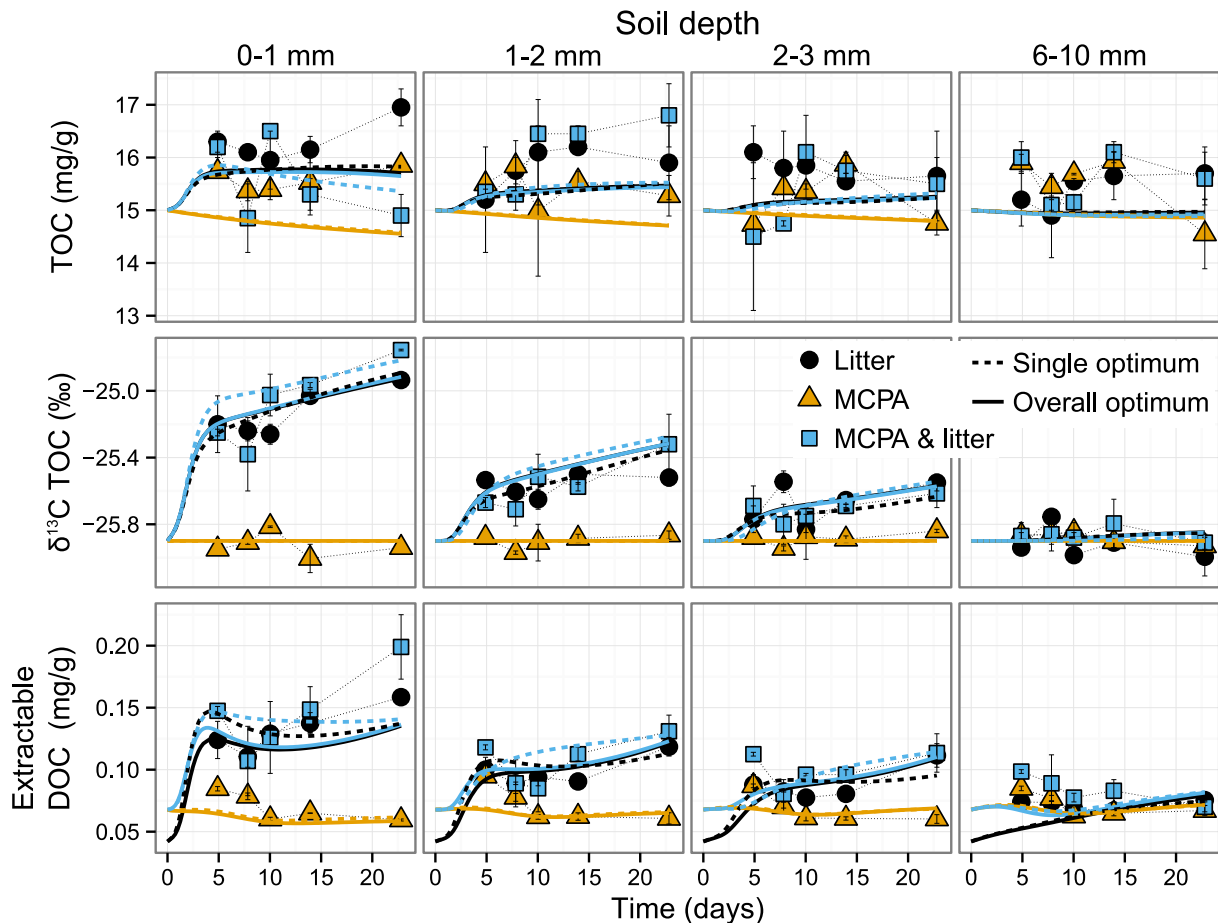


Fig. 3 Dynamics of organic C pools in three selected soil layers close to litter (0-3 mm) and one in “bulk” soil (6-10 mm). Symbols show means and error bars indicate standard errors of two replicates. Continuous lines show simulated values using either the treatment specific optimal parameters (dashed line) or the compromise parameter set (solid). See Appendix C: Fig. C1 for additional measurements and simulations of soil layers 3-4, 4-6 and 10-20 mm.

Other than in Poll et al. (2010), the ^{14}C mineralization kinetics as well as the total respiration rate differed only slightly between M and ML as well as L and ML treatments, respectively (Fig. 2). However, in another previous experiment (Ditterich et al. 2013), we also found no effect of MCPA addition on total C mineralization. In agreement with both studies (Poll et al. 2010, Ditterich et al. 2013) we found a strong increase of fungal ITS fragments close to the soil-litter interface and a slight synergistic effect of MCPA, whereas there was no effect of MCPA without litter addition (Fig. 4). The abundance of 16S rRNA and *tdA* genes responded exclusively to litter addition (Fig. 4), whereas an increased abundance of both genetic markers had been measured before in the case of the ML treatment (Poll et al. 2010, Ditterich et al. 2013). Poll et al. (2010) additionally found slightly increased 16S rRNA gene abundance in response to solely MCPA amendment without litter addition.

The observed CO_2 , MCPA and microbial dynamics remarkably differs within the current and the two previous experiments, although the same soil as well as very similar pre-treatments and experimental conditions were used. This finding emphasizes that the reproducibility of soil experiments is limited as soon as microbial interactions are studied. Slight differences in experimental conditions most probably affect the initial status of microorganisms and result in

system behavior variability. In consequence this i) enhances the uncertainty of inversely estimated biokinetic parameters and ii) limits their applicability between individual experiments (Brusseau et al. 2006). The variability inherent to natural microbial systems should also kept in mind with respect to the following assessment of model simulations.

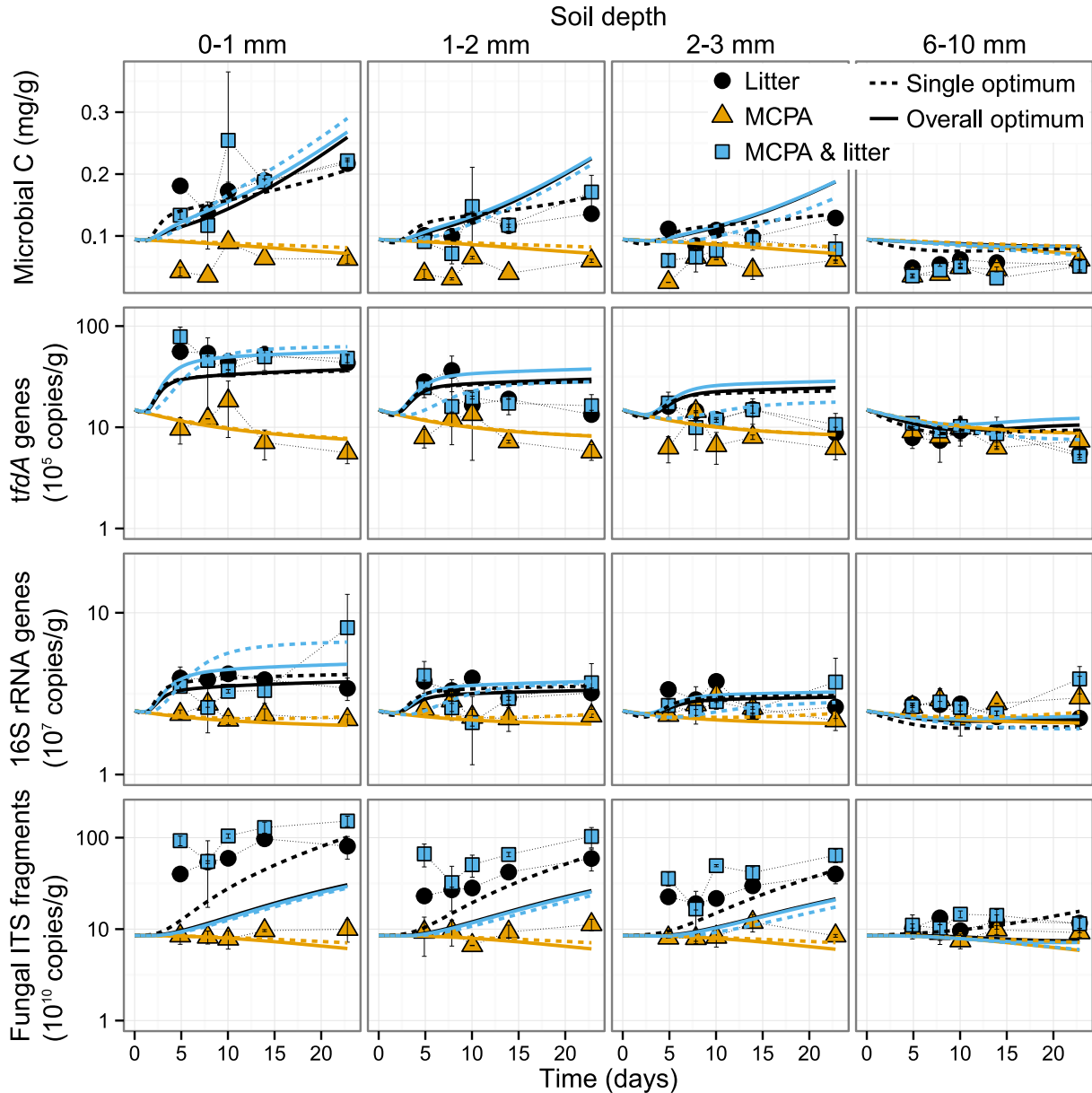


Fig. 4 Dynamics of microbial biomass C and genetic markers in three selected soil layers close to litter (0-3 mm) and one in “bulk” soil (6-10 mm). Symbols show means and error bars indicate standard errors of two replicates. Continuous lines show simulated values using either the treatment specific optimal parameters (dashed line) or the compromise parameter set (solid). See Appendix C: Fig. C2 for additional measurements and simulations of soil layers 3-4, 4-6 and 10-20 mm.

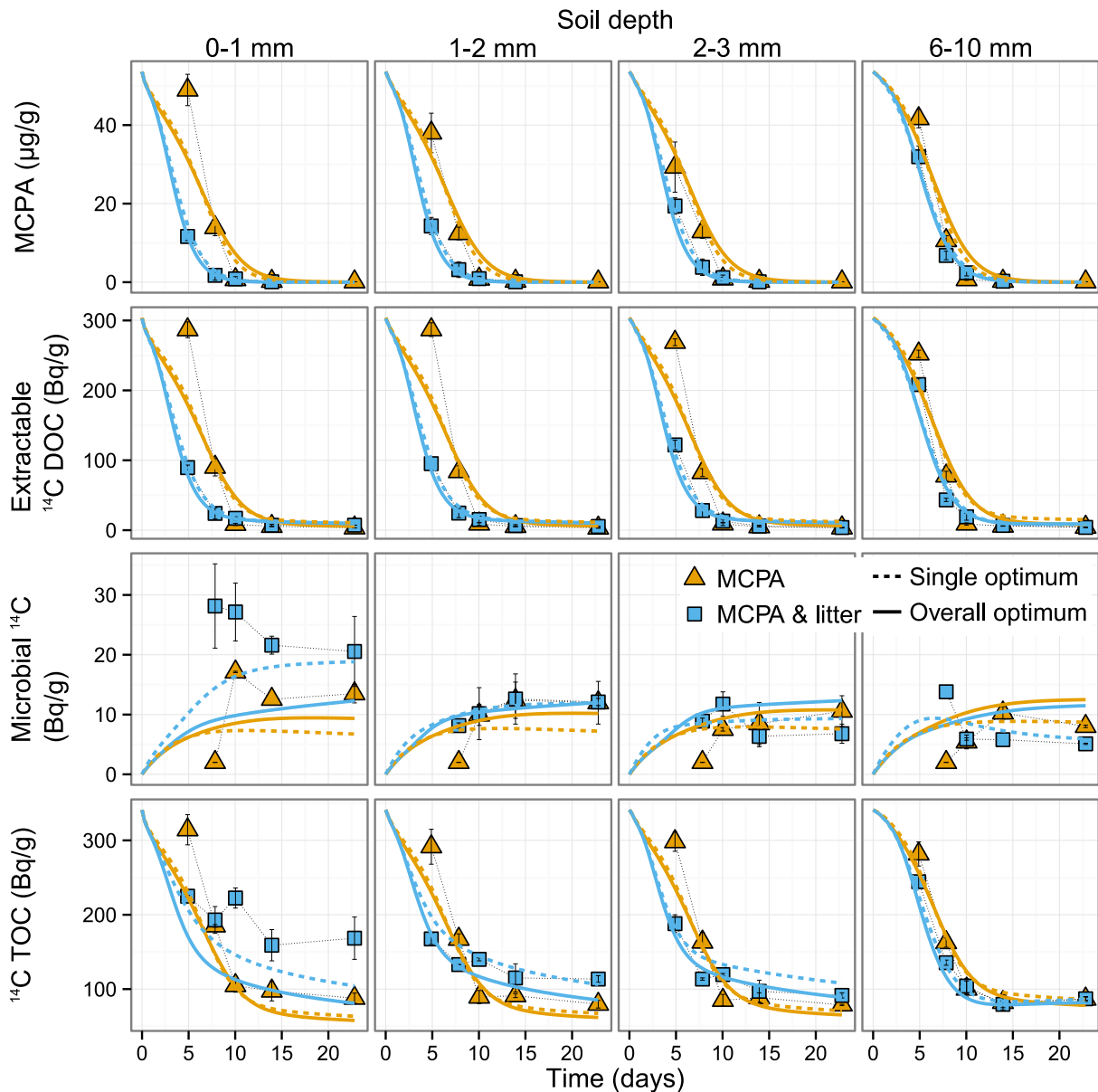


Fig. 5 Dynamics of MCPA and specific ^{14}C activity in organic C pools in three selected soil layers close to litter (0-3 mm) and one in “bulk” soil (6-10 mm). Symbols show means and error bars indicate standard errors of two replicates. Continuous lines show simulated values using either the treatment specific optimal parameters (dashed line) or the compromise parameter set (solid). See Appendix C: Fig. C3 for additional measurements and simulations of soil layers 3-4, 4-6 and 10-20 mm.

Model performance

The PECCAD model simulations agreed with the measured C and MCPA dynamics and nicely reproduced the impact of litter addition (Table 2, Fig. 2 - 5). The initial peak of soil respiration in the presence of litter was slightly underestimated, but the simulations predicted CO_2 production in the order $\text{ML} \sim \text{L} > \text{M}$ treatment in agreement with the data (Fig. 2). The model simulations correctly reflected the observed accelerated MCPA degradation in the detritosphere, but the observed initial lag phase of MCPA degradation in the case of the M treatment was not fully resolved as indicated by the simulated dynamics of $^{14}\text{CO}_2$ and MCPA in soil (Fig. 2, 5) and reflected in the initial overestimation of ^{14}C in microbial biomass (Fig. 5). The TOC dynamics could not be modeled well ($\text{EF} < 0$; Table 2), mostly because of uncertainty in the measured

data as indicated by the large standard deviations (Fig. 3). The uncertainty is probably due to the relatively small soil samples used in EA-IRMS measurements. In contrast, the accuracy of $\delta^{13}\text{C}$ data was high (Fig. 3) and so were the model efficiencies (Table 2). Note that model efficiency is low per se when measured variables show only little variation over time.

	EF _L *	EF _M	EF _{ML}		EF _L	EF _M	EF _{ML}
<i>MCPA concentration</i>				<i>Extractable DOC</i>			
M	-	0.90	0.88	L	0.75	-1.38	-19.7
ML	-	0.87	0.92	M	-6.14	-4.15	-4.61
Comp	-	0.86	0.91	ML	0.58	-3.12	0.37
				Comp	0.46	-3.44	0.18
<i>¹⁴C activity of microbial biomass</i>				<i>Extractable ¹⁴C DOC</i>			
M	-	-0.02	-0.19	M	-	0.86	0.88
ML	-	-0.45	0.49	ML	-	0.81	0.92
Comp	-	-0.07	-0.10	Comp	-	0.83	0.91
<i>¹⁴C activity of TOC</i>				<i>Microbial biomass</i>			
M	-	0.88	0.49	L	0.75	-1.38	-19.7
ML	-	0.83	0.75	M	-6.14	-4.15	-4.61
Comp	-	0.85	0.59	ML	0.38	-0.02	0.47
				Comp	0.46	-3.44	0.18
<i>Mean CO₂ production rate</i>				<i>Abundance of tfdA genes</i>			
L	0.71	0.02	0.53	L	0.56	-0.36	-24.3
M	0.56	0.43	0.54	M	0.43	-0.10	0.32
ML	0.67	0.09	0.65	ML	-0.73	-1.40	-0.12
Comp	0.69	0.04	0.65	Comp	-0.73	-1.40	-0.12
<i>Mean ¹⁴CO₂ production rate</i>				<i>Abundance of 16S rRNA genes</i>			
M	-	0.71	0.43	L	-0.02	-3.40	-25.6
ML	-	0.60	0.50	M	-0.06	-0.26	0.16
Comp	-	0.64	0.49	ML	-0.73	-1.40	-0.12
				Comp	0.10	-0.74	0.05
<i>TOC</i>				<i>Abundance of fungal ITS fragment</i>			
L	-0.50	-0.32	-0.36	L	0.46	-0.48	-0.39
M	-0.55	-0.30	-0.25	M	0.20	-0.42	-0.02
ML	-0.47	-0.33	-0.18	ML	-0.26	-0.98	-0.44
Comp	-0.50	-0.33	-0.23	Comp	-0.19	-0.90	-0.40
<i>$\delta^{13}\text{C}$ TOC</i>							
L	0.86	-0.01	0.43				
M	0.86	-0.01	0.69				
ML	0.77	-0.01	0.63				
Comp	0.85	-0.01	0.68				

Table 2 Performance of optimized parameter sets for best fits of the PECCAD model to the data of the three experimental treatments litter (L), MCPA (M) and MCPA & litter (ML) as well as for the compromise solution (Comp).

The model simulations could not match the observed decrease of microbial biomass accompanied by increased extractable DOC at the first two sampling dates in the M treatment (Fig. 3, 4). Note, however, that the initial decrease of microbial biomass was not reflected in the measured gene abundances (Fig. 4). The decrease of microbial biomass may indicate a toxic effect of MCPA on part of the soil microbial community (Cabral et al. 2003, Gonod et al. 2006, Poll et al. 2010). Dead microbes would directly lead to an increase of extractable DOC. The model simulation might have failed to match these measurements, because MCPA toxicity is not considered in the PECCAD model.

Although the PECCAD model simulations generally followed the observed increase of microbial biomass and gene abundances in the detritusphere (Fig. 4), the highest trade-offs in fitting the data of the three experimental data sets occurred with microbial dynamics (Table 2). In particular, the rapid, about tenfold increase of fungal ITS fragments close to the soil-litter interface could not be resolved. This discrepancy arises presumably because the relationship between the genetic marker abundance and biomass of each microbial pool was taken to be linear. We apply a simple conversion factor, calculated from the measured initial abundance of fungal ITS fragments and the inversely identified initial fungal biomass (see above). Yet, in real world, the abundance of fungal ITS fragments per biomass-C is probably strongly dependent on the physiological state and the composition of the fungal community in soil. In addition, Baldrian et al. (2013) showed that the quantification of fungal biomass by determination of ITS fragments is associated with high uncertainty because of high variation of rRNA gene copy numbers per biomass even within the same species. The authors pointed out that our ability to quantify fungal biomass pools in soil is limited, and that measurement methods must be improved to better catch reality. Summing up, the value of using fungal ITS fragments as genetic markers of fungal biomass is limited. The abundances of bacterial marker genes (*tfdA*, 16S rRNA genes) can be expected to be more reliable biomass proxies because of much lower variation of gene copies per biomass (see section “optimized parameters”). Future research should focus on model approaches that consider nonlinear relationships between gene abundance and biomass depending on physiological state and composition of microbial communities. At the same time, we need further progress in quantitative molecular techniques to improve the use of genetic proxies for integrating microbially explicit models with experiments.

Simulated pools and fluxes

The PECCAD model considers two pathways of MCPA degradation: i) the use of MCPA as growth and maintenance substrate by specific bacterial degraders and ii) co-metabolic transformation by fungi. There was no measured and simulated response of *tfdA* gene abundance to the MCPA amendment (i.e. no growth of bacterial MCPA degraders; Fig. 4). Consequently, in our simulations accelerated MCPA degradation in the detritusphere is predominantly regulated by fungal dynamics. According to the simulated dynamics in the first 3 mm soil layer close to litter (Fig. 6), input of litter-derived *hiq* and *loq* DOC by convective and diffusive transport (see Appendix D: Fig. D1) results in increased activity (physiological state r) and biomass of fungi (Fig. 6ab) as well as in accelerated fungal transformation of MCPA via co-metabolism (Fig. 6e).

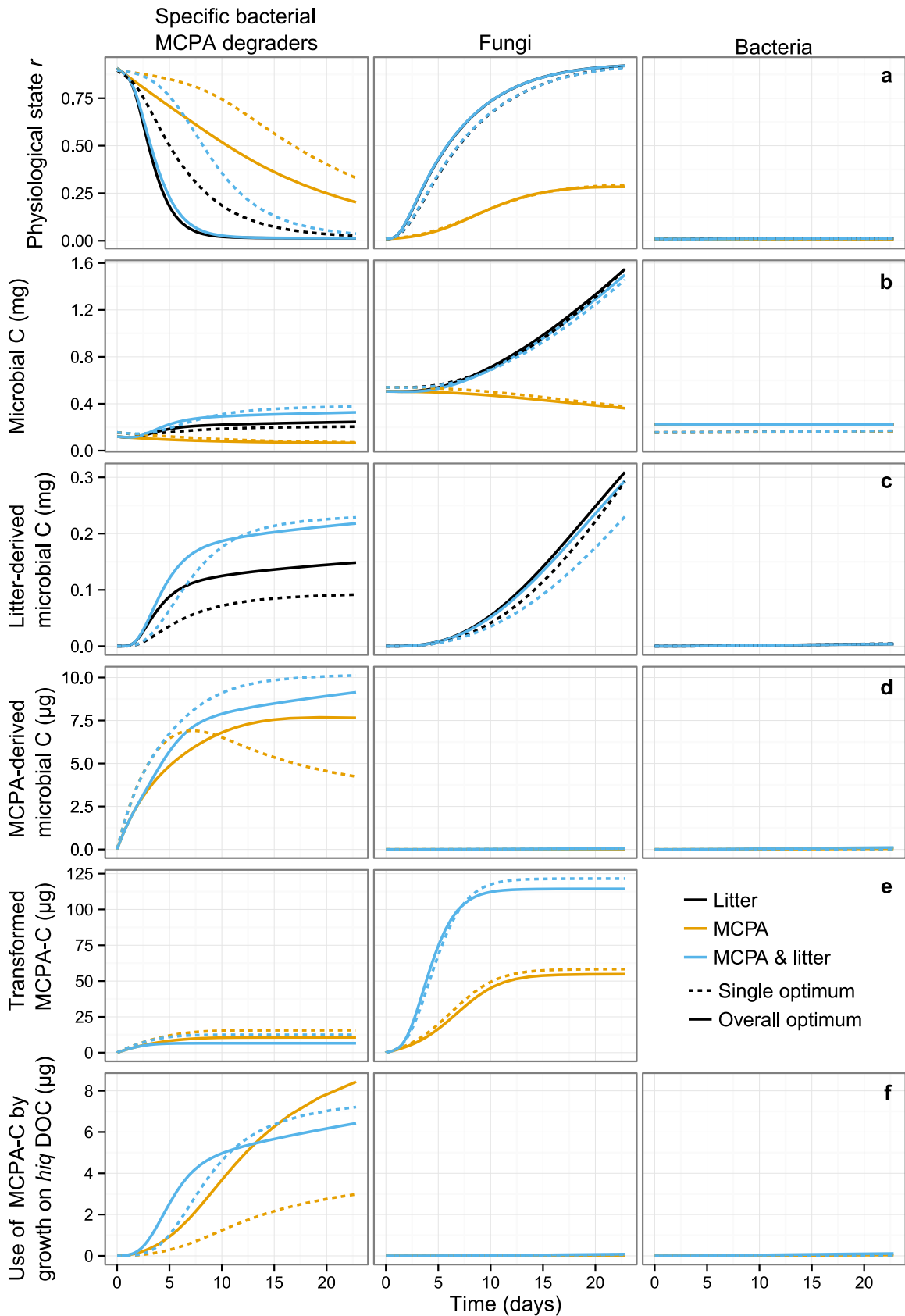


Fig. 6 Simulated microbial dynamics involved in coupled C turnover and MCPA degradation in the detritosphere (0-3 mm soil layer). Row **a** shows the mean simulated physiological state variable r that indicates which proportion of the total microbial pool is active (0 .. 1). Rows **b-d** represent total, litter-derived and MCPA-derived C in microbial biomass, respectively. Row **e** represents how much C of the parent MCPA compound was either used for growth and maintenance by specific bacterial degraders (left) or transformed to hiq DOC via fungal co-metabolism. Row **f** reflects the cumulated amount of MCPA-C from hiq DOC used for growth.

In contrast, the physiological state of bacterial MCPA degraders is mainly triggered by the availability of MCPA (see also section “optimized parameters”) resulting in a rapid reduction of physiologically active degraders as MCPA dissipates and only slightly enhanced biomass by litter-C (Fig. 6bc). The simulations show that MCPA is predominantly degraded via co-metabolic transformation by fungi (Fig. 6e), but specific MCPA degraders proliferate most from *hiq* DOC and thereby indirectly incorporate most MCPA-derived C in their biomass (Fig. 6df). However, in case of the ML treatment the model simulations failed to reflect the observed rapid ^{14}C incorporation into microbial biomass and TOC in the 0-1 mm soil layer directly adjacent to litter (Fig. 5). Thus, the indirect incorporation of MCPA-derived ^{14}C into the biomass of *tfdA*-harboring bacteria could not fully explain our measurements. We think this disagreement could be a consequence of the uncertainties associated with the use of the genetic proxies to constrain the modeled microbial pools. Indeed, it has been found that particularly *tfdA* class III genes are most strongly related to MCPA degradation, whereas *tfdA* class I genes typically dominate the total *tfdA* gene abundance (as measured in our study), but class I *tfdA* genes are not necessarily linked to MCPA degradation (Nielsen et al. 2011, Ditterich et al. 2013). Consequently, *tfdA* class III genes might have been a more sensitive genetic proxy for the bacterial MCPA degrader pool. Similarly, bacterial degraders harboring other genes than *tfdA* (see e.g.; Liu et al. 2013) that show different growth dynamics might have been involved in the degradation of MCPA in the present microcosm experiment and even fungal degraders that use MCPA as growth substrate may be responsible for MCPA degradation (see Shailubhai et al. 1983, Itoh et al. 2013). Thus, a biased dominance of co-metabolic vs. growth-linked MCPA degradation might be the reason that led to the underestimation of both i) the initial lag phase in case of the M treatment and ii) the observed rapid ^{14}C incorporation into microbial biomass and TOC in the 0-1 mm soil layer directly adjacent to litter in case of the ML treatment by PECCAD model simulations.

On the basis of our simulations we calculated the mass balance of total, litter-derived and MCPA-derived C pools and cumulated fluxes for the entire soil core, separated into 0-3 mm and 3-30 mm soil layers, at the end of the experiment (Appendix E: Fig. E1). Total C pools and cumulated fluxes clearly reflect increased C turnover in combination with accelerated MCPA degradation via stimulated microbial processes by litter-C input in the 0-3 mm compared to the 3-30 mm soil layer.

After 22.8 days 27% (56.1 mg) of total initial litter-C (206 mg) was decomposed. About 17% of decomposed litter-C corresponding to 4.6% of total litter-C was transferred to soil by convection and diffusion. This estimate is in the range of transfer rates found by two previous studies for diffusive transport of litter-C. Using young rye leaves and mature wheat straw stems with C/N ratios of 9 and 167, Galliard et al. (2003) calculated that 30% and 7% of initial litter-C were transferred to soil after 3 and 10 days. Similarly, Ingwersen et al. (2008) found that 31% of

initial litter-C were transferred to soil after 84 days, using rye residues with a similar C/N ratio of 40 as the maize residues used in this experiment. They further calculated that after 3 and 10 days about 1% and 4% of initial litter-C had been transferred. In their study 17% of the total litter-C transferred to soil was diffusively transported to soil at a distance of > 3 mm from the litter layer after 84 days. Our simulation predicted a higher transfer (see below). The increase is reasonable in view of the fact that litter-C was additionally transported by convection due to irrigation.

At the end of the experiment, after 22.8 days, most of the litter-C transferred to soil was found in the DOC pool within the 0-3 mm (65%) and 3-30 mm (23%) soil layers. In contrast, Ingwersen et al. (2008) found that most litter-C had been already transferred to the insoluble SOM pool via microbial turnover after 84 days. Consequently, in their experiment 31% of the total litter-derived CO₂ arose from mineralization processes in soil, whereas the litter-derived CO₂ in our experiment was almost completely produced directly in the litter layer. In accordance with Ingwersen et al. (2008), the largest part of litter-derived DOC was utilized for microbial growth: about 7% in the 0-3 mm and 1.4% in the 3-30 mm soil layer.

Essentially the same amounts of MCPA-C initially added (2.6 mg) were mineralized (69%) or leached (6.8%) from the entire soil core in both the M and ML treatments. In a previous experiment, conducted with the same soil and under similar experimental conditions, Poll et al. (2010) obtained a lower maximum percentage of mineralization of about 49% by fitting of a simple logistic model, but leached amounts of MCPA-derived ¹⁴C were similar.

Without litter addition the residual amounts of MCPA were clearly higher. In the 0-3 mm soil layer 16% of the total initially added MCPA parent compound were mineralized or transformed to DOC in the presence of litter compared to only 8% without litter addition. We found a net upward transport of the MCPA parent compound from the 3-30 mm to the upper 3 mm soil layer (5.8% of initially added MCPA) in the presence of litter, whereas in case of the M treatment 2.3% of initially added MCPA were transferred from the 0-3 mm soil layer to the subjacent soil. The increased co-metabolic transformation of MCPA by fungi in detritusphere soil resulted in a higher proportion of MCPA-C in DOC and higher export of MCPA-C as DOC out of the 0-3 mm soil layer than in the M treatment.

6.5 Conclusions

Our study revealed that complex biogeochemical models that explicitly consider microbial dynamics can be reasonably parameterized using sophisticated parameter optimization techniques in combination with biophysicochemical and genetic information provided by detailed experimental data. It is well recognized that mathematical modelling is a powerful tool to improve our understanding of environmental systems and its regulation (Wainwright and Mulligan 2013, p. 8). Here, simulations provide a comprehensive insight into the microbial regulation of

MCPA degradation coupled to C turnover in the detritusphere. They point to an important, albeit not yet well understood, role of fungi in the biodegradation of MCPA. We demonstrated that there are strong interactions between microbial dynamics and matter cycling at the mm-scale in soil. Diffusive and convective transport of litter-derived C control microbial dynamics in the detritusphere, which in turn impacts the diffusive transport of MCPA.

In future versions of the PECCAD model, a more complex representation of microbial traits within fungal and bacterial pools and the dynamics of extracellular enzymes will be explicitly considered on the basis of genomic and proteomic information to further improve the mechanistic representation of microbial population dynamics in soil. Recently the dynamics of MCPA degraders were coupled with that of water and solute transport in a three-dimensional model to evaluate how small-scale heterogeneity affects the leaching of MCPA in a loamy soil (Rosenbom et al. 2014). Similarly, a three-dimensional version of the PECCAD model will be applied in future studies to model coupled C turnover and pesticide degradation in natural soil, where biological and physicochemical processes intertwine at various hot spots (e.g. detritusphere – rhizosphere – drilosphere).

The PECCAD model provides the basis to study how microbial regulation mechanisms operative at the small-scale (mm) manifest at larger spatial scales using a bottom-up approach. In this context it can be applied as a tool to explore how the microbial dynamics in biogeochemical hot spots and elsewhere in soil regulate soil functions and ecosystem services, such as C cycling and pesticide degradation.

6.6 Acknowledgements

We thank Erhard Strohm, Elke Feiertag, Barbara von der Lüche, Sabine Rudolph, Heike Haslwimmer and Ingrid Tischer for their excellent technical assistance. Special thanks go to Marion Devers and Fabrice Martin-Laurent for their support with the analyses of genetic markers as well as to Jasper Vrugt for providing the MATLAB code of AMALGAM. We appreciate the stimulating discussions with Franziska Ditterich and gratefully acknowledge the funding (STR481/3-2 and KA1590/5-2) by Deutsche Forschungsgemeinschaft (DFG) in the frame of the priority program SPP 1315: “Biogeochemical Interfaces in Soil”.

6.7 Literature cited

- Allison, S. D. 2012. A trait-based approach for modelling microbial litter decomposition. *Ecology Letters* 15:1058–1070.
- Allison, S. D., M. D. Wallenstein, and M. A. Bradford. 2010. Soil-carbon response to warming dependent on microbial physiology. *Nature Geoscience* 3:336–340.
- Allison, S. D., M. N. Weintraub, T. B. Gartner, and M. P. Waldrop. 2011. Evolutionary-Economic Principles as Regulators of Soil Enzyme Production and Ecosystem Function. Pages 229–243 in G. Shukla and A. Varma, editors. *Soil Enzymology*. Springer Berlin Heidelberg.

- Alvarez-Cohen, L., and G. E. Speitel Jr. 2001. Kinetics of aerobic cometabolism of chlorinated solvents. *Biodegradation* 12:105–126.
- Anderson, T.-H., and K. H. Domsch. 1985a. Determination of ecophysiological maintenance carbon requirements of soil microorganisms in a dormant state. *Biology and Fertility of Soils* 1:81–89.
- Anderson, T.-H., and K. H. Domsch. 1985b. Maintenance carbon requirements of actively-metabolizing microbial populations under in situ conditions. *Soil Biology and Biochemistry* 17:197–203.
- Anderson, T.-H., and R. Martens. 2013. DNA determinations during growth of soil microbial biomasses. *Soil Biology and Biochemistry* 57:487–495.
- Aslam, S., P. Benoit, F. Chabauty, V. Bergheaud, C. Geng, L. Vieublé-Gonod, and P. Garnier. 2014. Modelling the impacts of maize decomposition on glyphosate dynamics in mulch. *European Journal of Soil Science* 65:231–247.
- Baelum, J., T. Henriksen, H. C. Bruun Hansen, and C. S. Jacobsen. 2006. Degradation of 4-Chloro-2-Methylphenoxyacetic Acid in Top- and Subsoil Is Quantitatively Linked to the Class III tfdA Gene. *Appl. Environ. Microbiol.* 72:1476–1486.
- Baelum, J., C. S. Jacobsen, and W. E. Holben. 2010. Comparison of 16S rRNA gene phylogeny and functional tfdA gene distribution in thirty-one different 2, 4-dichlorophenoxyacetic acid and 4-chloro-2-methylphenoxyacetic acid degraders. *Systematic and Applied Microbiology* 33:67–70.
- Baldrian, P., T. Větrovský, T. Cajthaml, P. Dobiášová, M. Petránková, J. Šnajdr, and I. Eichlerová. 2013. Estimation of fungal biomass in forest litter and soil. *Fungal Ecology* 6:1–11.
- Batoglu-Pazarbasi, M., N. Milosevic, F. Malaguerra, P. J. Binning, H. J. Albrechtsen, P. L. Bjerg, and J. Aamand. 2013. Discharge of landfill leachate to streambed sediments impacts the mineralization potential of phenoxy acid herbicides depending on the initial abundance of tfdA gene classes. *Environmental Pollution* 176:275–283.
- Battley, E. H. 2009. Is electron equivalence between substrate and product preferable to C-mol equivalence in representations of microbial anabolism applicable to “origin of life” environmental conditions? *Journal of Theoretical Biology* 260:267–275.
- Beare, M. H., D. C. Coleman, D. A. Crossley Jr, P. F. Hendrix, and E. P. Odum. 1995. A hierarchical approach to evaluating the significance of soil biodiversity to biogeochemical cycling. *Plant and Soil* 170:5–22.
- Berg, B., and C. McClaugherty. 2008. *Plant litter*. Springer, Berlin.
- Von Bergen, M., N. Jehmlich, M. Taubert, C. Vogt, F. Bastida, F.-A. Herbst, F. Schmidt, H.-H. Richnow, and J. Seifert. 2013. Insights from quantitative metaproteomics and protein-stable isotope probing into microbial ecology. *ISME Journal* 7:1877–1885.
- Bird, J. A., D. J. Herman, and M. K. Firestone. 2011. Rhizosphere priming of soil organic matter by bacterial groups in a grassland soil. *Soil Biology and Biochemistry* 43:718–725.
- Blagodatskaya, E., and Y. Kuzyakov. 2013. Active microorganisms in soil: Critical review of estimation criteria and approaches. *Soil Biology and Biochemistry* 67:192–211.
- Blagodatsky, S., E. Blagodatskaya, T. Yuyukina, and Y. Kuzyakov. 2010. Model of apparent and real priming effects: Linking microbial activity with soil organic matter decomposition. *Soil Biology and Biochemistry* 42:1275–1283.
- Blagodatsky, S., O. Heinemeyer, and J. Richter. 2000. Estimating the active and total soil microbial biomass by kinetic respiration analysis. *Biology and Fertility of Soils* 32:73–81.
- Blagodatsky, S., I. V. Yevdokimov, A. A. Larionova, and J. Richter. 1998. Microbial growth in soil and nitrogen turnover: Model calibration with laboratory data. *Soil Biology and Biochemistry* 30:1757–1764.
- Blazewicz, S. J., E. Schwartz, and M. K. Firestone. 2014. Growth and death of bacteria and fungi underlie rainfall-induced carbon dioxide pulses from seasonally dried soil. *Ecology* 95:1162–1172.

- Blouin, M., M. E. Hodson, E. A. Delgado, G. Baker, L. Brussaard, K. R. Butt, J. Dai, L. Dendooven, G. Peres, J. E. Tondoh, D. Cluzeau, and J. J. Brun. 2013. A review of earthworm impact on soil function and ecosystem services. *European Journal of Soil Science* 64:161–182.
- Van Bodegom, P. 2007. Microbial maintenance: A critical review on its quantification. *Microbial Ecology* 53:513–523.
- Boivin, A., S. Amellal, M. Schiavon, and M. T. Van Genuchten. 2005. 2,4-Dichlorophenoxyacetic acid (2,4-D) sorption and degradation dynamics in three agricultural soils. *Environmental Pollution* 138:92–99.
- Bottner, P., M. Pansu, and Z. Sallih. 1999. Modelling the effect of active roots on soil organic matter turnover. *Plant and Soil* 216:15–25.
- Brandt, B. W., I. M. M. Van Leeuwen, and S. A. L. M. Kooijman. 2003. A general model for multiple substrate biodegradation. Application to co-metabolism of structurally non-analogous compounds. *Water Research* 37:4843–4854.
- Brown, G. G., I. Barois, and P. Lavelle. 2000. Regulation of soil organic matter dynamics and microbial activity in the drilosphere and the role of interactions with other edaphic functional domains. *European Journal of Soil Biology* 36:177–198.
- Brusseau, M. L., S. K. Sandrin, L. Li, I. Yolcubal, F. L. Jordan, and R. M. Maier. 2006. Biodegradation during contaminant transport in porous media: 8. The influence of microbial system variability on transport behavior and parameter determination. *Water Resources Research* 42:W04406.
- Cabral, M. G., C. A. Viegas, M. C. Teixeira, and I. Sá-Correia. 2003. Toxicity of chlorinated phenoxyacetic acid herbicides in the experimental eukaryotic model *Saccharomyces cerevisiae*: Role of pH and of growth phase and size of the yeast cell population. *Chemosphere* 51:47–54.
- Campoy, S., M. L. Alvarez-Rodriguez, E. Recio, A. Rumbero, and J. J. R. Coque. 2009. Biodegradation of 2,4,6-TCA by the white-rot fungus *Phlebia radiata* is initiated by a phase I (O-demethylation)-phase II (O-conjugation) reactions system: Implications for the chlorine cycle. *Environmental Microbiology* 11:99–110.
- Castillo, M. d. P., A. Andersson, P. Ander, J. Stenström, and L. Torstensson. 2001. Establishment of the white rot fungus *Phanerochaete chrysosporium* on unsterile straw in solid substrate fermentation systems intended for degradation of pesticides. *World Journal of Microbiology and Biotechnology* 17:627–633.
- Cederlund, H., E. Borjesson, K. Onneby, and J. Stenstrom. 2007. Metabolic and cometabolic degradation of herbicides in the fine material of railway ballast. *Soil Biology & Biochemistry* 39:473–484.
- Chen, B., and M. Yuan. 2012. Enhanced dissipation of polycyclic aromatic hydrocarbons in the presence of fresh plant residues and their extracts. *Environmental Pollution* 161:199–205.
- Cheng, W. 2009. Rhizosphere priming effect: Its functional relationships with microbial turnover, evapotranspiration, and C-N budgets. *Soil Biology and Biochemistry* 41:1795–1801.
- Chen, Y.-M., T.-F. Lin, C. Huang, and J.-C. Lin. 2008. Cometabolic degradation kinetics of TCE and phenol by *Pseudomonas putida*. *Chemosphere* 72:1671–1680.
- Crespin, M. A., M. Gallego, M. Valcarcel, and J. L. Gonzalez. 2001. Study of the degradation of the herbicides 2,4-D and MCPA at different depths in contaminated agricultural soil. *Environmental Science & Technology* 35:4265–4270.
- Dalton, H., and D. I. Stirling. 1982. Co-metabolism. *Philosophical transactions of the Royal Society of London. Series B: Biological sciences* 297:481–496.
- Dazzo, F. B., and S. Ganter. 2009. Rhizosphere. Pages 335–349 in S. Editor-in-Chief: Moselio, editor. *Encyclopedia of Microbiology (Third Edition)*. Academic Press, Oxford.
- Dijkstra, P., S. C. Thomas, P. L. Heinrich, G. W. Koch, E. Schwartz, and B. A. Hungate. 2011. Effect of temperature on metabolic activity of intact microbial communities: Evidence for altered metabolic pathway activity but not for increased maintenance respiration and reduced carbon use efficiency. *Soil Biology and Biochemistry* 43:1848–1857.

- Ditterich, F., C. Poll, H. Pagel, D. Babin, K. Smalla, M. A. Horn, T. Streck, and E. Kandeler. 2013. Succession of bacterial and fungal 4-chloro-2-methylphenoxyacetic acid degraders at the soil-litter interface. *FEMS Microbiology Ecology* 86:85–100.
- Don, A., B. Steinberg, I. SchÄ¶ning, K. Pritsch, M. Joschko, G. Gleixner, and E. D. Schulze. 2008. Organic carbon sequestration in earthworm burrows. *Soil Biology and Biochemistry* 40:1803–1812.
- Don, R. H., and J. M. Pemberton. 1981. Properties of six pesticide degradation plasmids isolated from *Alcaligenes paradoxus* and *Alcaligenes eutrophus*. *Journal of Bacteriology* 145:681–686.
- Duah-Yentumi, S., and S. Kuwatsuka. 1980. Effect of organic matter and chemical fertilizers on the degradation of benthocarb and MCPA herbicides in the soil. *Soil Science and Plant Nutrition* 26:541–549.
- Efstratiadis, A., and D. Koutsoyiannis. 2010. One decade of multi-objective calibration approaches in hydrological modelling: A review [Une d cennie d'approches de calage multi-objectifs en mod lisation hydrologique: Une revue]. *Hydrological Sciences Journal* 55:58–78.
- Ellegaard-Jensen, L., J. Aamand, B. B. Kragelund, A. H. Johnsen, and S. Rosendahl. 2013. Strains of the soil fungus *Mortierella* show different degradation potentials for the phenylurea herbicide diuron. *Biodegradation* 24:765–774.
- Estrella, M. R., M. L. Brusseau, R. S. Maier, I. L. Pepper, P. J. Wierenga, and R. M. Miller. 1993. Biodegradation, sorption, and transport of 2,4-dichlorophenoxyacetic acid in saturated and unsaturated soils. *Applied and Environmental Microbiology* 59:4266–4273.
- European Commission. 2005. Review report for the active substance MCPA. Pages 1–62. Health & Consumer Protection Directorate-General.
- Faulkner, J. K., and D. Woodcock. 1965. 209. Fungal detoxication. Part VII. Metabolism of 2,4-dichloro- phenoxyacetic and 4-chloro-2-methylphenoxyacetic acids by *aspergillus niger*. *Journal of the Chemical Society (Resumed)*:1187–1191.
- Field, J., and R. Sierra-Alvarez. 2008. Microbial degradation of chlorinated phenols. *Reviews in Environmental Science and Bio/Technology* 7:211–241.
- F chslin, H. P., I. R egg, J. R. Van Der Meer, and T. Egli. 2003. Effect of integration of a GFP reporter gene on fitness of *Ralstonia eutropha* during growth with 2,4-dichlorophenoxyacetic acid. *Environmental Microbiology* 5:878–887.
- Fukumori, F., and R. P. Hausinger. 1993. *Alcaligenes eutrophus* JMP134 "2,4-dichlorophenoxyacetate monooxygenase" is an α -ketoglutarate-dependent dioxygenase. *Journal of Bacteriology* 175:2083–2086.
- Gaillard, V., C. Chenu, and S. Recous. 2003. Carbon mineralisation in soil adjacent to plant residues of contrasting biochemical quality. *Soil Biology and Biochemistry* 35:93–99.
- Gao, Z., J. W. Green, J. Vanderborght, and W. Schmitt. 2011. Improving uncertainty analysis in kinetic evaluations using iteratively reweighted least squares. *Environmental Toxicology and Chemistry* 30:2363–2371.
- Gerhardt, K. E., X. D. Huang, B. R. Glick, and B. M. Greenberg. 2009. Phytoremediation and rhizoremediation of organic soil contaminants: Potential and challenges. *Plant Science* 176:20–30.
- Ghani, A., and D. A. Wardle. 2001. Fate of ^{14}C from glucose and the herbicide metsulfuron-methyl in a plant-soil microcosm system. *Soil Biology and Biochemistry* 33:777–785.
- Gianfreda, L., and J. M. Bollag. 1994. Effect of soils on the behavior of immobilized enzymes. *Soil Science Society of America Journal* 58:1672–1681.
- Gignoux, J., J. House, D. Hall, D. Masse, H. B. Nacro, and L. Abbadie. 2001. Design and test of a generic cohort model of soil organic matter decomposition: The SOMKO model. *Global Ecology and Biogeography* 10:639–660.
- Gjettermann, B., M. Styczen, H. C. B. Hansen, F. P. Vinther, and S. Hansen. 2008. Challenges in modelling dissolved organic matter dynamics in agricultural soil using DAISY. *Soil Biology and Biochemistry* 40:1506–1518.

- Gommers, P. J. F., B. J. van Schie, J. P. van Dijken, and J. G. Kuenen. 1988. Biochemical limits to microbial growth yields: an analysis of mixed substrate utilization. *Biotechnology and Bioengineering* 32:86–94.
- Gonod, L. V., F. Martin-Laurent, and C. Chenu. 2006. 2,4-D impact on bacterial communities, and the activity and genetic potential of 2,4-D degrading communities in soil. *FEMS Microbiology Ecology* 58:529–537.
- Gras, A., M. Ginovart, J. Valls, and P. C. Baveye. 2011. Individual-based modelling of carbon and nitrogen dynamics in soils: Parameterization and sensitivity analysis of microbial components. *Ecological Modelling* 222:1998–2010.
- Green, J. L., B. J. M. Bohannan, and R. J. Whitaker. 2008. Microbial biogeography: From taxonomy to traits. *Science* 320:1039–1043.
- Haby, P. A., and D. E. Crowley. 1996. Biodegradation of 3-chlorobenzoate as affected by rhizodeposition and selected carbon substrates. *Journal of Environmental Quality* 25:304–310.
- Han Sung, O., and P. B. New. 1994. Effect of water availability on degradation of 2, 4-dichlorophenoxyacetic acid (2,4-D) by soil microorganisms. *Soil Biology and Biochemistry* 26:1689–1697.
- Van Hees, P. A. W., D. L. Jones, R. Finlay, D. L. Godbold, and U. S. Lundström. 2005. The carbon we do not see - The impact of low molecular weight compounds on carbon dynamics and respiration in forest soils: A review. *Soil Biology and Biochemistry* 37:1–13.
- Helal, H. M., and D. R. Sauerbeck. 1984. Influence of plant roots on C and P metabolism in soil. *Plant and Soil* 76:175–182.
- Helling, C. S., J. M. Bollag, and J. E. Dawson. 1968. Cleavage of ether-oxygen bond in phenoxyacetic acid by an arthrobacter species. *Journal of Agricultural Food and Chemistry* 16:538–539.
- He, Y., Q. Zhuang, J. W. Harden, A. D. McGuire, Z. Fan, Y. Liu, and K. P. Wickland. 2014. The implications of microbial and substrate limitation for the fates of carbon in different organic soil horizon types of boreal forest ecosystems: A mechanistically based model analysis. *Biogeosciences* 11:4477–4491.
- Ingwersen, J., C. Poll, T. Streck, and E. Kandeler. 2008. Micro-scale modelling of carbon turnover driven by microbial succession at a biogeochemical interface. *Soil Biology and Biochemistry* 40:872–886.
- Itoh, K., M. Kinoshita, S. Morishita, M. Chida, and K. Suyama. 2013. Characterization of 2,4-dichlorophenoxyacetic acid and 2,4,5-trichlorophenoxyacetic acid-degrading fungi in Vietnamese soils. *FEMS Microbiology Ecology* 84:124–132.
- Itoh, K., Y. Tashiro, K. Uobe, Y. Kamagata, K. Suyama, and H. Yamamoto. 2004. Root Nodule Bradyrhizobium spp. Harbor *tfdA?* and *cadA*, Homologous with Genes Encoding 2,4-Dichlorophenoxyacetic Acid-Degrading Proteins. *Applied and Environmental Microbiology* 70:2110–2118.
- Joergensen, R. G. 1996. The fumigation-extraction method to estimate soil microbial biomass: Calibration of the *kEC* value. *Soil Biology and Biochemistry* 28:25–31.
- Joergensen, R. G., and F. Wichern. 2008. Quantitative assessment of the fungal contribution to microbial tissue in soil. *Soil Biology and Biochemistry* 40:2977–2991.
- Kalbitz, K., J. Schmerwitz, D. Schwesig, and E. Matzner. 2003. Biodegradation of soil-derived dissolved organic matter as related to its properties. *Geoderma* 113:273–291.
- Kandeler, E., J. Luxhøi, D. Tschirko, and J. Magid. 1999. Xylanase, invertase and protease at the soil-litter interface of a loamy sand. *Soil Biology and Biochemistry* 31:1171–1179.
- Kembel, S. W., M. Wu, J. A. Eisen, and J. L. Green. 2012. Incorporating 16S Gene Copy Number Information Improves Estimates of Microbial Diversity and Abundance. *PLoS Computational Biology* 8:e1002743.
- Kiikkilä, O., A. Smolander, and V. Kitunen. 2013. Degradability, molecular weight and adsorption properties of dissolved organic carbon and nitrogen leached from different types of decomposing litter. *Plant and Soil* 373:787–798.
- Klappenbach, J. A., J. M. Dunbar, and T. M. Schmidt. 2000. rRNA operon copy number reflects ecological strategies of bacteria. *Applied and Environmental Microbiology* 66:1328–1333.

- Kovarova-Kovar, K., and T. Egli. 1998. Growth kinetics of suspended microbial cells: From single-substrate-controlled growth to mixed-substrate kinetics. *Microbiology and Molecular Biology Reviews* 62:646–666.
- Kramer, S., S. Marhan, H. Haslwimmer, L. Ruess, and E. Kandeler. 2013. Temporal variation in surface and sub-soil abundance and function of the soil microbial community in an arable soil. *Soil Biology and Biochemistry* 61:76–85.
- Krause, S., X. Le Roux, P. A. Niklaus, P. M. van Bodegom, J. T. Lennon, S. Bertilsson, H.-P. Grossart, L. Philippot, and P. L. E. Bodelier. 2014. Trait-based approaches for understanding microbial biodiversity and ecosystem functioning. *Frontiers in Microbiology* 5:251.
- Kügler, P. 2012. Moment fitting for parameter inference in repeatedly and partially observed stochastic biological models. *PLoS ONE* 7:e43001.
- Kuzyakov, Y. 2010. Priming effects: Interactions between living and dead organic matter. *Soil Biology and Biochemistry* 42:1363–1371.
- Laemmli, C., C. Werlen, and J. R. Van Der Meer. 2004. Mutation analysis of the different *tfd* genes for degradation of chloroaromatic compounds in *Ralstonia eutropha* JMP134. *Archives of Microbiology* 181:112–121.
- Laloy, E., B. Rogiers, J. A. Vrugt, D. Mallants, and D. Jacques. 2013. Efficient posterior exploration of a high-dimensional groundwater model from two-stage Markov chain Monte Carlo simulation and polynomial chaos expansion. *Water Resources Research* 49:2664–2682.
- Langner, H. W., W. P. Inskeep, H. M. Gaber, W. L. Jones, B. S. Das, and J. M. Wraith. 1998. Pore water velocity and residence time effects on the degradation 2,4-D during transport. *Environmental Science and Technology* 32:1308–1315.
- Lashermes, G., Y. Zhang, S. Houot, J. P. Steyer, D. Patureau, E. Barriuso, and P. Garnier. 2013. Simulation of organic matter and pollutant evolution during composting: The COP-compost model. *Journal of Environmental Quality* 42:361–372.
- Lavelle, P. 1988. Earthworm activities and the soil system. *Biology and Fertility of Soils* 6:237–251.
- Ledger, T., D. H. Pieper, and B. Gonzalez. 2006. Chlorophenol Hydroxylases Encoded by Plasmid pJP4 Differentially Contribute to Chlorophenoxyacetic Acid Degradation. *Appl. Environ. Microbiol.* 72:2783–2792.
- Lendenmann, U., and T. Egli. 1998. Kinetic models for the growth of *Escherichia coli* with mixtures of sugars under carbon-limited conditions. *Biotechnology and Bioengineering* 59:99–107.
- Lennon, J. T., and S. E. Jones. 2011. Microbial seed banks: The ecological and evolutionary implications of dormancy. *Nature Reviews Microbiology* 9:119–130.
- Liu, Y.-J., S.-J. Liu, H. L. Drake, and M. A. Horn. 2013. Consumers of 4-chloro-2-methylphenoxyacetic acid from agricultural soil and drilosphere harbor *cadA*, *r/sdpA*, and *tfdA*-like gene encoding oxygenases. *FEMS Microbiology Ecology* 86:114–129.
- Liu, Y.-J., A. Zapras, S.-J. Liu, H. L. Drake, and M. A. Horn. 2011. The earthworm *Aporrectodea caliginosa* stimulates abundance and activity of phenoxyalkanoic acid herbicide degraders. *ISME Journal* 5:473–485.
- Loos, M. A., I. F. Schlosser, and W. R. Mapham. 1979. Phenoxy herbicide degradation in soils: Quantitative studies of 2,4-D- and MCPA-degrading microbial populations. *Soil Biology and Biochemistry* 11:377–385.
- Malik, A., and G. Gleixner. 2013. Importance of microbial soil organic matter processing in dissolved organic carbon production. *FEMS Microbiology Ecology* 86:139–148.
- Manzoni, S., P. Taylor, A. Richter, A. Porporato, and G. I. Ågren. 2012. Environmental and stoichiometric controls on microbial carbon-use efficiency in soils. *New Phytologist* 196:79–91.
- Marschner, P., S. Marhan, and E. Kandeler. 2012. Microscale distribution and function of soil microorganisms in the interface between rhizosphere and detritusphere. *Soil Biology and Biochemistry* 49:174–183.
- McGill, W. B., H. W. Hunt, R. G. Woodmansee, and J. O. Reuss. 1981. PHOENIX, a model of the dynamics of carbon and nitrogen in grassland soils. Pages 49–115 in F. E. Clark and T. Rosswall, editors. *Terrestrial*

- nitrogen cycles. Processes, ecosystem strategies and management impacts. Swedish Natural Science Research Council, Stockholm.
- Mcmahon, S., and J. Parnell. 2014. Weighing the deep continental biosphere. *FEMS Microbiology Ecology* 87:113–120.
- Minkevich, I. G., and V. K. Eroshin. 1973. Theoretical calculation of mass balance during the cultivation of microorganisms. *Biotechnology Bioengineering Symposium* 4:21–25.
- Monga, O., P. Garnier, V. Pot, E. Coucheney, N. Nunan, W. Otten, and C. Chenu. 2014. Simulating microbial degradation of organic matter in a simple porous system using the 3-D diffusion-based model MOSAIC. *Biogeosciences* 11:2201–2209.
- Moore, C., T. Wöhling, and J. Doherty. 2011. Efficient regularization and uncertainty analysis using a global optimization methodology. *Water Resources Research* 46:W08527.
- Moore, J. C., R. B. Boone, A. Koyama, and K. Holfelder. 2014. Enzymatic and detrital influences on the structure, function, and dynamics of spatially-explicit model ecosystems. *Biogeochemistry* 117:205–227.
- Moorhead, D. L. ., Z. L. . Rinkes, R. L. . Sinsabaugh, and M. N. . Weintraub. 2013. Dynamic relationships between microbial biomass, respiration, inorganic nutrients and enzyme activities: Informing enzyme-based decomposition models. *Frontiers in Microbiology* 4.
- Moorhead, D. L., and R. L. Sinsabaugh. 2006. A theoretical model of litter decay and microbial interaction. *Ecological Monographs* 76:151–174.
- Mueller, T., L. S. Jensen, J. Magid, and N. E. Nielsen. 1997. Temporal variation of C and N turnover in soil after oilseed rape straw incorporation in the field: Simulations with the soil-plant-atmosphere model DAISY. *Ecological Modelling* 99:247–262.
- Müller, T. A., T. Fleischmann, J. R. Van Der Meer, and H. P. E. Kohler. 2006. Purification and characterization of two enantioselective α -ketoglutarate-dependent dioxygenases, RdpA and SdpA, from *Sphingomonas herbicidovorans* MH. *Applied and Environmental Microbiology* 72:4853–4861.
- Myrold, D. D., L. H. Zeglin, and J. K. Jansson. 2014. The potential of metagenomic approaches for understanding soil microbial processes. *Soil Science Society of America Journal* 78:3–10.
- Nicolaisen, M. H., J. Bælum, C. S. Jacobsen, and J. Sørensen. 2008. Transcription dynamics of the functional *tfdA* gene during MCPA herbicide degradation by *Cupriavidus necator* AEO106 (pRO101) in agricultural soil. *Environmental Microbiology* 10:571–579.
- Nielsen, M. S., J. Bælum, M. B. Jensen, and C. S. Jacobsen. 2011. Mineralization of the herbicide MCPA in urban soils is linked to presence and growth of class III *tfdA* genes. *Soil Biology and Biochemistry* 43:984–990.
- Nielsen, T. K., Z. Xu, E. Gözdereliler, J. Aamand, L. H. Hansen, and S. R. Sørensen. 2013. Novel Insight into the Genetic Context of the *cadAB* Genes from a 4-chloro-2-methylphenoxyacetic Acid-Degrading *Sphingomonas*. *PLoS ONE* 8:e83346.
- Pagel, H., J. Ingwersen, C. Poll, E. Kandeler, and T. Streck. 2014. Micro-scale modeling of pesticide degradation coupled to carbon turnover in the detritusphere: Model description and sensitivity analysis. *Biogeochemistry* 117:185–204.
- Parton, W. J. 1993. Observations and modeling of biomass and soil organic matter dynamics for the grassland biome worldwide. *Global Biogeochemical Cycles* 7:785–809.
- Parton, W. J., D. S. Schimel, C. V. Cole, and D. S. Ojima. 1987. Analysis of factors controlling soil organic matter levels in Great Plains grasslands. *Soil Science Society of America Journal* 51:1173–1179.
- Paustian, K., and J. Schnürer. 1987. Fungal growth response to carbon and nitrogen limitation: Application of a model to laboratory and field data. *Soil Biology and Biochemistry* 19:621–629.
- PDE_Solutions. 2011. FlexPDE 6.20 - finite element model builder for Partial Differential Equations. PDE Solutions Inc., WA, USA.

- Perveen, N., S. Barot, G. Alvarez, K. Klumpp, R. Martin, A. Rapaport, D. Herfurth, F. Louault, and S. Fontaine. 2014. Priming effect and microbial diversity in ecosystem functioning and response to global change: A modeling approach using the SYMPHONY model. *Global Change Biology* 20:1174–1190.
- Pieper, D. H., W. Reineke, K. H. Engesser, and H. J. Knackmuss. 1988. Metabolism of 2,4-dichlorophenoxyacetic acid, 4-chloro-2-methylphenoxyacetic acid and 2-methylphenoxyacetic acid by *Alcaligenes eutrophus* JMP 134. *Archives of Microbiology* 150:95–102.
- Pietramellara, G., J. Ascher, F. Borgogni, M. T. Ceccherini, G. Guerri, and P. Nannipieri. 2009. Extracellular DNA in soil and sediment: Fate and ecological relevance. *Biology and Fertility of Soils* 45:219–235.
- Poll, C., J. Ingwersen, M. Stemmer, M. H. Gerzabek, and E. Kandeler. 2006. Mechanisms of solute transport affect small-scale abundance and function of soil microorganisms in the detritosphere. *European Journal Of Soil Science* 57:583–595.
- Poll, C., S. Marhan, J. Ingwersen, and E. Kandeler. 2008. Dynamics of litter carbon turnover and microbial abundance in a rye detritosphere. *Soil Biology and Biochemistry* 40:1306–1324.
- Poll, C., H. Pagel, M. Devers-Lamrani, F. Martin-Laurent, J. Ingwersen, T. Streck, and E. Kandeler. 2010. Regulation of bacterial and fungal MCPA degradation at the soil-litter interface. *Soil Biology and Biochemistry* 42:1879–1887.
- Polson, A. 1950. Some aspects of diffusion in solution and a definition of a colloidal particle. *Journal of Physical and Colloid Chemistry* 54:649–652.
- Price, K., S. T. Purucker, S. R. Kraemer, and J. E. Babendreier. 2012. Tradeoffs among watershed model calibration targets for parameter estimation. *Water Resources Research* 48:W10542.
- Rampazzo Todorovic, G., M. Stemmer, M. Tatzber, C. Katzlberger, H. Spiegel, F. Zehetner, and M. H. Gerzabek. 2010. Soil-carbon turnover under different crop management: Evaluation of RothC-model predictions under Pannonian climate conditions. *Journal of Plant Nutrition and Soil Science* 173:662–670.
- Reddy, G. V. B., D. K. Joshi, and M. H. Gold. 1997. Degradation of chlorophenoxyacetic acids by the lignin-degrading fungus *Dichomitus squalens*. *Microbiology* 143:2353–2360.
- Reed, D. C., C. K. Algar, J. A. Huber, and G. J. Dick. 2014. Gene-centric approach to integrating environmental genomics and biogeochemical models. *Proceedings of the National Academy of Sciences of the United States of America* 111:1879–1884.
- Reemtsma, T. 2009. Determination of molecular formulas of natural organic matter molecules by (ultra-) high-resolution mass spectrometry. Status and needs. *Journal of Chromatography A* 1216:3687–3701.
- Rinkes, Z. L. ., J. L. . DeForest, A. S. . Grandy, D. L. . Moorhead, and M. N. . Weintraub. 2014. Interactions between leaf litter quality, particle size, and microbial community during the earliest stage of decay. *Biogeochemistry* 117:153–168.
- Rosenbom, A. E. ., P. J. . Binning, J. . Aamand, A. . Dechesne, B. F. . Smets, and A. R. . Johnsen. 2014. Does microbial centimeter-scale heterogeneity impact MCPA degradation in and leaching from a loamy agricultural soil? *Science of the Total Environment* 472:90–98.
- Roth, V.-N., T. Dittmar, R. Gaupp, and G. Gleixner. 2014. Ecosystem-specific composition of dissolved organic matter. *Vadose Zone Journal* 13.
- Rousk, J. . b, and E. . Bååth. 2011. Growth of saprotrophic fungi and bacteria in soil. *FEMS Microbiology Ecology* 78:17–30.
- Rubilar, O., M. C. Diez, and L. Gianfreda. 2008. Transformation of chlorinated phenolic compounds by white rot fungi. *Critical Reviews in Environmental Science and Technology* 38:227–268.
- Sambridge, M. 2013. A parallel tempering algorithm for probabilistic sampling and multimodal optimization. *Geophysical Journal International* 196:357–374.

- Schenck zu Schweinsberg-Mickan, M., R. G. Jörgensen, and T. Müller. 2012. Rhizodeposition: Its contribution to microbial growth and carbon and nitrogen turnover within the rhizosphere. *Journal of Plant Nutrition and Soil Science* 175:750–760.
- Sedighi, M., and F. Vahabzadeh. 2014. Kinetic Modeling of cometabolic degradation of ethanethiol and phenol by *Ralstonia eutropha*. *Biotechnology and Bioprocess Engineering* 19:239–249.
- Shailubhai, K., S. R. Sahasrabudhe, K. A. Vora, and V. V. Modi. 1983. Degradation of chlorinated derivatives of phenoxyacetic acid and benzoic acid by *Aspergillus niger*. *FEMS Microbiology Letters* 18:279–282.
- Shaw, L. J., and R. G. Burns. 2005. Rhizodeposition and the enhanced mineralization of 2,4-dichlorophenoxyacetic acid in soil from the *Trifolium pratense* rhizosphere. *Environmental Microbiology* 7:191–202.
- Shelton, D. R., and M. A. Doherty. 1997. A model describing pesticide bioavailability and biodegradation in soil. *Soil Science Society of America Journal* 61:1078–1084.
- Simkins, S., and M. Alexander. 1984. Models for mineralization kinetics with the variables of substrate concentration and population density. *Applied and Environmental Microbiology* 47:1299–1306.
- Sinsabaugh, R. L., S. Manzoni, D. L. Moorhead, and A. Richter. 2013. Carbon use efficiency of microbial communities: Stoichiometry, methodology and modelling. *Ecology Letters* 16:930–939.
- Sistla, S. A., E. B. Rastetter, and J. P. Schimel. 2014. Responses of a tundra system to warming using SCAMPS: A stoichiometrically coupled, acclimating microbeplantsoil model. *Ecological Monographs* 84:151–170.
- Smejkal, C. W., T. Vallaey, S. K. Burton, and H. M. Lappin-Scott. 2001. Substrate specificity of chlorophenoxyalkanoic acid-degrading bacteria is not dependent upon phylogenetically related *tfdA* gene types. *Biology and Fertility of Soils* 33:507–513.
- Smith, O. L. 1979. An analytical model of the decomposition of soil organic matter. *Soil Biology and Biochemistry* 11:585–606.
- Soulas, G. 1993. Evidence for the existence of different physiological groups in the microbial community responsible for 2,4-D mineralization in soil. *Soil Biology and Biochemistry* 25:443–449.
- Spohn, M., and Y. Kuzyakov. 2014. Spatial and temporal dynamics of hotspots of enzyme activity in soil as affected by living and dead roots—a soil zymography analysis. *Plant and Soil* 379:67–77.
- Sträuber, H., R. H. Müller, and W. Babel. 2003. Evidence of cytochrome P450-catalyzed cleavage of the ether bond of phenoxybutyrate herbicides in *Rhodococcus erythropolis* K2-3. *Biodegradation* 14:41–50.
- Talbot, J. M., T. D. Bruns, J. W. Taylor, D. P. Smith, S. Branco, S. I. Glassman, S. Erlandson, R. Vilgalys, H.-L. Liao, M. E. Smith, and K. G. Peay. 2014. Endemism and functional convergence across the North American soil mycobiome. *Proceedings of the National Academy of Sciences of the United States of America* 111:6341–6346.
- Thiet, R. K., S. D. Frey, and J. Six. 2006. Do growth yield efficiencies differ between soil microbial communities differing in fungal:bacterial ratios? Reality check and methodological issues. *Soil Biology and Biochemistry* 38:837–844.
- Tipping, E., P. M. Chamberlain, M. Fröberg, P. J. Hanson, and P. M. Jardine. 2012. Simulation of carbon cycling, including dissolved organic carbon transport, in forest soil locally enriched with ¹⁴C. *Biogeochemistry* 108:91–107.
- Tiunov, A. V., M. Bonkowski, M. Bonkowski, J. A. Tiunov, and S. Scheu. 2001. Microflora, protozoa and nematoda in *Lumbricus terrestris* burrow walls: A laboratory experiment. *Pedobiologia* 45:46–60.
- Toal, M. E., C. Yeomans, K. Killham, and A. A. Meharg. 2000. A review of rhizosphere carbon flow modelling. *Plant and Soil* 222:263–281.
- Torstensson, N. T. L., J. Stark, and B. Goransson. 1975. The effect of repeated applications of 2,4-D and MCPA on their breakdown in soil. *Weed Research* 15:159–164.

- Totsche, K. U., T. Rennert, M. H. Gerzabek, I. Kögel-Knabner, K. Smalla, M. Spiteller, and H. J. Vogel. 2010. Biogeochemical interfaces in soil: The interdisciplinary challenge for soil science. *Journal of Plant Nutrition and Soil Science* 173:88–99.
- Trigueros, D. E. G., A. N. Módenes, A. D. Kroumov, and F. R. Espinoza-Quiñones. 2010. Modeling of biodegradation process of BTEX compounds: Kinetic parameters estimation by using Particle Swarm Global Optimizer. *Process Biochemistry* 45:1355–1361.
- Trivedi, P., I. C. Anderson, and B. K. Singh. 2013. Microbial modulators of soil carbon storage: Integrating genomic and metabolic knowledge for global prediction. *Trends in Microbiology* 21:641–651.
- Vance, E. D., P. C. Brookes, and D. S. Jenkinson. 1987. An extraction method for measuring soil microbial biomass C. *Soil Biology and Biochemistry* 19:703–707.
- Vroumsia, T., R. Steiman, F. Seigle-Murandi, and J. L. Benoit-Guyod. 2005. Fungal bioconversion of 2,4-dichlorophenoxyacetic acid (2,4-D) and 2,4-dichlorophenol (2,4-DCP). *Chemosphere* 60:1471–1480.
- Vrugt, J. A., H. V. Gupta, L. A. Bastidas, W. Bouten, and S. Sorooshian. 2003. Effective and efficient algorithm for multiobjective optimization of hydrologic models. *Water Resources Research* 39:SWC51–SWC519.
- Vrugt, J. A., and B. A. Robinson. 2007. Improved evolutionary optimization from genetically adaptive multimethod search. *Proceedings of the National Academy of Sciences of the United States of America* 104:708–711.
- Vrugt, J. A., and M. Sadegh. 2013. Toward diagnostic model calibration and evaluation: Approximate Bayesian computation. *Water Resources Research* 49:4335–4345.
- Wainwright, J., and M. Mulligan. 2013. *Environmental modelling: finding simplicity in complexity.* (J. Wainwright and M. Mulligan, Eds.). John Wiley & Sons Ltd, Chichester.
- Wallenstein, M. D., and E. K. Hall. 2012. A trait-based framework for predicting when and where microbial adaptation to climate change will affect ecosystem functioning. *Biogeochemistry* 109:35–47.
- Wang, G., M. A. Mayes, L. Gu, and C. W. Schadt. 2014. Representation of dormant and active microbial dynamics for ecosystem modeling. *PLoS ONE* 9.
- Wang, G., and W. M. Post. 2012. A theoretical reassessment of microbial maintenance and implications for microbial ecology modeling. *FEMS Microbiology Ecology* 81:610–617.
- Wieder, W. R., A. S. Grandy, C. M. Kallenbach, and G. B. Bonan. 2014. Integrating microbial physiology and physio-chemical principles in soils with the Microbial-Mineral Carbon Stabilization (MIMICS) model. *Biogeosciences* 11:3899–3917.
- Wöhling, T., S. Gayler, E. Priesack, J. Ingwersen, H.-D. Witzmann, P. Högy, M. Cuntz, S. Attinger, V. Wulfmeyer, and T. Streck. 2013. Multiresponse, multiobjective calibration as a diagnostic tool to compare accuracy and structural limitations of five coupled soil-plant models and CLM3.5. *Water Resources Research* 49:8200–8221.
- Wöhling, T., and J. A. Vrugt. 2011. Multiresponse multilayer vadose zone model calibration using Markov chain Monte Carlo simulation and field water retention data. *Water Resources Research* 47:W04510.
- WRB, I. W. G. 2006. *World reference base for soil resources 2006.*
- Wutzler, T., S. A. Blagodatsky, E. Blagodatskaya, and Y. Kuzyakov. 2012. Soil microbial biomass and its activity estimated by kinetic respiration analysis - Statistical guidelines. *Soil Biology and Biochemistry* 45:102–112.
- Wutzler, T., and M. Reichstein. 2013. Priming and substrate quality interactions in soil organic matter models. *Biogeosciences* 10:2089–2103.
- Young, I. M., J. W. Crawford, N. Nunan, W. Otten, and A. Spiers. 2009. Chapter 4 Microbial Distribution in Soils. *Physics and Scaling. Advances in Agronomy* 100:81–121.
- Zapras, A., Y. J. Liu, S. J. Liu, H. L. Drake, and M. A. Horn. 2010. Abundance of novel and diverse tfdA-like genes, encoding putative phenoxyalkanoic acid herbicide-degrading dioxygenases, in soil. *Applied and Environmental Microbiology* 76:119–128.

- Zelenev, V. V., A. H. C. Van Bruggen, and A. M. Semenov. 2005. Modeling wave-like dynamics of oligotrophic and copiotrophic bacteria along wheat roots in response to nutrient input from a growing root tip. *Ecological Modelling* 188:404–417.
- Zhang, G., D. Lu, M. Ye, M. Gunzburger, and C. Webster. 2013. An adaptive sparse-grid high-order stochastic collocation method for Bayesian inference in groundwater reactive transport modeling. *Water Resources Research* 49:6871–6892.
- Zsolnay, Á. 2003. Dissolved organic matter: Artefacts, definitions, and functions. *Geoderma* 113:187–209.

6.8 Appendices

Appendix A (Table A1). Basic characteristics of soil and maize litter. In parentheses: standard errors.

	Total C	Total N	$\delta^{13}\text{C}$	pH (CaCl ₂)	sand	silt	clay
	mg/g	mg/g	‰		%	%	%
Soil	14.9 (0.4)	1.85 (0.02)	-25.9 (0.04)	5.3	19 (0.4)	63 (0.5)	17 (0.1)
Maize litter	412 (5)	8.81 (0.20)	-12.8 (0.01)	-	-	-	-

Appendix B (Table B1). Parameters and further model input of the PECCAD model with defined ranges.

Parameter	Range	Unit	Parameter	Range	Unit
$Y_{L,hiq}$	0.01 ... 1	Unitless	q_{max-F}	0.1 ... 10	d^{-1}
$Y_{L,loq}$	0.01 ... 1	Unitless	K_{I-B}	1 ... 100	$g \cdot (mg C)^{-1}$
μ_{max-B}	0.1 ... 50	d^{-1}	K_{I-F}	1 ... 100	$g \cdot (mg C)^{-1}$
μ_{max-F}	0.1 ... 50	d^{-1}	$k_{r-B,hiq}$	0.001 ... 10	$mg C \cdot g^{-1}$
μ_{max-BP}	0.1 ... 50	d^{-1}	$k_{r-B,loq}$	0.001 ... 10	$mg C \cdot g^{-1}$
$k_{B,hiq}$	1 ... 500	$g \cdot (mg C \cdot d)^{-1}$	$k_{r-F,hiq}$	0.001 ... 10	$mg C \cdot g^{-1}$
$k_{B,loq}$	1 ... 500	$g \cdot (mg C \cdot d)^{-1}$	$k_{r-F,loq}$	0.001 ... 10	$mg C \cdot g^{-1}$
$k_{F,hiq}$	1 ... 500	$g \cdot (mg C \cdot d)^{-1}$	$k_{r-BP,P}$	0.001 ... 10	$mg C \cdot g^{-1}$
$k_{F,loq}$	1 ... 500	$g \cdot (mg C \cdot d)^{-1}$	$k_{r-BP,hiq}$	0.001 ... 10	$mg C \cdot g^{-1}$
$k_{BP,P}$	1 ... 500	$g \cdot (mg C \cdot d)^{-1}$	$k_{r-BP,loq}$	0.001 ... 10	$mg C \cdot g^{-1}$
$k_{BP,hiq}$	1 ... 500	$g \cdot (mg C \cdot d)^{-1}$	Y_{r-B}	0.1 ... 1	Unitless
$k_{BP,loq}$	1 ... 500	$g \cdot (mg C \cdot d)^{-1}$	Y_{r-F}	0.1 ... 1	Unitless
m_{max-B}	0.01 ... 2	d^{-1}	$Y_{R-F,P}$	0.1 ... 1	Unitless
m_{max-BP}	0.01 ... 2	d^{-1}	$Y_{S-B,hiq}$	0.5 ... 1	Unitless
$k_{m-B,hiq}$	1 ... 1500	$g \cdot (mg C \cdot d)^{-1}$	$Y_{S-B,loq}$	0.5 ... 1	Unitless
$k_{m-B,loq}$	1 ... 1500	$g \cdot (mg C \cdot d)^{-1}$	$Y_{S-F,hiq}$	0.5 ... 1	Unitless
$k_{m-BP,P}$	1 ... 1500	$g \cdot (mg C \cdot d)^{-1}$	$Y_{S-F,loq}$	0.5 ... 1	Unitless
$k_{m-BP,hiq}$	1 ... 1500	$g \cdot (mg C \cdot d)^{-1}$	$Y_{S-BP,P}$	0.5 ... 1	Unitless
$k_{m-BP,loq}$	1 ... 1500	$g \cdot (mg C \cdot d)^{-1}$	$Y_{S-BP,hiq}$	0.5 ... 1	Unitless
$k_{F,P}$	1×10^{-5} ... 10	d^{-1}	$Y_{S-BP,loq}$	0.5 ... 1	Unitless
T_{y-F}	1×10^{-5} ... 1	$mg C \cdot (mg C)^{-1}$	D_{hiq}	1 ... 100	$mm^2 \cdot d^{-1}$
$K_{S-F,P}$	0.1 ... 100	$mg C \cdot g^{-1}$	D_{loq}	1 ... 100	$mm^2 \cdot d^{-1}$
$T_{F,P}$	1 ... 1×10^5	$mg C \cdot (mg C)^{-1}$	K_{d-hiq}	1 ... 100	$mm^3 \cdot mg^{-1}$
a_{max-B}	0.1 ... 3	d^{-1}	K_{d-loq}	1 ... 100	$mm^3 \cdot mg^{-1}$
a_{max-F}	0.1 ... 3	d^{-1}	λ	1 ... 50	mm
a_{max-BP}	0.1 ... 3	d^{-1}	$r_B(t=0)$	0.01 ... 1	Unitless
$K_{a-B,hiq}$	1 ... 100	$g \cdot (mg C)^{-1}$	$r_F(t=0)$	0.01 ... 1	Unitless
$K_{a-B,loq}$	1 ... 100	$g \cdot (mg C)^{-1}$	$r_{BP}(t=0)$	0.01 ... 1	Unitless
$K_{a-F,hiq}$	1 ... 100	$g \cdot (mg C)^{-1}$	$f_B(t=0)$	0.05 ... 0.95	Unitless
$K_{a-F,loq}$	1 ... 100	$g \cdot (mg C)^{-1}$	$f_{BP-B}(t=0)$	1×10^{-6} ... 1	Unitless
$K_{a-BP,P}$	1 ... 100	$g \cdot (mg C)^{-1}$	$f_{DOC,hiq}(t=0)$	1×10^{-5} ... 1	Unitless
$K_{a-BP,hiq}$	1 ... 100	$g \cdot (mg C)^{-1}$	f_{DOC}	0.1 ... 1	Unitless
$K_{a-BP,loq}$	1 ... 100	$g \cdot (mg C)^{-1}$	f_p	0.76 ... 0.90	Unitless
q_{max-B}	0.1 ... 10	d^{-1}			

Appendix C. Measured and simulated dynamics of C, MCPA and microorganisms in all soil layers.

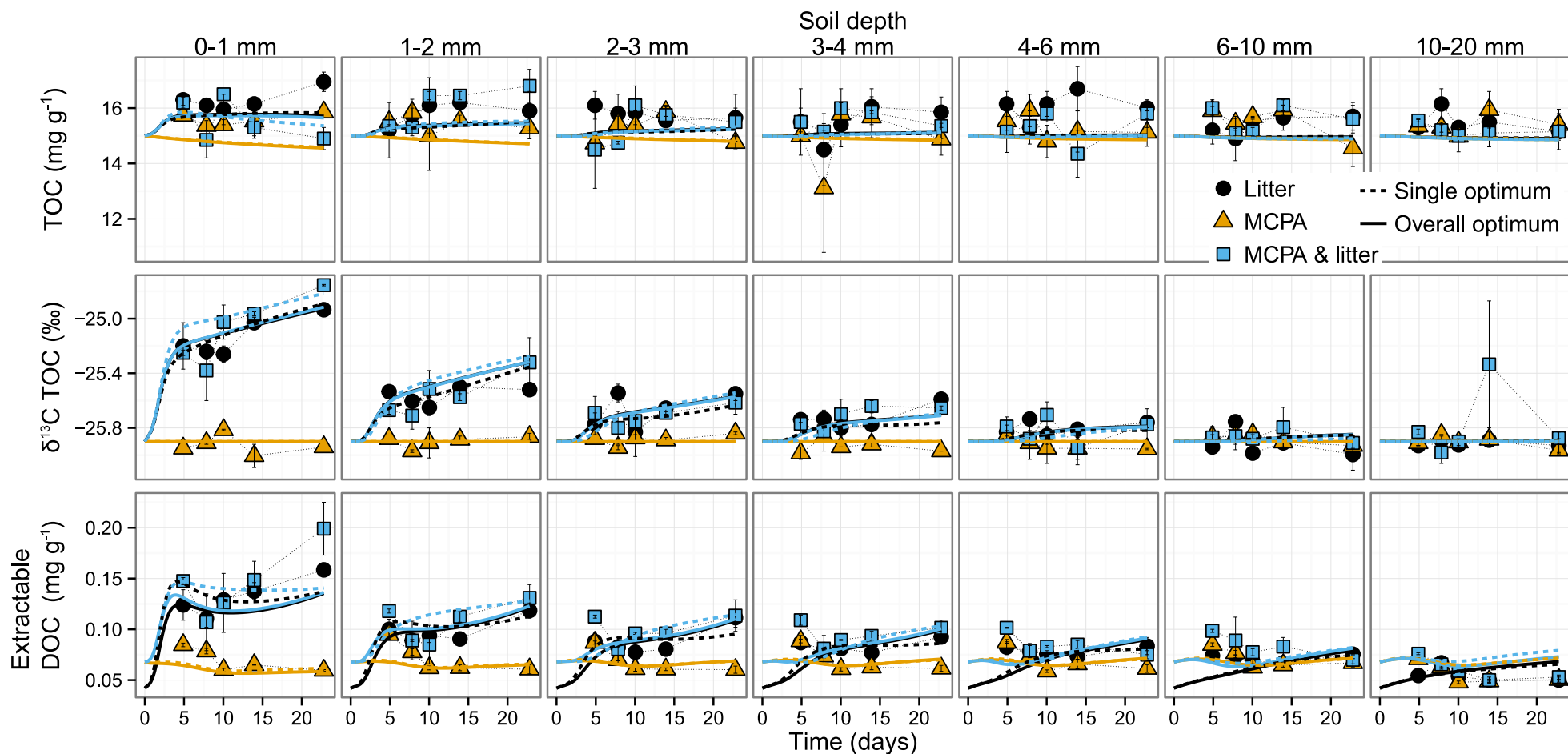


Fig. C1 Dynamics of organic C pools in three selected soil layers close to litter (0-3 mm) and one in “bulk” soil (6-10 mm). Symbols show means and error bars indicate standard errors of two replicates. Continuous lines show simulated values using either the treatment specific optimal parameters (dashed line) or the compromise parameter set (solid).

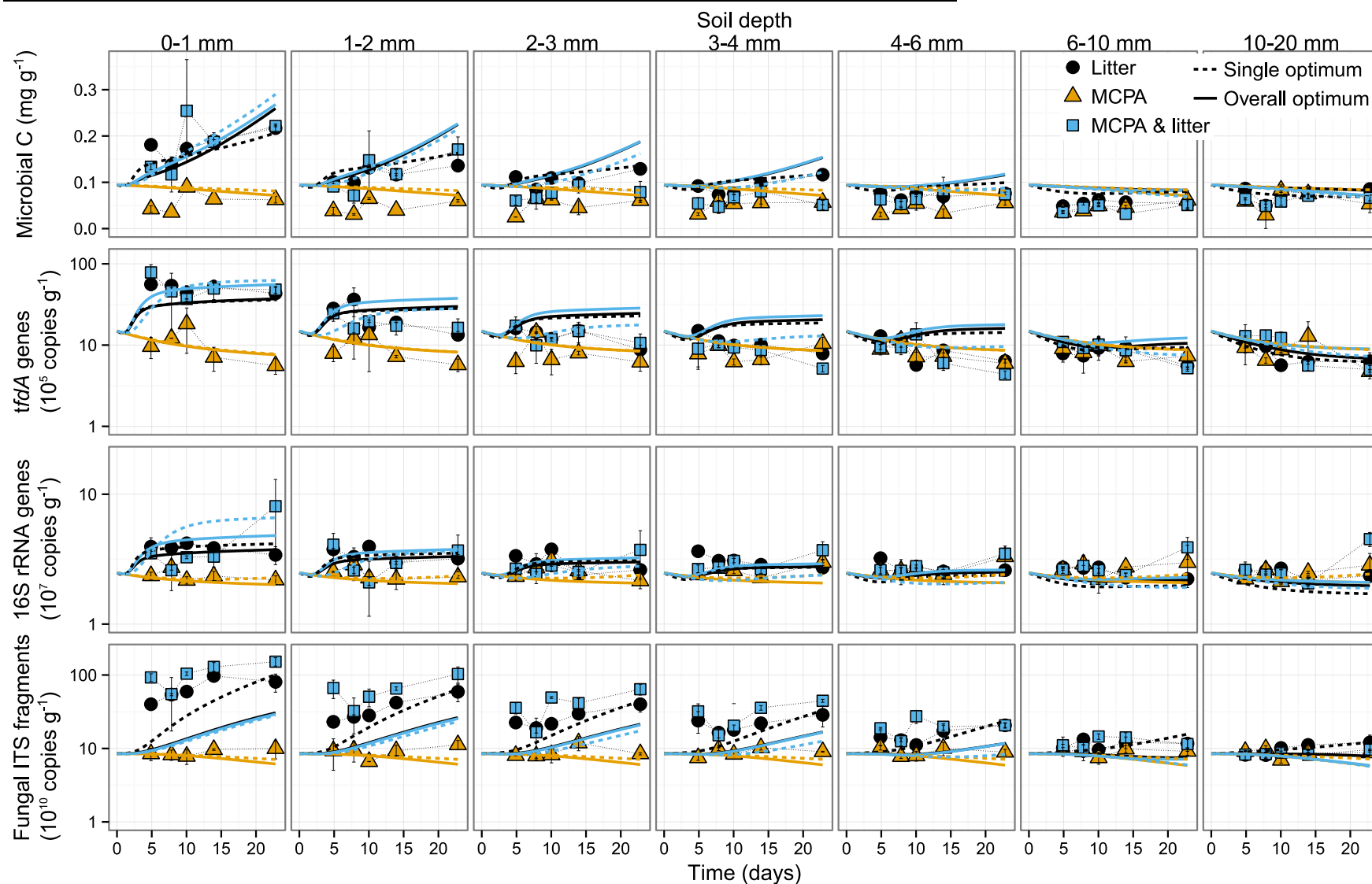


Fig. C2 Dynamics of microbial biomass C and genetic markers in three selected soil layers close to litter (0-3 mm) and one in “bulk” soil (6-10 mm). Symbols show means and error bars indicate standard errors of two replicates. Continuous lines show simulated values using either the treatment specific optimal parameters (dashed line) or the compromise parameter set (solid).

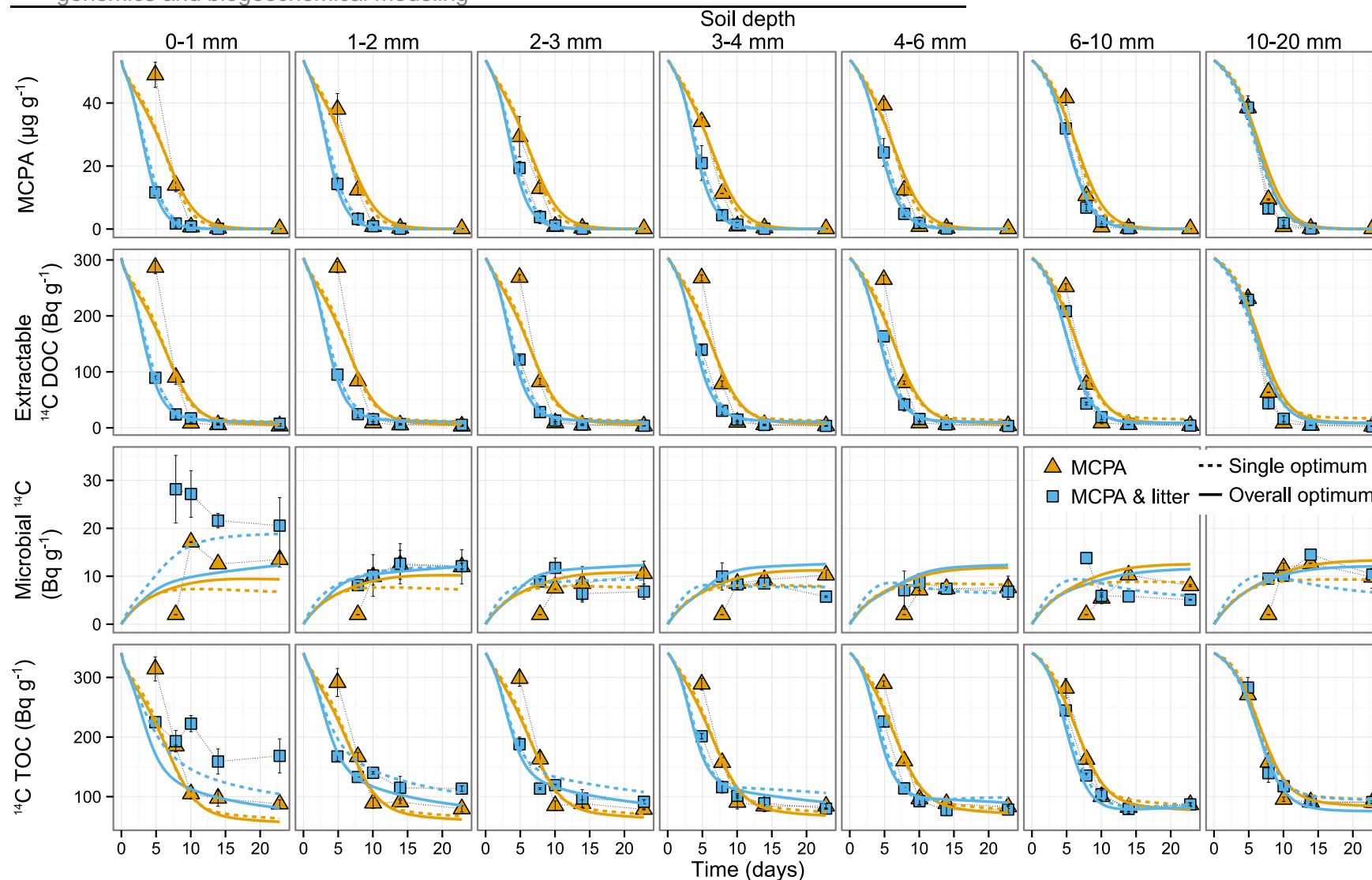
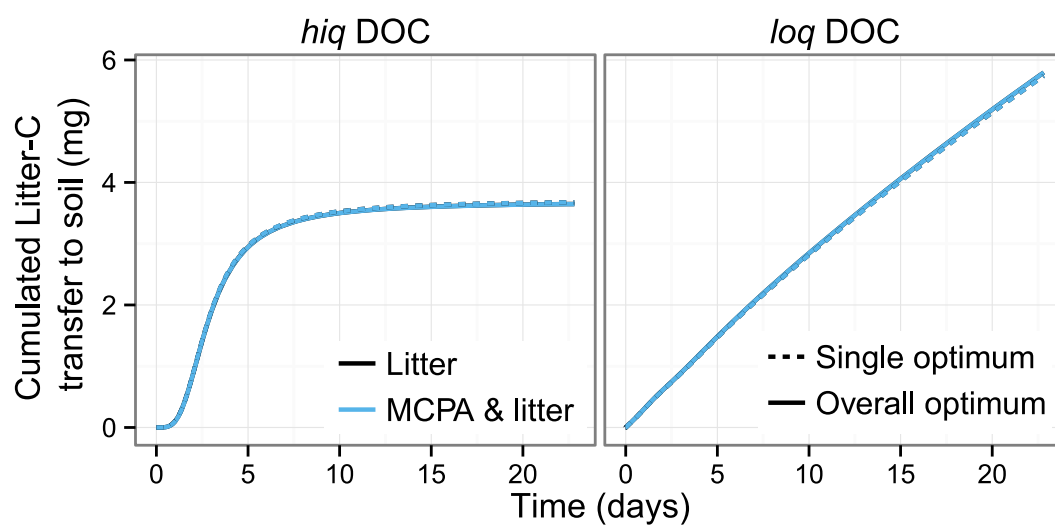


Fig. C3 Dynamics of MCPA and specific ^{14}C activity in organic C pools in three selected soil layers close to litter (0-3 mm) and one in “bulk” soil (6-10 mm). Symbols show means and error bars indicate standard errors of two replicates. Continuous lines show simulated values using either the treatment specific optimal parameters (dashed line) or the compromise parameter set (solid).

Appendix D. Simulated input of *hiq* and *loq* DOC at the upper soil boundary**Fig. D1** Simulated dynamics of *hiq* and *loq* litter-C input at the top of the soil cores (upper boundary).

Appendix E. Mass balance of total, litter- and MCPA-derived C after 22.8 days.

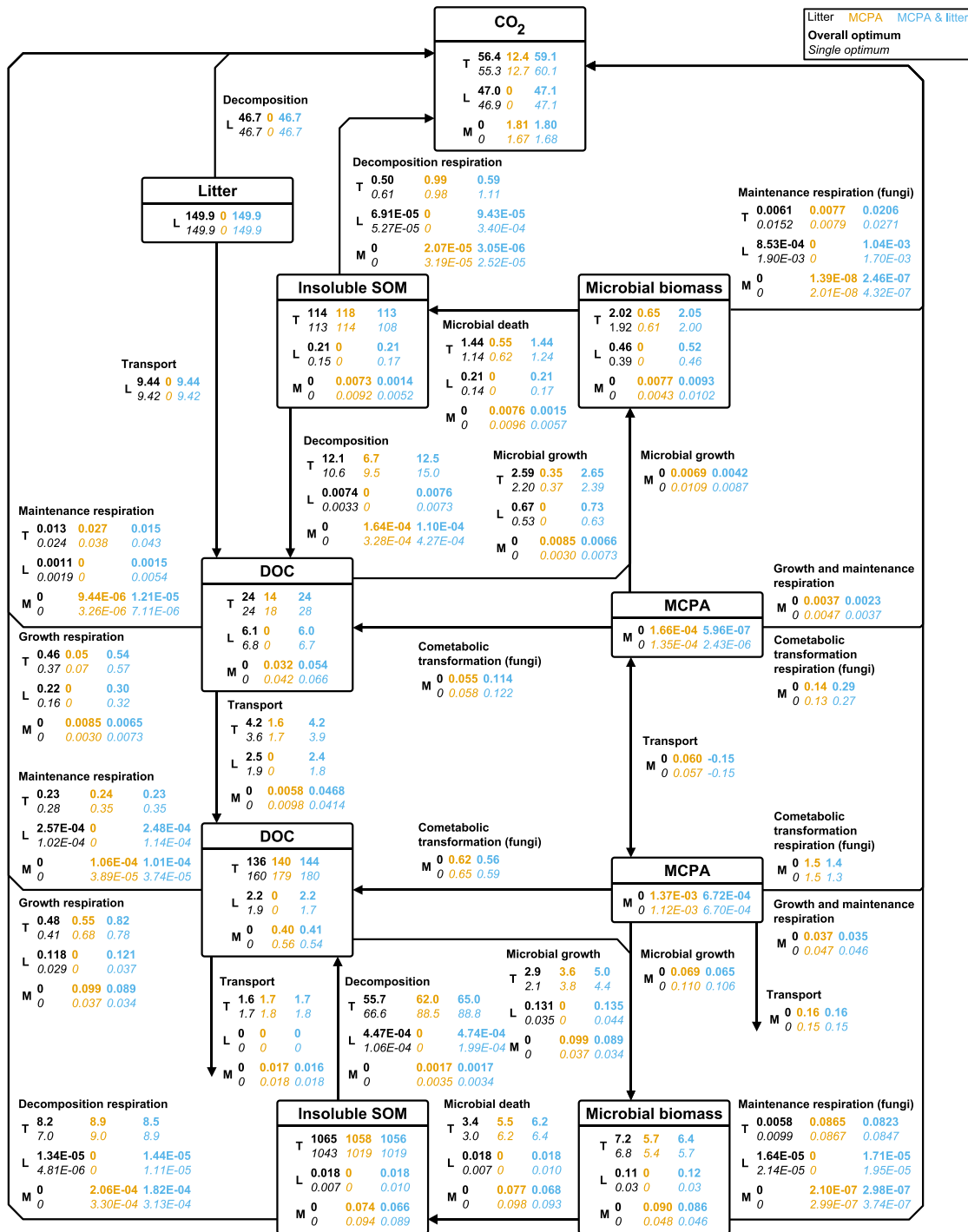


Fig. E1 Simulated pool sizes and cumulated fluxes of total C (T), litter-derived C (L) and MCPA-derived C (M) after 22.8 days. For each pool and cumulated flux the values of the three treatments are shown in black (Litter), orange (MCPA) and blue (MCPA & litter). Within each data group the first (bold) and second (italic) lines indicate model results using the compromise or the best treatment specific optimal parameter set. All pools and fluxes are given in mg C.

7 General discussion

Using the detritusphere as a model system, my thesis elucidated how the availability of C resources regulates microbial dynamics involved in MCPA degradation. Readily utilizable C stimulates microbial activity and C turnover in soil (Kuzyakov 2010). This was confirmed by the results of my thesis. It was additionally shown that increased microbial activity and C turnover triggers accelerated MCPA degradation. Stimulation of biogeochemical processes (particularly C/N turnover and pesticide degradation) as a result of increased availability of readily utilizable C can be similarly found in other biogeochemical hot spots, such as the rhizo- and drilosphere, or in macropores (Bundt et al. 2001a; Gerhardt et al. 2009; Liu et al. 2011; Schenck zu Schweinsberg-Mickan et al. 2012; Badawi et al. 2013; Blouin et al. 2013).

Kandeler et al. (1999a) stated that litter-derived dissolved organic substances provide the energy for microbial activity in the detritusphere. This statement nicely expresses the underlying principle of three possible regulation mechanisms of accelerated MCPA degradation identified in my thesis:

- (1) The major bacterial pathway of MCPA degradation involves the initial cleavage of the ether bond of MCPA by α -ketoglutarate-linked dioxygenases (Liu et al. 2013). In this reaction, the co-substrate α -ketoglutarate is oxidized to CO_2 plus succinate (Müller and Babel 2001; Hausinger 2004). Note, that other α -ketoacids can be utilized as cosubstrate as well (Fukumori and Hausinger 1993). Litter might supply α -ketoglutarate, other α -ketoacids or metabolic precursors to the detritusphere soil. As a result, resources and energy required by bacteria for co-substrate (re)generation would be substantially reduced.
- (2) Additional supply of C, N and energy can generally increase the production of enzymes by alleviating resource limitation (Schimel and Weintraub 2003; Allison 2005). Consequently, litter-C input might shift resource allocation towards increased production of MCPA degrading enzymes by specific bacteria and bacterial consortia.
- (3) In accordance with previous studies (Berg and McClaugherty 2008, p.36; Ingwersen et al. 2008), my thesis revealed that fungi most strongly benefit from additional supply of litter-C. Litter-derived compounds probably facilitate fungal MCPA degradation via co-metabolism involving unspecific enzymes (Reddy et al. 1997; Castillo et al. 2001; Sträuber et al. 2003; Vroumsia et al. 2005; Campoy et al. 2009; Itoh et al. 2013). Primary substrates supplied by litter might act as inducers of enzyme production, or provide the energy required for the enzymatically catalyzed reaction to attack MCPA as secondary substrate (Dalton and Stirling 1982; Brandt et al. 2003).

These regulation mechanisms are reflected in the PECCAD (PEsticide degradation Coupled to CARbon turnover in the Detritosphere) model, which I developed in the frame of my thesis. In the model, specific bacterial degraders utilize MCPA as growth and energy substrate, whereas fungi perform co-metabolic MCPA transformation. Availability of dissolved organic C controls physiological activity, growth, death and maintenance of microorganisms. Consequently, the model implicitly reflects accelerated MCPA degradation in response to litter-C input i) via additional resource and energy supply to specific bacterial MCPA degraders and ii) via increased production of unspecific fungal enzymes as a result of stimulated fungal growth and activity.

The consideration of microbial feedbacks to C availability in PECCAD is in accordance with formulations used in current state-of-the-art C turnover models (Blagodatsky et al. 2010; Neill and Guenet 2010; Allison 2012; Wutzler and Reichstein 2013; Moore et al. 2014; Perveen et al. 2014; Wang et al. 2014; Wieder et al. 2014). Other than PECCAD, however, some of these models explicitly account for enzyme dynamics. The mechanism of accelerated co-metabolic MCPA transformation in response to higher availability of dissolved organic C as incorporated in PECCAD was similarly applied to model glyphosate degradation in mulch and adjacent soil (Aslam et al. 2014). Beyond these approaches, PECCAD does not treat soil as a bulk. Instead it explicitly considers sorption and one-dimensional transport of solutes (DOC and MCPA). It thereby mechanistically accounts for interactions between microbial dynamics and physico-chemical processes. Likewise other models combine the simulation of microbial dynamics and reactive transport (Chalhoub et al. 2013; Rosenbom et al. 2014). Recent approaches additionally consider the pore network architecture in real soil (Gharasoo et al. 2014; Monga et al. 2014). In contrast to PECCAD, such studies focus on C and N turnover only and have not yet considered regulation mechanisms of C availability on microbial dynamics involved in the degradation of pesticides or other xenobiotics.

“Biogeochemical models, however, are trailing in the wake of the environmental genomics revolution...” (Reed et al. 2014). That means, modern molecular tools provide huge amounts of information about composition and function of microbial communities in soil (von Bergen et al. 2013; Myrold et al. 2014), but this knowledge has largely not yet been utilized for modeling (Trivedi et al. 2013). In extension of much simpler approaches (Batoglu-Pazarbasi et al. 2013), my thesis contributes to integrate soil genomics and mathematical modeling. Microbial pools of the PECCAD model are set up in correspondence to quantifiable genetic proxies. I demonstrated that the PECCAD model can be parameterized using detailed microbial (incl. genetic proxies) and physicochemical data in combination with a sophisticated parameter optimization approach. The application of the parameterized PECCAD model allows an in-depth analysis of matter cycling in the detritosphere. Nevertheless, my thesis points to severe challenges in

integrating genetic information and mechanistic models that need to be solved in future research. Here, the identification of functional microbial traits by molecular tools (including genomics, proteomics, transcriptomics, and metabolomics; Green et al. 2008; Prosser 2012; Krause et al. 2014; Talbot et al. 2014) and their integration in mechanistic models (Allison 2012; Wallenstein and Hall 2012; Manzoni et al. 2014) provide a promising way to gain further progress.

8 Final conclusions

The detritosphere is a hot spot of matter turnover in soil. The input of C from the litter layer into the adjacent soil strongly affects the dynamics of fungi and specific bacterial MCPA degraders in this microhabitat, which in turn regulate the biogeochemical processes there. According to the PECCAD simulations about 90% of initially applied MCPA is degraded co-metabolically by fungi, whereas only about 4% of applied MCPA is used as growth and energy substrate by specialized bacterial degraders. Although these numbers may be somewhat affected by uncertainties in the model parameters and in the genetic proxies utilized, my results clearly suggest a distinct dominance of co-metabolic over growth-linked MCPA transformation implying that unspecific fungal enzymes play a more important role in the biodegradation of MCPA than previously thought.

Soil is a complex system with self-organizing properties (Young and Crawford 2004). “Three key concepts that characterize self-organizing systems are feedback, complexity and emergence” (Wainwright and Mulligan 2013, p.49). Accordingly, my thesis clarifies the complexity of a system response (accelerated MCPA degradation coupled to C turnover) emerging from small-scale feedbacks (or interactions) between physicochemical processes and microbial dynamics. My thesis makes a contribution to tackle the challenge of integrating genetic information in mechanistic models, which is important to improve “our understanding of the key role microbes play in modulating Earth’s biogeochemistry” (Reed et al. 2014). Further improvements of the representation of complex soil microbial communities and their dynamics in mathematical models will be probably gained in future research by explicitly considering functional traits of soil microorganisms, which are identified and quantified using molecular biological analyses.

My thesis highlights that we need to understand microbial functioning to grasp how soil functions are regulated. I demonstrated the benefit of closely integrating complex mathematical models and sophisticated experiments in order to facilitate the interpretation of observations and to test theory. The applied modeling approach provides a promising perspective for future studies aiming at an improved understanding of microbial functioning in soil.

9 References

- Allison S.D. (2012). A trait-based approach for modelling microbial litter decomposition. *Ecology Letters*, 15(9), 1058–1070.
- Allison S.D. (2005). Cheaters, diffusion and nutrients constrain decomposition by microbial enzymes in spatially structured environments. *Ecology Letters*, 8(6), 626–635.
- Allison S.D. and Jastrow J.D. (2006). Activities of extracellular enzymes in physically isolated fractions of restored grassland soils. *Soil Biology and Biochemistry*, 38(11), 3245–3256.
- Ananyeva K., Wang W., Smucker A.J.M., Rivers M.L. and Kravchenko A.N. (2013). Can intra-aggregate pore structures affect the aggregate's effectiveness in protecting carbon? *Soil Biology and Biochemistry*, 57, 868–875.
- Ashman M.R., Hallett P.D. and Brookes P.C. (2003). Are the links between soil aggregate size class, soil organic matter and respiration rate artefacts of the fractionation procedure? *Soil Biology and Biochemistry*, 35(3), 435–444.
- Aslam S., Benoit P., Chabauty F., Bergheaud V., Geng C., Vieubl e-Gonod L. and Garnier P. (2014). Modelling the impacts of maize decomposition on glyphosate dynamics in mulch. *European Journal of Soil Science*, 65(2), 231–247.
- Bach E.M. and Hofmockel K.S. (2014). Soil aggregate isolation method affects measures of intra-aggregate extracellular enzyme activity. *Soil Biology and Biochemistry*, 69(0), 54 – 62.
- Badawi N., Johnsen A.R., Brandt K.K., S orensen J. and Aamand J. (2013). Hydraulically active biopores stimulate pesticide mineralization in agricultural subsoil. *Soil Biology and Biochemistry*, 57, 533–541.
- Baelum J., Jacobsen C.S. and Holben W.E. (2010). Comparison of 16S rRNA gene phylogeny and functional *tfdA* gene distribution in thirty-one different 2, 4-dichlorophenoxyacetic acid and 4-chloro-2-methylphenoxyacetic acid degraders. *Systematic and Applied Microbiology*, 33(2), 67–70.
- Bailey V.L., Fansler S.J., Stegen J.C. and McCue L.A. (2013). Linking microbial community structure to β -glucosidic function in soil aggregates. *ISME Journal*, 7(10), 2044–2053.
- Banitz T., Johst K., Wick L.Y., Schamfu s S., Harms H. and Frank K. (2013). Highways versus pipelines: Contributions of two fungal transport mechanisms to efficient bioremediation. *Environmental Microbiology Reports*, 5(2), 211.
- Batoglu-Pazarbasi M., Milosevic N., Malaguerra F., Binning P.J., Albrechtsen H.J., Bjerg P.L. and Aamand J. (2013). Discharge of landfill leachate to streambed sediments impacts the mineralization potential of phenoxy acid herbicides depending on the initial abundance of *tfdA* gene classes. *Environmental Pollution*, 176, 275–283.
- Beare M.H., Coleman D.C., Crossley Jr D.A., Hendrix P.F. and Odum E.P. (1995). A hierarchical approach to evaluating the significance of soil biodiversity to biogeochemical cycling. *Plant and Soil*, 170(1), 5–22.
- Berg B. and McClaugherty C. (2008). *Plant litter*. Berlin: Springer.
- Von Bergen M., Jehmlich N., Taubert M., Vogt C., Bastida F., Herbst F.-A., Schmidt F., Richnow H.-H. and Seifert J. (2013). Insights from quantitative metaproteomics and protein-stable isotope probing into microbial ecology. *ISME Journal*, 7(10), 1877–1885.
- Bird J.A., Herman D.J. and Firestone M.K. (2011). Rhizosphere priming of soil organic matter by bacterial groups in a grassland soil. *Soil Biology and Biochemistry*, 43(4), 718–725.
- Blagodatskaya E. and Kuzyakov Y. (2013). Active microorganisms in soil: Critical review of estimation criteria and approaches. *Soil Biology and Biochemistry*, 67(0), 192–211.
- Blagodatskaya E. and Kuzyakov Y. (2008). Mechanisms of real and apparent priming effects and their dependence on soil microbial biomass and community structure: Critical review. *Biology and Fertility of Soils*, 45(2), 115–131.

- Blagodatsky S., Blagodatskaya E., Yuyukina T. and Kuzyakov Y. (2010). Model of apparent and real priming effects: Linking microbial activity with soil organic matter decomposition. *Soil Biology and Biochemistry*, 42(8), 1275–1283.
- Blagodatsky S. and Richter O. (1998). Microbial growth in soil and nitrogen turnover: A theoretical model considering the activity state of microorganisms. *Soil Biology and Biochemistry*, 30(13), 1743–1755.
- Blouin M., Hodson M.E., Delgado E.A., Baker G., Brussaard L., Butt K.R., Dai J., Dendooven L., Peres G., Tondoh J.E., Cluzeau D. and Brun J.J. (2013). A review of earthworm impact on soil function and ecosystem services. *European Journal of Soil Science*, 64(2), 161–182.
- Blume H.-P., Brümmer G.W., Horn R., Kandeler E., Kögel-Knabner I., Kretzschmar R., Stahr K. and Wilke B.-M. (2010). *Scheffer/Schachtschabel: Lehrbuch der Bodenkunde*. Heidelberg: Spektrum Akademischer Verlag.
- Boivin A., Amellal S., Schiavon M. and Van Genuchten M.T. (2005). 2,4-Dichlorophenoxyacetic acid (2,4-D) sorption and degradation dynamics in three agricultural soils. *Environmental Pollution*, 138(1), 92–99.
- Bottner P., Pansu M. and Sallih Z. (1999). Modelling the effect of active roots on soil organic matter turnover. *Plant and Soil*, 216(1-2), 15–25.
- Bouckaert L., Sleutel S., Van Loo D., Brabant L., Cnudde V., Van Hoorebeke L. and De Neve S. (2013). Carbon mineralisation and pore size classes in undisturbed soil cores. *Soil Research*, 51(1), 14–22.
- Brandt B.W., Van Leeuwen I.M.M. and Kooijman S.A.L.M. (2003). A general model for multiple substrate biodegradation. Application to co-metabolism of structurally non-analogous compounds. *Water Research*, 37(20), 4843–4854.
- British Crop Protection Council. (2009). *The pesticide manual: a world compendium*. 15th ed. C. Tomlin, ed. Alton, Hampshire: British Crop Protection Council.
- Bundt M., Jäggi M., Blaser P., Siegwolf R. and Hagedorn F. (2001a). Division S-7 - Forest & range soils: Carbon and nitrogen dynamics in preferential flow paths and matrix of a forest soil. *Soil Science Society of America Journal*, 65(5), 1529–1538.
- Bundt M., Widmer F., Pesaro M., Zeyer J. and Blaser P. (2001b). Preferential flow paths: Biological 'hot spots' in soils. *Soil Biology and Biochemistry*, 33(6), 729–738.
- Burns R.G., DeForest J.L., Marxsen J., Sinsabaugh R.L., Stromberger M.E., Wallenstein M.D., Weintraub M.N. and Zoppini A. (2013). Soil enzymes in a changing environment: Current knowledge and future directions. *Soil Biology and Biochemistry*, 58, 216–234.
- BVL. (2014). *Absatz an Pflanzenschutzmitteln in der Bundesrepublik Deutschland - Ergebnisse der Meldungen gemäß § 64 Pflanzenschutzgesetz für das Jahr 2013*. Bundesamt für Verbraucherschutz und Lebensmittelsicherheit.
- Campoy S., Alvarez-Rodriguez M.L., Recio E., Rumbero A. and Coque J.J.R. (2009). Biodegradation of 2,4,6-TCA by the white-rot fungus *Phlebia radiata* is initiated by a phase I (O-demethylation)-phase II (O-conjugation) reactions system: Implications for the chlorine cycle. *Environmental Microbiology*, 11(1), 99–110.
- Castillo M. d. P., Andersson A., Ander P., Stenström J. and Torstensson L. (2001). Establishment of the white rot fungus *Phanerochaete chrysosporium* on unsterile straw in solid substrate fermentation systems intended for degradation of pesticides. *World Journal of Microbiology and Biotechnology*, 17(6), 627–633.
- Caux P.Y., Kent R.A., Bergeron V., Fan G.T. and Macdonald D.D. (1995). Environmental Fate And Effects Of Mcpa - A Canadian Perspective. *Critical Reviews In Environmental Science And Technology*, 25(4), 313–376.
- Cazelles K., Otten W., Baveye P.C. and Falconer R.E. (2013). Soil fungal dynamics: Parameterisation and sensitivity analysis of modelled physiological processes, soil architecture and carbon distribution. *Ecological Modelling*, 248, 165–173.
- Cederlund H., Borjesson E., Onneby K. and Stenstrom J. (2007). Metabolic and cometabolic degradation of herbicides in the fine material of railway ballast. *Soil Biology & Biochemistry*, 39(2), 473–484.

- Chalhoub M., Garnier P., Coquet Y., Mary B., Lafolie F. and Houot S. (2013). Increased nitrogen availability in soil after repeated compost applications: Use of the PASTIS model to separate short and long-term effects. *Soil Biology and Biochemistry*, 65, 144–157.
- Chen B. and Yuan M. (2012). Enhanced dissipation of polycyclic aromatic hydrocarbons in the presence of fresh plant residues and their extracts. *Environmental Pollution*, 161, 199–205.
- Cheng W. (2009). Rhizosphere priming effect: Its functional relationships with microbial turnover, evapotranspiration, and C-N budgets. *Soil Biology and Biochemistry*, 41(9), 1795–1801.
- Chenu C. and Cosentino D. (2011). Microbial regulation of soil structural dynamics. In *The Architecture and biology of soils: Life in inner space*. CABI Publishing, pp. 37–70.
- Chorover J., Kretzschmar R., Garica-Pichel F. and Sparks D.L. (2007). Soil biogeochemical processes within the critical zone. *Elements*, 3(5), 321–326.
- Christensen B.T. (2001). Physical fractionation of soil and structural and functional complexity in organic matter turnover. *European Journal of Soil Science*, 52(3), 345–353.
- Crawford J.W., Deacon L., Grinev D., Harris J.A., Ritz K., Singh B.K. and Young I. (2012). Microbial diversity affects self-organization of the soil - Microbe system with consequences for function. *Journal of the Royal Society Interface*, 9(71), 1302–1310.
- Crespin M.A., Gallego M., Valcarcel M. and Gonzalez J.L. (2001). Study of the degradation of the herbicides 2,4-D and MCPA at different depths in contaminated agricultural soil. *Environmental Science & Technology*, 35(21), 4265–4270.
- Dalton H. and Stirling D.I. (1982). Co-metabolism. *Philosophical transactions of the Royal Society of London. Series B: Biological sciences*, 297(1088), 481–496.
- Don A., Steinberg B., Schöning I., Pritsch K., Joschko M., Gleixner G. and Schulze E.D. (2008). Organic carbon sequestration in earthworm burrows. *Soil Biology and Biochemistry*, 40(7), 1803–1812.
- Don R.H. and Pemberton J.M. (1981). Properties of six pesticide degradation plasmids isolated from *Alcaligenes paradoxus* and *Alcaligenes eutrophus*. *Journal of Bacteriology*, 145(2), 681–686.
- Dorodnikov M., Blagodatskaya E., Blagodatsky S., Marhan S., Fangmeier A. and Kuzyakov Y. (2009). Stimulation of microbial extracellular enzyme activities by elevated CO₂ depends on soil aggregate size. *Global Change Biology*, 15(6), 1603–1614.
- Ettema C.H. and Wardle D.A. (2002). Spatial soil ecology. *Trends in Ecology and Evolution*, 17(4), 177–183.
- European Commission. (2005). *Review report for the active substance MCPA*. Health & Consumer Protection Directorate-General.
- Fontaine S., Henault C., Amor A., Bdioui N., Bloor J.M.G., Maire V., Mary B., Revalliot S. and Maron P.A. (2011). Fungi mediate long term sequestration of carbon and nitrogen in soil through their priming effect. *Soil Biology and Biochemistry*, 43(1), 86–96.
- Foster R.C. (1988). Microenvironments of soil microorganisms. *Biology and Fertility of Soils*, 6(3), 189–203.
- Franklin R.B. and Mills A.L. (2009). Importance of spatially structured environmental heterogeneity in controlling microbial community composition at small spatial scales in an agricultural field. *Soil Biology and Biochemistry*, 41(9), 1833–1840.
- Fukumori F. and Hausinger R.P. (1993). Purification and characterization of 2,4-dichlorophenoxyacetate/α- ketoglutarate dioxygenase. *Journal of Biological Chemistry*, 268(32), 24311–24317.
- Gaillard V., Chenu C. and Recous S. (2003). Carbon mineralisation in soil adjacent to plant residues of contrasting biochemical quality. *Soil Biology and Biochemistry*, 35(1), 93–99.
- Garnier P., Néel C., Aita C., Recous S., Lafolie F. and Mary B. (2003). Modelling carbon and nitrogen dynamics in a bare soil with and without straw incorporation. *European Journal of Soil Science*, 54(3), 555–568.
- Gaston L.A. and Locke M.A. (2002). Differences in microbial biomass, organic carbon, and dye sorption between flow and no-flow regions of unsaturated soil. *Journal of Environmental Quality*, 31(4), 1406–1408.

- Gerhardt K.E., Huang X.D., Glick B.R. and Greenberg B.M. (2009). Phytoremediation and rhizoremediation of organic soil contaminants: Potential and challenges. *Plant Science*, 176(1), 20–30.
- Gharasoo M., Centler F., Fetzer I. and Thullner M. (2014). How the chemotactic characteristics of bacteria can determine their population patterns. *Soil Biology and Biochemistry*, 69, 346–358.
- Gharasoo M., Centler F., Regnier P., Harms H. and Thullner M. (2012). A reactive transport modeling approach to simulate biogeochemical processes in pore structures with pore-scale heterogeneities. *Environmental Modelling and Software*, 30, 102–114.
- Girish Shukla and A. Varma eds. (2011). *Soil enzymology*. Heidelberg: Springer.
- Gleixner G. (2013). Soil organic matter dynamics: A biological perspective derived from the use of compound-specific isotopes studies. *Ecological Research*, 28(5), 683–695.
- Grant R.F., Juma N.G. and McGill W.B. (1993). Simulation of carbon and nitrogen transformations in soil: Microbial biomass and metabolic products. *Soil Biology and Biochemistry*, 25(10), 1331–1338.
- Gras A., Ginovart M., Valls J. and Baveye P.C. (2011). Individual-based modelling of carbon and nitrogen dynamics in soils: Parameterization and sensitivity analysis of microbial components. *Ecological Modelling*, 222(12), 1998–2010.
- Green J.L., Bohannon B.J.M. and Whitaker R.J. (2008). Microbial biogeography: From taxonomy to traits. *Science*, 320(5879), 1039–1043.
- Grundmann G.L. (2004). Spatial scales of soil bacterial diversity - The size of a clone. *FEMS Microbiology Ecology*, 48(2), 119–127.
- Haby P.A. and Crowley D.E. (1996). Biodegradation of 3-chlorobenzoate as affected by rhizodeposition and selected carbon substrates. *Journal of Environmental Quality*, 25(2), 304–310.
- Hagedorn F. and Bellamy P. (2011). Hot Spots and Hot Moments for Greenhouse Gas Emissions from Soils. In R. Jandl, M. Rodeghiero, & M. Olsson, eds. *Soil Carbon in Sensitive European Ecosystems: From Science to Land Management*. John Wiley & Sons, Ltd, pp. 13–32.
- Hallett P.D., Karim K.H., Glyn Bengough A. and Otten W. (2013). Biophysics of the vadose zone: From reality to model systems and back again. *Vadose Zone Journal*, 12(4). DOI 10.2136/vzj2013.05.0090.
- Hausinger R.P. (2004). Fe(II)/alpha-ketoglutarate-dependent hydroxylases and related enzymes. *Critical Reviews in Biochemistry and Molecular Biology*, 39(1), 21–68.
- Helal H.M. and Sauerbeck D.R. (1984). Influence of plant roots on C and P metabolism in soil. *Plant and Soil*, 76(1-3), 175–182.
- Helling C.S., Bollag J.M. and Dawson J.E. (1968). Cleavage of ether-oxygen bond in phenoxyacetic acid by an arthrobacter species. *Journal of Agricultural Food and Chemistry*, 16(3), 538–539.
- Hissett R. and Gray T.R.G. (1976). Microsites and time changes in soil microbe ecology. In J. M. Anderson & A. Macfadyen, eds. *The role of terrestrial and aquatic organisms in decomposition processes*. Symposium of the British Ecological Society. Oxford: Blackwell, pp. 23–39.
- Hoffmann H., Schloter M. and Wilke B.-M. (2007). Microscale-scale measurement of potential nitrification rates of soil aggregates. *Biology and Fertility of Soils*, 44(2), 411–413.
- Ingwersen J., Poll C., Streck T. and Kandeler E. (2008). Micro-scale modelling of carbon turnover driven by microbial succession at a biogeochemical interface. *Soil Biology and Biochemistry*, 40(4), 872–886.
- Itoh K., Kinoshita M., Morishita S., Chida M. and Suyama K. (2013). Characterization of 2,4-dichlorophenoxyacetic acid and 2,4,5-trichlorophenoxyacetic acid-degrading fungi in Vietnamese soils. *FEMS Microbiology Ecology*, 84(1), 124–132.
- Itoh K., Tashiro Y., Uobe K., Kamagata Y., Suyama K. and Yamamoto H. (2004). Root Nodule Bradyrhizobium spp. Harbor tfdA? and cadA, Homologous with Genes Encoding 2,4-Dichlorophenoxyacetic Acid-Degrading Proteins. *Applied and Environmental Microbiology*, 70(4), 2110–2118.

- Jarvis N.J. (2007). A review of non-equilibrium water flow and solute transport in soil macropores: Principles, controlling factors and consequences for water quality. *European Journal of Soil Science*, 58(3), 523–546.
- Jastrow J.D., Amonette J.E. and Bailey V.L. (2007). Mechanisms controlling soil carbon turnover and their potential application for enhancing carbon sequestration. *Climatic Change*, 80(1-2), 5–23.
- Jensen P.H., Hansen H.C.B., Rasmussen J. and Jacobsen O.S. (2004). Sorption-controlled degradation kinetics of MCPA in soil. *Environmental Science & Technology*, 38(24), 6662–6668.
- Jury W.A. and Horton R. (2004). *Soil physics*. Hoboken, NJ [u.a.]: Wiley.
- Kandeler E. and Dick R.P. (2007). Soil Enzymes - Spatial Distribution and Function in Agroecosystems. In G. Benckiser & S. Schnell, eds. *Biodiversity in agricultural production systems*. Books in Soils, Plants, and the Environment. Boca Raton, FL: CRC Taylor & Francis.
- Kandeler E., Luxhøi J., Tschierko D. and Magid J. (1999a). Xylanase, invertase and protease at the soil-litter interface of a loamy sand. *Soil Biology and Biochemistry*, 31(8), 1171–1179.
- Kandeler E., Stemmer M. and Klimanek E.-M. (1999b). Response of soil microbial biomass, urease and xylanase within particle size fractions to long-term soil management. *Soil Biology and Biochemistry*, 31(2), 261–273.
- Kandeler E., Tschierko D., Bruce K.D., Stemmer M., Hobbs P.J., Bardgett R.D. and Amelung W. (2000). Structure and function of the soil microbial community in microhabitats of a heavy metal polluted soil. *Biology and Fertility of Soils*, 32(5), 390–400.
- Kandeler E., Tschierko D., Stemmer M., Schwarz S. and Gerzabek M.H. (2001). Organic matter and soil microorganisms - Investigations from the micro- to the macro-scale. *Bodenkultur*, 52(2), 117–131.
- Kögel-Knabner I., Guggenberger G., Kleber M., Kandeler E., Kalbitz K., Scheu S., Eusterhues K. and Leinweber P. (2008). Organo-mineral associations in temperate soils: Integrating biology, mineralogy, and organic matter chemistry. *Journal of Plant Nutrition and Soil Science*, 171(1), 61–82.
- Krause S., Le Roux X., Niklaus P.A., van Bodegom P.M., Lennon J.T., Bertilsson S., Grossart H.-P., Philippot L. and Bodelier P.L.E. (2014). Trait-based approaches for understanding microbial biodiversity and ecosystem functioning. *Frontiers in Microbiology*, 5:251. DOI 10.3389/fmicb.2014.00251.
- Kravchenko L.V., Strigul N.S. and Shvytov I.A. (2004). Mathematical simulation of the dynamics of interacting populations of rhizosphere microorganisms. *Microbiology*, 73(2), 189–195.
- Kuzyakov Y. (2010). Priming effects: Interactions between living and dead organic matter. *Soil Biology and Biochemistry*, 42(9), 1363–1371.
- Kuzyakov Y., Blagodatskaya E. and Blagodatsky S. (2009). Comments on the paper by Kemmitt et al. (2008) 'Mineralization of native soil organic matter is not regulated by the size, activity or composition of the soil microbial biomass - A new perspective' [*Soil Biology & Biochemistry* 40, 61-73]: The biology of the Regulatory Gate. *Soil Biology and Biochemistry*, 41(2), 435–439.
- Kuzyakov Y., Friedel J.K. and Stahr K. (2000). Review of mechanisms and quantification of priming effects. *Soil Biology and Biochemistry*, 32(11-12), 1485–1498.
- Laemmli C., Werlen C. and Van Der Meer J.R. (2004). Mutation analysis of the different tfd genes for degradation of chloroaromatic compounds in *Ralstonia eutropha* JMP134. *Archives of Microbiology*, 181(2), 112–121.
- Lagomarsino A., Grego S. and Kandeler E. (2012). Soil organic carbon distribution drives microbial activity and functional diversity in particle and aggregate-size fractions. *Pedobiologia*, 55(2), 101–110.
- Ledger T., Pieper D.H. and Gonzalez B. (2006). Chlorophenol Hydroxylases Encoded by Plasmid pJP4 Differentially Contribute to Chlorophenoxyacetic Acid Degradation. *Appl. Environ. Microbiol.*, 72(4), 2783–2792.
- Lin H. (2012). *Understanding Soil Architecture and Its Functional Manifestation Across Scales*. Elsevier.
- Liu Y.-J., Liu S.-J., Drake H.L. and Horn M.A. (2013). Consumers of 4-chloro-2-methylphenoxyacetic acid from agricultural soil and drilosphere harbor cadA, r/sdpA, and tfdA-like gene encoding oxygenases. *FEMS Microbiology Ecology*, 86(1), 114–129.

- Liu Y.-J., Zaprasis A., Liu S.-J., Drake H.L. and Horn M.A. (2011). The earthworm *Aporrectodea caliginosa* stimulates abundance and activity of phenoxyalkanoic acid herbicide degraders. *ISME Journal*, 5(3), 473–485.
- Loos M.A., Schlosser I.F. and Mapham W.R. (1979). Phenoxy herbicide degradation in soils: Quantitative studies of 2,4-D- and MCPA-degrading microbial populations. *Soil Biology and Biochemistry*, 11(4), 377–385.
- Von Lützow M., Kögel-Knabner I., Ekschmitt K., Flessa H., Guggenberger G., Matzner E. and Marschner B. (2007). SOM fractionation methods: Relevance to functional pools and to stabilization mechanisms. *Soil Biology and Biochemistry*, 39(9), 2183–2207.
- Manzoni S., Schaeffer S.M., Katul G., Porporato A. and Schimel J.P. (2014). A theoretical analysis of microbial eco-physiological and diffusion limitations to carbon cycling in drying soils. *Soil Biology and Biochemistry*, 73, 69–83.
- Marx M.-C., Kandeler E., Wood M., Wermbter N. and Jarvis S.C. (2005). Exploring the enzymatic landscape: Distribution and kinetics of hydrolytic enzymes in soil particle-size fractions. *Soil Biology and Biochemistry*, 37(1), 35–48.
- Masse D., Cambier C., Brauman A., Sall S., Assigbetse K. and Chotte J.L. (2007). MIOR: An individual-based model for simulating the spatial patterns of soil organic matter microbial decomposition. *European Journal of Soil Science*, 58(5), 1127–1135.
- McClain M.E., Boyer E.W., Dent C.L., Gergel S.E., Grimm N.B., Groffman P.M., Hart S.C., Harvey J.W., Johnston C.A., Mayorga E., McDowell W.H. and Pinay G. (2003). Biogeochemical Hot Spots and Hot Moments at the Interface of Terrestrial and Aquatic Ecosystems. *Ecosystems*, 6(4), 301–312.
- Möller A. and Hansen A.M. (2012). Dynamics of xenobiotic transformation processes in soil systems: A zero-dimensional system model applied to ethylenethiourea. *Applied Geochemistry*, 27(9), 1807–1813.
- Monga O., Garnier P., Pot V., Coucheney E., Nunan N., Otten W. and Chenu C. (2014). Simulating microbial degradation of organic matter in a simple porous system using the 3-D diffusion-based model MOSAIC. *Biogeosciences*, 11(8), 2201–2209.
- Moore J.C., Boone R.B., Koyama A. and Holfelder K. (2014). Enzymatic and detrital influences on the structure, function, and dynamics of spatially-explicit model ecosystems. *Biogeochemistry*, 117(1), 205–227.
- Moorhead D.L., Lashermes G. and Sinsabaugh R.L. (2012). A theoretical model of C- and N-acquiring exoenzyme activities, which balances microbial demands during decomposition. *Soil Biology and Biochemistry*, 53, 133–141.
- Moorhead D.L. and Sinsabaugh R.L. (2006). A theoretical model of litter decay and microbial interaction. *Ecological Monographs*, 76(2), 151–174.
- Müller R.H. and Babel W. (2001). Pseudo-recalcitrance of chlorophenoxyalkanoate herbicides - Correlation to the availability of α -ketoglutarate. *Acta Biotechnologica*, 21(3), 227–242.
- Müller T.A., Fleischmann T., Van Der Meer J.R. and Kohler H.P.E. (2006). Purification and characterization of two enantioselective α -ketoglutarate-dependent dioxygenases, RdpA and SdpA, from *Sphingomonas herbicidovorans* MH. *Applied and Environmental Microbiology*, 72(7), 4853–4861.
- Myrold D.D., Zeglin L.H. and Jansson J.K. (2014). The potential of metagenomic approaches for understanding soil microbial processes. *Soil Science Society of America Journal*, 78(1), 3–10.
- Nannipieri P., Ascher J., Ceccherini M.T., Landi L., Pietramellara G. and Renella G. (2003). Microbial diversity and soil functions. *European Journal of Soil Science*, 54(4), 655–670.
- Nannipieri P., Kandeler E. and Ruggiero P. (2002). Enzyme activities and microbiological and biochemical processes in soil. In R. G. Burns & R. Dick, eds. *Enzymes in the Environment*. New York: Marcel Dekker, pp. 1–33.
- Neill C. and Guenet B. (2010). Comparing two mechanistic formalisms for soil organic matter dynamics: A test with in vitro priming effect observations. *Soil Biology and Biochemistry*, 42(8), 1212–1221.

- Nielsen T.K., Xu Z., Gözdereliler E., Aamand J., Hansen L.H. and Sørensen S.R. (2013). Novel Insight into the Genetic Context of the *cadAB* Genes from a 4-chloro-2-methylphenoxyacetic Acid-Degrading *Sphingomonas*. *PLoS ONE*, 8(12), e83346.
- Nishiyama M., Senoo K., Wada H. and Matsumoto S. (1992). Identification of soil microhabitats for growth, death and survival of a bacterium, γ -1,2,3,4,5,6-hexachlorocyclohexane-assimilating *Sphingomonas paucimobilis*, by fractionation of soil. *FEMS Microbiology Letters*, 101(3), 145–150.
- Nunan N., Wu K., Young I.M., Crawford J.W. and Ritz K. (2003). Spatial distribution of bacterial communities and their relationships with the micro-architecture of soil. *FEMS Microbiology Ecology*, 44(2), 203–215.
- Or D., Smets B.F., Wraith J.M., Dechesne A. and Friedman S.P. (2007). Physical constraints affecting bacterial habitats and activity in unsaturated porous media - a review. *Advances in Water Resources*, 30(6-7), 1505–1527.
- Parkin T.B. (1993). Spatial variability of microbial processes in soil - A review. *Journal of Environmental Quality*, 22(3), 409–417.
- Parnas H. (1976). A theoretical explanation of the priming effect based on microbial growth with two limiting substrates. *Soil Biology and Biochemistry*, 8(2), 139–144.
- Paul E.A. (2007). *Soil microbiology, ecology, and biochemistry*. 3rd ed. E. A. Paul, ed. Amsterdam: Academic Press.
- Perveen N., Barot S., Alvarez G., Klumpp K., Martin R., Rapaport A., Herfurth D., Louault F. and Fontaine S. (2014). Priming effect and microbial diversity in ecosystem functioning and response to global change: A modeling approach using the SYMPHONY model. *Global Change Biology*, 20(4), 1174–1190.
- Pieper D.H., Reineke W., Engesser K.H. and Knackmuss H.J. (1988). Metabolism of 2,4-dichlorophenoxyacetic acid, 4-chloro-2-methylphenoxyacetic acid and 2-methylphenoxyacetic acid by *Alcaligenes eutrophus* JMP 134. *Archives of Microbiology*, 150(1), 95–102.
- Pivetz B.E. and Steenhuis T.S. (1995). Soil matrix and macropore biodegradation of 2,4-D. *Journal of Environmental Quality*, 24(4), 564–570.
- Poll C., Ingwersen J., Stemmer M., Gerzabek M.H. and Kandeler E. (2006). Mechanisms of solute transport affect small-scale abundance and function of soil microorganisms in the detritusphere. *European Journal Of Soil Science*, 57(4), 583–595.
- Poll C., Marhan S., Ingwersen J. and Kandeler E. (2008). Dynamics of litter carbon turnover and microbial abundance in a rye detritusphere. *Soil Biology and Biochemistry*, 40(6), 1306–1324.
- Poll C., Thiede A., Wermbter N., Sessitsch A. and Kandeler E. (2003). Micro-scale distribution of microorganisms and microbial enzyme activities in a soil with long-term organic amendment. *European Journal of Soil Science*, 54(4), 715–724.
- Postma J. and Van Veen J.A. (1990). Habitable pore space and survival of *Rhizobium leguminosarum* biovar *trifolii* introduced into soil. *Microbial Ecology*, 19(2), 149–161.
- Prosser J.I. (2012). Ecosystem processes and interactions in a morass of diversity. *FEMS Microbiology Ecology*, 81(3), 507–519.
- Rabbi S.M.F., Wilson B.R., Lockwood P.V., Daniel H. and Young I.M. (2014). Soil organic carbon mineralization rates in aggregates under contrasting land uses. *Geoderma*, 216, 10–18.
- Ranjard L., Poly F., Combrisson J., Richaume A., Gourbière F., Thioulouse J. and Nazaret S. (2000). Heterogeneous cell density and genetic structure of bacterial pools associated with various soil microenvironments as determined by enumeration and DNA fingerprinting approach (RISA). *Microbial Ecology*, 39(4), 263–272.
- Ranjard L. and Richaume A. (2001). Quantitative and qualitative microscale distribution of bacteria in soil. *Research in Microbiology*, 152(8), 707–716.
- Raynaud X. and Nunan N. (2014). Spatial ecology of bacteria at the microscale in soil. *PLoS ONE*, 9(1), e87217.

- Reddy G.V.B., Joshi D.K. and Gold M.H. (1997). Degradation of chlorophenoxyacetic acids by the lignin-degrading fungus *Dichomitus squalens*. *Microbiology*, 143(7), 2353–2360.
- Reed D.C., Algar C.K., Huber J.A. and Dick G.J. (2014). Gene-centric approach to integrating environmental genomics and biogeochemical models. *Proceedings of the National Academy of Sciences of the United States of America*, 111(5), 1879–1884.
- Rennert T., Totsche K.U., Heister K., Kersten M. and Thieme J. (2012). Advanced spectroscopic, microscopic, and tomographic characterization techniques to study biogeochemical interfaces in soil. *Journal of Soils and Sediments*, 12(1), 3–23.
- Resat H., Bailey V., McCue L.A. and Konopka A. (2012). Modeling Microbial Dynamics in Heterogeneous Environments: Growth on Soil Carbon Sources. *Microbial Ecology*, 63(4), 883–897.
- Rosenbom A.E., Binning P.J., Aamand J., Dechesne A., Smets B.F. and Johnsen A.R. (2014). Does microbial centimeter-scale heterogeneity impact MCPA degradation in and leaching from a loamy agricultural soil? *Science of the Total Environment*, 472, 90–98.
- Ruamps L.S., Nunan N. and Chenu C. (2011). Microbial biogeography at the soil pore scale. *Soil Biology and Biochemistry*, 43(2), 280–286.
- Ruamps L.S., Nunan N., Pouteau V., Leloup J., Raynaud X., Roy V. and Chenu C. (2013). Regulation of soil organic C mineralisation at the pore scale. *FEMS Microbiology Ecology*, 86(1), 26–35.
- Schenck zu Schweinsberg-Mickan M., Jörgensen R.G. and Müller T. (2012). Rhizodeposition: Its contribution to microbial growth and carbon and nitrogen turnover within the rhizosphere. *Journal of Plant Nutrition and Soil Science*, 175(5), 750–760.
- Schimel J.P. and Weintraub M.N. (2003). The implications of exoenzyme activity on microbial carbon and nitrogen limitation in soil: A theoretical model. *Soil Biology and Biochemistry*, 35(4), 549–563.
- Sessitsch A., Weilharter A., Gerzabek M.H., Kirchmann H. and Kandeler E. (2001). Microbial Population Structures in Soil Particle Size Fractions of a Long-Term Fertilizer Field Experiment. *Applied and Environmental Microbiology*, 67(9), 4215–4224.
- Sexstone A.J., Revsbech N.P., Parkin T.B. and Tiedje J.M. (1985). Direct measurement of oxygen profiles and denitrification rates in soil aggregates. *Soil Science Society of America Journal*, 49(3), 645–651.
- Shaw L.J. and Burns R.G. (2003). Biodegradation of Organic Pollutants in the Rhizosphere. *Advances in Applied Microbiology*, 53, 1–47.
- Sistla S.A., Rastetter E.B. and Schimel J.P. (2014). Responses of a tundra system to warming using SCAMPS: A stoichiometrically coupled, acclimating microbeplantsoil model. *Ecological Monographs*, 84(1), 151–170.
- Six J., Bossuyt H., Degryze S. and Deneff K. (2004). A history of research on the link between (micro)aggregates, soil biota, and soil organic matter dynamics. *Soil and Tillage Research*, 79(1), 7–31.
- Six J. and Paustian K. (2014). Aggregate-associated soil organic matter as an ecosystem property and a measurement tool. *Soil Biology and Biochemistry*, 68, A4–A9.
- Smejkal C.W., Vallaeyts T., Burton S.K. and Lappin-Scott H.M. (2001). Substrate specificity of chlorophenoxyalkanoic acid-degrading bacteria is not dependent upon phylogenetically related *tfdA* gene types. *Biology and Fertility of Soils*, 33(6), 507–513.
- Soulas G. (1993). Evidence for the existence of different physiological groups in the microbial community responsible for 2,4-D mineralization in soil. *Soil Biology and Biochemistry*, 25(4), 443–449.
- Spohn M. and Kuzyakov Y. (2013). Distribution of microbial- and root-derived phosphatase activities in the rhizosphere depending on P availability and C allocation - Coupling soil zymography with ¹⁴C imaging. *Soil Biology and Biochemistry*, 67, 106–113.
- Sträuber H., Müller R.H. and Babel W. (2003). Evidence of cytochrome P450-catalyzed cleavage of the ether bond of phenoxybutyrate herbicides in *Rhodococcus erythropolis* K2-3. *Biodegradation*, 14(1), 41–50.

- Strong D.T., De Wever H., Merckx R. and Recous S. (2004). Spatial location of carbon decomposition in the soil pore system. *European Journal of Soil Science*, 55(4), 739–750.
- Talbot J.M., Bruns T.D., Taylor J.W., Smith D.P., Branco S., Glassman S.I., Erlandson S., Vilgalys R., Liao H.-L., Smith M.E. and Peay K.G. (2014). Endemism and functional convergence across the North American soil mycobiome. *Proceedings of the National Academy of Sciences of the United States of America*, 111(17), 6341–6346.
- Tisdall J.M. and Oades J.M. (1982). Organic matter and water-stable aggregates in soils. *Journal of Soil Science*, 33(2), 141–163.
- Torstensson N.T.L., Stark J. and Goransson B. (1975). The effect of repeated applications of 2,4-D and MCPA on their breakdown in soil. *Weed Research*, 15, 159–164.
- Totsche K.U., Rennert T., Gerzabek M.H., Kögel-Knabner I., Smalla K., Spiteller M. and Vogel H.J. (2010). Biogeochemical interfaces in soil: The interdisciplinary challenge for soil science. *Journal of Plant Nutrition and Soil Science*, 173(1), 88–99.
- Trivedi P., Anderson I.C. and Singh B.K. (2013). Microbial modulators of soil carbon storage: Integrating genomic and metabolic knowledge for global prediction. *Trends in Microbiology*, 21(12), 641–651.
- Vinther F.P., Eiland F., Lind A.-M. and Elsgaard L. (1999). Microbial biomass and numbers of denitrifiers related to macropore channels in agricultural and forest soils. *Soil Biology and Biochemistry*, 31(4), 603–611.
- Vogel H.-J. and Roth K. (2003). Moving through scales of flow and transport in soil. *Journal of Hydrology*, 272(1–4), 95–106.
- Vos M., Wolf A.B., Jennings S.J. and Kowalchuk G.A. (2013). Micro-scale determinants of bacterial diversity in soil. *FEMS Microbiology Reviews*, 37(6), 936–954.
- Vroumsia T., Steiman R., Seigle-Murandi F. and Benoit-Guyod J.L. (2005). Fungal bioconversion of 2,4-dichlorophenoxyacetic acid (2,4-D) and 2,4-dichlorophenol (2,4-DCP). *Chemosphere*, 60(10), 1471–1480.
- Wainwright J. and Mulligan M. (2013). *Environmental modelling: finding simplicity in complexity*. J. Wainwright & M. Mulligan, eds. Chichester: John Wiley & Sons Ltd.
- Wallenstein M.D. and Hall E.K. (2012). A trait-based framework for predicting when and where microbial adaptation to climate change will affect ecosystem functioning. *Biogeochemistry*, 109(1–3), 35–47.
- Wang G., Mayes M.A., Gu L. and Schadt C.W. (2014). Representation of dormant and active microbial dynamics for ecosystem modeling. *PLoS ONE*, 9(2). DOI 10.1371/journal.pone.0089252.
- Wieder W.R., Grandy A.S., Kallenbach C.M. and Bonan G.B. (2014). Integrating microbial physiology and physiochemical principles in soils with the Microbial-Mineral Carbon Stabilization (MIMICS) model. *Biogeosciences*, 11(14), 3899–3917.
- Wutzler T. and Reichstein M. (2008). Colimitation of decomposition by substrate and decomposers – A comparison of model formulations. *Biogeosciences*, 5(3), 749–759.
- Wutzler T. and Reichstein M. (2013). Priming and substrate quality interactions in soil organic matter models. *Biogeosciences*, 10(3), 2089–2103.
- Young I.M. and Crawford J.W. (2004). Interactions and self-organization in the soil-microbe complex. *Science*, 304(5677), 1634–1637.
- Young I.M. and Ritz K. (2005). The habitat of soil microbes. In R. D. Bardgett, M. B. Usher, & D. W. Hopkins, eds. *Biological Diversity and Function in Soils*. Ecological Reviews. Cambridge: Cambridge University Press, pp. 31–43.
- Zapras A., Liu Y.J., Liu S.J., Drake H.L. and Horn M.A. (2010). Abundance of novel and diverse tfdA-like genes, encoding putative phenoxyalkanoic acid herbicide-degrading dioxygenases, in soil. *Applied and Environmental Microbiology*, 76(1), 119–128.
- Zhang S., Li Q., Lü Y., Zhang X. and Liang W. (2013). Contributions of soil biota to C sequestration varied with aggregate fractions under different tillage systems. *Soil Biology and Biochemistry*, 62, 147–156.

Curriculum vitae

Name	Holger Pagel
Date of -Birth	26.03.1979
Place of Birth	Rostock
Marital status	married, 3 children

Education

2008-2014	PhD student at the Institute of Soil Science and Land Evaluation, Biogeophysics (Prof. Thilo Streck), University of Hohenheim
1998-2007	Studies in environmental science and technology (TU Berlin) with focus on water quality control, soil science and environmental hygiene
1997	General qualification for university entrance (Abitur) at Goethe-Gymnasium, Schwerin (Germany)

Work experience

2007	Three-month internship at the Institute of Soil Science and Agrochemistry, Siberian Branch of the Russian Academy of Sciences in Novosibirsk
2007	Self-employee in Graduate Research Programme "Perspectives on Urban Ecology II" funded by DFG (TU Berlin)
2005-2006	Student assistant in DFG project „Mobilization and Mobility of colloidal phosphorus in sandy soils“ (TU Berlin)
1999-2000	Team member of „Youth initiative World Exposition Expo 2000“ („Verein der Freunde der Jugendinitiative Weltausstellung 2000“)
1997-1998	Civilian service Diakoniewerk Neues Ufer gGmbH

Uhingen, 29.11.2014

Acknowledgements

I am grateful to:

Katrin Ilg for sharing all ups and downs, her extensive support as well as her stamina when I talked the hind leg off a donkey on modeling while having a fag in the evening. Thank you for showing me your “Ländle”. Without you, I would never have started (and finished?) my PhD in Hohenheim.

Prof. Thilo Streck for supervising my thesis, thought-provoking discussions about science and other things as well as for his support and for giving me the freedom to find my own scientific way.

Prof. Ellen Kandeler for co-supervising my thesis, her motivation, support and her confidence in my competence.

Prof. Claire Chenu for acting as co-referee.

Christian Poll for introducing me to the soil-litter interface as well as for sharing ideas and frustration (particularly when we jointly set-up our first experiment from 9 a.m. until 11 p.m.) in the lab, at conferences and elsewhere.

Joachim Ingwersen for always having an ear for small and big problems with experiments, modeling and organisation. Thank you for your motivation and the flowers for the manuscripts.

Franziska Ditterich for nice collaboration, many discussions and broadening my knowledge on molecular biology.

Erhard Strohm for his support with experiments, equipment and analyses as well as for the insider information on agricultural practices.

Sabine Rudolph, Heike Haslwimmer, Ingrid Tischer, Christoph Schweizer, David Bru, Barbara von der Lühe, Jacob Schunck and Elke Feiertag for analytical support. Special thanks go to Elke for coping with my chaos in the lab.

Omar Saleh, Rieke Trittin, Tatiana Yuyukina, Thomas Herbert Angermeier, Milena Schulz, Katharina Lennard and last but not least Aurela Gebala for their valuable contributions to my research.

The team of the mechanics workshop for doing a good job.

Fabrice Martin-Laurent and Marion Devers-Lamrani for nice collaboration.

Katrin Ilg, Joachim Ingwersen and Christian Poll for critically reading the manuscript of my thesis.

All colleagues and friends in Hohenheim for many talks, discussions and shared problems.

Olga Fishkis, Marc Lamers, Iris Palmer, Claudia Kreschnak and Sven Marhan for giving me a good start in Hohenheim.

My office colleagues Susanne Kramer and Anna Georgiades for inspiring discussions about science and daily life. Special thanks go to Susanne for her immediate help in all formality questions regarding the submission of the thesis and for always sharing her tobacco with me.

Hilde Ilg for being such a great grandmother, her commitment and support with the kids and her cooking skills (always critically looking at my supply with fresh salad).